EFFECT OF PARTICLE FABRIC ON THE ONE-DIMENSIONAL COMPRESSION RESPONSE OF FRASER RIVER SAND

by

Sheri Lynn Northcutt

B.S. Civil Engineering, University of Illinois at Urbana-Champaign, 2007

A THESIS SUBMITTED IN PARTIAL FULFILLMENT OF THE REQUIREMENTS FOR THE DEGREE OF

MASTER OF APPLIED SCIENCE

in

The Faculty of Graduate Studies

(Civil Engineering)

THE UNIVERSITY OF BRITISH COLUMBIA
(Vancouver)

January 2010

ABSTRACT

One-dimensional compression of sand with lateral stress measurement allows for laboratory determination of the coefficient of lateral pressure at rest, K_o. Commonly used to define the initial state of stress in soil where no lateral strain occurs, K_o is calculated as the ratio of horizontal to vertical effective stress. The present study aims to investigate the role of initial particle fabric in one-dimensional compression and to determine the effect of fabric on the coefficient of lateral pressure at rest in Fraser River sand.

One-dimensional compression with lateral stress measurement was carried out on reconstituted Fraser River sand specimens using an instrumented oedometer. Laboratory specimen reconstitution methods were developed in order to construct different particle fabrics. Three different techniques were utilized: air pluviation, tamping and vibration. In addition, the effects of initial relative density and loading history on the compression response were evaluated. Each one-dimensional compression test was executed in three distinct phases: virgin loading, unloading and reloading. The key results from the testing program were compared with current methods available for estimation of K_o.

The results from the present study show that specimens resulting from different laboratory reconstitution methods (i.e., initial particle fabrics) exhibit different one-dimensional compression responses. For Fraser River sand in one-dimensional compression, air-pluviated specimens yield the highest K_o values, tamped specimens produce the lowest K_o values and vibrated specimens rank intermediate. With increasing initial relative density, regardless of the initial specimen preparation method, the measured K_o values generally decrease. Upon reloading, measured K_o values are slightly reduced from those observed during virgin loading.

Furthermore, results from the present study indicate that the current methods commonly used for determination of K_o do not necessarily provide suitable estimations for variable granular particle fabrics arising from different specimen reconstitution techniques. A new method for determination of K_o is proposed, as a function of the constant-volume friction angle, initial relative density and a factor accounting for the initial particle fabric.

TABLE OF CONTENTS

LIST OF TABLES

LIST OF FIGURES

LIST OF SYMBOLS

C_u	coefficient of uniformity
d	double-amplitude of vibration
D_{50}	average particle size
D_r	relative density
e_{max}	maximum void ratio
e_{min}	minimum void ratio
F	fabric factor
F_{AP}	fabric factor for air-pluviated specimens
F_N	fabric factor for non-densified specimens
F_T	fabric factor for tamped specimens
F_V	fabric factor for vibrated specimens
K_o	coefficient of lateral pressure at rest
K_{onc}	coefficient of lateral pressure at rest during virgin loading, originally proposed by Mayne & Kulhawy (1982)
K_{op}	coefficient of lateral pressure at rest for end-of-primary loading of granular materials not subject to densification, from Mesri & Hayat (1993)
K_{or}	coefficient of lateral pressure at rest during reloading, originally proposed by Mayne & Kulhawy (1982)

K_{ou} coefficient of lateral pressure at rest during unloading, originally proposed by Mayne & Kulhawy (1982)

$\overset{o}{K}$ coefficient of lateral pressure at rest, defined by the slope of the horizontal versus vertical effective stress plot in one-dimensional compression, from Mesri & Hayat (1993)

$\overset{o}{K}_r$ coefficient of lateral pressure at rest in recompression, defined by the slope of the horizontal versus vertical effective stress plot in one-dimensional compression, from Mesri & Hayat (1993)

m density parameter

m_r reload coefficient, from Mayne & Kulhawy (1982)

OCR overconsolidation ratio

OCR_{max} maximum overconsolidation ratio, from Mayne & Kulhawy (1982)

α at-rest rebound parameter, from Schmidt (1967)

ϕ angle of internal friction, from Jaky (1944)

ϕ' effective stress friction angle

ϕ'_{cv} constant-volume effective friction angle

σ'_h horizontal effective pressure

σ'_p preconsolidation effective pressure

σ'_v vertical effective pressure

$\sigma'_{v,max}$ maximum vertical effective pressure previously experienced by the soil, from Mayne & Kulhawy (1982)

$\sigma'_{v,min}$ minimum vertical effective pressure to which the soil was unloaded, from Mayne & Kulhawy (1982)

$\Delta\sigma'$ incremental increase in effective stress

ACKNOWLEDGMENTS

I would like to express my sincerest appreciation to my research supervisor, Dr. Dharma Wijewickreme. His skilled guidance, enthusiastic support and continued patience made the completion of this thesis possible. I also wish to express my genuine gratitude to Dr. Mahdi Taiebat, for his constructive feedback and assistance in timely submission of this manuscript.

Additionally, I would like to extend my appreciation to all of my colleagues and friends at the University of British Columbia, including Alireza Ahmadnia, Kaley Crawford-Flett, Antone Dabeet, Greg Lewsley, Mavi Sanin, Atitep Srikongsri, Mark Styler and Lalinda Weerasekara, for helping to make my time at UBC both fulfilling and enjoyable. I am also grateful to the technical support staff of the Department of Civil Engineering, specifically Bill Leung, Harald Schrempp, Scott Jackson and John Wong, for their friendly advice and expert assistance in the geotechnical laboratory.

Finally, I wish to acknowledge my Mom, Dad and sister, Michelle, to whom I am forever indebted for their unwavering support and encouragement throughout the years.

1 INTRODUCTION

1.1 Purpose of the study

The coefficient of lateral pressure at rest, K_o, is a parameter used to define the initial state of stress in soil. For in-situ deposits where no lateral deformation occurs, the state of stress is termed "at-rest." The at-rest condition is described by the following equation:

$$K_o = \frac{\sigma'_h}{\sigma'_v}; \qquad \text{where} \quad \sigma'_h = \text{horizontal effective pressure}$$

$$\sigma'_v = \text{vertical effective pressure}$$

Eq. 1.1

While the vertical effective stress can be easily estimated for a given depth of overburden, the horizontal effective stress is a complex function of the soil type and structure, as well as geologic history (Mitchell & Soga, 2005). The coefficient of lateral pressure at rest allows for the determination of the in-situ horizontal effective stress and therefore, is an important parameter in engineering design.

A valuable tool used in the investigation of soil behaviour is laboratory element testing. Through soil testing in a controlled laboratory setting, researchers aim to better understand how and why a soil behaves as observed in the field. Ultimately, knowledge gained in the laboratory can be translated into practical engineering design by helping predict the behaviour of soils in-situ.

The purpose of this study is to investigate the effect of initial particle fabric on the behaviour of granular soil, specifically Fraser River sand, in one-dimensional compression. Laboratory specimens of Fraser River sand were prepared by three different reconstitution methods over a range of initial relative densities. One-dimensional compression responses were compared for specimens comprised of identical granular material and packing density but prepared by dissimilar reconstitution methods (i.e., initial particle fabrics). Special attention was paid to the influences of specimen densification and to the effects of loading history on the stress state during compression.

1.2 Organization of this thesis

Chapter 2 presents a review of literature pertaining to the coefficient of lateral pressure at rest. Notable studies of K_o in granular soils are discussed and current methods for determination of K_o are presented. Additionally, the concept of "particle fabric" in granular soil is introduced, and the development of fabric in reconstituted soil specimens is reviewed. Finally, the role of particle fabric in one-dimensional compression of sand is discussed.

Chapters 3 and 4 present the experimental aspects of the present study. Chapter 3 outlines the testing apparatus and procedure. Also, the testing program is identified. Chapter 4 discusses the development of the specimen reconstitution techniques for the present study, in the context of relevant literature.

The results from one-dimensional compression testing of Fraser River sand are presented in Chapter 5. Results are organized according to the preparation method used to reconstitute the test specimens. Observed effects of specimen densification and loading history on the compression response are presented.

Chapter 6 offers an in-depth analysis and discussion of the one-dimensional compression test results. Primarily, the role of initial particle fabric in the behaviour of sand in one-dimensional compression is explored. Further, the results from the present study are compared with the methods for K_o determination from literature, and a new determination method is proposed.

Chapter 7 provides conclusions and recommendations from the present study.

The full set of testing data is provided in Appendices A, B and C.

2 LITERATURE REVIEW

2.1 Coefficient of lateral pressure at rest in granular soils

2.1.1 Background

Countless studies have been conducted to better understand the coefficient of lateral pressure at rest. The first notable study attempting to quantify K_o was conducted by Jaky (1944). The following equation was presented for determination of the coefficient of lateral pressure at rest:

$$K_o = (1 - \sin\phi)\frac{1+\frac{2}{3}\sin\phi}{1+\sin\phi}; \quad \text{where} \quad \phi = \text{angle of internal friction}$$

Eq. 2.1

This equation was derived from theoretical analysis of a free-standing cone of granular material (Jaky, 1944). Later, a simplified version of the relation was presented (Jaky, 1948):

$$K_o = 1 - \sin\phi$$

Eq. 2.2

In 1967, two separate studies emerged, both aimed at evaluating the coefficient of lateral pressure at rest through an empirical approach (Alpan, 1967; Schmidt, 1967). Similar observations of the behaviour of soil in one-dimensional compression were made by both authors. It was noted that during virgin loading, K_o is generally constant. During unloading, a rebound effect is observed and K_o increases. If the soil is subjected to recompression, K_o is again affected, as an even more complex stress state is developed (Alpan, 1967; Schmidt, 1967).

2.1.2 Effects of loading history and densification

One of the most comprehensive studies concerning the coefficient of lateral pressure at rest was presented by Mayne and Kulhawy (1982). In an effort to characterize K_o

behaviour during virgin loading (K_{onc}), unloading (K_{ou}) and reloading (K_{or}), published laboratory testing data was amassed for ninety different granular soils from a variety of sources. For granular soils under virgin loading, the reported coefficient of lateral pressure at rest was plotted in relation to the effective stress friction angle, ϕ' (see Figure 2.1). It was concluded that the formula introduced by Jaky (1948) (Eq. 2.2) was "moderately valid" for normally consolidated, cohesionless soils (Mayne & Kulhawy, 1982).

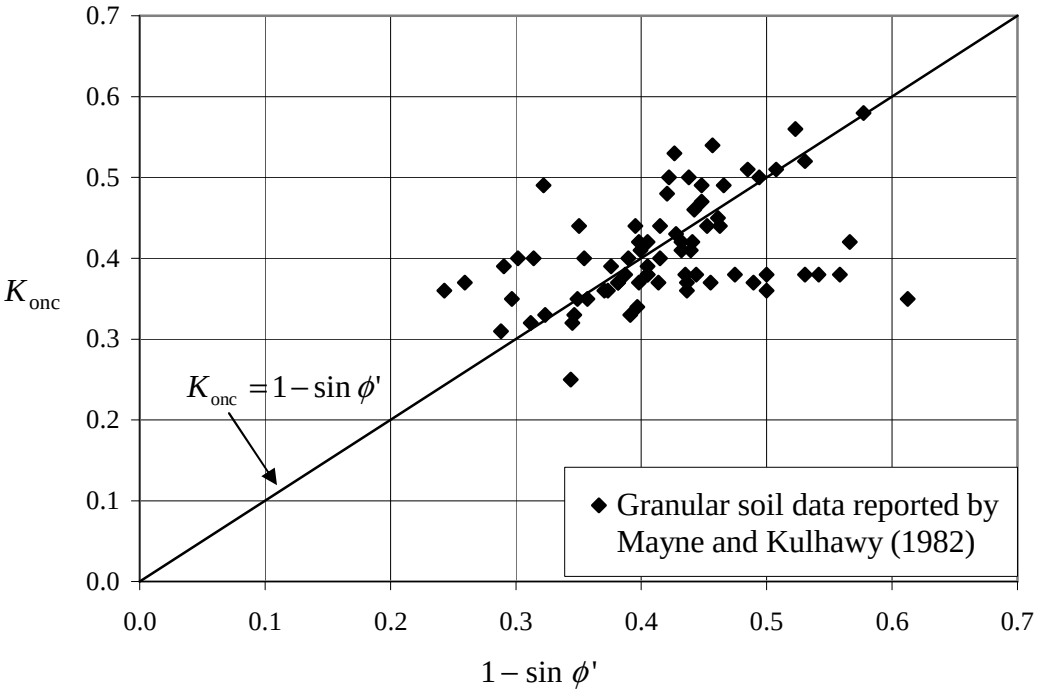

Figure 2.1. Relationship between K_{onc} and effective friction angle (modified from Mayne & Kulhawy, 1982)

For granular soils experiencing unloading, Mayne and Kulhawy (1982) observed the coefficient of lateral pressure at rest to be a function of the overconsolidation ratio (OCR) and the effective stress friction angle. This observation stemmed from a relation originally proposed in a study by Schmidt (1967), who identified the following equation for soils during unloading:

$$K_{ou} = K_{onc}\text{OCR}^{\alpha}; \quad \text{where} \quad \alpha = \text{at-rest rebound parameter}$$

Eq. 2.3

For sands, the at-rest rebound parameter (α) was empirically shown to be a constant value between 0.3 and 0.5 (Schmidt, 1967).

Mayne and Kulhawy (1982) utilized linear regression analyses to determine α values for their catalogued data. Figure 2.2 plots these α values against the effective friction angle.

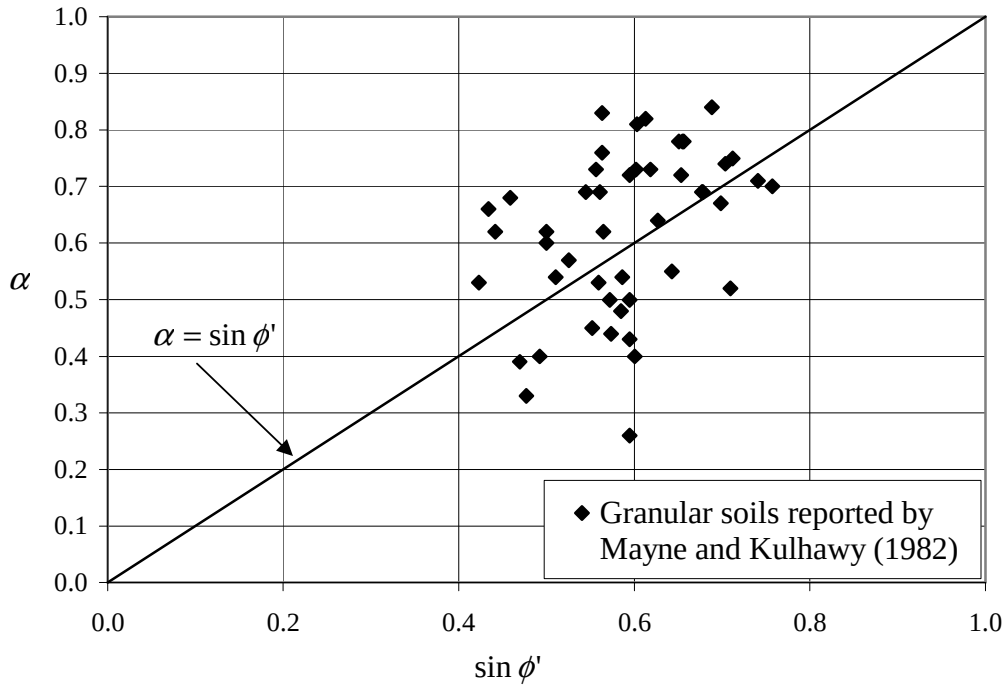

Figure 2.2. Relationship between α and effective friction angle (modified from Mayne & Kulhawy, 1982)

Although Figure 2.2 appears tentative, it was concluded that the α parameter proposed by Schmidt (1967) was roughly equal to $\sin\phi'$ for granular soils (Mayne & Kulhawy, 1982). Therefore, the K_{ou} can be expressed as the following:

$$K_{ou} = (1 - \sin\phi')\text{OCR}^{\sin\phi'}$$

Eq. 2.4

For granular soils during reloading, Mayne and Kulhawy (1982) were able to derive an empirical relationship for the coefficient of lateral pressure at rest, though markedly less test data was available. Using the concept of overconsolidation ratio, a new stress history parameter, OCR_{max}, was conceived for this purpose, as defined by the following equation:

$$\mathrm{OCR}_{\max} = \frac{\sigma'_{v,\max}}{\sigma'_{v,\min}};$$

where $\sigma'_{v,\max}$ = maximum vertical effective pressure previously experienced by the soil

$\sigma'_{v,\min}$ = minimum vertical effective pressure to which the soil was unloaded

Eq. 2.5

Consistent with available test data, Mayne and Kulhawy (1982) assumed a linear relationship between the horizontal and vertical effective stresses in reloading. A reload coefficient (m_r) was used to describe the slope of the observed linear effective stress relationship. The resulting equation is as follows:

$$K_{or} = K_{onc}\left(\frac{\mathrm{OCR}}{\mathrm{OCR}_{\max}^{(1-\alpha)}}\right) + m_r\left(1 - \frac{\mathrm{OC}R}{\mathrm{OCR}_{\max}}\right); \text{where} \quad m_r = \text{reload coefficient}$$

Eq. 2.6

Empirically, the reload coefficient (m_r) was determined to be a function of the effective friction angle or K_o during virgin loading (see Figure 2.3). Therefore, the m_r can be expressed as the following:

$$m_r = \left(\frac{3}{4}\right)(1 - \sin\phi') = \left(\frac{3}{4}\right)K_{onc}$$

Eq. 2.7

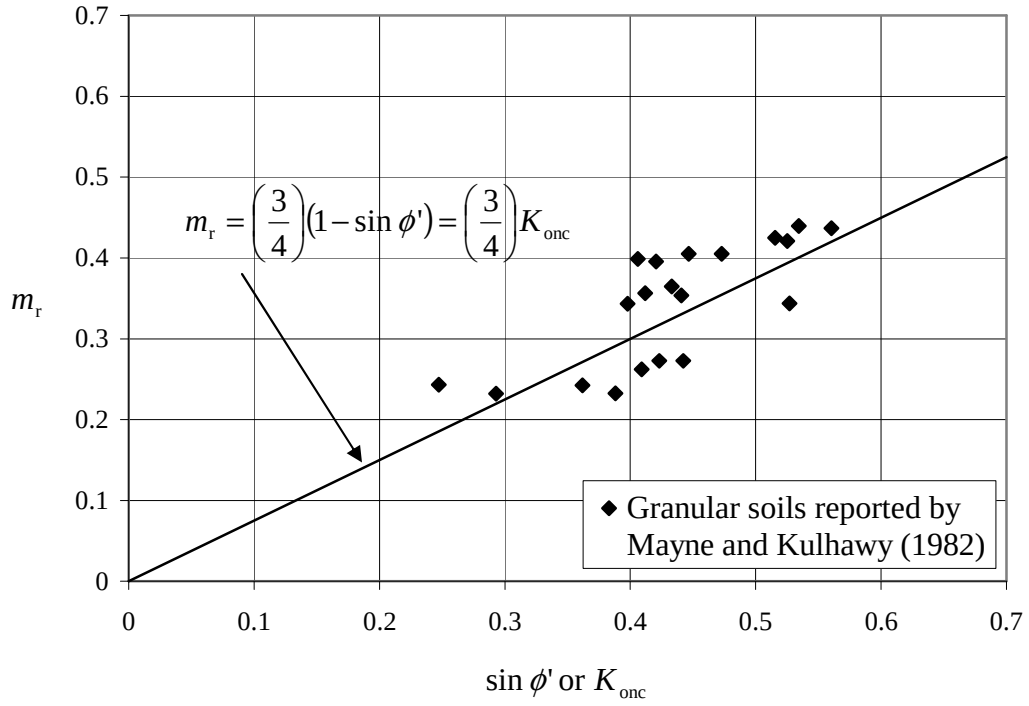

Figure 2.3. Relationship between m_r and effective friction angle or K_{onc} (modified from Mayne & Kulhawy, 1982)

Combining the equations for the coefficient of lateral pressure at rest during virgin loading, unloading and reloading from Mayne and Kulhawy (1982), the following general equation results:

$$K_o = (1-\sin\phi')\left[\left(\frac{OCR}{OCR_{max}^{(1-\sin\phi')}}\right)+\frac{3}{4}\left(1-\frac{OCR}{OCR_{max}}\right)\right]$$

Eq. 2.8

It should be noted that a degree of uncertainty exists in the conclusions drawn by Mayne and Kulhawy (1982). Particularly, the authors acknowledge in their paper that the effective friction angles reported by the various researchers were determined by variable, unspecified methods and as such, may be unsuitable for direct comparison.

More recently, a study investigating the coefficient of lateral pressure at rest in granular materials was conducted by Mesri and Hayat (1993). Special attention was paid to the

nomenclature employed in discussion of the coefficient of lateral pressure at rest, in an effort to more accurately discern the applicability of quantitative relationships presented in related literature.

First, Mesri and Hayat (1993) noted that the Jaky formulations for the coefficient of lateral pressure at rest (Eq. 2.1, Eq. 2.2) were intended for use with the friction angle equal to the angle of repose, or the constant-volume effective friction angle (ϕ'_{cv}). Therefore, Jaky's equations could arguably only be of use for granular soils not subject to densification, where $\phi' = \phi'_{cv}$. Often, laboratory testing described in literature involves densified granular soils and hence, should not be evaluated with Jaky's formulations. The Mayne and Kulhawy (1982) paper does not make this distinction (Mesri & Hayat, 1993).

With this in mind, Mesri and Hayat (1993) established a more decisive parameter, K_{op}, the coefficient of lateral pressure at rest for the end-of-primary loading of sedimented, normally consolidated clays and granular soils not subject to densification. Jaky's simplified relation (Eq. 2.2) then becomes:

$$K_{op} = 1 - \sin\phi'_{cv}$$

Eq. 2.9

More prominently, Mesri and Hayat (1993) challenged the equation presented by Mayne and Kulhawy (1982) for the coefficient of lateral pressure at rest during unloading (Eq. 2.4). The parameter α from Schmidt's original equation (Eq. 2.3) was concluded by Mayne and Kulhawy (1982) to be a function of the effective friction angle of the soil. Instead, Mesri and Hayat (1993) contended that α was independent of the initial density (i.e., effective friction angle) and was actually a function of the constant-volume effective friction angle. Graphical evidence supporting this claim from a limited number of one-dimensional compression tests is presented in Figure 2.4.

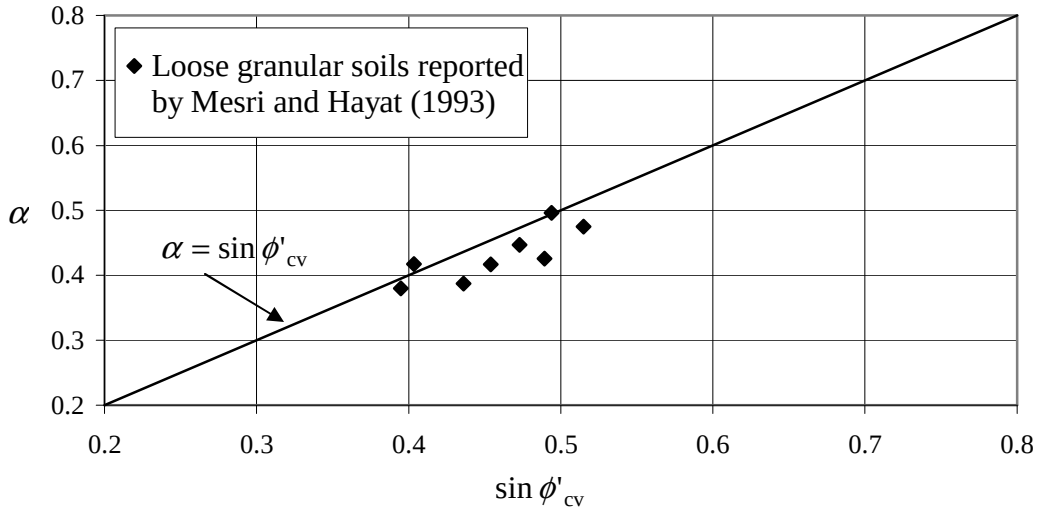

Figure 2.4. Relationship between α and constant-volume friction angle (modified from Mesri & Hayat, 1993)

Hence, the equation for K_{ou} may be expressed as:

$$K_{ou} = \left(1 - \sin\phi'_{cv}\right)\mathrm{OCR}^{\alpha}; \qquad \text{where} \quad \alpha = \sin\phi'_{cv}$$

Eq. 2.10

Lastly, a new parameter closely related to K_o was established by Mesri and Hayat (1993). The parameter $\overset{o}{K}$ describes the coefficient of lateral pressure at rest defined by the slope of the horizontal versus vertical effective stress plot in one-dimensional compression, such that:

$$\overset{o}{K} = \frac{\Delta\sigma'_h}{\Delta\sigma'_v}; \qquad \text{where} \quad \Delta\sigma' = \text{incremental increase in effective stress}$$

Eq. 2.11

From Mesri and Hayat (1993), the following observations of $\overset{o}{K}$ in one-dimensional compression were presented. For virgin loading of non-densified granular soils, $\overset{o}{K}$ is equal to K_{op}. When granular soils are densified and subsequently subjected to one-dimensional compression from $\sigma'_h = \sigma'_v = 0$, $\overset{o}{K}$ can be estimated from Jaky's formula

(Eq. 2.2), using the densified or effective friction angle (ϕ'). For granular soils in recompression, a stiffer response is observed and $\overset{o}{K}$ is reduced to equal $\overset{o}{K}_r$. Mesri and Hayat (1993) presented the following equation for relating $\overset{o}{K}_r$ to K_o:

$$K_o = \overset{o}{K}_r + \frac{\sigma'_p}{\sigma'_v}\left(K_{op} - \overset{o}{K}_r\right), \text{ where } \sigma'_p = \text{preconsolidation pressure}$$

Eq. 2.12

Therefore, for a given sand, the greatest $\overset{o}{K}$ value is observed at the loosest condition, and the least $\overset{o}{K}$ value is observed at the densest condition. However, at high pressures when grain crushing occurs, $\overset{o}{K}$ has been shown to increase to K_{op} (Mesri & Hayat, 1993).

Despite the empirical evidence presented by various researchers in general support of Jaky's original theory (Eq. 2.2), the theoretical basis for the formulation is still being called into question. Michalowski (2005) performed a rigorous critique of the stress distribution in a wedge-shaped prism of loose, granular material. It was concluded that not only was Jaky's equation an unrealistic representation of a highly variable stress state, but also, the stress state of a wedge-shaped prism is unrelated to the typical stress path observed in one-dimensional compression. In other words, despite the reported empirical evidence, there is no rational basis for the application of Jaky's equation to describe the coefficient of lateral pressure at rest (Michalowski, 2005).

2.2 Particle fabric in reconstituted sand specimens

According to Oda (1972), the particle fabric of a granular media may be described as "the spatial arrangement of solid particles and associated void." For a homogeneous specimen, the orientation of individual particles and the relative configuration of the particles collectively define the specimen fabric. In general, initial particle fabric is a function of both characteristic grain shape and specimen reconstitution method. Moreover, studies have shown that soil's mechanical response is often a function of its particle fabric (Oda, 1972a).

The fabric of a soil specimen is inherently problematic to directly observe. To examine fabric attributes both qualitatively and quantitatively, soil specimens are often preserved and dissected by a variety of methods. Generally, prior to preservation, any pore fluids present in the specimen must be removed. A resin or plastic may then be injected into the specimen voids and allowed to harden. It is critical to preclude any disturbance to the particle fabric during impregnation and curing. Once preserved, the specimen may be sawed into various sections, which are polished as needed. Microscopic imaging is then performed on representative sections to measure grain orientations or other fabric characteristics (Mitchell & Soga, 2005).

In addition, it has been shown that the mechanical response of soil specimens can be directionally dependent upon the applied loading (Oda, 1972a). In the present study, which utilizes one-dimensional compression testing, loading and deformations occur in the vertical direction only. Therefore, the stress-strain response of the specimen will be influenced primarily by the fabric characteristics observed in the vertical plane.

At this time, it is important to acknowledge the primary goal of specimen reconstitution in the laboratory. Unlike cohesive soils which may be sampled intact from the field for use in laboratory testing, it is remarkably difficult and expensive to obtain undisturbed granular samples. Instead, researchers must retrieve disturbed samples and then reconstitute the material in a laboratory setting. Ideally, the particle fabric of the reconstituted specimen should mimic the fabric exhibited naturally in the field. Similarly, particle fabric may also be modeled after the fabric generated by field compaction methods.

2.2.1 Air pluviation method

Pluviation, through air or water, is a reconstitution technique often used to imitate natural, alluvial deposition in the field. The mechanical deposition process of air-pluviated sand may be idealized as the free-falling behaviour of identical spheres. However, this model does not account for non-spherical grains, particle variability and particle interference during deposition (Vaid & Negussey, 1984).

Given that many sands have a significant amount of flat or elongated particles, it is important to account for this characteristic when considering pluviation behaviour. If ellipsoidal particles are deposited freely through the air under the influence of gravity, more particles will tend to deposit with their long axes normal to the direction of free-fall. Consequently, anisotropic fabric is developed (Mahmood & Mitchell, 1974).

Mahmood and Mitchell (1974) investigated the different granular fabrics formed by various specimen reconstitution techniques. Crushed basalt specimens were prepared by simple pouring, static compaction with a piston and dynamic compaction from a vibrating table. Prepared specimens were preserved and grain orientations in the vertical plane were measured. Poured specimens, comparable to air-pluviated specimens, exhibited a strongly preferential grain orientation, with the long particles axes normal to the vertical plane. This effect is likely due to the aforementioned behaviour of ellipsoids in free-fall (Mahmood & Mitchell, 1974).

2.2.2 Tamping method

Tamping is a reconstitution method often used to imitate field compaction techniques. Tamping or sheepsfoot rollers are commonly used for compacting layers of fills in engineering practice (Terzaghi, Peck, & Mesri, 1996).

For specimens prepared with tamping, the compactive effort imposed on the specimen results in a rearrangement of grains into a configuration which better resists applied normal stresses. Tamping, in specific, enacts a one-dimensional deformation force which is resisted by particle friction and interlocking. Densification occurs by slippage at grain contacts and some overturning of particles into voids (Mahmood & Mitchell, 1974).

In their study, Mahmood and Mitchell (1974) noted moderate anisotropy for crushed basalt specimens prepared with static compaction, a form of tamping. A weakly bimodal preferential grain orientation was observed at about 45° from the horizontal.

2.2.3 Vibration method

Similar to tamping, vibration may be used to imitate field compaction methods. Vibratory rollers and vibrating-plate compactors are often used for compacting layers of fills in the field (Terzaghi et al., 1996).

For specimens prepared by vibration, grains are rearranged into a more stable configuration, but by a different densification mechanism than observed in tamping. The pulsating force imposed by a vibrator induces a periodic decrease of the energy barriers created by particle interlocking and friction (Mahmood & Mitchell, 1974).

In their study, Mahmood and Mitchell (1974) observed practically random grain orientations in crushed basalt specimens prepared by vibration.

It should be noted that the research by others has been presented herein solely to promote an understanding of how diverse reconstitution methods generate unique fabrics. There is no evidence to suggest that the specimen fabrics from the studies described in Chapter 2.2 will be replicated by the reconstitution methods performed in the present study. Particle fabric is shown to be highly sensitive to the granular material used, the specimen container and the exact preparation technique. Only resin impregnation, sectioning and microscopic observation of the specimen in question can define its particle fabric with certainty.

2.3 Role of particle fabric in response behaviour of sand

The influence of the initial particle fabric generated by a specific preparation method may be detected through distinctions in the soil's mechanical response. Earlier studies addressing the effects of fabric on specimen response focused primarily on liquefaction behaviour (Ladd, 1974; Mulilis, Seed, Chan, Mitchell, & Arulanandan, 1977). For the present study, the influence of initial particle fabric on the one-dimensional compression response of sand is of interest.

Mahmood, Mitchell and Lindblom (1976) presented one of the first investigations focused on fabric effects in one-dimensional compressibility of clean, uniform sand. A

primitive instrumented oedometer-type device was designed to conduct one-dimensional compression tests of reconstituted Monterey sand specimens. Specimens were prepared in a dry condition, by either air pluviation or vibration. Limited test results indicated that measured K_o values decreased with increasing density. Moreover, K_o values for vibrated specimens were less than those for air-pluviated specimens at a given density (Mahmood, Mitchell, & Lindblom, 1976).

In 1984, Okochi and Tatsuoka conducted a series of K_o-consolidation tests on reconstituted sand specimens using a triaxial apparatus. Toyoura sand, a uniform, clean, angular sand, was selected as the test material. Specimens were reconstituted by two different methods, air pluviation of dry sand and tamping of moist sand (Okochi & Tatsuoka, 1984).

From Figure 2.5, test results yielded slightly larger K_o values for air-pluviated specimens of a given initial density than for tamped specimens of the same density. This deviation indicates a relationship between the virgin loading specimen response in one-dimensional compression and the reconstituted particle fabric.

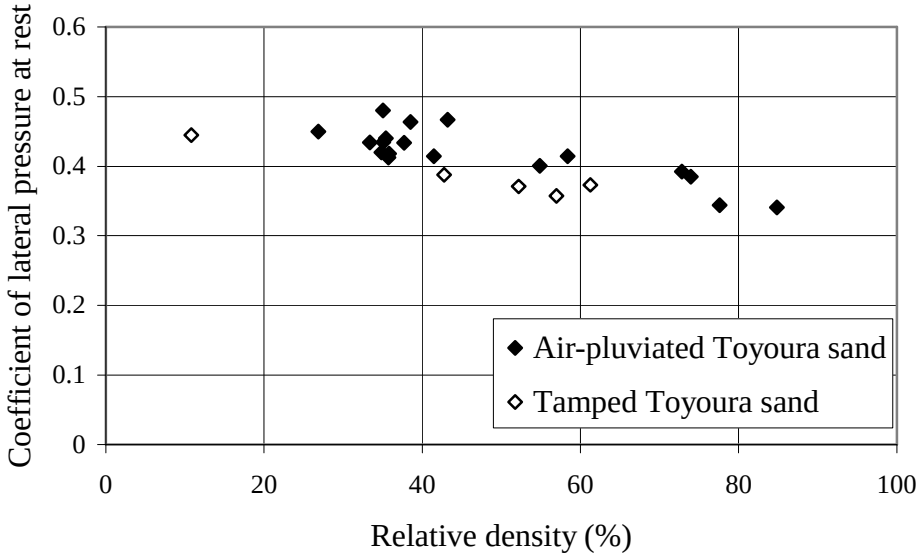

Figure 2.5. Relationship between K_o and initial relative density for different particle fabrics ($\sigma'_v = 200$ kPa) (modified from Okochi & Tatsuoka, 1984)

Using these test results, Okochi and Tatsuoka (1984) critiqued the applicability of the Jaky (1948) relation for K_o as a function of the effective friction angle during virgin loading (Eq. 2.2). Strictly speaking, the test results indicated Jaky's formulation was inaccurate because K_o varied with reconstituted particle fabric while the effective friction angle did not. The effective friction angle for Toyoura sand was shown to be a function of initial void ratio alone. However, the authors acknowledged that such a rigorous critique may be inappropriate, due to the limitations associated with laboratory determination of the effective friction angle. It was the authors' opinion that overall, Jaky's equation provided a suitable estimation for K_o during virgin loading (Okochi & Tatsuoka, 1984).

Similarly, different specimen response behaviour was observed by Okochi and Tatsuoka (1984) for air-pluviated and tamped specimens during the unloading phase. Figure 2.6 illustrates this difference by plotting the at-rest rebound parameter versus the specimen's initial relative density. Recall from Schmidt (1976), the at-rest rebound parameter (α) was used to define the coefficient of lateral pressure at rest during unloading (Eq. 2.3).

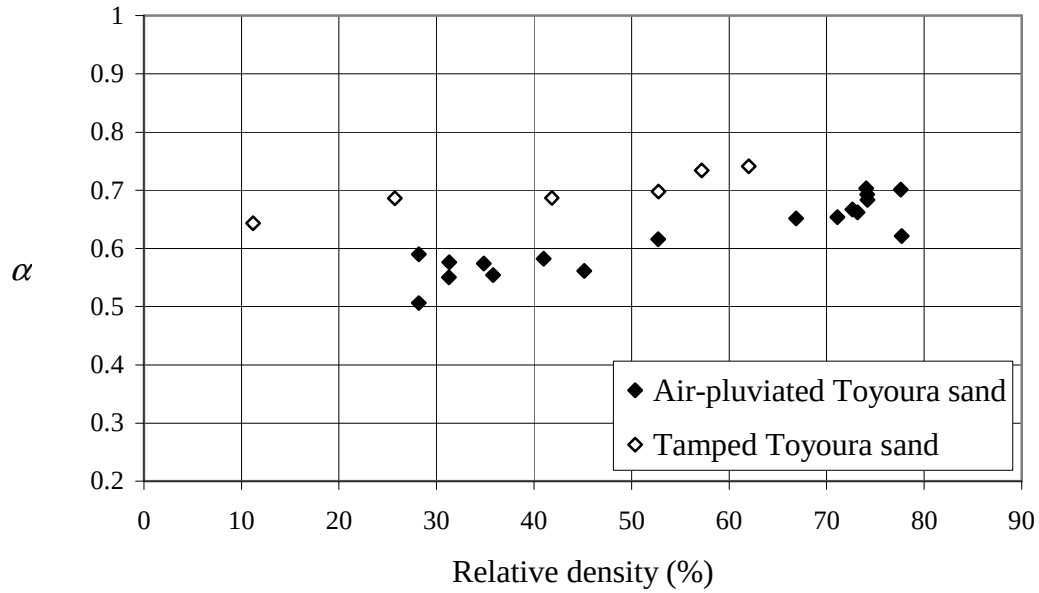

Figure 2.6. Relationship between α and initial relative density for different particle fabrics (modified from Okochi & Tatsuoka, 1984)

Using these results, Okochi and Tatsuoka (1984) assessed the Mayne and Kulhawy (1982) equation expressing α as a function of the effective friction angle (Eq. 2.4). Again, the test results indicated such a formulation was inaccurate because α varied with reconstituted particle fabric while the effective friction angle did not. Even so, it was the authors' opinion that the Mayne and Kulhawy (1982) equation provided a reasonable approximation (Okochi & Tatsuoka, 1984).

In a similar study, Wanatowski and Chu (2008) performed K_o-consolidation testing of reconstituted sand specimens in a plane-strain device. Changi sand, a uniform, clean and subangular sand, was selected as the test material. Specimens were reconstituted by two different methods, water pluviation and moist tamping (Wanatowski & Chu, 2008).

In agreement with Okochi and Tatsuoka (1984), Wanatowski and Chu (2008) found that K_o values from specimens prepared by moist tamping were usually lower than those from specimens reconstituted by pluviation. Additionally, it was observed that K_o values from specimens prepared by moist tamping varied with the initial relative density, with increasing K_o noted for decreasing density. For pluviated specimens, however, no strong relationship was noted between K_o and reconstituted relative density (Wanatowski & Chu, 2008).

A final study of note examines the effect of fabric and particle shape on K_o of granular materials using both experimental testing and theoretical micromechanical analysis (Guo & Stolle, 2006). In the laboratory, Guo and Stolle (2006) performed one-dimensional compression testing on different mixtures of glass beads of variable shape and surface textures. The beads were carefully placed in the testing apparatus, without any densification. To compliment their testing program, Guo and Stolle (2006) assessed a probabilistic theory originally proposed by Harr (1977). The theory describes the coefficient of lateral pressure at rest for a granular medium as a unique function of particle geometry and distribution of contact normals between particles (Harr, 1977).

Guo and Stolle (2006) concluded from their study that the coefficient of lateral pressure at rest of granular materials depends on particle shape and arrangement, in addition to the effective friction angle. Furthermore, the orientation of the particle fabric with reference

to the direction of one-dimensional compression is critical. However, no unique relationships between K_o and particle shape could be identified (Guo & Stolle, 2006).

When considering the effects of initial particle fabric on response behaviour, it is imperative to recognize the evolving nature of the fabric itself. Commonly, the inherent or initial fabric upon specimen reconstitution may be described by researchers. However, once testing and specimen deformation commences, the particle fabric begins to evolve in response. This concept is termed "fabric reconstruction" (Oda, 1972b). As testing progresses through loading and unloading phases, it may become increasingly difficult to discern the influence of particle fabric alone. Not only is the particle fabric continually changing, but also, compression-induced densification and developing stress history concurrently affect specimen response.

To better understand the mechanisms of fabric reconstruction, advanced constitutive models are currently being developed (Papadimitriou, Dafalias, & Yoshimine, 2005). However, to successfully create such modelling tools, the complexity of particle fabric must first be more thoroughly investigated in the laboratory. Therefore, extreme care must be taken when attempting to decouple and interpret the influences of both initial and evolving particle fabric in laboratory element testing.

3 EXPERIMENTAL ASPECTS: TEST APPARATUS AND PROCEDURE

Different testing devices have been used in one-dimensional compression testing, including the triaxial apparatus and instrumented oedometer. Outlined here are the general requirements for laboratory determination of the coefficient of lateral pressure at rest (Bishop, 1958):

- The testing device commissioned should compress the specimen in the vertical direction, while fully constraining it in the horizontal direction;
- The setup should provide accurate measurement of both the vertical and horizontal stresses experienced by the specimen;
- The boundaries imposing horizontal constraint should not inflict any vertical shear forces during compression testing; and
- For saturated testing, free-draining boundaries must be maintained to prevent excess pore pressures.

3.1 Test apparatus

The apparatus used in this study for one-dimensional compression of sand consists of three primary components: the instrumented oedometer, the compression frame and the data acquisition system.

3.1.1 Instrumented oedometer

Test specimens were reconstituted in a highly polished, rigid, stainless steel consolidation ring or oedometer (see Figure 3.1, Figure 3.2). The inner dimensions of the ring measure 76 mm in diameter and 38 mm in height. Circumscribing the steel ring is a series of strain gauges cased in protective plastic. The strain gauges are capable of detecting very small hoop strains produced upon radial loading of the practically rigid steel ring. The ring is seated on a steel base, equipped with a drainage port. The base is also inlaid with a small circular porous stone, measuring 45 mm in diameter and 6.5 mm in thickness.

The stiffness of the instrumented oedometer is approximately 2×10^{-5} % radial strain per 100 kPa lateral pressure.

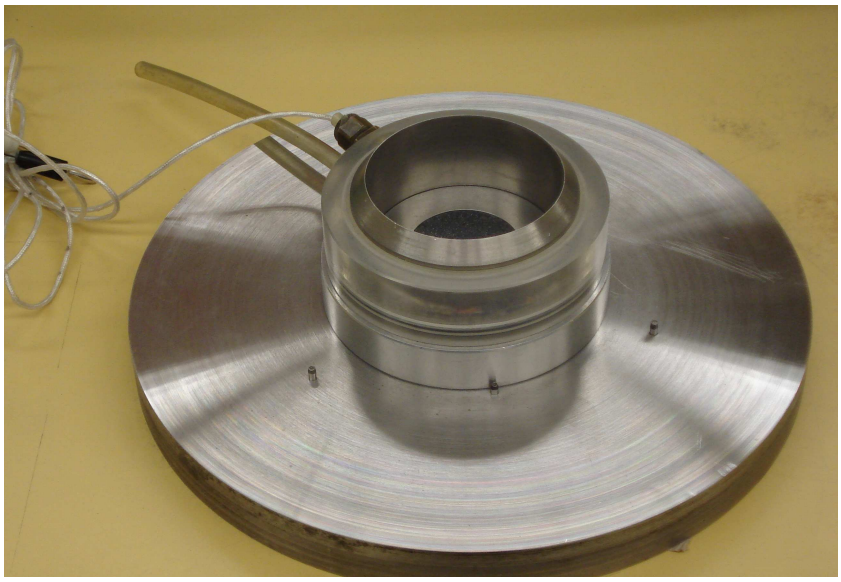

Figure 3.1. Photograph of instrumented oedometer

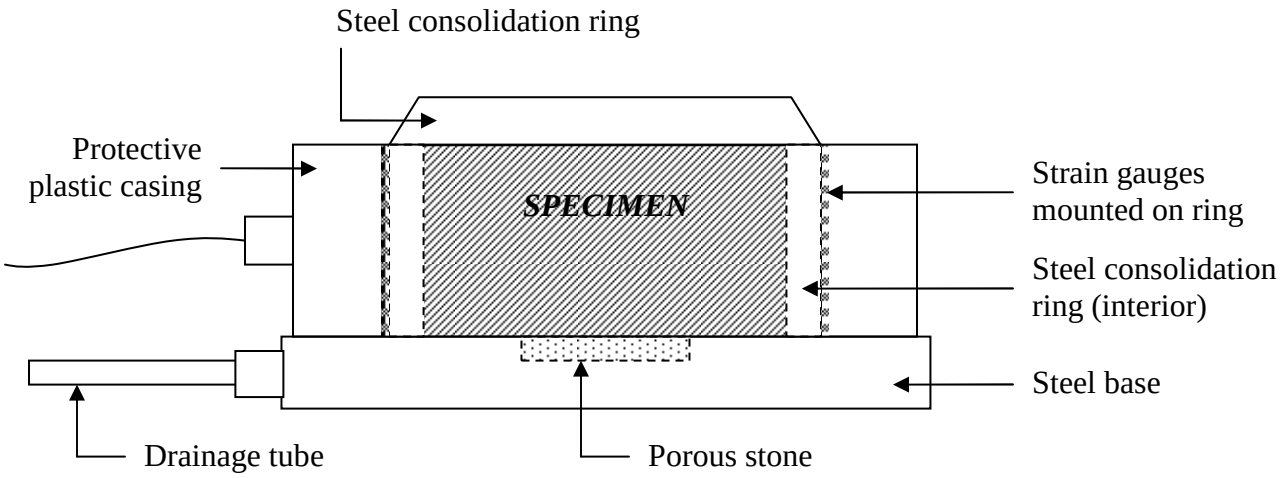

Figure 3.2. Schematic of instrumented oedometer

Calibration of the instrumented oedometer was achieved using a regulated compressed air supply with a maximum air pressure of about 700 kPa. The open ends of the steel ring

were capped with steel end platens to create an air-tight cavity. The resulting chamber was then pressurized with known pressures and the corresponding output voltages from the instrumented ring were used to calibrate the device. The precision of the instrumented oedometer is ±0.04 kPa.

3.1.2 Compression frame

A five ton Wykeham Farrance Eng. Ltd. compression machine was used to apply normal loads to the test specimens at a constant strain rate of 0.015 mm per minute (see Figure 3.3, Figure 3.4). The machine was fitted with a 400 kg-force capacity load cell to measure the applied axial force. The precision of the load cell is $\pm 3\times10^{-5}$ kN, which is equivalent to ±0.006 kPa normal pressure on the specimen. Also, a linear variable differential transformer (LVDT) was attached to the loading platform to measure the axial strain of the specimen. The precision of the LVDT is $\pm 8\times10^{-4}$ mm.

Figure 3.3. Photograph of compression frame

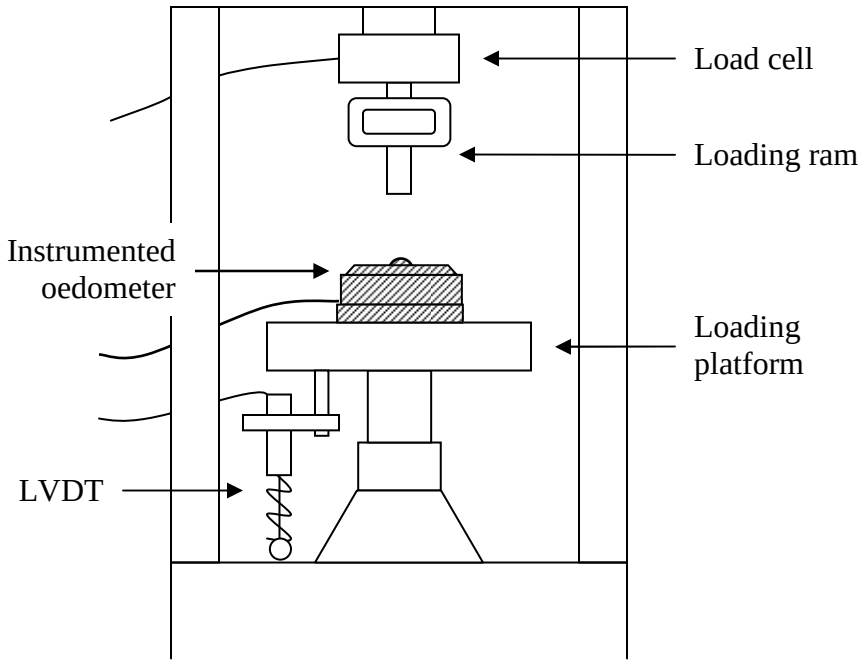

Figure 3.4. Schematic of compression frame

3.1.3 Data acquisition system

A computerized data acquisition system was used to receive and record voltage signals from the instrumented oedometer, load cell and LVDT. The system is comprised of a signal conditioning unit, a desktop computer and data acquisition software. The signal conditioning unit is custom-designed with a high resolution 4.5 digit analog to digital converter and a low-noise input amplifier. The DOS-based data acquisition software is also custom-designed and is capable of recording voltage readings from up to five signal channels. The program's frequency of data recording is set by the user.

3.2 Test procedure

At the beginning of each test, all electronic components were connected to the signal conditioning unit to establish zero voltage readings. Once thermal equilibrium was satisfied and zero readings were recorded, the instrumented oedometer was disconnected and transferred to the specimen preparation area.

Each test specimen was carefully reconstituted in the oedometer by air pluviation, tamping or vibration. For details on the techniques utilized for each of the reconstitution methods, see Chapter 4. After preparation, the top cap was gently placed on the surface of the specimen. The top cap is fixed with a porous stone and weighs about 220 grams, leading to a vertical stress of 0.5 kPa on the specimen. Extreme care was taken so that the specimen was not disturbed during placing of the top cap. The height of the specimen was then measured, with respect to a fixed reference height. The weight of the specimen was also measured, and the relative density was calculated.

Next, the specimen was transported to the compression frame and carefully placed on the loading platform. The specimen was aligned with the loading ram, and the loading platform was raised so that the ram was nearly in contact with the top cap. Then the oedometer was reconnected to the signal conditioning unit, and the system was permitted to reach thermal equilibrium.

Compression testing consisted of three distinct phases: virgin loading, unloading and reloading. During the virgin loading phase, the specimen was loaded to a vertical pressure of 250 kPa. During the unloading phase, the specimen was unloaded to 0 kPa. Finally, for the reloading phase, the specimen was reloaded to a vertical pressure of 400 kPa. All loading and unloading phases were performed at a constant strain rate of 0.015 mm per minute. Output voltages from the instrumented oedometer, load cell and LVDT were automatically recorded every fifteen seconds during testing.

3.3 Testing program

The testing program, as described herein, was designed to investigate the behaviour of sand in one-dimensional compression with respect to reconstituted specimen fabric. Also considered were the effects of initial relative density and loading history. Supplementary to the core testing program, a series of tests was performed at varied strain rates, to investigate if results would be significantly impacted from testing at other rates of strain. Similarly, a series of tests was performed upon saturated specimens, to determine if any significant impact would arise from saturated versus dry conditions.

3.3.1 One-dimensional compression of dry sand specimens

A total of sixty (60) one-dimensional compression tests were performed on dry, reconstituted Fraser River sand specimens (see Table 3.1, Table 3.2, Table 3.3). Of these sixty (60) tests, twenty-six (26) tests were performed on air-pluviated specimens, seventeen (17) tests were performed on tamped specimens, and seventeen (17) tests were performed on vibrated specimens. Tests were carried out on specimens prepared at four distinct levels of particle packing: very loose, medium loose, dense and very dense. The degree of particle packing roughly corresponds to relative densities of 0, 30, 60 and 85%, respectively.

Table 3.1. Testing program for air-pluviated specimens

Test ID	Degree of particle packing	Reconstituted relative density (%)
AP_L_201	Very loose	1
AP_L_202		2
AP_L_203		2
AP_L_204		1
AP_L_205		0
AP_L_206		1
AP_M_201	Medium loose	32
AP_M_202		30
AP_M_203		33
AP_M_204		32
AP_M_205		33
AP_M_206		32
AP_M_207		30
AP_D_201	Dense	57
AP_D_202		62
AP_D_203		60
AP_D_204		59
AP_D_205		58
AP_D_206		60
AP_D_207		61
AP_V_201	Very dense	88
AP_V_202		86
AP_V_203		85
AP_V_204		84
AP_V_205		88
AP_V_206		87

Table 3.2. Testing program for tamped specimens

Test ID	**Degree of particle packing**	**Reconstituted relative density (%)**
T_M_201	Medium loose	33
T_M_202		30
T_M_203		29
T_M_204		31
T_M_205		29
T_M_206		30
T_D_201	Dense	60
T_D_202		63
T_D_203		62
T_D_204		62
T_D_205		63
T_D_206		61
T_V_201	Very Dense	87
T_V_202		86
T_V_203		87
T_V_204		86
T_V_205		85

Table 3.3. Testing program for vibrated specimens

Test ID	**Degree of particle packing**	**Reconstituted relative density (%)**
V_M_201	Medium loose	26
V_M_202		24
V_M_203		28
V_M_204		34
V_M_205		26
V_M_206		26
V_D_201	Dense	62
V_D_202		62
V_D_203		64
V_D_204		63
V_D_205		64
V_D_206		58
V_V_201	Very Dense	86
V_V_202		84
V_V_203		86
V_V_204		85
V_V_205		84

3.3.2 One-dimensional compression at varied strain rates

Six (6) one-dimensional compression tests were carried out on dry, reconstituted Fraser River sand specimens at varied strain rates (see Table 3.4, Table 3.5). Two strain rates were selected that differed by an approximate factor of ten from the 0.015 mm per minute standard rate used for all other tests. A rate of 0.0018 mm per minute, or about ten times slower than the standard rate, and a rate of 0.15 mm per minute, or about ten times faster than the standard rate, were chosen. For a given strain rate, one (1) test was performed for each specimen reconstitution technique. All six (6) tests were performed on dense specimens, with a relative density of about 60%.

Table 3.4. Testing program for strain rate of 0.0018 mm per min.

Test ID	**Reconstitution method**	**Reconstituted relative density (%)**
AP_D_301	Air pluviation	60
T_D_301	Tamping	61
V_D_301	Vibration	65

Table 3.5. Testing program for strain rate of 0.15 mm per min.

Test ID	**Reconstitution method**	**Reconstituted relative density (%)**
AP_D_302	Air pluviation	60
T_D_302	Tamping	63
V_D_302	Vibration	62

3.3.3 One-dimensional compression of saturated sand specimens

Three (3) one-dimensional compression tests were completed on saturated, reconstituted Fraser River sand specimens (see Table 3.6). For each specimen reconstitution technique, one (1) test was performed. All three (3) tests were performed on dense specimens, with a relative density of approximately 60%. After reconstitution and subsequent saturation, these specimens were tested under a constant water head of 1 cm, to ensure saturated conditions over the entire test.

Table 3.6. Testing program for saturated specimens

Test ID	**Reconstitution method**	**Reconstituted relative density (%)**
AP_D_401	Air pluviation	57
T_D_401	Tamping	63
V_D_401	Vibration	62

4 EXPERIMENTAL ASPECTS: RECONSTITUTED SPECIMEN PREPARATION

4.1 Material tested

Testing was performed on dredged sand from the Fraser River, located immediately south of Vancouver, British Columbia, Canada. From gradation analyses, the Fraser River sand utilized in this study was found to be a medium-sized sand with less than 1% fines and an average particle size (D_{50}) of 0.28 mm (see Figure 4.1). The sand is uniformly-graded, with a coefficient of uniformity (C_u) of 1.80.

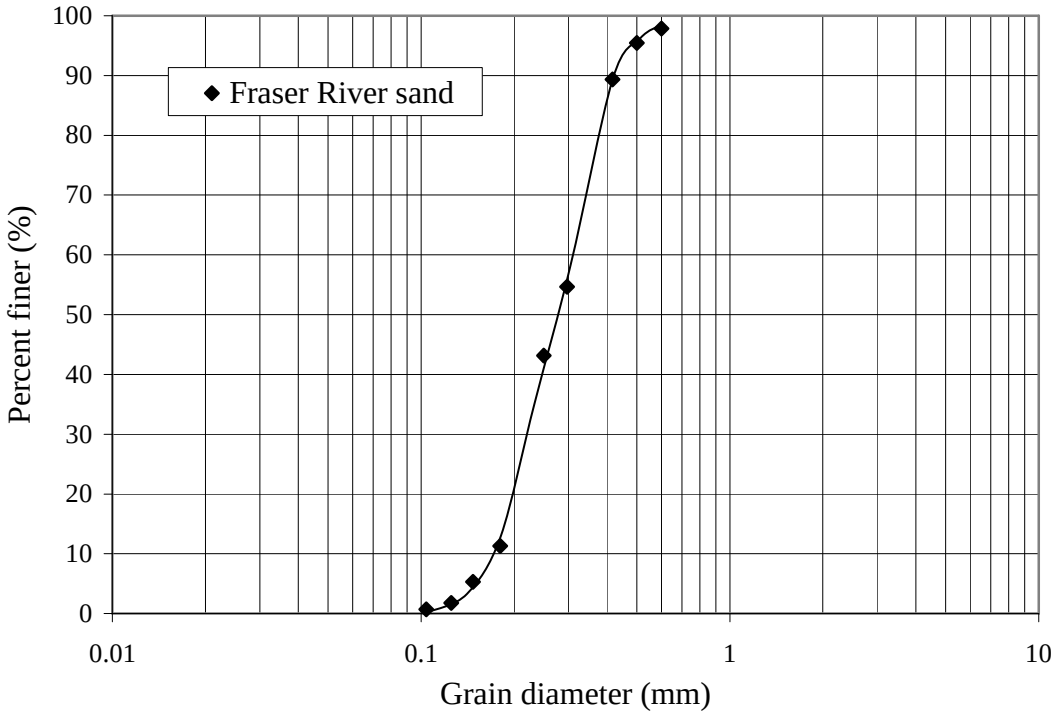

Figure 4.1. Particle size distribution of Fraser River sand

A specific gravity of 2.71 was measured for the sand and maximum and minimum void ratios (e_{max} and e_{min}) of 0.962 and 0.620, respectively, were assumed (Sivathayalan & Vaid, 2002).

Optical microscopic inspection of the sand showed angular to sub-rounded particles (see Figure 4.2). Fraser River sand has an average mineral composition of 40% quartz, 11% feldspar, 45% unaltered rock fragments, and 4% other minerals (Garrison, Luternauer, Grill, Macdonald, & Murray, 1969).

Figure 4.2. Optical microscope photograph of Fraser River sand

Fraser River sand was chosen for this study due to its local availability and its frequent use in fundamental laboratory research at the University of British Columbia over the past fifteen years (Wijewickreme, Sriskandakumar, & Byrne, 2005).

In preparation for this study, the dredged sand was carefully divided or "split" into approximately 150 individual samples for testing, each containing from 250 to 300 grams of sand. A splitter was used to ensure consistent gradations among the samples. Gradation analyses performed on select samples confirmed their consistency. All test specimens were reconstituted in an air-dried state.

4.2 Air pluviation reconstitution method

The most basic of the three methods of specimen reconstitution selected for this study is air pluviation. In general, air pluviation implies the pouring or raining of granular particles through the air into a specimen container (Kolbuszewski, 1948). A specific air pluviation technique was developed for use with dry Fraser River sand and the

instrumented oedometer. This technique was shown to produce high quality specimens that were sufficiently uniform and easily replicable.

4.2.1 Background

Air pluviation is a method which has been used extensively in laboratory specimen preparation and subsequently, is relatively well understood (Kolbuszewski, 1948; Rad & Tumay, 1987; Vaid & Negussey, 1988; Lo Presti, Pedroni, & Crippa, 1992; Cresswell, Barton, & Brown, 1999). Early investigations into the behaviour of air-pluviated sands have shown that the relative density in reconstituted specimens can be controlled through variations of the pluviation technique (Kolbuszewski, 1948). Specifically, particle drop height, with respect to the specimen container, and depositional intensity are the primary factors in controlling reconstituted specimen density (Vaid & Negussey, 1988).

Figure 4.3 shows the effects of drop height and deposition intensity for two gradations of Ottawa sand. With increasing drop height, the relative density of the specimen increases. With increasing depositional intensity or mass flow rate, the relative density of the specimen decreases.

Air pluviation of sand may be accomplished through a variety of deposition techniques, ranging from pouring deposition in a concentrated stream to true pluviation or raining deposition through a series of diffuser meshes. (Rad & Tumay, 1987); (Cresswell et al., 1999). Figure 4.4 illustrates the general depositional behaviour for both pouring and raining techniques.

Cresswell et al. (1999) prepared a series of air-pluviated specimens to explore the effects of pouring versus raining deposition. Pouring deposition yielded specimens with notably lower densities than raining deposition, for the majority of depositional intensities tested. However, at very low deposition intensity, specimens prepared by pouring and raining were of comparable density (see Figure 4.5). Furthermore, Cresswell et al. (1999) observed that pouring deposition had a tendency to create a “cone of particles,” leading to specimen non-uniformities. This effect was especially evident at small drop heights.

(a)

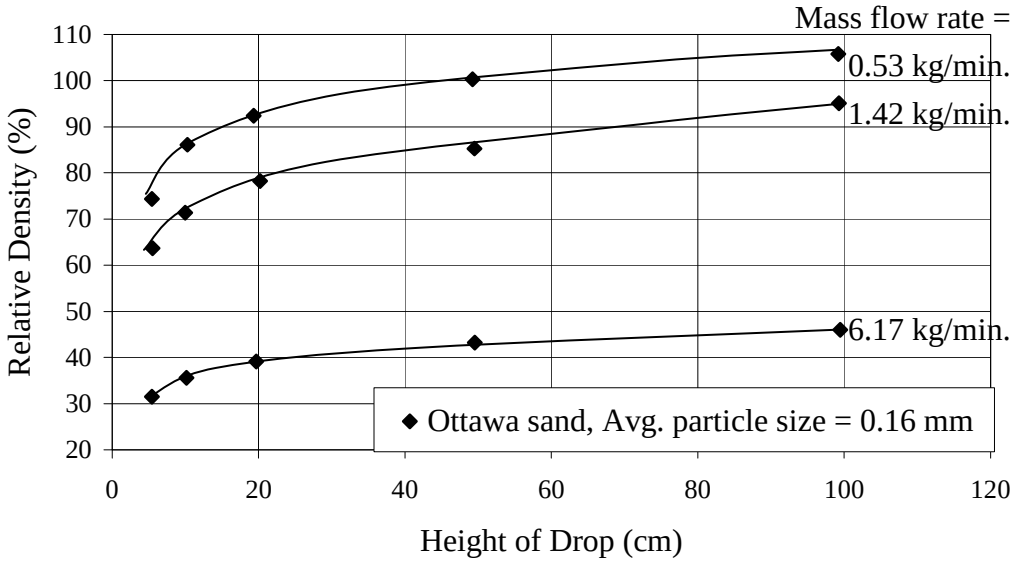

(b)

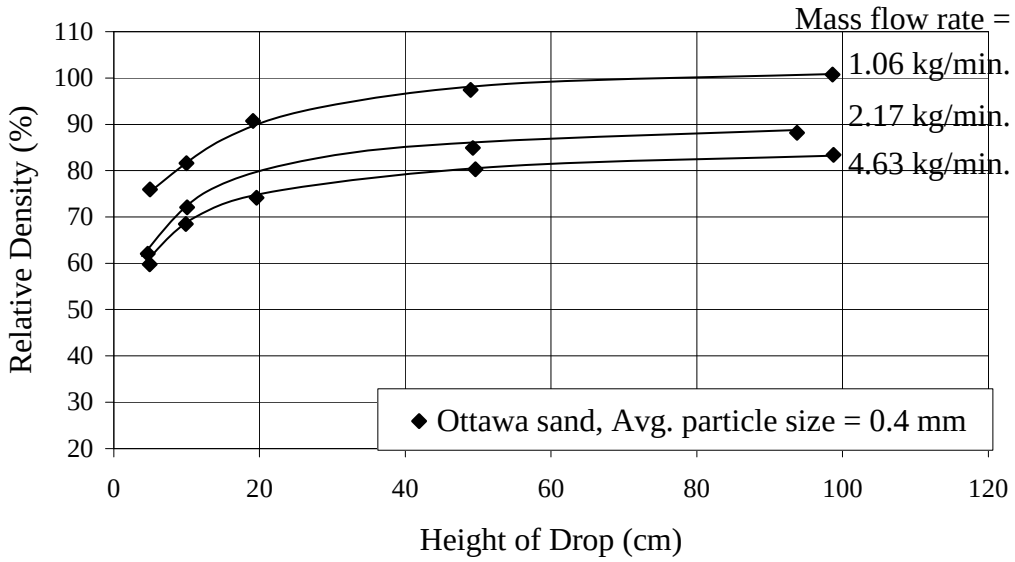

Figure 4.3. Effect of height of drop and mass flow rate on relative density of (a) Ottawa sand, D_{50} = 0.16 mm and (b) Ottawa sand, D_{50} = 0.4 mm (modified from Vaid & Negussey, 1988)

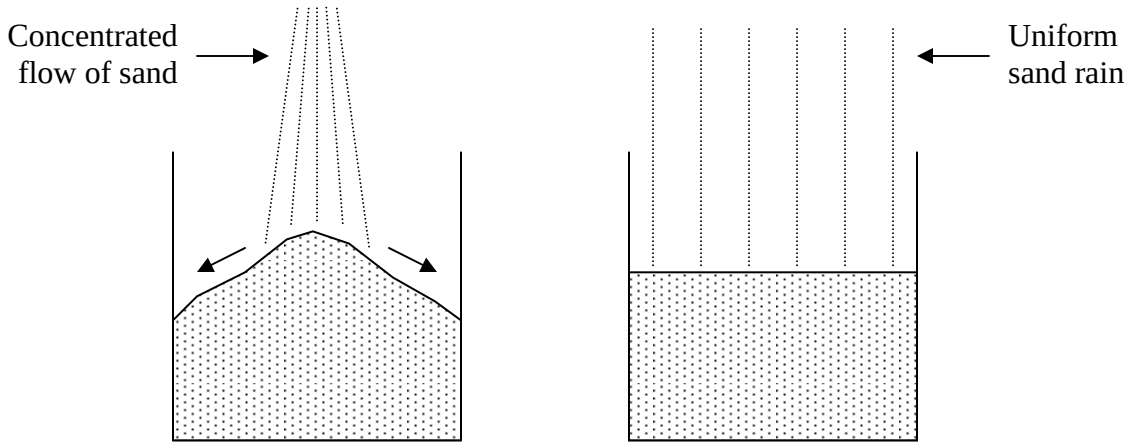

Figure 4.4. Schematic of air-pluviated sand deposition: pouring (left) vs. raining (right) (reproduced from Cresswell et al., 1999)

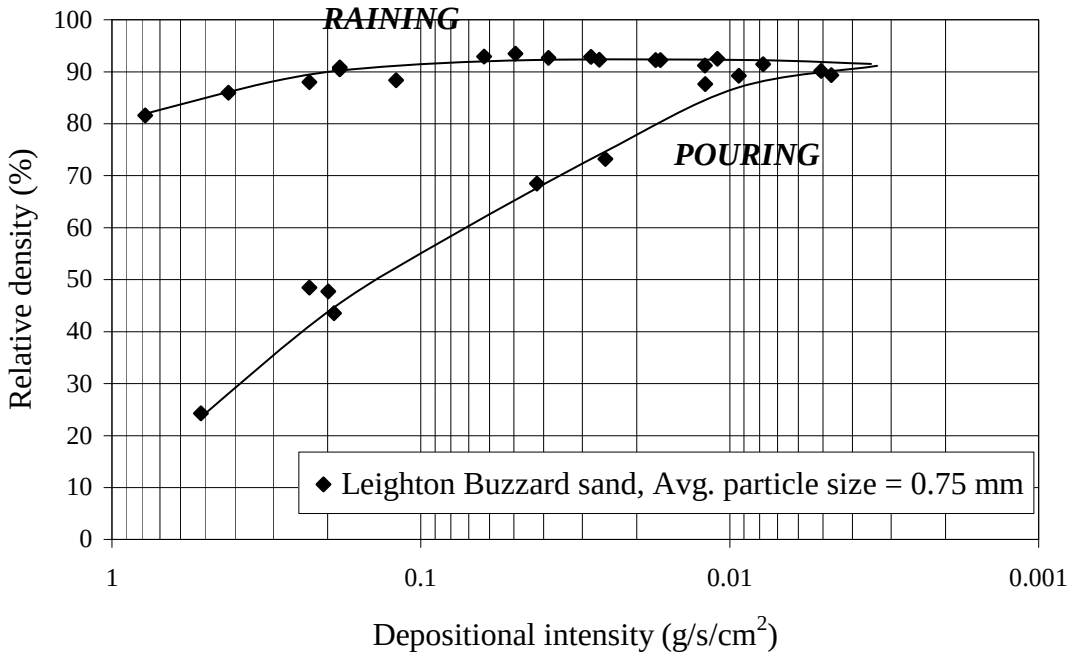

Figure 4.5. Effect of deposition technique and intensity on relative density of Leighton Buzzard sand, D_{50} = 0.75 mm (modified from Cresswell et al., 1999)

4.2.2 Technique development

For the purpose of this study, the air pluviation technique or techniques developed should:

- Generate four distinct degrees of packing density, from very loose to very dense,
- Produce homogeneous specimens with consistent density over specimen height,
- Avoid irregular particle deposition and coning effects,
- Be suitable for use with designated test material and apparatus, and
- Be simple and replicable.

First, a technique for very loose, air-pluviated specimens was developed. A small funnel with a 7-mm spout opening was used to deposit a concentrated flow of sand directly into the specimen container (see Figure 4.6). Specimens were reconstituted in two separate lifts, each approximately 12 mm thick. After each lift was deposited by funnel, a siphon connected to a vacuum was used to level the specimen surface (see Figure 4.7). The siphon was passed over the specimen surface at a fixed height with a vacuum force of about 33 kPa, until no more particles could be removed and the specimen surface was level.

Figure 4.6. Photograph of funnel deposition

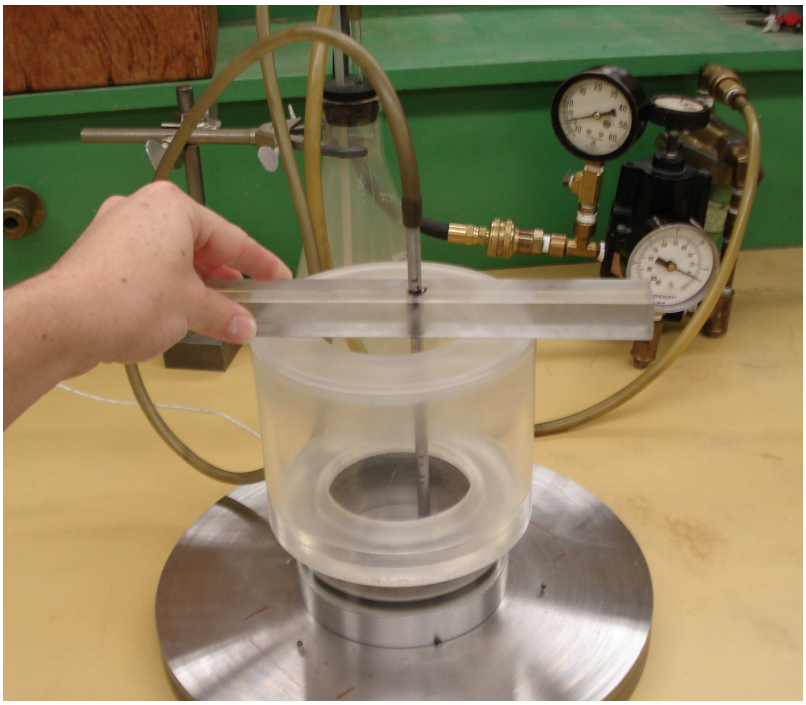

Figure 4.7. Photograph of siphon and vacuum setup

To produce very loose specimens of about 0% relative density, the funnel was positioned at a drop height of near zero. As the level of sand in the container was elevated, the funnel was also raised to maintain a consistent drop height.

It should be noted that deposition by funnel at near zero drop height closely mimics pouring behaviour and may be prone to particle coning. To produce an effect similar to raining, either the drop height must be raised or diffuser meshes must be introduced. However, both of these alterations result in an undesirable increase in relative density. Instead, an effort was made to maintain regular deposition by traversing the funnel in a circular motion over the container during pluviation. Additionally, reconstituting specimens in two levelled lifts aided in preventing particle cones from developing.

For specimens with a medium loose relative density of about 30%, the air pluviation technique was modified slightly. As discussed in Chapter 4.2.1, the relative density of air-pluviated sand specimens can be controlled by adjusting the drop height and/or deposition intensity. For medium loose specimens, the drop height from the funnel to the specimen container was raised to about 22 cm. To keep the funnel level during

deposition, a pluviation crossbar and cylinder were introduced to the setup (see Figure 4.8). As shown in Figure 4.8, the deposition funnel may be fitted into the center of the crossbar, which is then laid across the top of the pluviation cylinder. The crossbar and funnel can then easily traverse the specimen container while maintaining a constant drop height.

Figure 4.8. Photograph of funnel deposition with pluviation crossbar and cylinder

As before, specimens were reconstituted in two levelled lifts. In contrast to very loose preparation, the height of the funnel was not raised with respect to specimen height during deposition. The drop height was judged high enough such that no noticeable effect on deposition density would result. This judgment was later proven reasonable by specimen dissections, as noted in Chapter 4.2.3.

For dense and very dense specimens, with respective target relative densities of about 60% and 85%, the air pluviation technique used for medium loose specimens was further modified. In addition to an elevated drop height of approximately 22 cm, the funnel spout was constricted to lower depositional intensity. A small plastic collar was fixed

beneath the funnel spout, effectively narrowing the spout opening. For dense specimen preparation, the spout opening was restricted to 3.6 mm. For very dense specimen preparation, the spout opening was restricted to 2.0 mm.

Both dense and very dense specimens were reconstituted in two levelled lifts. The pluviation crossbar and cylinder were used to maintain constant drop height as the funnel was traversed over the specimen container.

4.2.3 Specimen quality

As the aim of this study is to observe the effects of particle fabric, it is imperative that reconstituted specimens be of homogeneous fabric. To verify the uniformity of reconstituted specimens, dissections were performed for all reconstitution methods and degrees of particle packing. The method employed for specimen dissection was modeled about that presented by Sriskandakumar (2004).

First, an air-pluviated specimen was prepared as described in Chapter 4.2.2 for the desired degree of particle packing. After reconstitution, the top cap was gently placed on the specimen surface and height and weight measurements were taken. To perform the dissection, the top cap was subsequently removed and the siphon and vacuum setup was used to carefully remove a layer of sand about 12 mm thick from the top of the specimen. This equates to approximately half of the original specimen thickness. Once more, the specimen height and weight were recorded. The dissection process allows the relative density to be calculated separately for the top and bottom lifts of the reconstituted specimen.

Figure 4.9, Figure 4.10 and Figure 4.11 show the results from dissections of very loose, medium loose and dense air-pluviated specimens, respectively. For all three dissections, specimen lifts exhibited about ±1% deviation from the average specimen relative density. Sriskandakumar (2004) also performed dissections on medium loose, air-pluviated Fraser River sand specimens. Deviations from the average relative density reported are ±5%, indicating a comparatively high degree of uniformity in air-pluviated specimens prepared for the present study (Sriskandakumar, 2004).

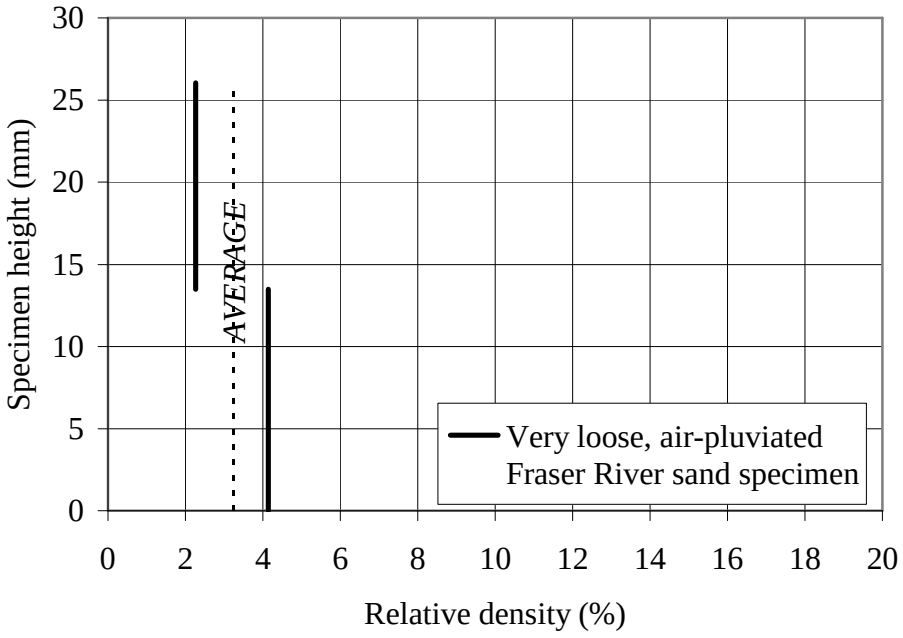

Figure 4.9. Dissection of very loose, air-pluviated Fraser River sand specimen

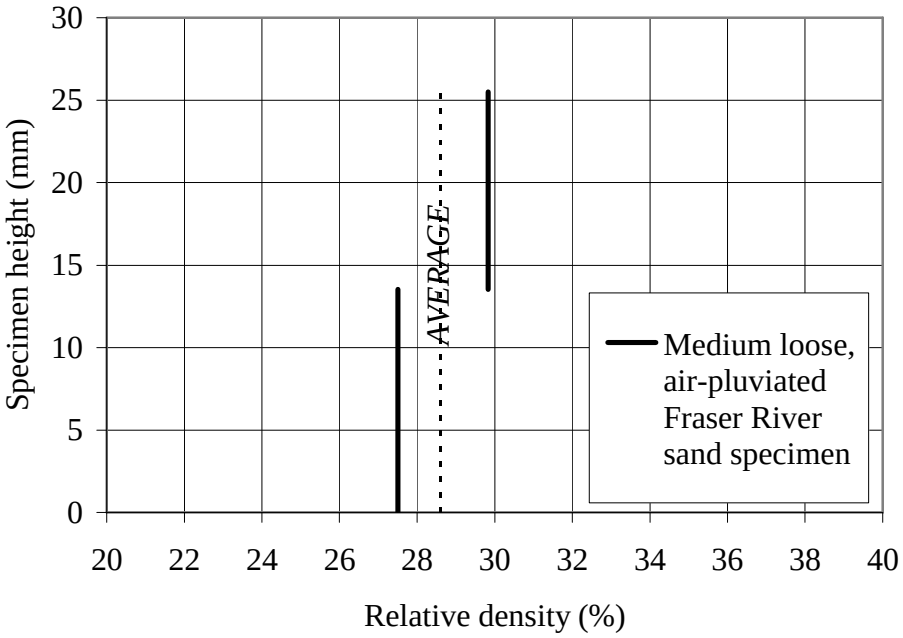

Figure 4.10. Dissection of medium loose, air-pluviated Fraser River sand specimen

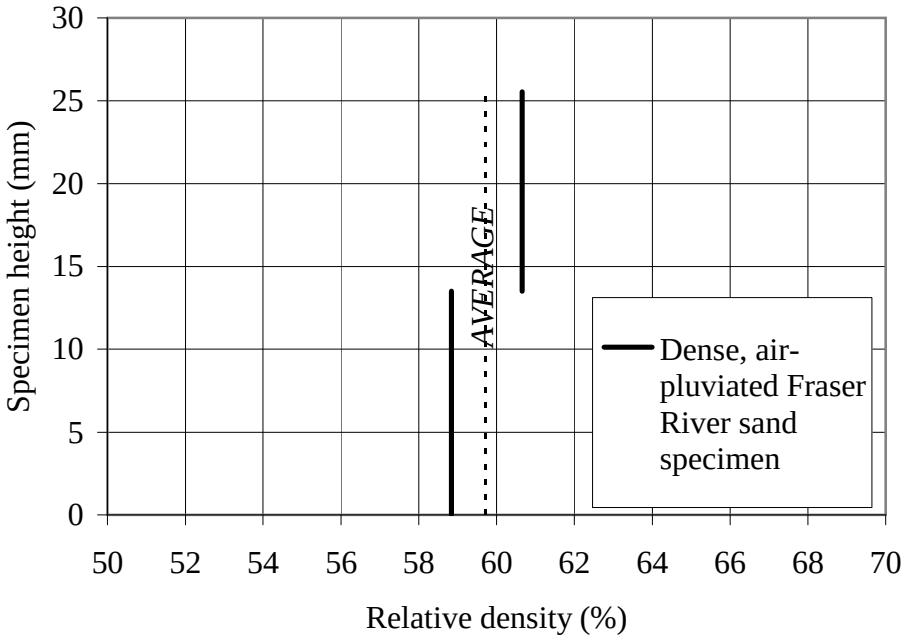

Figure 4.11. Dissection of dense, air-pluviated Fraser River sand specimen

Figure 4.12 shows the results from a dissection of a very dense, air-pluviated specimen. Very dense, air-pluviated specimens showed a much higher degree of non-uniformity than the other air-pluviated specimens. Very dense specimen lifts exhibited a maximum of ±7% deviation from the average relative density, in contrast to the ±1% deviation observed in very loose, medium loose and dense air-pluviated specimens. Still, this disparity is not too far from the deviations reported by Sriskandakumar (2004) for medium loose, air-pluviated Fraser River sand. Moreover, this level of deviation can be considered acceptable, considering the limitations on measurement accuracy for this size of specimen (Sriskandakumar, 2004).

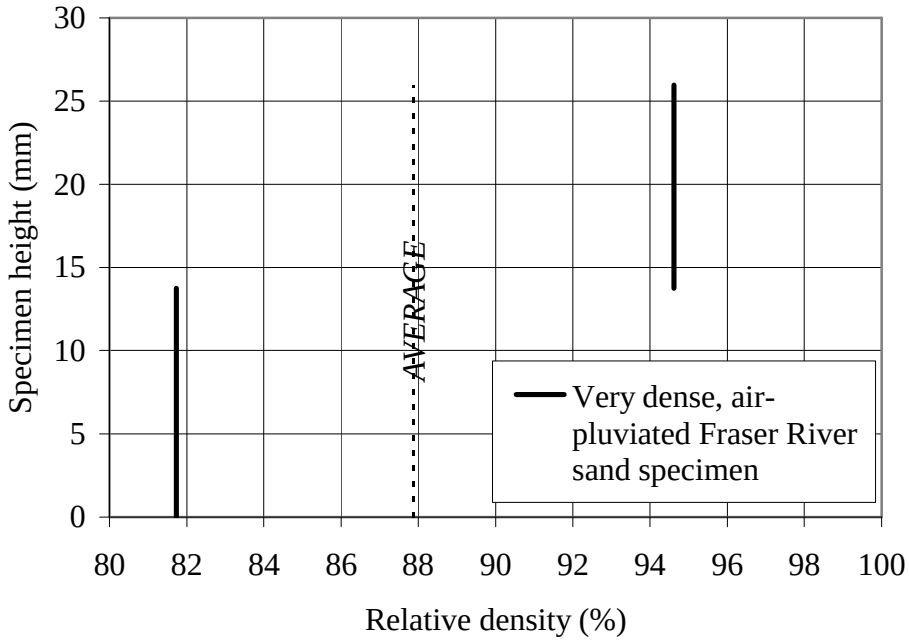

Figure 4.12. Dissection of very dense, air-pluviated Fraser River sand specimen

4.3 Tamping reconstitution method

The second method of specimen reconstitution selected for this study is tamping. Tamping is a form of specimen compaction, characterized by repetitive blows of a dead weight compaction foot to a lift of soil (Ladd, 1974). For the purpose of this study, a tamping technique was specifically tailored for use with dry Fraser River sand and the instrumented oedometer. This technique was shown to produce high quality specimens that were sufficiently uniform and easily replicable.

4.3.1 Background

Variations of the tamping method are often employed for laboratory testing of reconstituted sands, most commonly in a moist state (Ladd, 1974); (Mulilis et al., 1977); (Ladd, 1978); (Vaid & Sivathayalan, 2000); (Frost & Park, 2003). Although specific techniques may differ, a common thread in nearly all tamping studies is difficulty in achieving homogeneous specimens.

In an effort to address this concern, Ladd (1978) developed a moist tamping technique known as "undercompaction." When tamping force is applied to a lift of soil, the compactive effort will not only densify the current lift, but also, lower layers will experience increased densification. Undercompaction requires that when reconstituting specimens, lower lifts be compacted to a decreased percentage of the desired relative density. As successive lifts are prepared, the tamping force will further densify the lower layers to the desired relative density (Ladd, 1978). The concept of the undercompaction tamping technique is illustrated in Figure 4.13.

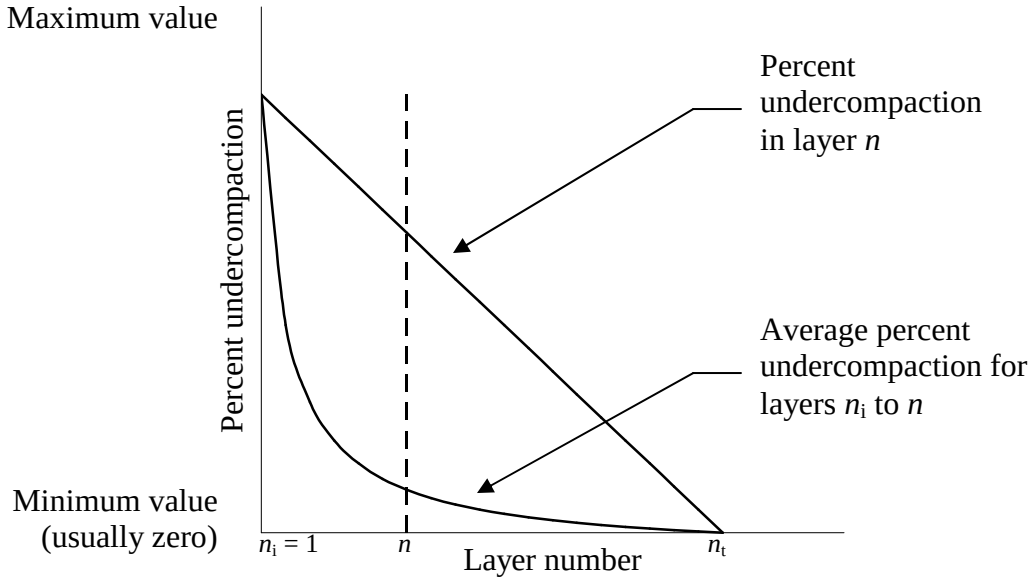

Figure 4.13. Illustration of undercompaction tamping technique (reproduced from Ladd, 1978)

More recently, Frost and Park (2003) conducted a study to critically assess the mechanism of tamping in specimen preparation. To measure the forces imparted to the specimen during reconstitution, the tamping device was equipped with a load cell. After reconstitution, X-ray and optical imaging were utilized to evaluate specimen uniformity. Specimens were prepared using Ladd's undercompaction tamping technique (Frost & Park, 2003).

As expected, Frost and Park (2003) observed that overall, greater tamping force was required to compact layers to greater relative densities. However, they also noted that the bottom layer in the tamped specimens, which was compacted to the lowest relative density, was not the layer that required the least compaction force. The authors point to the influence of the rigid specimen container influenced the compaction behaviour of the bottom layer (Frost & Park, 2003). This observation suggests that adaptation of the original undercompaction technique may be warranted.

From image analyses, variances of up to 10% in relative density were detected between tamped layers. Moreover, variations of up to 15% in relative density were measured within individual reconstituted layers. This evidence indicates that tamped specimens are inherently non-uniform in their fabric, in comparison to specimens prepared by pluviation methods (Frost & Park, 2003).

4.3.2 Technique development

For the purpose of this study, the tamping technique or techniques developed should:

- Generate three distinct degrees of packing density, from medium loose to very dense,
- Produce homogeneous specimens with consistent density over specimen height,
- Be suitable for use with designated test material and apparatus, and
- Be simple and replicable.

Tamped specimens were reconstituted in two distinct stages: initial deposition and compactive tamping. For all specimens prepared with tamping, dry lifts of soil were initially deposited using the technique developed for very loose, air-pluviated specimens. Each 12-mm lift was deposited at zero drop height by a small funnel with a 7-mm spout opening (see Figure 4.6). After each lift was deposited by funnel, a siphon connected to a vacuum was used to level the specimen surface (see Figure 4.7). Once a lift was initially deposited, a tamping technique was applied to achieve the desired degree of particle packing.

A custom tamping apparatus was devised for use with the specimen container (see Figure 4.14, Figure 4.15, Figure 4.16). The apparatus consists of a compactive foot, with a diameter equal to that of the specimen, connected to a tamping rod. The rod is inserted into the tamping frame, where it is permitted to slide freely in the vertical direction but restricted from horizontal movement. The frame serves to accurately guide the tamping rod and compactive foot in a strictly vertical path centered over the instrumented oedometer. To impart a tamping blow, the rod is simply raised to a desired height and then released under gravity. The combination of the rod and foot weighs about 415 grams.

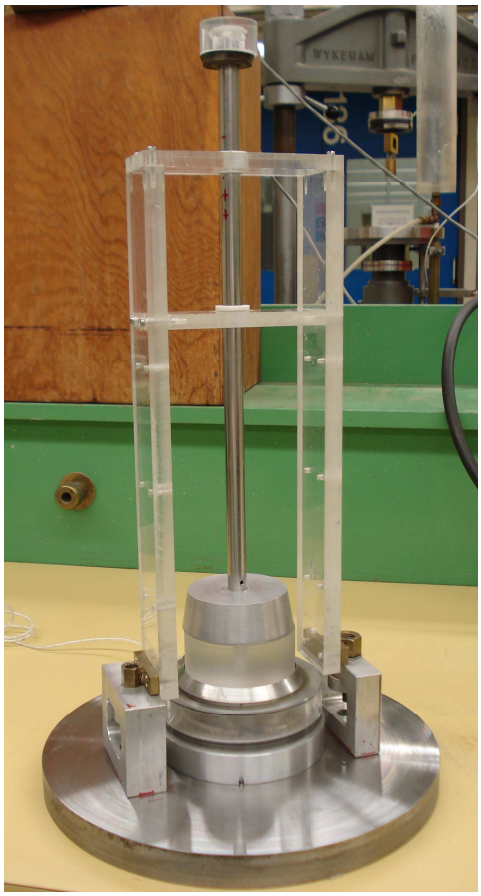

Figure 4.14. Photograph of tamping apparatus

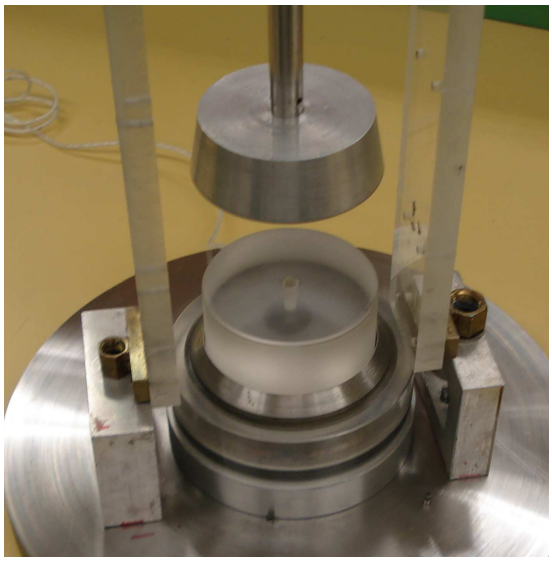

Figure 4.15. Photograph of tamping apparatus (close-up)

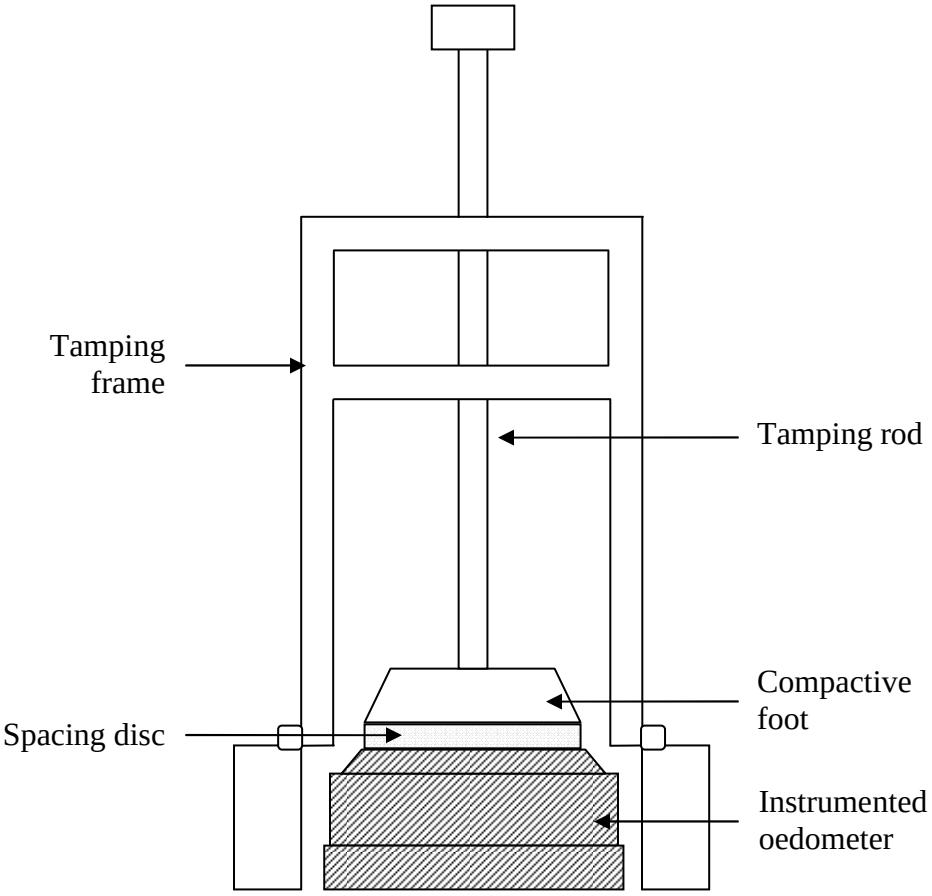

Figure 4.16. Schematic of tamping apparatus

Used in conjunction with the tamping apparatus is a plastic spacing disc which is placed on top of the specimen during the tamping stage. The disc prevents particle scatter upon impact or superficial particle damage. Also, the disc ensures that the surface of the specimen remains levels during the tamping stages and that the foot makes full contact with the specimen cross-section. The disc is practically rigid and fairly light, imposing less than 0.5 kPa on the specimen.

Two aspects were considered when developing the tamping technique for specimen reconstitution. First, the appropriate compactive force should be applied to the specimen as a whole to achieve the desired degree of particle packing. The compactive force from the tamping apparatus is controlled by the number of tamping blows applied to the specimen and the drop height of the compactive foot. Second, the concept of undercompaction should be acknowledged so that the relative density is reasonably uniform over the height of the specimen.

A tamping technique for specimens of a medium loose density near 30% was developed. As aforementioned, each lift was initially deposited by funnel and levelled before tamping was applied. Each lift was also re-levelled with the siphon and vacuum after the prescribed tamping was completed. For medium loose, tamped specimens, the drop height from the base of the compaction foot to the top surface of the spacing disc was chosen to be 25 mm. At this height, only two blows for each layer were required to reach the desired relative density. With such small amount of compactive force used, undercompaction of the bottom lift was not a concern.

For dense, tamped specimens of about 60% relative density, a similar tamping technique was used. As before, each lift was initially deposited by funnel and levelled before tamping was applied. Each lift was also re-levelled after the prescribed tamping was completed. For dense, tamped specimens, the drop height used was also 25 mm. It was determined that about 20% undercompaction of the bottom layer would result in the most uniform reconstituted specimen. Therefore, the bottom layer required eight tamping blows and the top layer received nine blows.

The tamping technique was modified only slightly for the preparation of very dense specimens at about 85% relative density. Like both medium loose and dense specimens, each lift was initially deposited by funnel and levelled before tamping was applied. Each lift was also re-levelled after the prescribed tamping was completed. For very dense, tamped specimens, the drop height was raised to 35 mm. At this height, 20% undercompaction of the bottom layer was again deemed appropriate. To achieve the desired degree of particle packing, 38 blows were applied to the bottom lift and 45 blows were applied to the top lift.

No very loose specimens were prepared by tamping, given the compactive nature of the method.

4.3.3 Specimen quality

Dissections were performed on medium loose, dense and very dense tamped specimens to confirm fabric uniformity. The details of the dissection method are fully described in Chapter 4.2.3.

Figure 4.17, Figure 4.18 and Figure 4.19 show the results from dissections of medium loose, dense and very dense tamped specimens, respectively. For all three dissections, specimen lifts exhibited a maximum of ±2% deviation from the average specimen relative density. In another study using Fraser River sand, Vaid and Sivathayalan (2000) also prepared tamped specimens and performed dissections to evaluate uniformity. In contrast to the results presented here, a 10% variation from the average relative density was experienced in tamped specimens (Vaid & Sivathayalan, 2000).

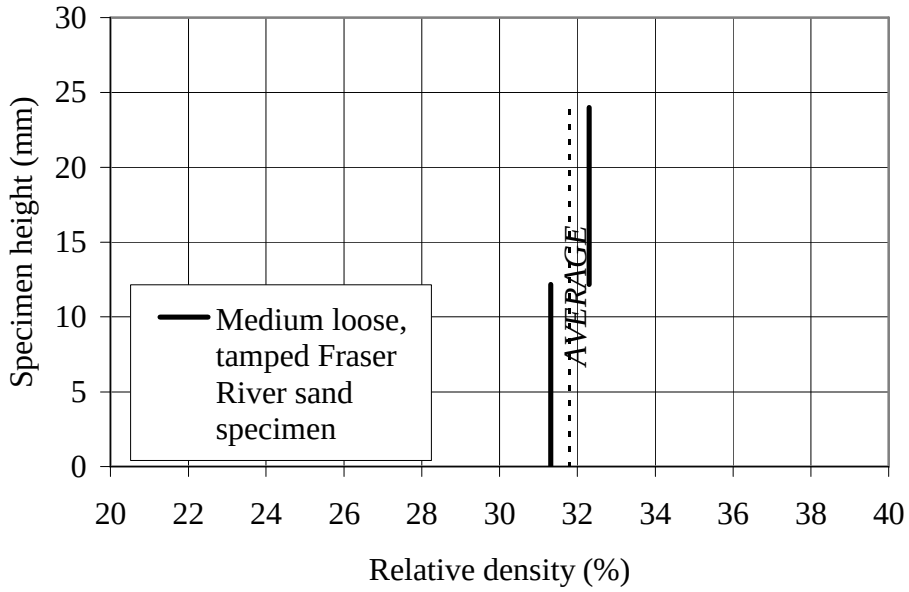

Figure 4.17. Dissection of medium loose, tamped Fraser River sand specimen

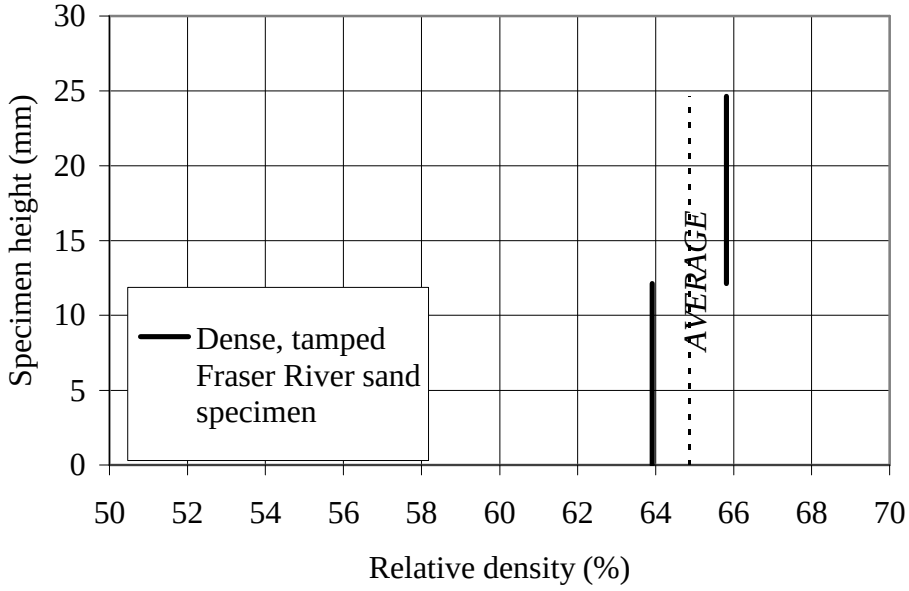

Figure 4.18. Dissection of dense, tamped Fraser River sand specimen

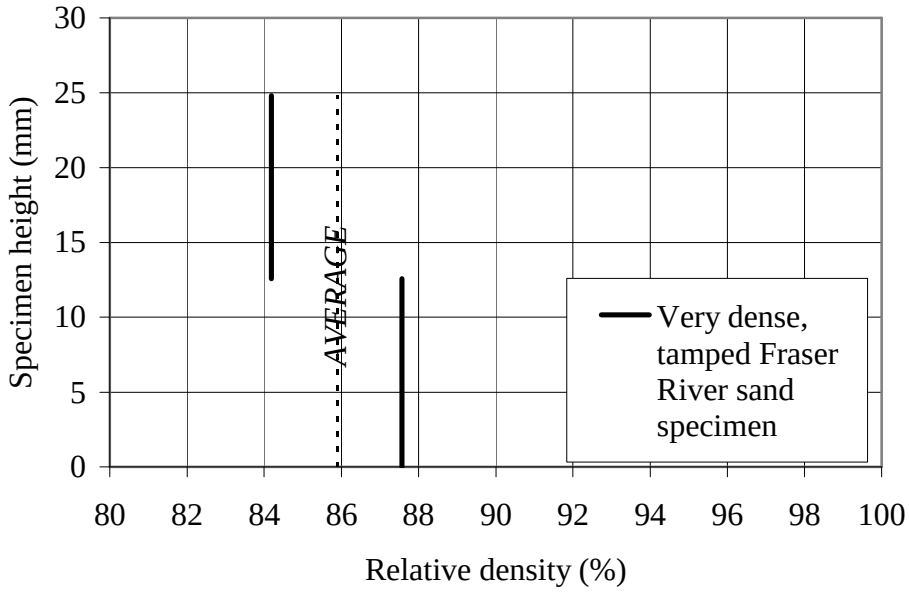

Figure 4.19. Dissection of very dense, tamped Fraser River sand specimen

As many authors have reported difficulties in achieving homogeneous specimens with tamping, the tamping technique developed for this study yielded surprisingly uniform specimens. It is unknown why such difficulties were not experienced here. Possible influences may be the size of the specimen container, thickness of the lifts and dry condition of the sand.

4.4 Vibration reconstitution method

The third and final method of specimen reconstitution selected for this study is vibration. Vibration is a form of specimen compaction where oscillating frequencies are transmitted to a specimen via a vibrating table, modified tamping device or other vibrating instrument. Vibration behaviour can be controlled by an electromagnetic or pneumatic vibrating mechanism and is described by its unique frequency and amplitude (Pettibone & Hardin, 1965). A specific vibration reconstitution technique was developed for use with dry Fraser River sand and the instrumented oedometer. This technique was shown to produce high quality specimens that were sufficiently uniform and easily replicable.

4.4.1 Background

Although vibration is a frequently used method for reconstituted specimen preparation, a consistent approach of laboratory vibration compaction has not yet been generally accepted (Selig, 1963; Pettibone & Hardin, 1965; Brand, 1973; Dobry & Whitman, 1973; Mulilis et al., 1977). Mechanisms used in research to apply vibrations include electromagnetic and pneumatic one-degree-of-freedom vibrating tables; electric "engraver-type" vibrators and hand-held pneumatic vibrators applied to the exterior of the specimen container; and electromagnetic and pneumatic hammer-type vibrators applied directly to the specimen surface, often through a modified tamping device. As well, the vibration behaviour itself has varied widely in its frequency and amplitude for the studies listed. Other significant experimental variables noted include the duration of vibrations, the orientation of applied vibrations, the surcharge, if any, used during vibrations and the attributes of the specimen container.

To better understand the factors controlling vibration behaviour in reconstituted specimens, Selig (1963) conducted a study on vibrated, dry sand specimens. A vibrating apparatus where the specimen container was suspended on springs and the entire setup was vibrated in a vertical fashion. For a given frequency and amplitude, considerable densification was reported immediately after vibrations began, and practically no further compaction was observed after a few minutes. Moreover, for double-amplitudes less than 1.0 mm, the density of a specimen was shown to increase when either the frequency or amplitude of vibration was increased (see Figure 4.20) (Selig, 1963).

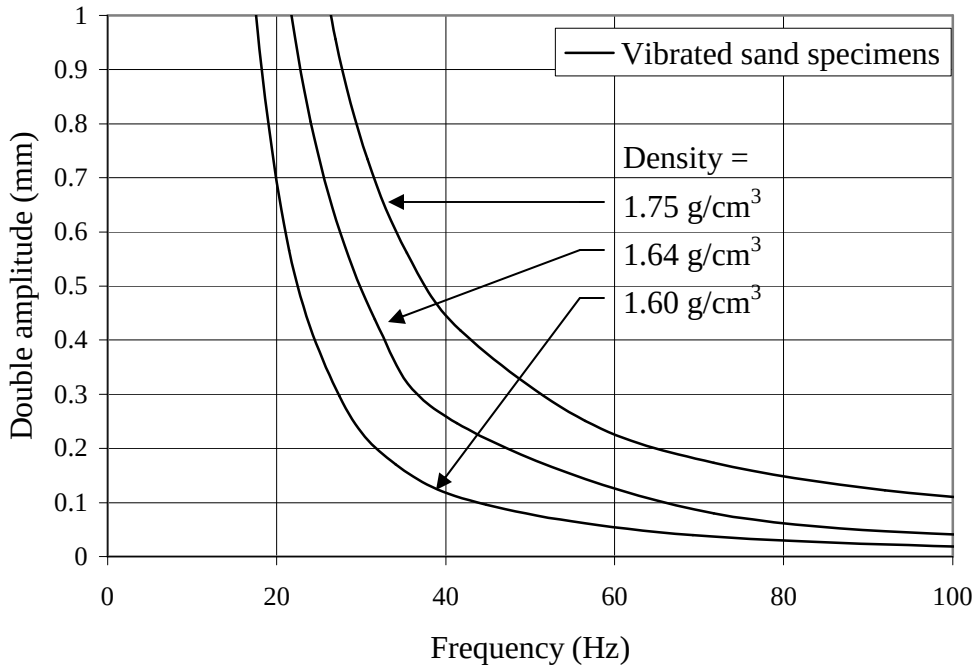

Figure 4.20. Effect of frequency and amplitude on density of vibrated sand specimens (modified from Selig, 1963)

Brand (1973) also investigated the factors controlling vibration behaviour, with a focus on reconstituted specimen uniformity. Variations in relative density from the specimen average ranged from around 5% to near 20%. The degree of variability of relative density within the specimens was found to be largely influenced by the frequency and amplitude of vibrations (see Figure 4.21) (Brand, 1973).

(a)

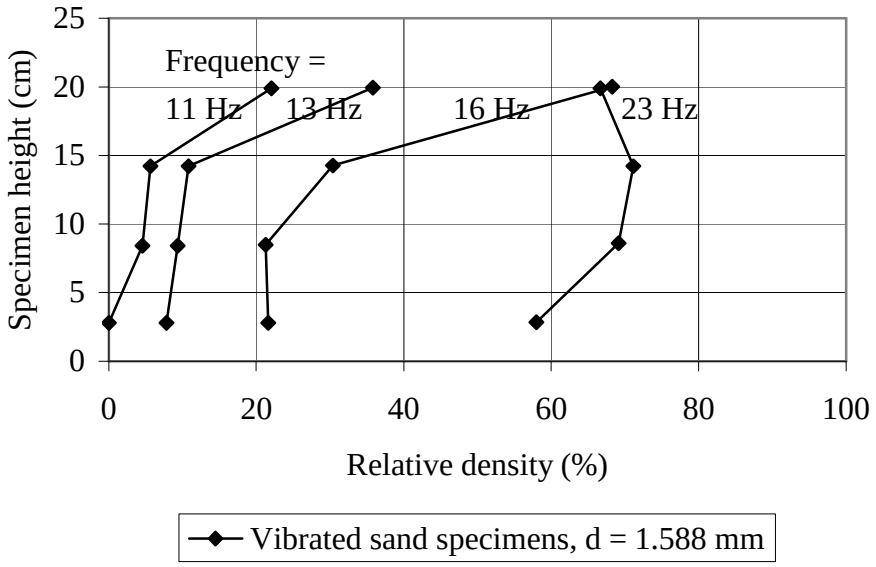

(b)

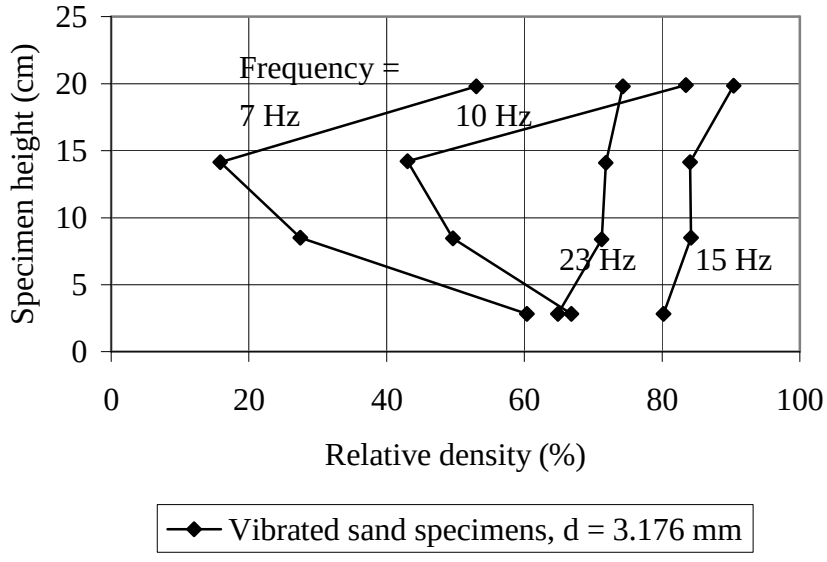

Figure 4.21. Dissections of sand specimens vibrated at various frequencies, where double-amplitude of vibration is (a) 1.588 mm and (b) 3.176 mm (modified from Brand, 1973)

4.4.2 Technique development

For the purpose of this study, the vibration technique or techniques developed should:

- Generate three distinct degrees of packing density, from medium loose to very dense,
- Produce homogeneous specimens with consistent density over specimen height,
- Be suitable for use with designated test material and apparatus, and
- Be simple and replicable.

Vibrated specimens were reconstituted in two distinct stages: initial deposition and compactive vibration. For all specimens prepared with vibration, dry lifts of soil were initially deposited using the technique developed for very loose, air-pluviated specimens. Each 12-mm lift was deposited at zero drop height by a small funnel with a 7-mm spout opening (see Figure 4.6). After each lift was deposited by funnel, a siphon connected to a vacuum was used to level the specimen surface (see Figure 4.7).

A vibrating table was chosen for use in this study. The apparatus available was the Soiltest CN-166 vibrating table, equipped with a cushioned steel vibrating deck and an electromagnetic vibrator (Soiltest, 1990). The table operates at a frequency of 60 Hz and has a double-amplitude range of 0.05 to 0.38 mm. Because the table was designed for use with a much larger specimen mould, the vibrating deck was modified for use with the instrumented oedometer. A specimen preparation platform was mounted to the table and steel guides posts and a fitted collar were used to secure the oedometer in place (see Figure 4.22, Figure 4.23, Figure 4.24).

Figure 4.22. Photograph of vibration apparatus

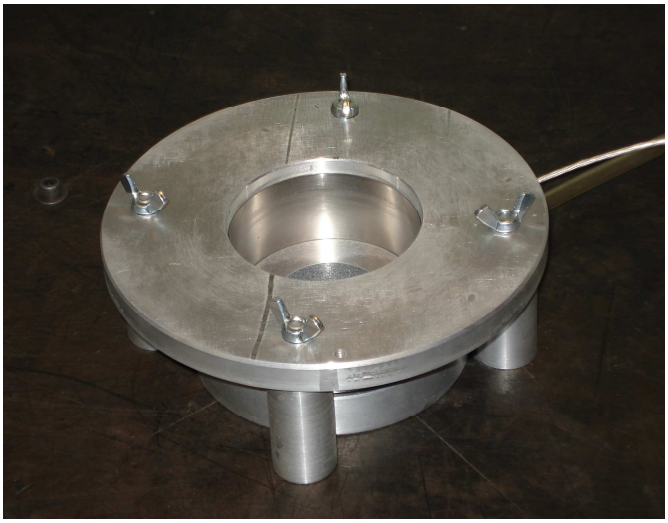

Figure 4.23. Photograph of vibration apparatus (close-up)

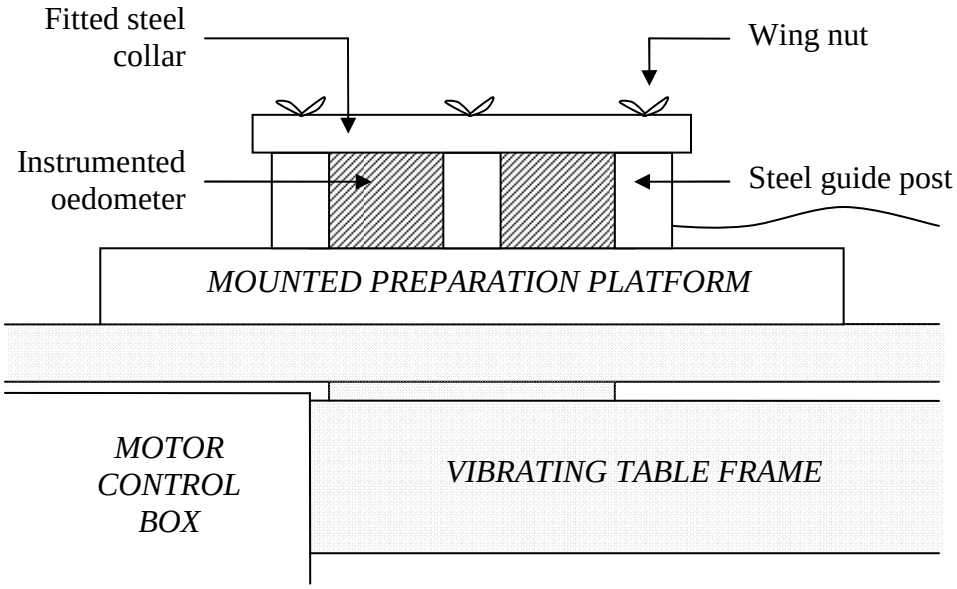

Figure 4.24. Schematic of vibration apparatus

As discussed in Chapter 4.4.1, published studies have not yet presented a unified method for vibrated specimen preparation nor have they resolved the many factors influencing vibration behaviour. Without a strong consensus from literature, the vibration technique developed for this study was chiefly based on a series of reconstitution trials performed with the specific test material and specimen container.

Similar to the tamping technique developed, two aspects were considered when developing the vibration technique for specimen reconstitution. First, suitable vibrations should be applied to the specimen as a whole to achieve the desired degree of particle packing. Given the predetermined operating frequency of the table, the parameters of vibration amplitude and time were used to control the densification. Second, the relative density should be reasonably uniform over the height of the specimen.

For specimens of a medium loose density near 30%, a vibration technique using the vibrating table was developed. Each specimen was initially deposited in two lifts. The vibratory compaction was applied over the entire specimen, as opposed to individual lifts. Subsequent to vibration, the specimen was again re-levelled with the siphon and vacuum. From reconstitution trials performed for this study and in reports from literature, it was

observed that the densification effect upon commencing vibrations was immediate. Therefore, only very short vibration times were needed.

For the medium loose specimens, a double-amplitude of 0.08 mm was chosen. This amplitude was the smallest amount that was practically possible with the vibrating table. Although the table is specified as low as 0.05 mm, the vibrator did not operate consistently at such a low threshold. At this chosen amplitude, the vibrator was simply "pulsed," imparting only an instantaneous moment of vibration to the specimen. While a "pulse" may not be a uniquely defined quantity, a high degree of repeatability of this technique was confirmed. Also, imposing vibrations for any longer than an instant pulse resulted in relative densities markedly higher than desired.

For dense, vibrated specimens of about 60% relative density, a similar vibration technique was used. As before, both lifts were initially deposited by funnel and levelled before vibration was applied over the entire specimen. The specimen was also re-levelled after the prescribed vibration was completed. For dense, vibrated specimens, a slightly greater double-amplitude of 0.10 mm was chosen. Two pulses of the vibrator were used to achieve the desired degree of particle packing.

The vibration technique was altered for the preparation of very dense specimens at about 85% relative density. Reconstitution trials for very dense specimens showed that longer vibration times were required to reach the higher level relative density. However, it was also observed that non-uniformities within the specimen emerged over even marginally extended vibration times. Best results were achieved when vibratory compaction was applied after reconstitution of each lift, instead of only to the specimen as a whole. Consequently, each of the two lifts was initially deposited by funnel and levelled, and then the prescribed amount of vibration was applied to the lift. Both lifts were re-levelled after vibration.

For very dense, vibrated specimens, the double-amplitude was kept constant at 0.10 mm. To achieve the desired degree of particle packing, approximately one second of vibration was delivered to each lift.

It should be noted that a dead weight surcharge of 415 grams or 0.9 kPa on the specimen surface was used when applying vibrations to all specimens. A surcharge was used to prevent particle scatter during vibration and to promote regular vibratory compaction throughout the specimen, as suggested by Vaid and Negussey (1988).

No very loose specimens were prepared by vibration, given the compactive nature of the method.

4.4.3 Specimen quality

Dissections were performed on medium loose, dense and very dense vibrated specimens to verify fabric uniformity. The details of the dissection method are fully described in Chapter 4.2.3.

Figure 4.25, Figure 4.26 and Figure 4.27 show the results from dissections of medium loose, dense and very dense vibrated specimens, respectively. The dissection of the medium loose specimen showed ±4% deviation from the average specimen relative density. The dissections of the dense and very dense specimens exhibited a maximum of ±2% deviation from the average specimen relative density. No dissection data specifically for vibrated Fraser River sand specimens was available in literature. When compared to the dissection data from Brand (1973) presented in Chapter 4.4.1, these deviations are certainly reasonable (see Figure 4.21). Moreover, they are comparable with the deviations in relative density experienced with both air-pluviation and tamping techniques developed for this study.

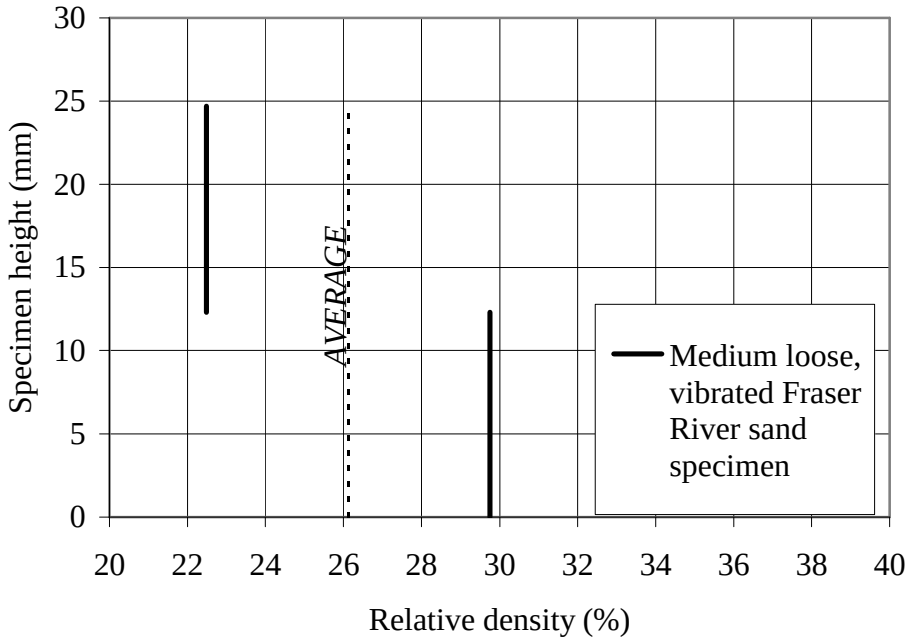

Figure 4.25. Dissection of medium loose, vibrated Fraser River sand specimen

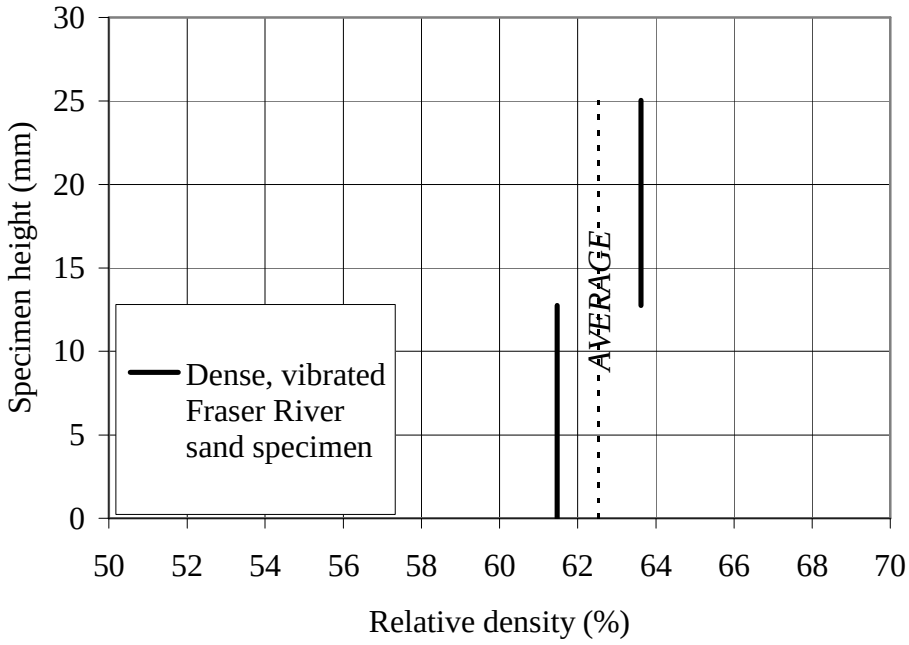

Figure 4.26. Dissection of dense, vibrated Fraser River sand specimen

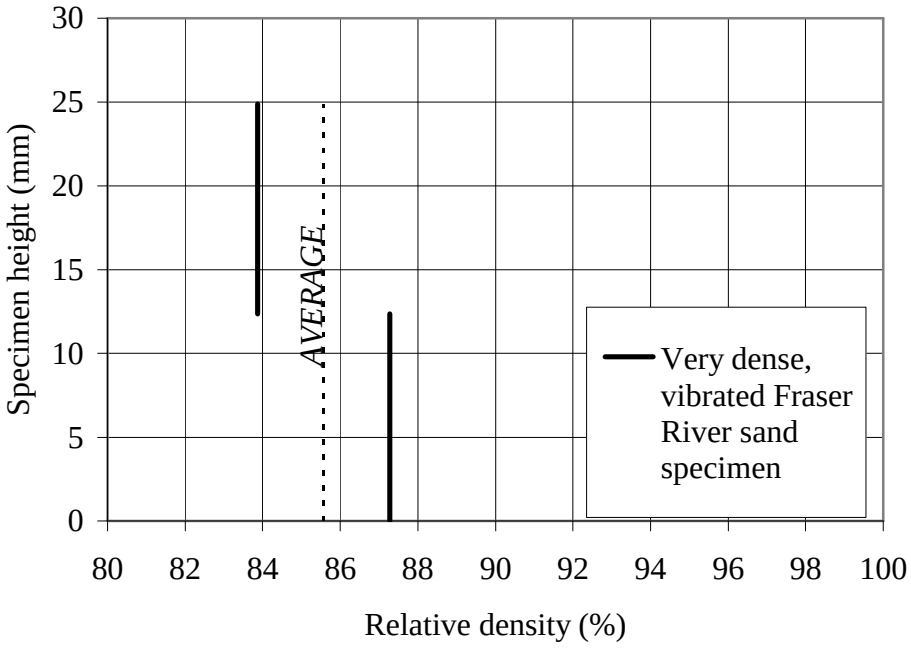

Figure 4.27. Dissection of very dense, vibrated Fraser River sand specimen

4.5 Specimen saturation

A limited number of saturated compression tests were performed on Fraser River sand specimens that were reconstituted in a dry state and then saturated prior to testing. The method used for saturating the reconstituted specimens is modeled after Wijewickreme, Sriskandakumar and Byrne (2005) and is described herein.

First, the testing apparatus was prepared for saturated testing, as shown in Figure 4.28. A plastic water reservoir was attached to the loading platform of the compression frame. The positioning of the reservoir ensures that its height with respect to the oedometer remains constant during testing. On the instrumented oedometer, where the steel ring meets the base, a thin coat of water-resistant silicone grease was applied. Also, the porous stone from the base of the oedometer and the porous stone attached to the top cap were boiled in water until saturated.

Figure 4.28. Photograph of specimen saturation setup

Once the apparatus was properly assembled, the reconstituted specimen was prepared and transported to the loading platform, as detailed in Chapter 3.2. The drainage tube at the base of the instrumented oedometer was connected to the water reservoir, and a plastic cylinder was seated flush atop the oedometer to contain the water passed through the specimen. The contact between the plastic cylinder and oedometer was also thinly coated with water-resistant silicone grease.

Finally, de-aired water, prepared in advance under vacuum, was slowly percolated from the reservoir up through the base of the specimen. Only a small differential head of water was permitted, not greater than 5 cm, to prevent any specimen disturbance. As recommended, about 20 pore volumes of de-aired water were passed through the specimen to achieve saturation (Wijewickreme et al., 2005). Excess water was siphoned from the plastic cylinder as it collected during the saturation process.

After saturation was completed, the flow from the reservoir through the specimen was permitted to equalize. A constant head of water approximately 1 cm above the specimen was retained to ensure continued saturation throughout testing.

5 RESULTS

The main objective of this chapter is to present the factual results from experimental work. A detailed analysis and discussion is presented in Chapter 6.

5.1 General

A series of plots generated from test data is presented in this section, to characterize the typical stress-strain specimen response of Fraser River sand in one-dimensional compression. The general observations of specimen response noted in this section apply to all specimens tested.

A typical stress-strain response for Fraser River sand in one-dimensional compression is shown in Figure 5.1 as specimen void ratio versus logarithm of vertical stress. The plotted series of concave-down curves coincides with the three distinct loading phases: virgin loading, unloading and reloading.

First, the specimen undergoes virgin loading to 250 kPa vertical stress. During this stage, shown in black in Figure 5.1, the specimen is considered normally consolidated (OCR = 1). Note that the majority of the axial strain experienced by the specimen occurs during this loading phase.

Immediately following virgin loading, the specimen is unloaded to approximately zero vertical stress. However, due to soil creep, the shift from virgin loading to unloading phases is not truly instantaneous. The unloading phase, shown in white in Figure 5.1, exhibits a slightly flatter slope than observed in virgin loading. The specimen is overconsolidated in this phase (OCR > 1), with OCR continually increasing as unloading progresses.

Finally, the specimen is compressed to 400 kPa in the reloading phase, shown in grey in Figure 5.1. Upon reloading, the specimen is initially in an overconsolidated state (OCR > 1). As the vertical effective stress increases, OCR decreases, approaching unity. A relatively stiff recompression response is initially observed, as the reloading curve

follows essentially the same reduced slope as in the unloading phase. When the preconsolidation pressure (σ'_p) of 250 kPa is reached the specimen is again considered normally consolidated (OCR = 1). The compression response exhibited at vertical stresses greater than 250 kPa seems to follow the same compression slope as in the virgin loading phase. These observations are in accord with previous observations of the one-dimensional compression response of sands (Hendron, 1963).

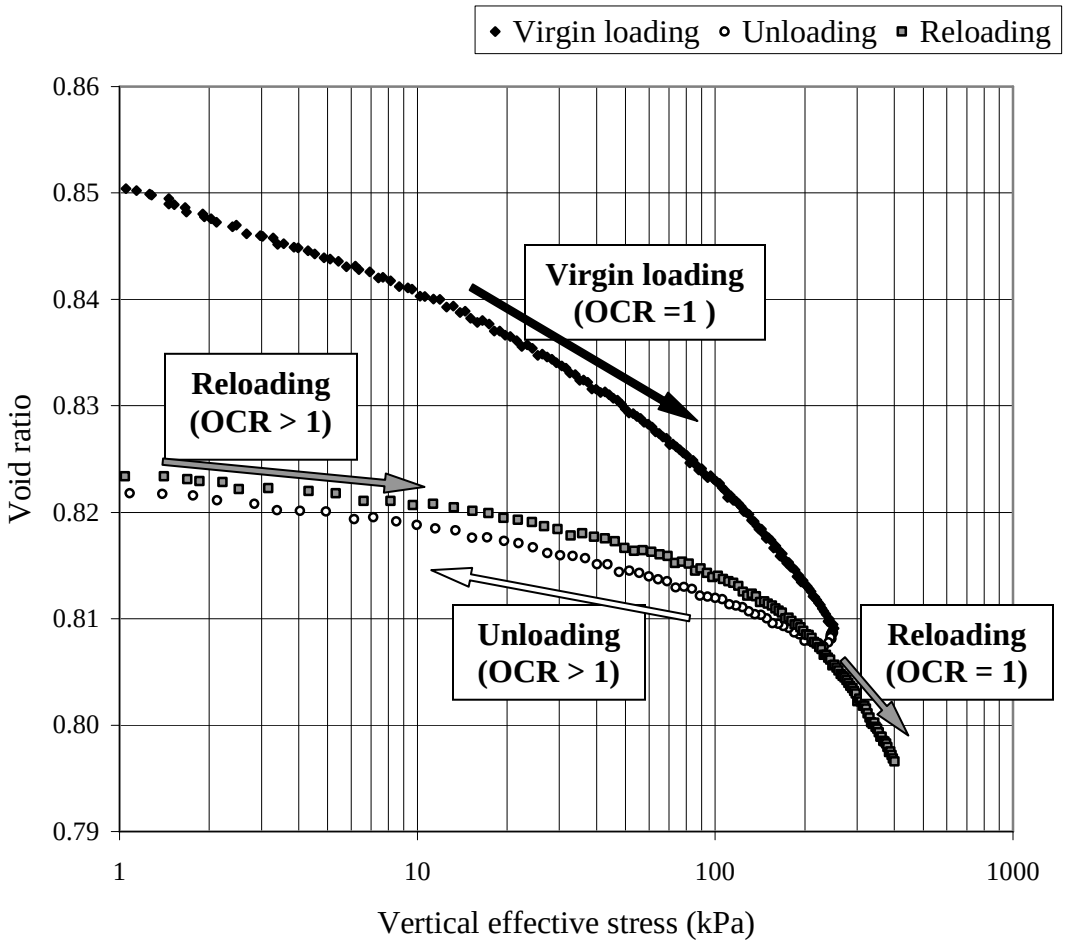

Figure 5.1. Typical void ratio vs. vertical effective stress plot for Fraser River sand

A typical vertical versus horizontal effective stress plot for Fraser River sand in one-dimensional compression is shown in Figure 5.2. Each loading phase is plotted separately, for clarity.

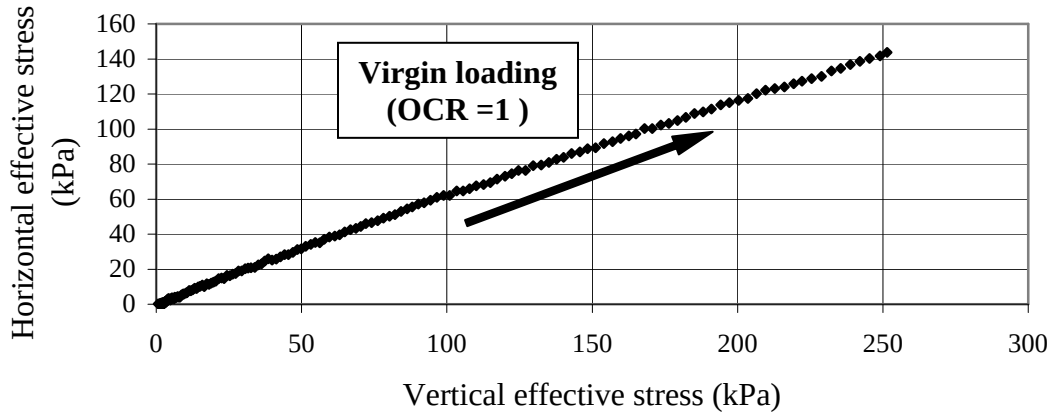

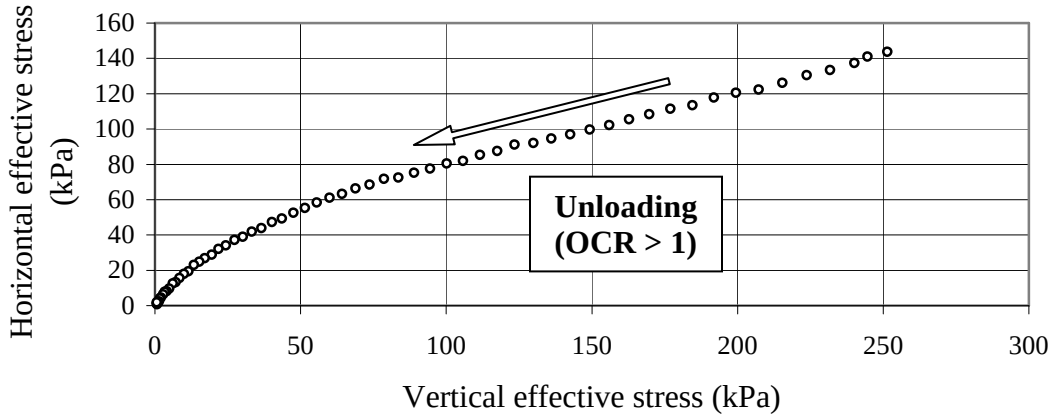

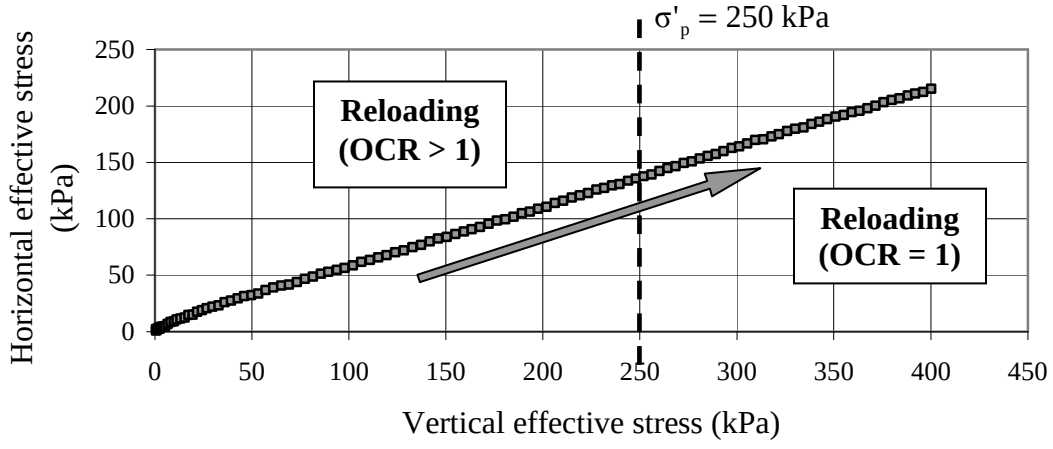

Figure 5.2. Typical one-dimensional compression response of Fraser River sand as $\sigma_h^{'}$ vs. $\sigma_v^{'}$ during virgin loading, unloading, and reloading

A strong linear relation through the origin is apparent during both the virgin loading and reloading phases. For these phases, the slope of the best fit line is equivalent to $\overset{o}{K}$, as defined in Eq. 2.11. For reloading, note that the slope of the best fit line does not appear to change as the specimen is loaded above the preconsolidation pressure. During the unloading phase, a mildly "S-shaped" curve is exhibited.

A typical plot of the coefficient of lateral pressure at rest for Fraser River sand in one-dimensional compression is shown in Figure 5.3, as $K_o\left(=\frac{\sigma'_h}{\sigma'_v}\right)$ versus vertical stress. Each loading phase is plotted separately, for clarity.

During the virgin loading phase, K_o levels off to a relatively constant value, in excess of about 25 kPa vertical stress. A slight decrease may be noted in K_o with increasing vertical stress, although the change is not significant. For unloading, K_o increases considerably, usually in excess of unity. During reloading, K_o once again levels off to a reasonably constant value, in excess of about 125 kPa.

When considering plots of K_o versus vertical stress, recall the definition of K_o (Eq. 1.1). As a numerical ratio of measured stresses, K_o is susceptible to error when measured stresses are very low. As the vertical stress is reduced to near zero, electronic instability combined with limited precision increases the error observed in stress measurements. While this is not a major problem for the accuracy of the stress measurements themselves, a ratio of the values at such low stresses would be inherently inaccurate. Therefore, K_o values calculated very near to zero vertical stress should not necessarily be considered as an accurate representation of the specimen response.

In subsequent sections, the one-dimensional compression response of different reconstituted specimens of Fraser River sand will be investigated in more detail. Test results for each reconstituted fabric type will be examined. Data collected to study the effects of densification and loading history on the observed behaviour for each fabric type will be presented in a systematic manner.

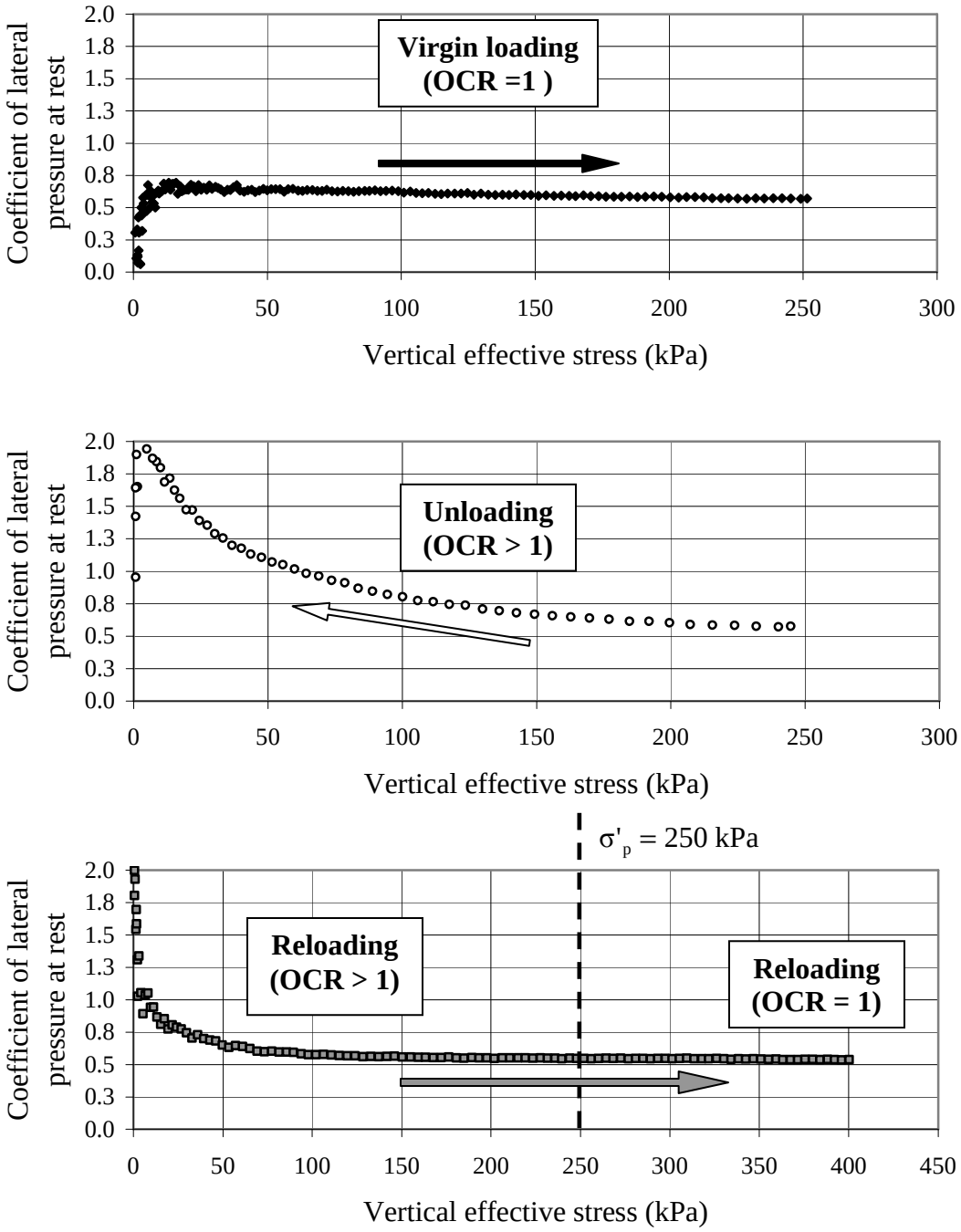

Figure 5.3. Typical K_o vs. vertical effective stress for Fraser River sand

5.2 Air-pluviated Fraser River sand specimens

5.2.1 Very loose specimens

Six (6) one-dimensional compression tests were performed on very loose, air-pluviated (AP_L) Fraser River sand specimens. The initial relative densities ranged from 0 to 2%, with an average of 1%. The test data presented herein represents the typical one-dimensional compression response of very loose, air-pluviated sand specimens. The full set of data for very loose, air-pluviated specimens is available in Appendix A.1. Repeatability was verified from comparisons of the plots in Appendix A.1.

Figure 5.4 plots a typical compression curve. Figure 5.5 depicts the horizontal versus vertical effective stress, with each loading phase displayed separately. Figure 5.6 shows the coefficient of lateral pressure at rest as a function of the vertical effective stress, with each loading phases plotted individually.

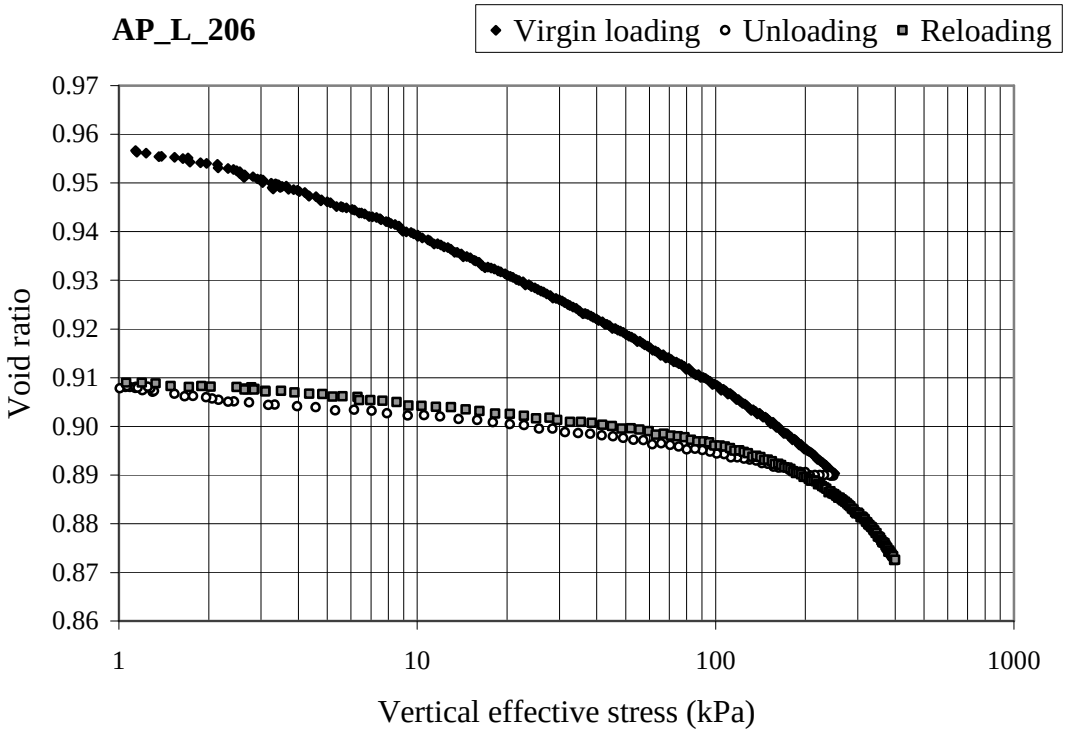

Figure 5.4. Void ratio vs. vertical effective stress for AP_L_206

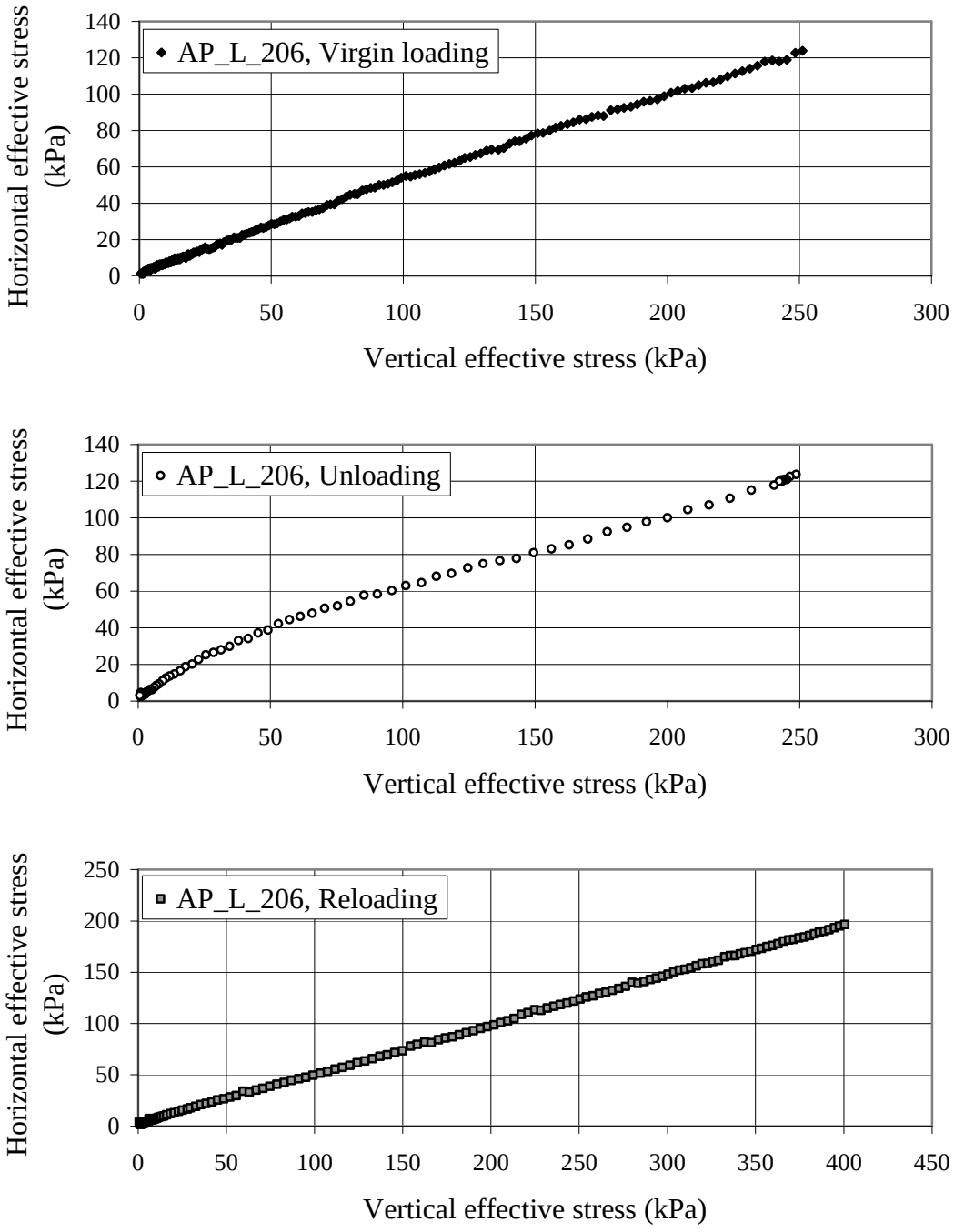

Figure 5.5. Horizontal vs. vertical effective stress for AP_L_206

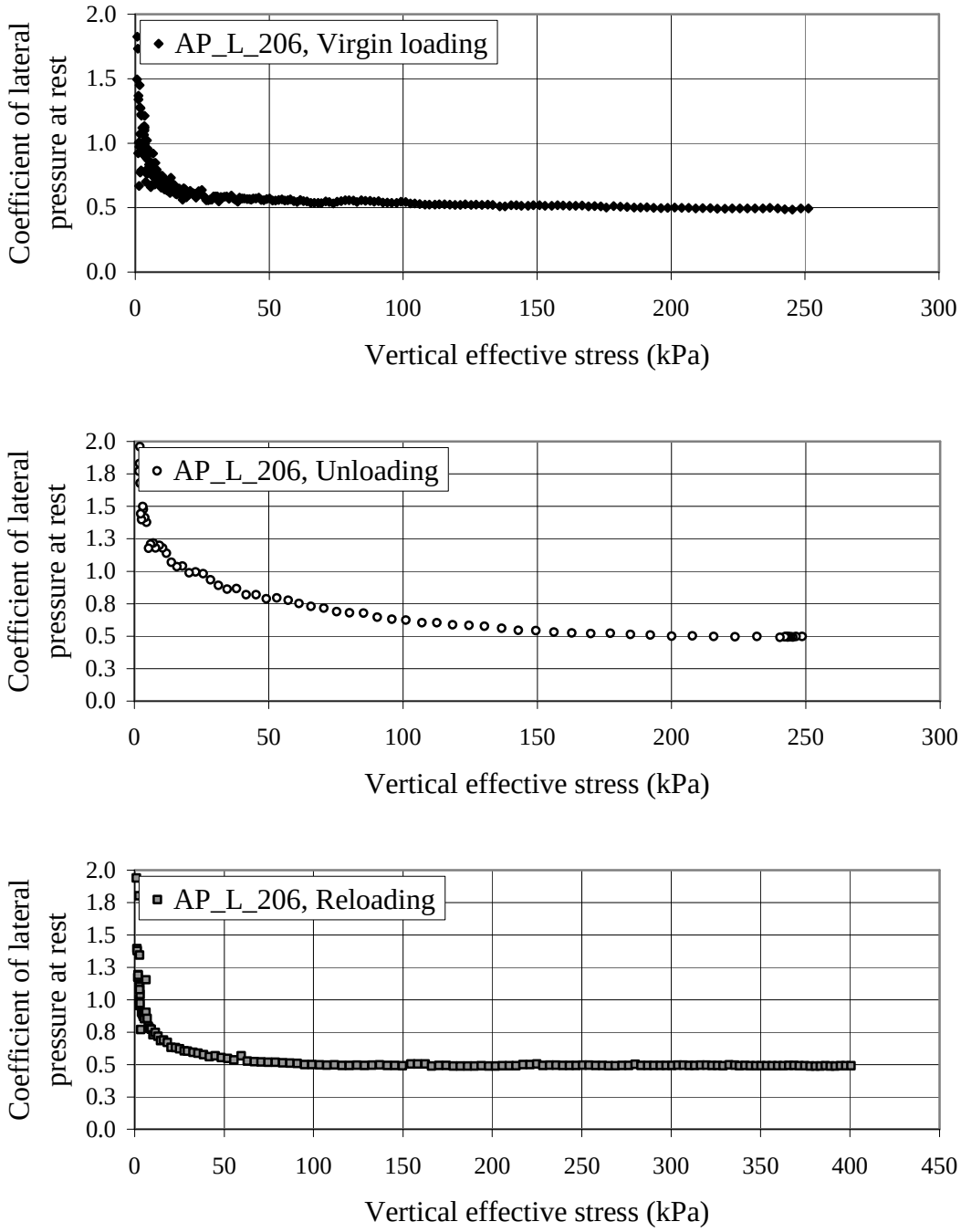

Figure 5.6. K_o vs. vertical effective stress for AP_L_206

The coefficient of lateral pressure at rest for very loose, air-pluviated specimens was computed for virgin loading, unloading and reloading phases. For both virgin loading and reloading, the values were calculated at the end of the loading phases, since K_o is a relatively constant value over the phase. For unloading, K_o was calculated at a given OCR value, over a representative range. Approximate OCR values of 2, 5, 10 and 25 were chosen. The results are listed in Table 5.1, Table 5.2, Table 5.3 and Table 5.4. Note that the reloading phase in specimens AP_L_201 through AP_L_205, inclusive, was only carried out to a maximum vertical effective stress of 300 kPa. Reloading for AP_L_206, presented separately, was carried out to 400 kPa.

Table 5.1. K_o values for AP_L specimens subject to virgin loading

Test ID	**Reconstituted relative density (%)**	**K_o at end of virgin loading** (σ'_v = 250 kPa)
AP_L_201	1	0.428
AP_L_202	2	0.528
AP_L_203	2	0.501
AP_L_204	1	0.472
AP_L_205	0	0.477
AP_L_206	1	0.493

Table 5.2. K_o values for AP_L specimens subject to unloading

Test ID	**Reconstituted relative density (%)**	**K_o for unloading**			
		OCR = 2	**OCR = 5**	**OCR = 10**	**OCR = 25**
AP_L_201	1	0.546	0.784	0.883	0.947
AP_L_202	2	0.661	0.891	1.10	1.33
AP_L_203	2	0.610	0.874	1.05	1.28
AP_L_204	1	0.555	0.711	0.846	0.851
AP_L_205	0	0.555	0.725	0.795	0.808
AP_L_206	1	0.583	0.788	0.981	1.20

Table 5.3. K_o values for AP_L specimens 201 through 205 subject to reloading

Test ID	**Reconstituted relative density (%)**	**K_o at end of reloading** $\left(\sigma'_v = 300 \text{ kPa}\right)$*
AP_L_201	1	0.391
AP_L_202	2	0.518
AP_L_203	2	0.489
AP_L_204	1	0.435
AP_L_205	0	0.466

*Note that AP_L tests 201 through 205, inclusive, were only carried out to a maximum of σ'_v = 300 kPa during the reloading phase.

Table 5.4. K_o value for AP_L_206 subject to reloading

Test ID	**Reconstituted relative density (%)**	**K_o at end of reloading** $\left(\sigma'_v = 400 \text{ kPa}\right)$
AP_L_206	1	0.491

5.2.2 Medium loose specimens

Seven (7) one-dimensional compression tests were performed on medium loose, air-pluviated (AP_M) Fraser River sand specimens. The relative densities of the test specimens ranged from 30 to 33%, with an average value of 32%. The test data is presented herein and represents the characteristic one-dimensional compression response of medium loose, air-pluviated sand specimens (Figure 5.7, Figure 5.8 and Figure 5.9). The complete set of testing data for medium loose, air-pluviated specimens is available in Appendix A.2. Repeatability of the results was verified from comparisons of the compression responses plotted in Appendix A.2.

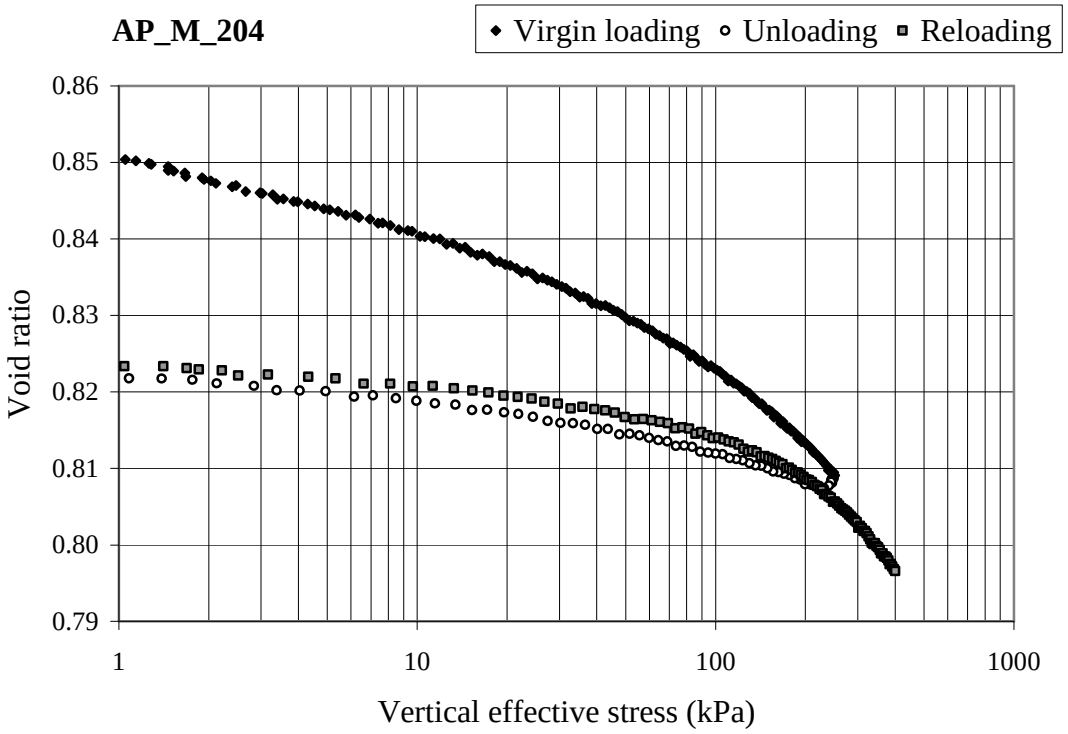

Figure 5.7. Void ratio vs. vertical effective stress for AP_M_204

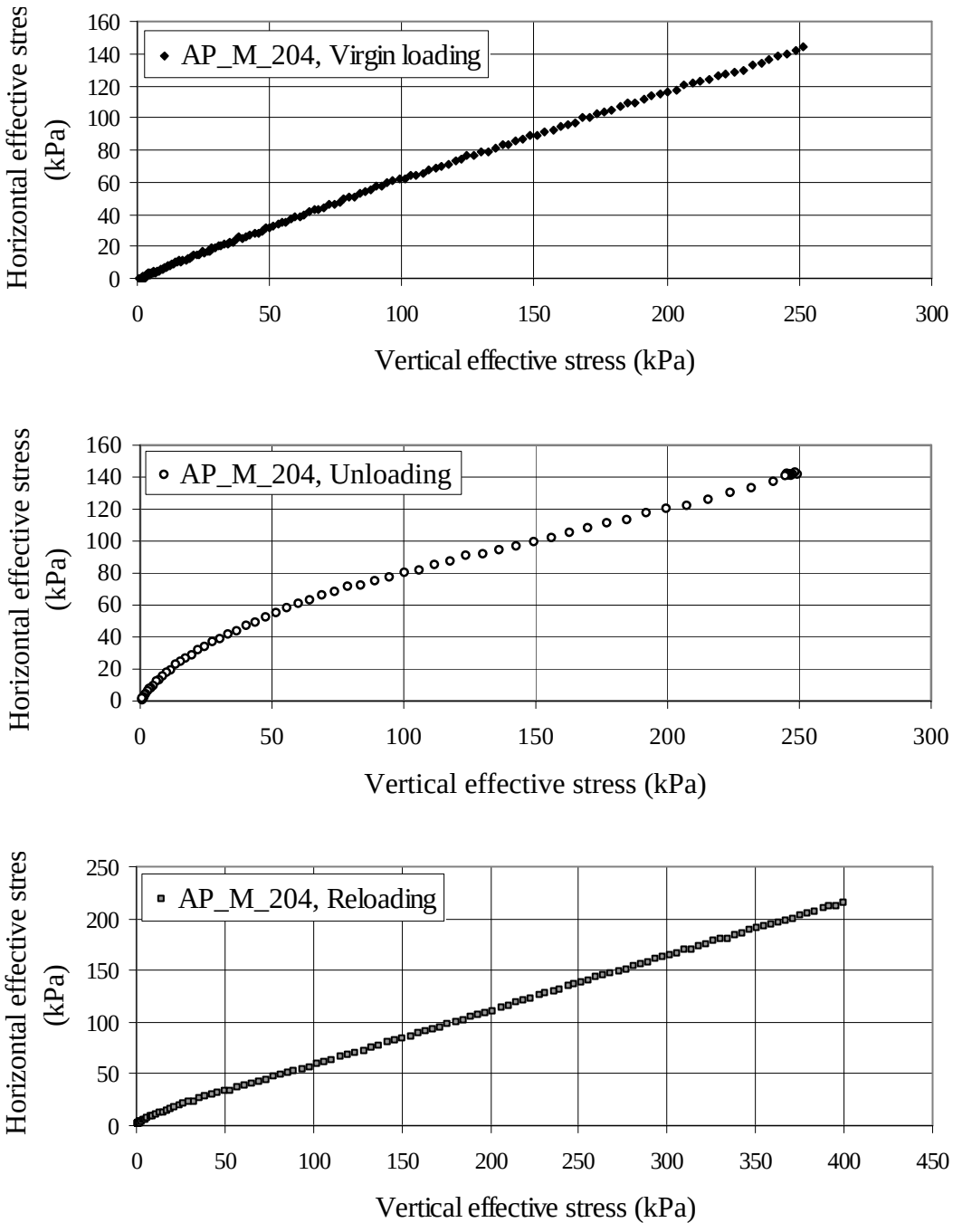

Figure 5.8. Horizontal vs. vertical effective stress for AP_M_204

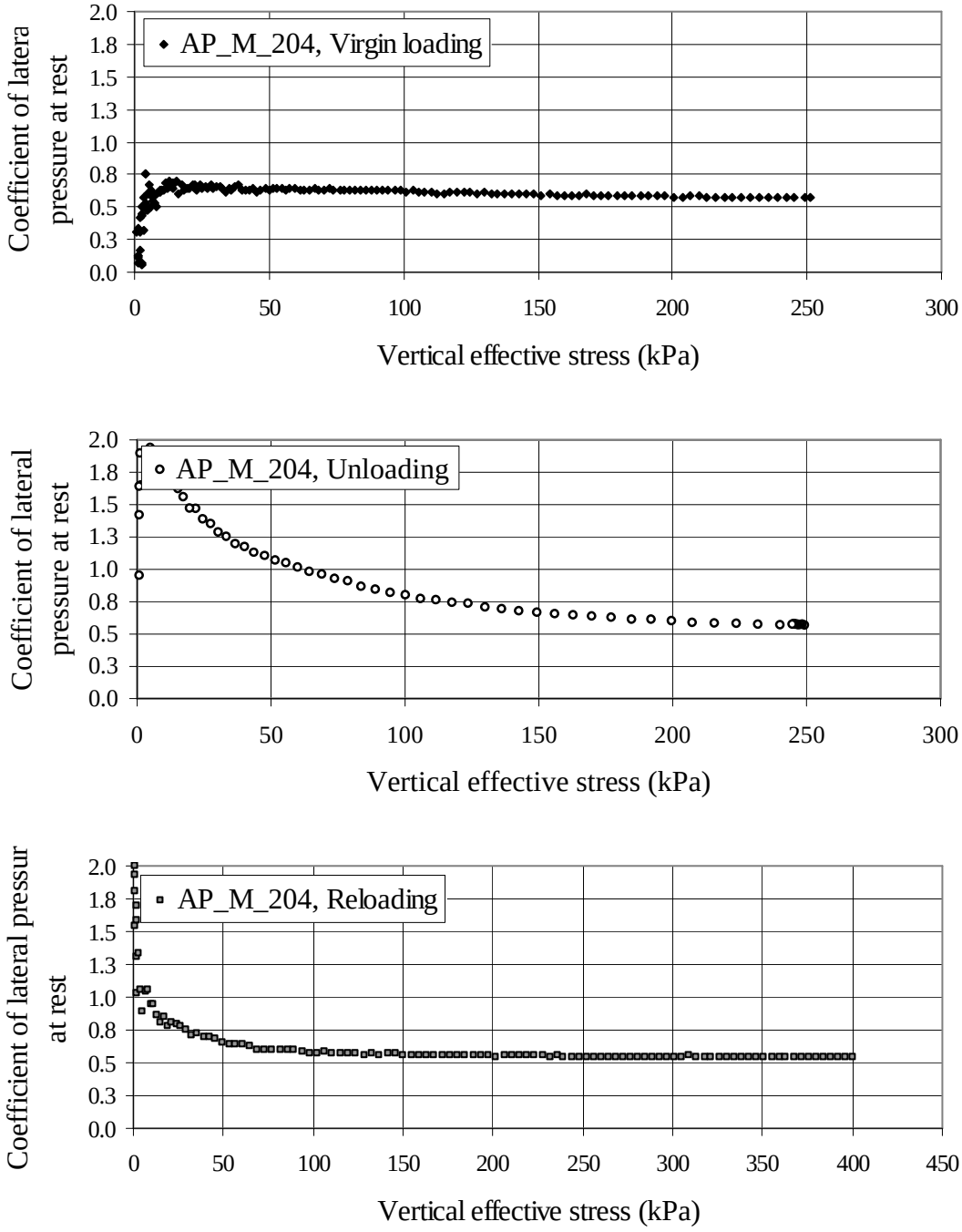

Figure 5.9. K_o vs. vertical effective stress for AP_M_204

The coefficient of lateral pressure at rest for medium loose, air-pluviated specimens was determined for virgin loading, unloading and reloading phases. The results are listed in Table 5.5, Table 5.6 and Table 5.7.

Table 5.5. K_o values for AP_M specimens subject to virgin loading

Test ID	**Reconstituted relative density (%)**	**K_o at end of virgin loading** (σ'_v = 250 kPa)
AP_M_201	32	0.509
AP_M_202	30	0.596
AP_M_203	33	0.555
AP_M_204	32	0.572
AP_M_205	33	0.465
AP_M_206	32	0.649
AP_M_207	30	0.571

Table 5.6. K_o values for AP_M specimens subject to unloading

Test ID	**Reconstituted relative density (%)**	**K_o for unloading**			
		OCR = 2	**OCR = 5**	**OCR = 10**	**OCR = 25**
AP_M_201	32	0.585	0.779	0.897	0.997
AP_M_202	30	0.760	1.11	1.44	1.81
AP_M_203	33	0.703	0.995	1.29	1.64
AP_M_204	32	0.911	1.47	1.87	2.21
AP_M_205	33	0.620	0.919	1.19	1.41
AP_M_206	32	0.820	1.19	1.50	1.87
AP_M_207	30	0.748	1.09	1.33	1.67

Table 5.7. K_o values for AP_M specimens subject to reloading

Test ID	**Reconstituted relative density (%)**	**K_o at end of reloading** $\left(\sigma'_v = 400 \text{ kPa}\right)$
AP_M_201	32	0.473
AP_M_202	30	0.548
AP_M_203	33	0.523
AP_M_204	32	0.538
AP_M_205	33	0.460
AP_M_206	32	0.590
AP_M_207	30	0.531

5.2.3 Dense specimens

Seven (7) one-dimensional compression tests were performed on dense, air-pluviated (AP_D) Fraser River sand specimens. The relative densities of the test specimens ranged from 57 to 62%, with an average of 60%. Presented herein, the test data represents the typical one-dimensional compression response of dense, air-pluviated sand specimens (Figure 5.10, Figure 5.11 and Figure 5.12). The full set of testing data for dense, air-pluviated specimens is presented in Appendix A.3. From comparisons of the compression responses plotted in Appendix A.3, repeatability of the testing results was verified.

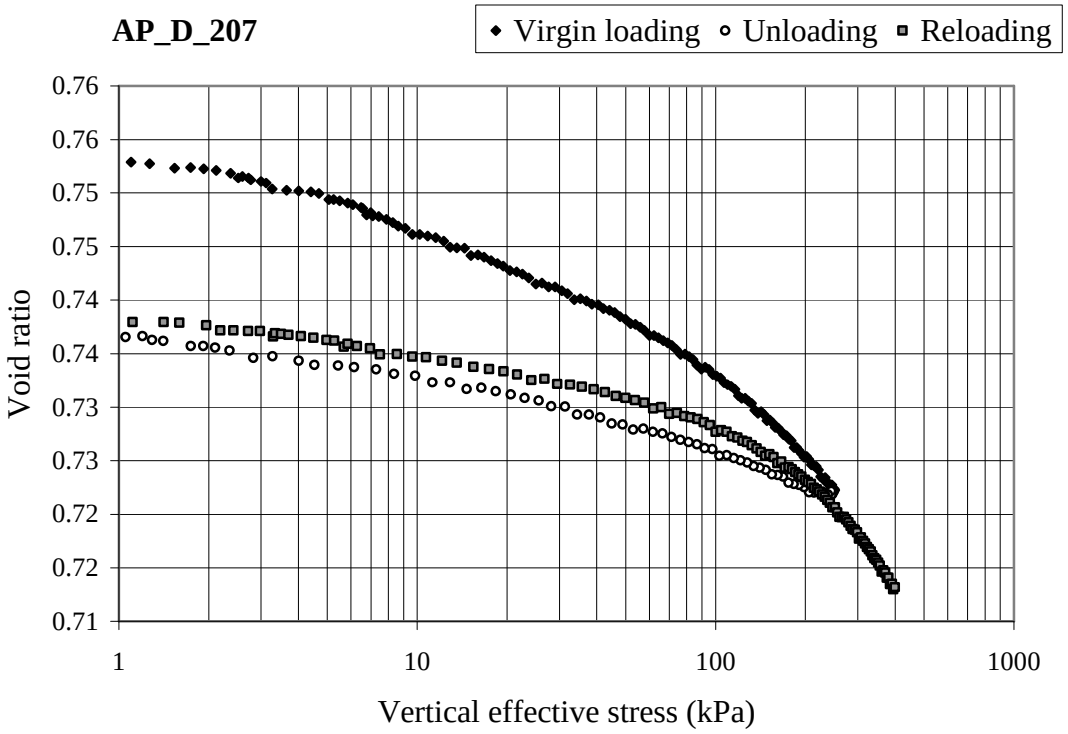

Figure 5.10. Void ratio vs. vertical effective stress for AP_D_207

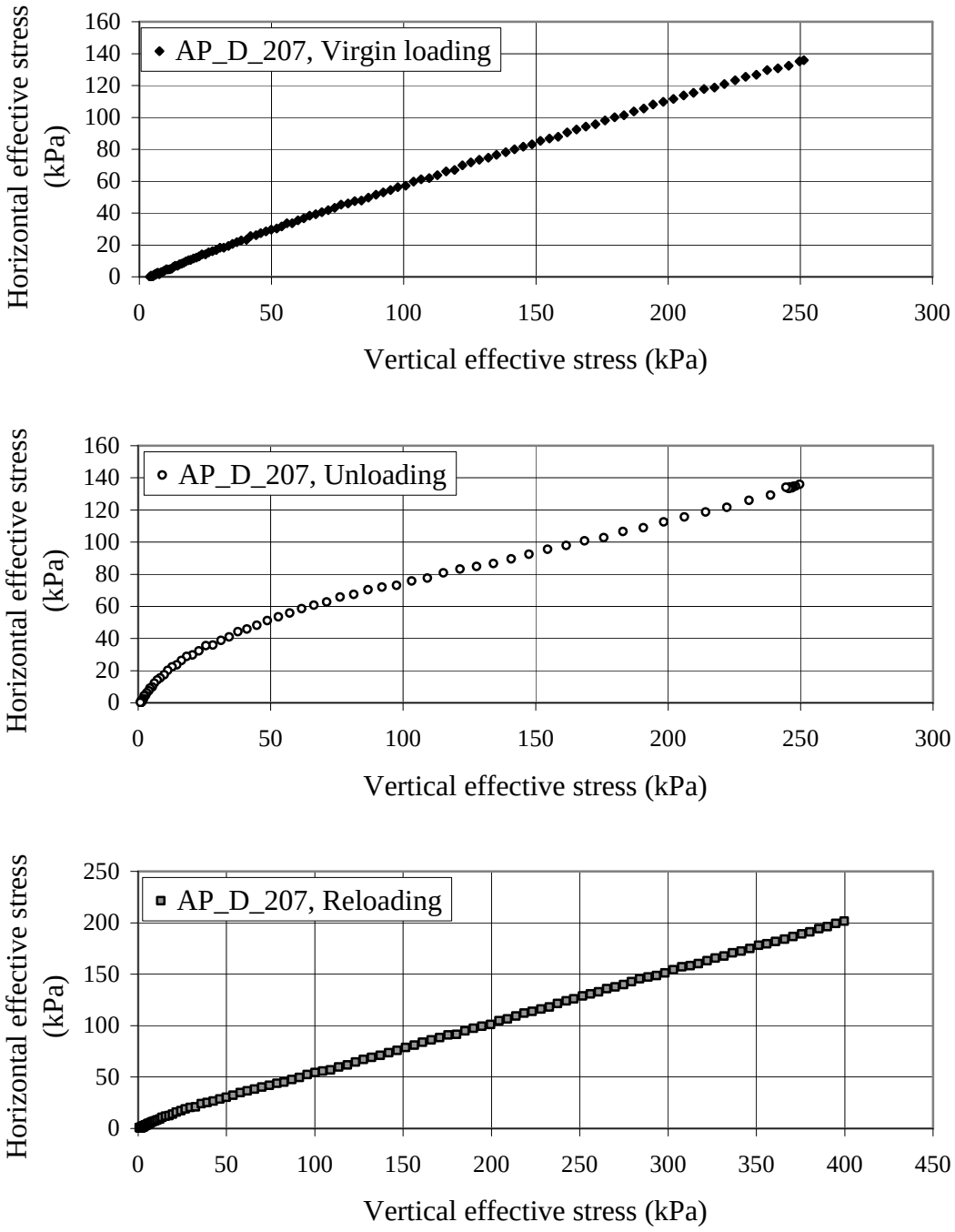

Figure 5.11. Horizontal vs. vertical effective stress for AP_D_207

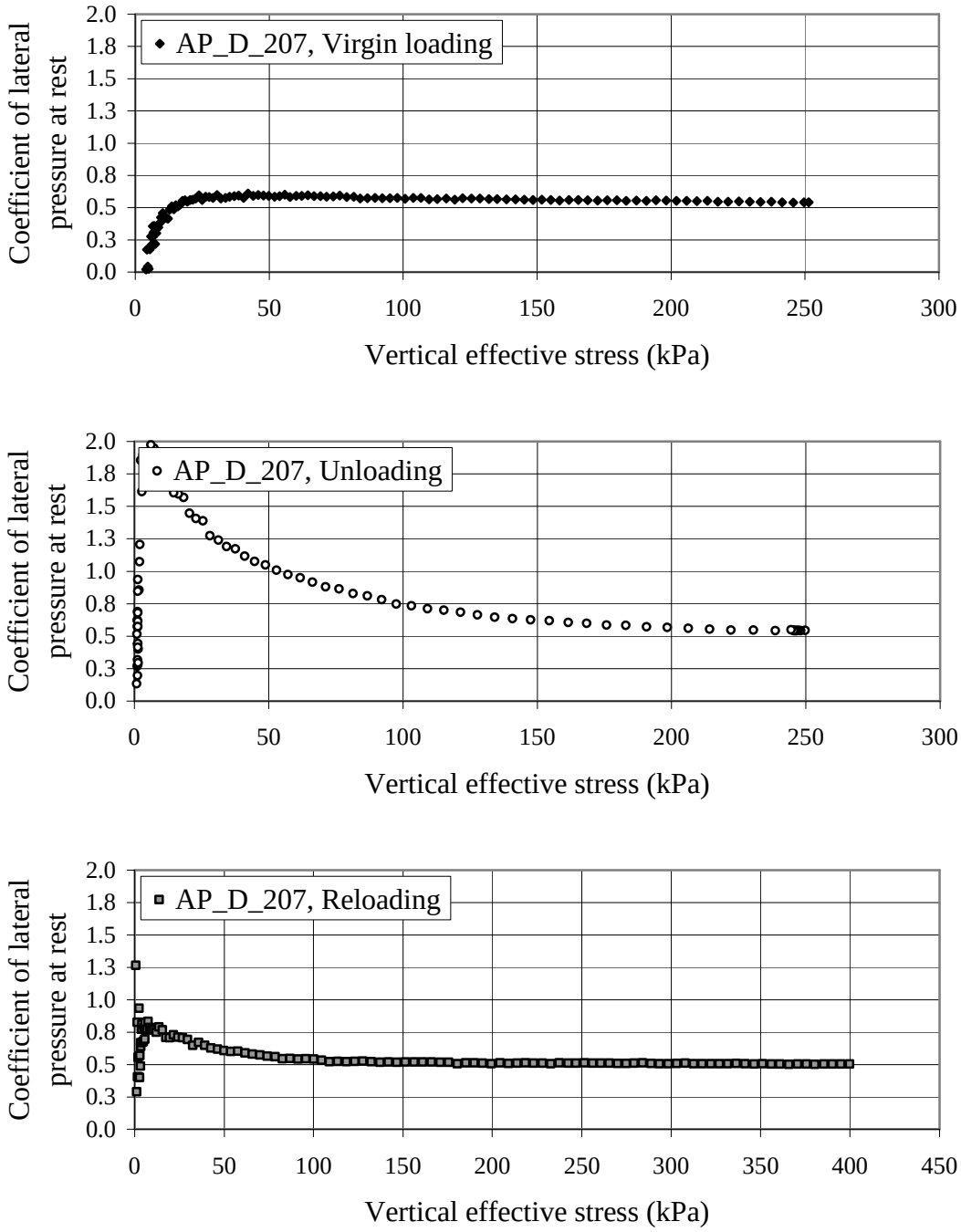

Figure 5.12. K_o vs. vertical effective stress for AP_D_207

The coefficient of lateral pressure at rest for dense, air-pluviated specimens was computed for virgin loading, unloading and reloading phases (Table 5.8, Table 5.9 and Table 5.10).

Table 5.8. K_o values for AP_D specimens subject to virgin loading

Test ID	**Reconstituted relative density (%)**	**K_o at end of virgin loading** (σ'_v = 250 kPa)
AP_D_201	57	0.565
AP_D_202	62	0.553
AP_D_203	60	0.472
AP_D_204	59	0.519
AP_D_205	58	0.424
AP_D_206	60	0.558
AP_D_207	61	0.541

Table 5.9. K_o values for AP_D specimens subject to unloading

Test ID	**Reconstituted relative density (%)**	**K_o for unloading**			
		OCR = 2	**OCR = 5**	**OCR = 10**	**OCR = 25**
AP_D_201	57	0.690	0.989	1.22	1.46
AP_D_202	62	0.671	1.05	1.36	1.91
AP_D_203	60	0.580	0.880	1.11	1.45
AP_D_204	59	0.641	0.983	1.30	1.81
AP_D_205	58	0.513	0.767	0.977	1.21
AP_D_206	60	0.706	1.06	1.47	2.03
AP_D_207	61	0.685	1.05	1.39	1.76

Table 5.10. K_o values for AP_D specimens subject to reloading

Test ID	**Reconstituted relative density (%)**	**K_o at end of reloading** $\left(\sigma'_v = 400 \text{ kPa}\right)$
AP_D_201	57	0.522
AP_D_202	62	0.519
AP_D_203	60	0.457
AP_D_204	59	0.480
AP_D_205	58	0.415
AP_D_206	60	0.517
AP_D_207	61	0.504

5.2.4 Very dense specimens

Six (6) one-dimensional compression tests were performed on very dense, air-pluviated (AP_V) Fraser River sand specimens. The relative densities of the test specimens varied from 84 to 88%, with an average of 86%. The test data, presented herein, represents the typical one-dimensional compression response of very dense, air-pluviated sand specimens (Figure 5.13, Figure 5.14 and Figure 5.15). The complete set of testing data for very dense, air-pluviated specimens is provided in Appendix A.4. Repeatability of the testing results was verified from comparisons of the compression responses plotted in Appendix A.4.

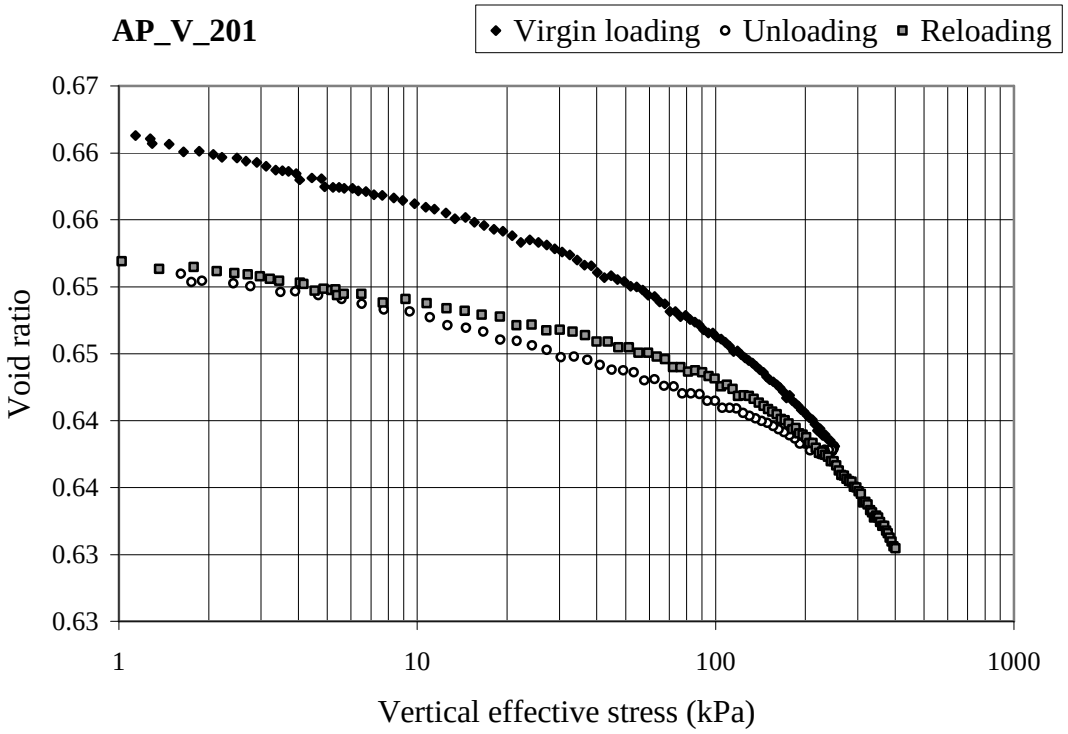

Figure 5.13. Void ratio vs. vertical effective stress for AP_V_201

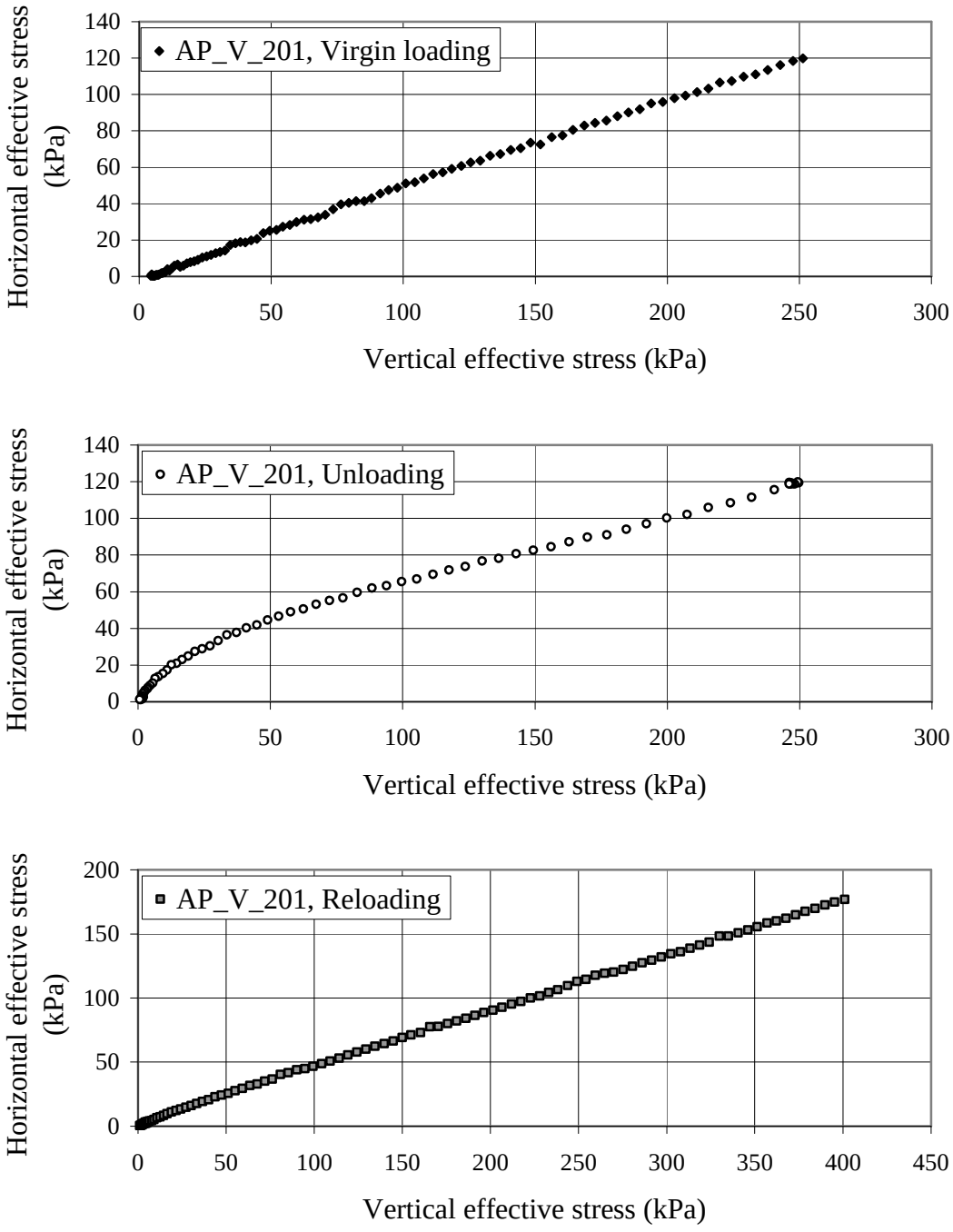

Figure 5.14. Horizontal vs. vertical effective stress for AP_V_201

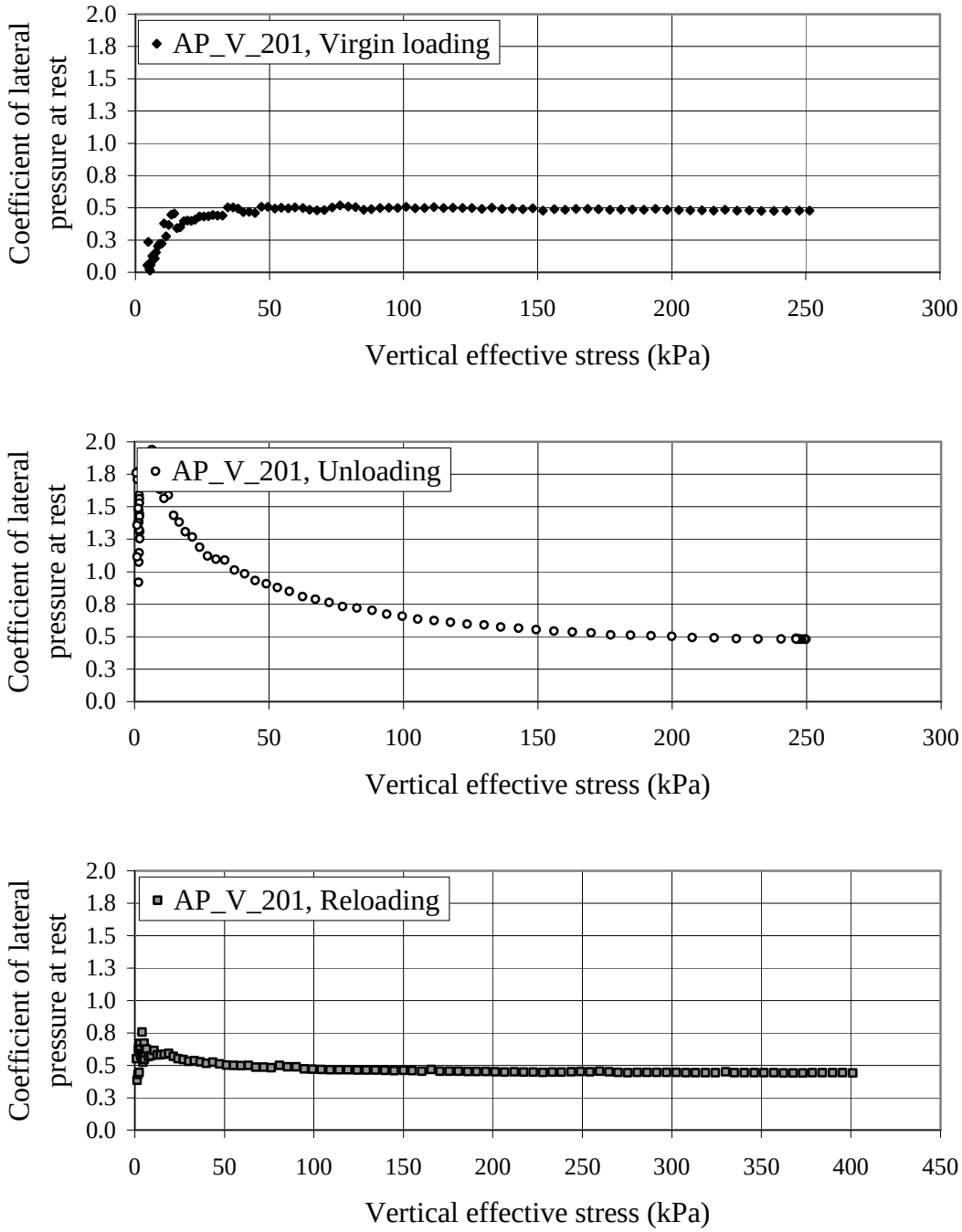

Figure 5.15. K_o vs. vertical effective stress for AP_V_201

The coefficient of lateral pressure at rest for very dense, air-pluviated specimens was computed for virgin loading, unloading and reloading phases (Table 5.11, Table 5.12 and Table 5.13).

Table 5.11. K_o values for AP_V specimens subject to virgin loading

Test ID	**Reconstituted relative density (%)**	**K_o at end of virgin loading** (σ'_v = 250 kPa)
AP_V_201	88	0.477
AP_V_202	86	0.485
AP_V_203	85	0.423
AP_V_204	84	0.531
AP_V_205	88	0.420
AP_V_206	87	0.515

Table 5.12. K_o values for AP_V specimens subject to unloading

Test ID	**Reconstituted relative density (%)**	**K_o for unloading**			
		OCR = 2	**OCR = 5**	**OCR = 10**	**OCR = 25**
AP_V_201	88	0.597	0.908	1.19	1.63
AP_V_202	86	0.601	0.958	1.21	1.65
AP_V_203	85	0.454	0.686	0.947	1.35
AP_V_204	84	0.682	1.10	1.55	2.25
AP_V_205	88	0.476	0.742	1.08	1.69
AP_V_206	87	0.655	0.991	1.36	2.00

Table 5.13. K_o values for AP_V specimens subject to reloading

Test ID	**Reconstituted relative density (%)**	**K_o at end of reloading** $\left(\sigma'_v = 400 \text{ kPa}\right)$
AP_V_201	88	0.441
AP_V_202	86	0.446
AP_V_203	85	0.422
AP_V_204	84	0.475
AP_V_205	88	0.388
AP_V_206	87	0.474

5.2.5 Effect of densification

For air-pluviated specimens, the effect of densification during reconstitution may be observed by comparing typical compression response curves. Figure 5.16 depicts the horizontal versus vertical effective stress response during virgin loading, unloading and reloading for very loose, medium loose, dense and very dense air-pluviated specimens.

With the exception of the data for the very loose specimen, it may be observed from Figure 5.16 that the slope of the stress plot, $\overset{o}{K}$, for virgin loading and reloading phases, increases with decreasing reconstituted relative density. During unloading, a similar "S-shaped" curvature is observed for all reconstituted densities. As unloading progresses to zero effective vertical stress, the curves gradually converge.

It is unclear why the very loose specimen behaviour does not follow the trend observed in medium loose, dense and very dense specimens. It is thought that the very loose reconstitution method may produce a "collapsible" structure. Very loose specimens, prepared near zero relative density, may be prone to disproportionate compressibility upon loading. Figure 5.17 shows the axial strain versus the square root of vertical effective stress for very loose, medium loose, dense and very dense air-pluviated specimens. Clearly, the compressibility in the very loose specimen is markedly greater, thus supporting the above hypothesis. Still, further research is needed to confirm this supposition.

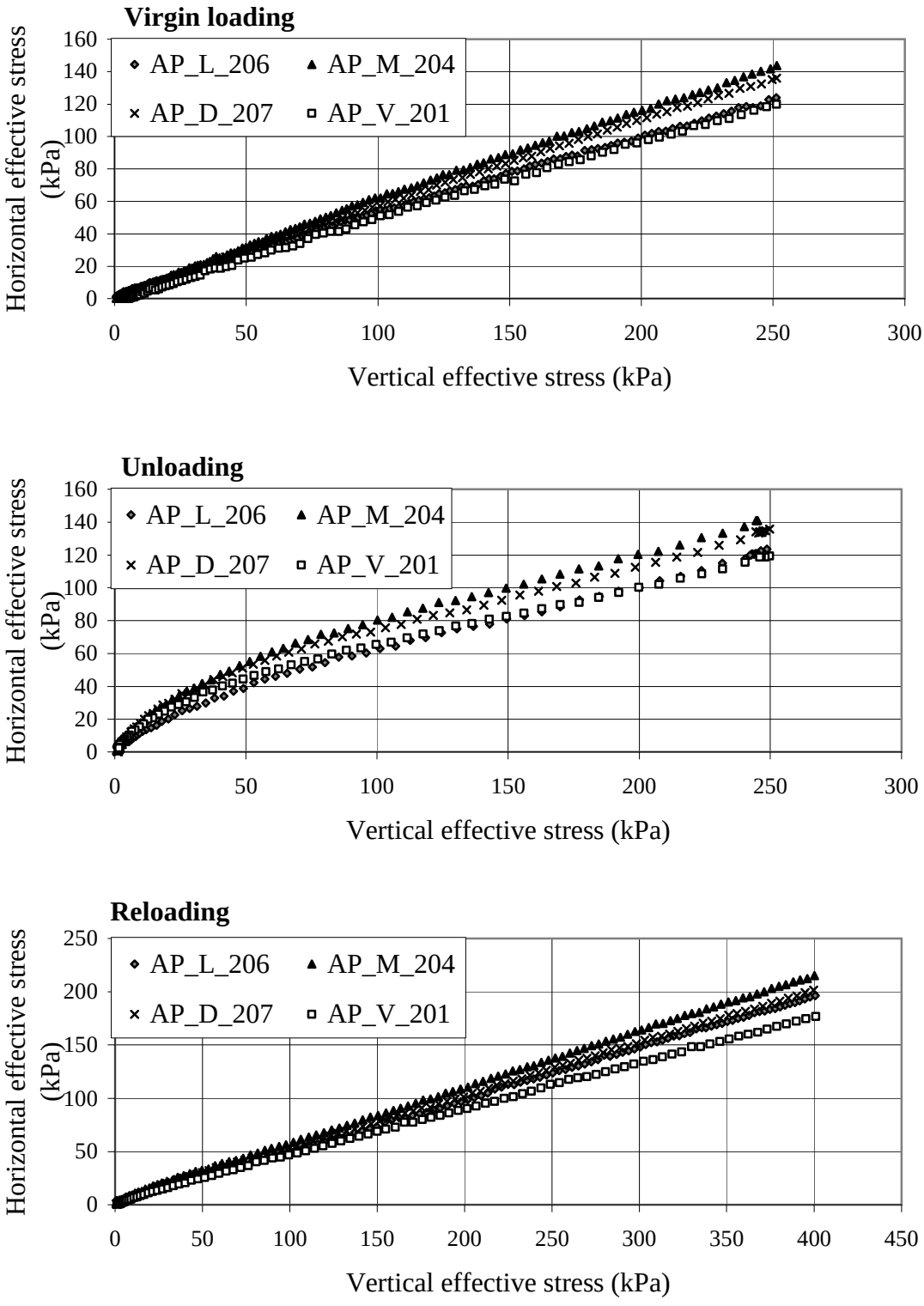

Figure 5.16. Comparison of horizontal vs. vertical effective stress for AP specimens

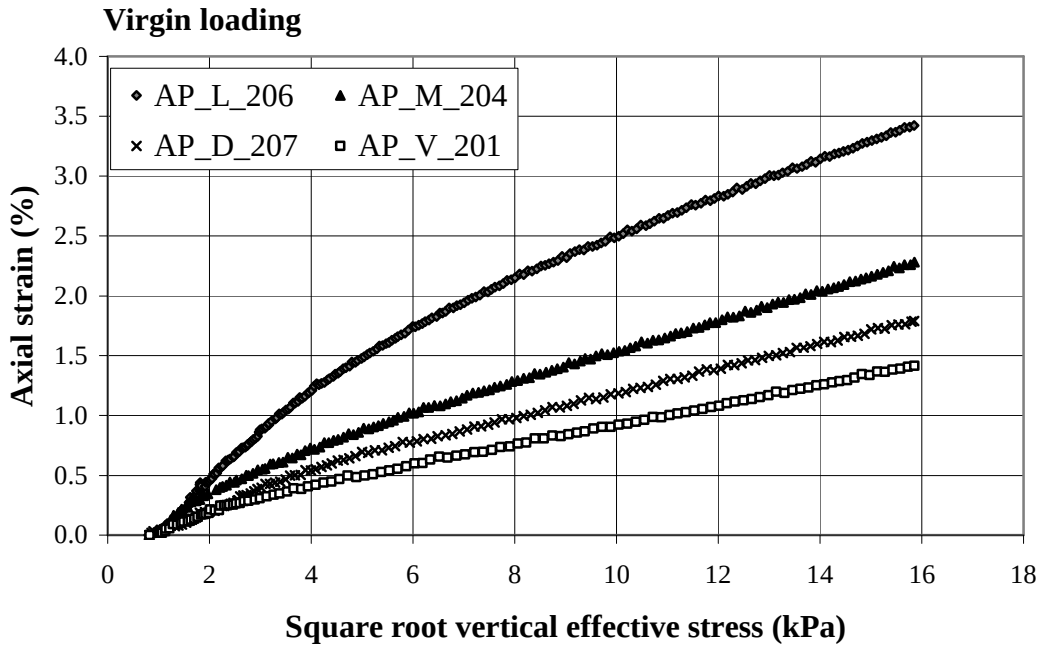

Figure 5.17. Comparison of axial strain vs. vertical effective stress of AP specimens

Figure 5.18 depicts the coefficient of lateral pressure at rest during compression for very loose, medium loose, dense and very dense air-pluviated specimens. As noted previously, K_o during both virgin loading and reloading becomes reasonably constant soon after loading commences. This constant K_o value increases with decreasing reconstituted relative density, with the exception of the very loose specimen. During unloading, all reconstituted densities exhibit a similar concave-up curve. As unloading progresses to zero effective vertical stress, the curves slightly diverge.

To best observe the effect of densification, the coefficient of lateral pressure at rest, calculated at the end of virgin loading, was compared for all twenty-six (26) one-dimensional compression tests performed on air-pluviated specimens (see Figure 5.19). Note that the shaded region in Figure 5.19 corresponds to a general envelope derived from the compression test results.

Figure 5.19 reiterates the decrease in K_o with increasing relative density. Also, the plot suggests that with increasing relative density, the scatter in measured K_o values somewhat decreases.

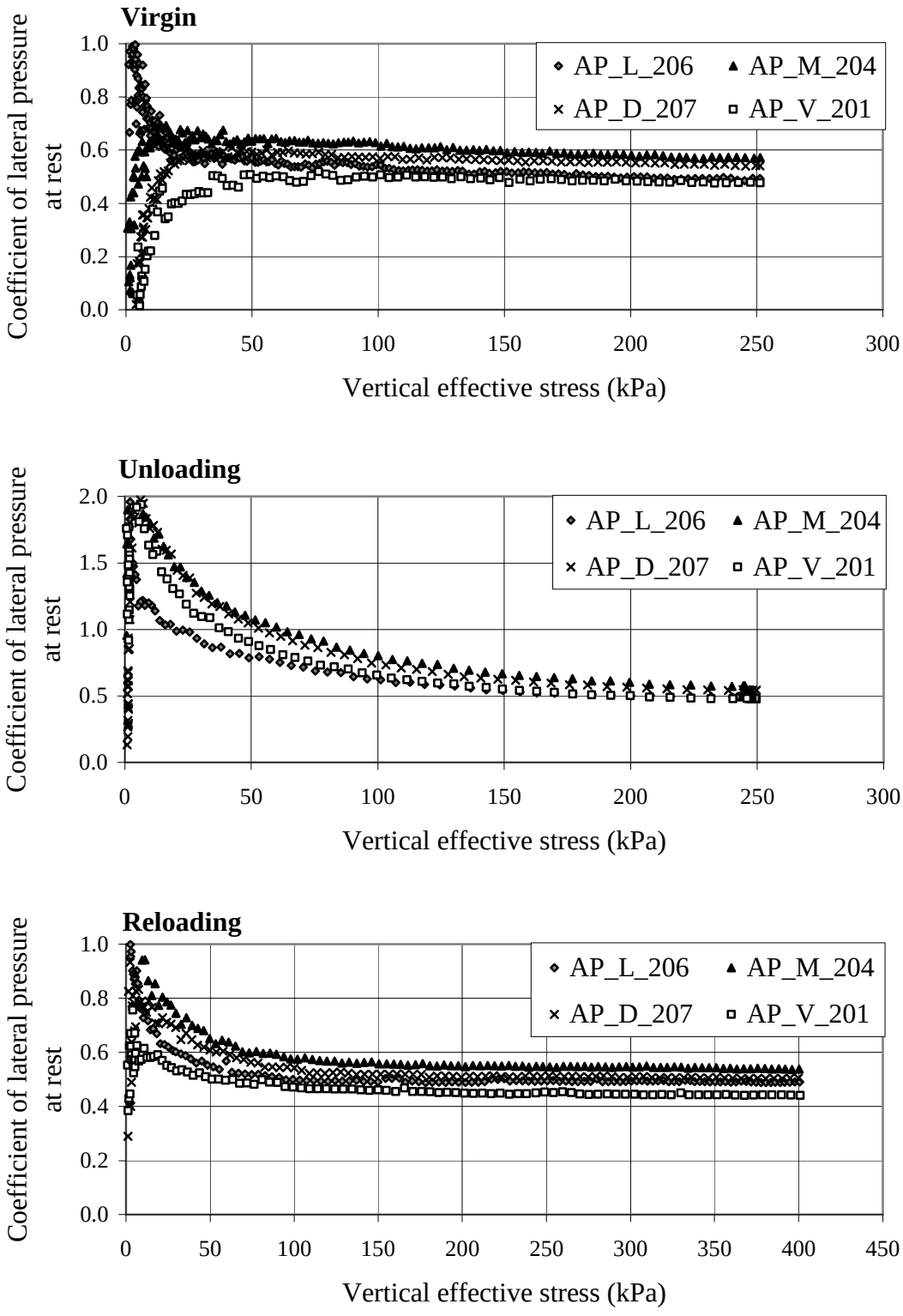

Figure 5.18. Comparison of K_o vs. vertical effective stress for AP specimens

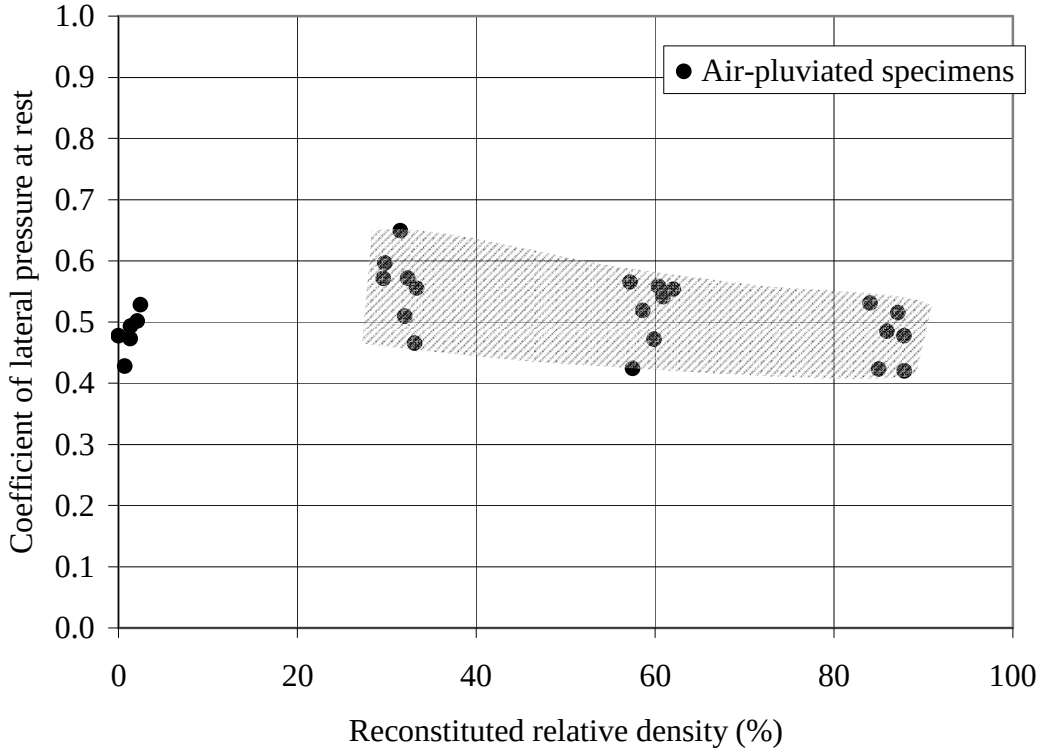

Figure 5.19. K_o at the end of virgin loading for AP specimens

5.2.6 Effect of loading history

For air-pluviated specimens, the effect of loading history may be observed by comparing the plotted compression test data for a given reconstituted density. Figure 5.20 depicts a comparison of horizontal versus vertical effective stress during virgin loading and reloading for a dense, air-pluviated specimen. While slight non-linearity exists near the origin, both the virgin loading and reloading curves appear distinctly linear in excess of 100 kPa vertical stress. Note that the slope exhibited in the reloading phase is slightly decreased from the slope observed in the virgin loading phase.

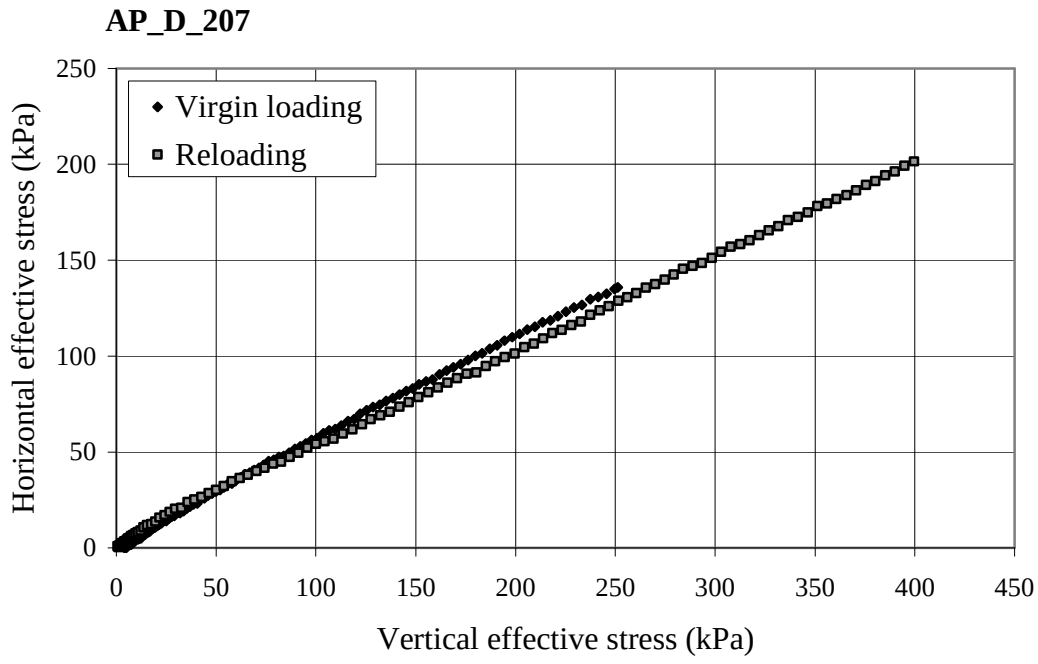

Figure 5.20. Comparison of horizontal vs. vertical effective stress during virgin loading and reloading for AP_D_207

Figure 5.21 plots the coefficient of lateral pressure at rest during virgin loading and reloading for a dense, air-pluviated specimen. Above roughly 100 kPa vertical stress, the plot shows a lower K_o value for the reloading phase than for virgin loading, consistent with observations from Figure 5.20. As the specimen is reloaded past its preconsolidation pressure of 250 kPa, no noticeable change in K_o is demonstrated.

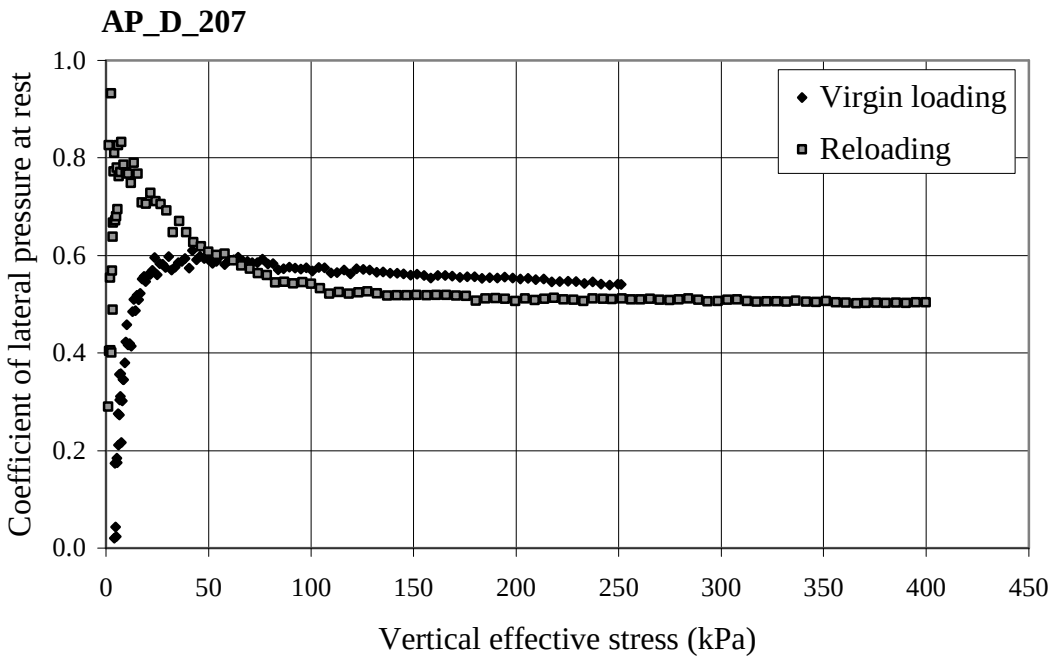

Figure 5.21. Comparison K_o vs. vertical effective stress during virgin loading and reloading for AP_D_207

Although not shown here, the effect of loading history on very loose, medium loose and very dense air-pluviated specimens was found to be similar to that observed in dense, air-pluviated specimens (see Figure 5.20, Figure 5.21).

To best observe the effect of loading history, the coefficient of lateral pressure at rest, calculated at the end of both virgin loading and reloading, was compared for all twenty-six (26) one-dimensional compression tests performed on air-pluviated specimens (see Figure 5.22). For all reconstituted densities, K_o values measured at the end of reloading are slightly lower than those at the end of virgin loading.

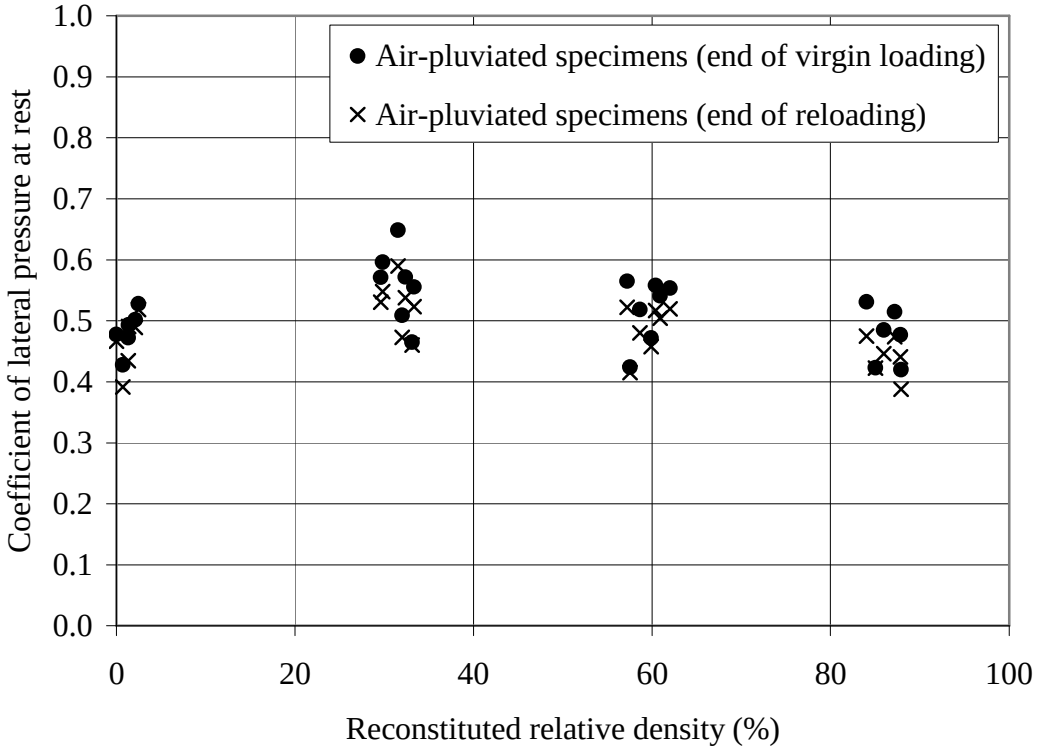

Figure 5.22. K_o at the end of virgin loading and reloading for AP specimens

Additionally, the coefficient of lateral pressure at rest, computed for selected OCR values over the unloading phase, was compared for all twenty-six (26) one-dimensional compression tests performed on air-pluviated specimens (see Figure 5.23). For all reconstituted densities, K_o values increase appreciably as OCR increases. Also, the scatter in K_o values seem to increase markedly with increasing OCR.

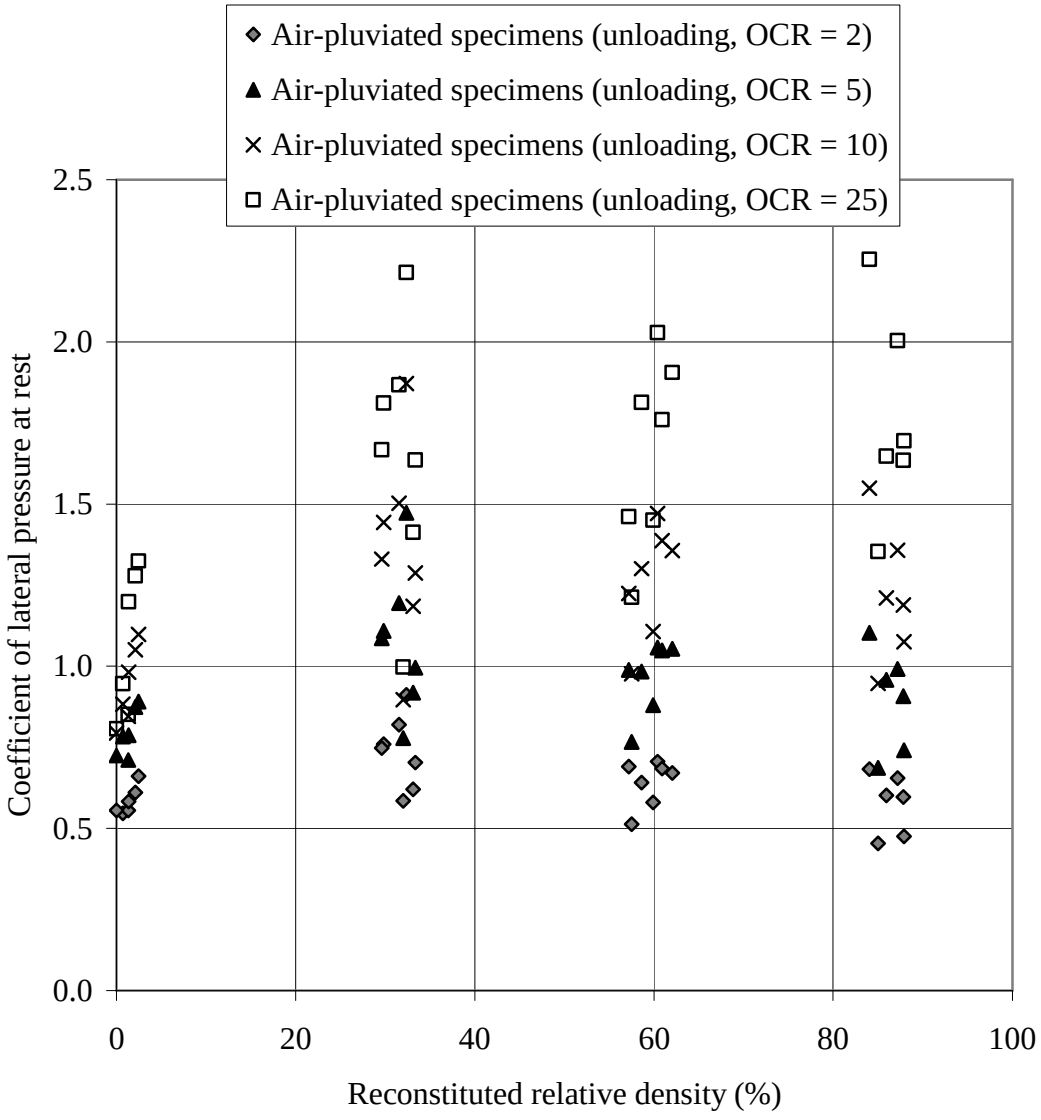

Figure 5.23. K_o at varied OCR values during unloading for AP specimens

5.3 Tamped Fraser River sand specimens

5.3.1 Medium loose specimens

Six (6) one-dimensional compression tests were performed on medium loose, tamped (T_M) Fraser River sand specimens. The relative densities of the test specimens ranged from 29 to 33%, with an average value of 30%. The test data presented herein represents the typical one-dimensional compression response of medium loose, tamped sand

specimens. Refer to Appendix B.1 for the full set of medium loose, tamped specimen test data. Repeatability of the results was verified from comparisons of the compression response plots in Appendix B.1.

Figure 5.24 illustrates a typical compression curve. The horizontal versus vertical effective stress is displayed in Figure 5.25, with each loading phase plotted separately. Figure 5.26 depicts the coefficient of lateral pressure at rest versus the vertical effective stress, with each loading phases plotted individually.

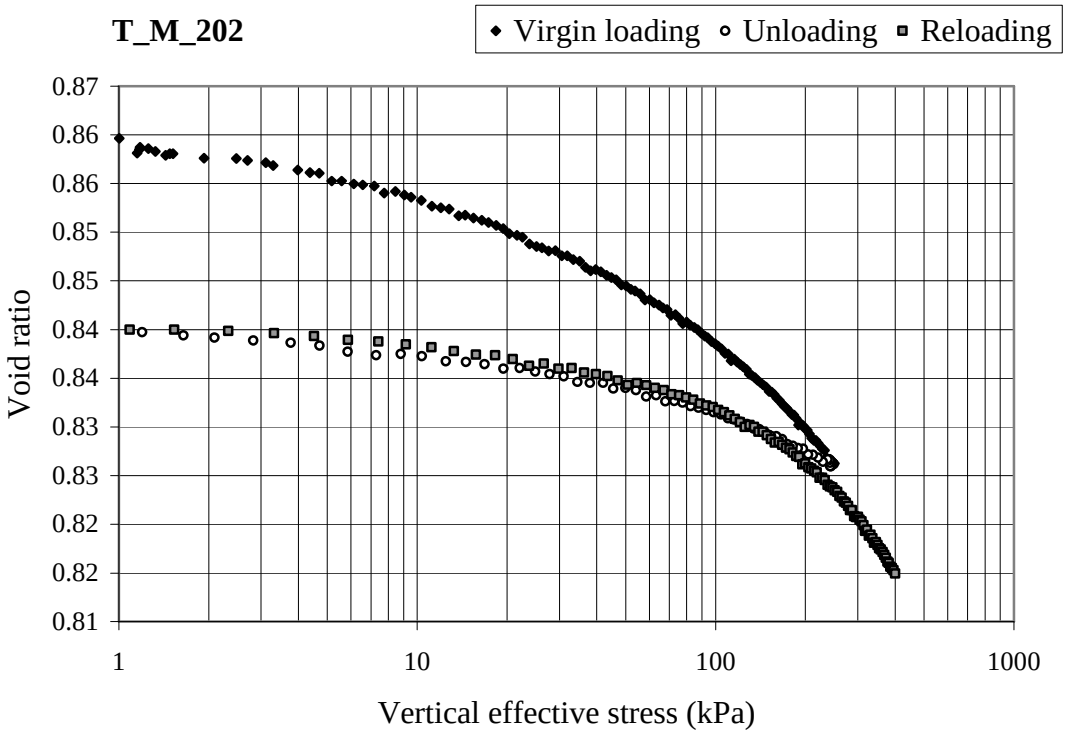

Figure 5.24. Void ratio vs. vertical effective stress for T_M_202

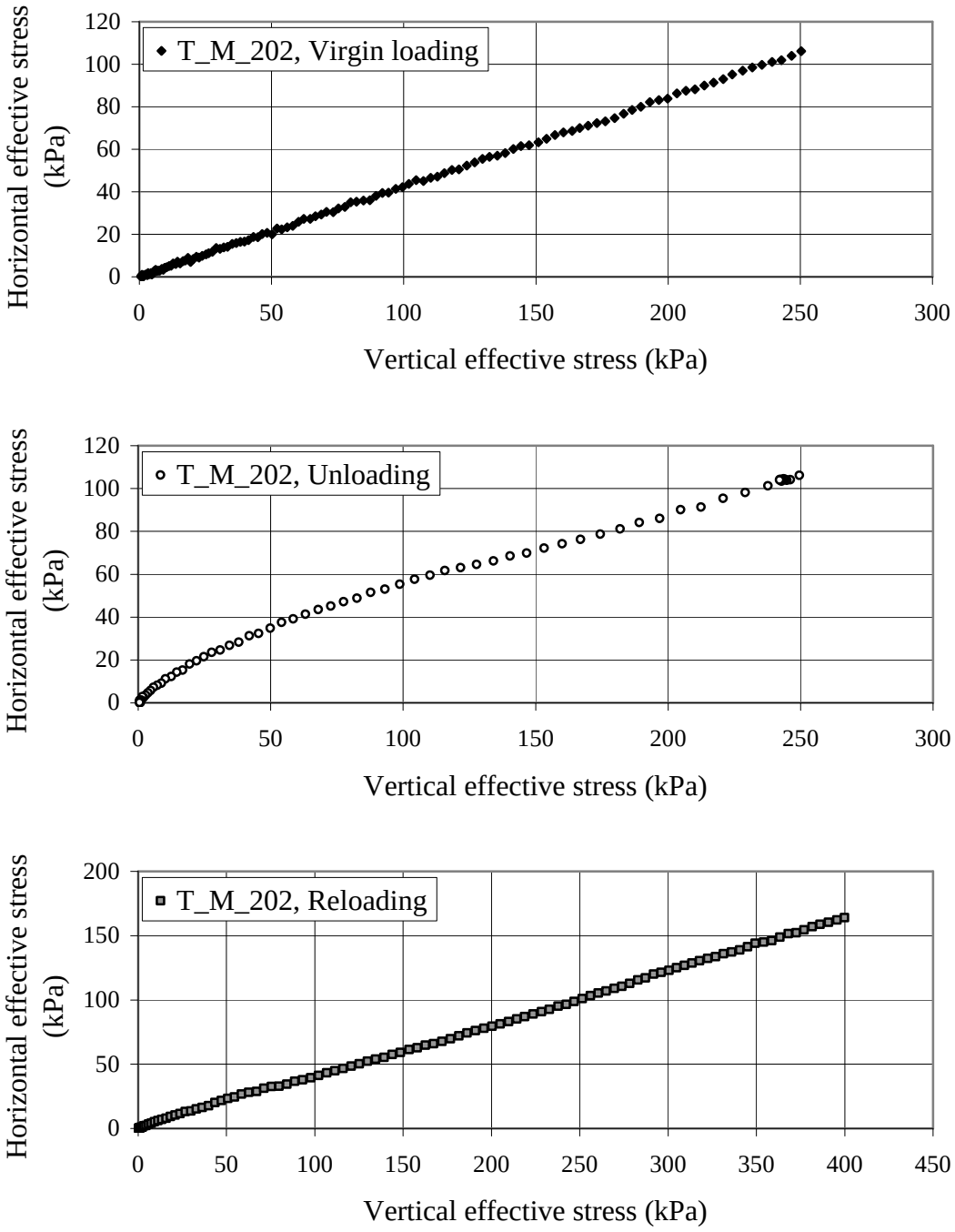

Figure 5.25. Horizontal vs. vertical effective stress for T_M_202

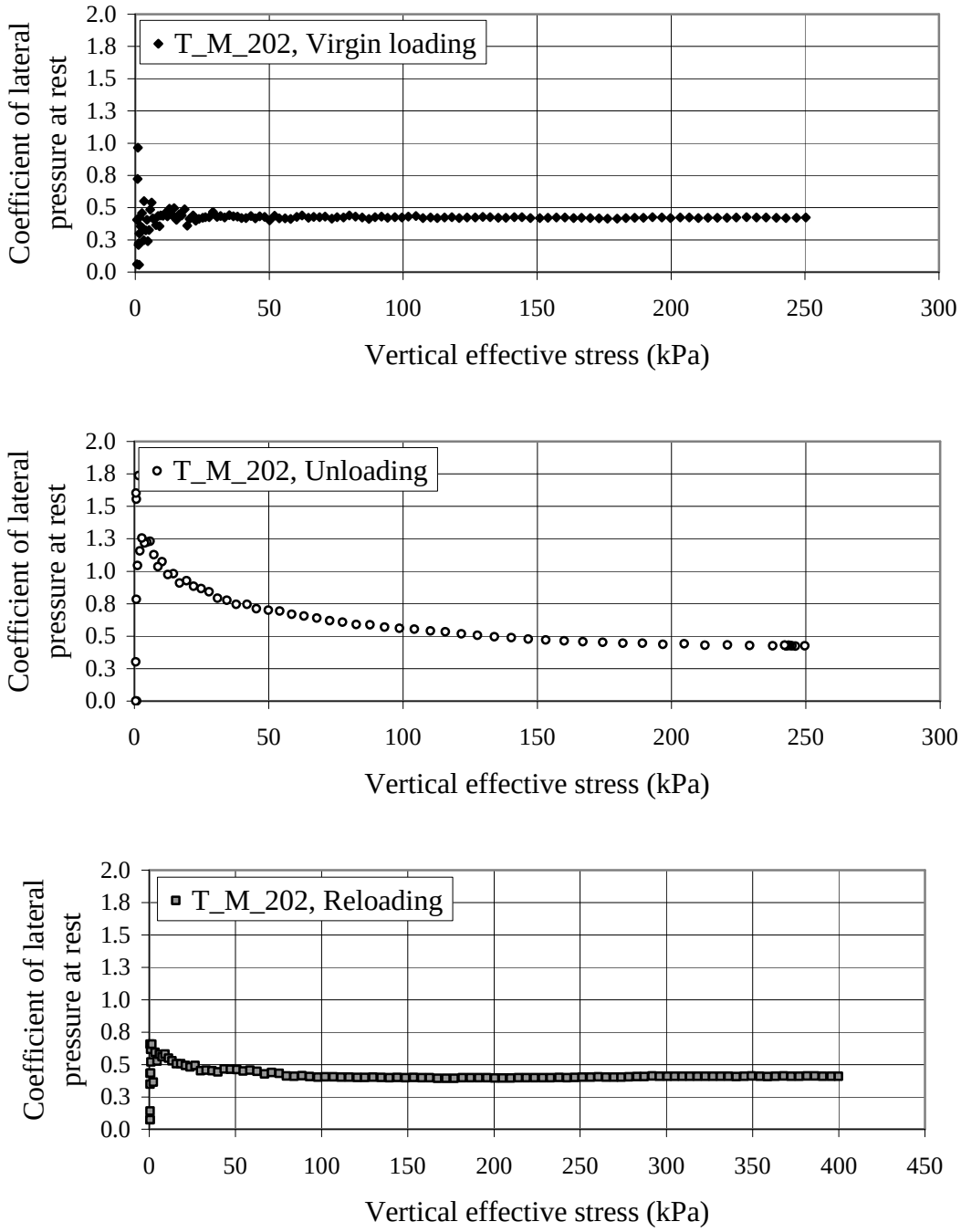

Figure 5.26. K_o vs. vertical effective stress for T_M_202

The coefficient of lateral pressure at rest for medium loose, tamped specimens was computed for virgin loading, unloading and reloading phases. The results are listed in Table 5.14, Table 5.15 and Table 5.16.

Table 5.14. K_o values for T_M specimens subject to virgin loading

Test ID	**Reconstituted relative density (%)**	**K_o at end of virgin loading** (σ'_v = 250 kPa)
T_M_201	33	0.362
T_M_202	30	0.424
T_M_203	29	0.414
T_M_204	31	0.432
T_M_205	29	0.472
T_M_206	30	0.443

Table 5.15. K_o values for T_M specimens subject to unloading

Test ID	**Reconstituted relative density (%)**	**K_o for unloading**			
		OCR = 2	**OCR = 5**	**OCR = 10**	**OCR = 25**
T_M_201	33	0.476	0.720	0.903	1.05
T_M_202	30	0.505	0.699	0.865	1.07
T_M_203	29	0.492	0.662	0.781	0.835
T_M_204	31	0.505	0.684	0.750	0.730
T_M_205	29	0.566	0.788	0.896	0.983
T_M_206	30	0.563	0.818	0.907	1.19

Table 5.16. K_o values for T_M specimens subject to reloading

Test ID	**Reconstituted relative density (%)**	**K_o at end of reloading** $\left(\sigma'_v = 400 \text{ kPa}\right)$
T_M_201	33	0.363
T_M_202	30	0.410
T_M_203	29	0.406
T_M_204	31	0.420
T_M_205	29	0.456
T_M_206	30	0.412

5.3.2 Dense specimens

Six (6) one-dimensional compression tests were performed on dense, tamped (T_D) Fraser River sand specimens. The relative densities of the test specimens ranged from 60 to 63%, with an average of 62%. Presented herein, the test data represents the characteristic one-dimensional compression response of dense, tamped sand specimens (Figure 5.27, Figure 5.28 and Figure 5.29). The full set of testing data for dense, tamped specimens is available in Appendix B.2. From comparisons of the compression responses in Appendix B.2, repeatability of the testing results was verified.

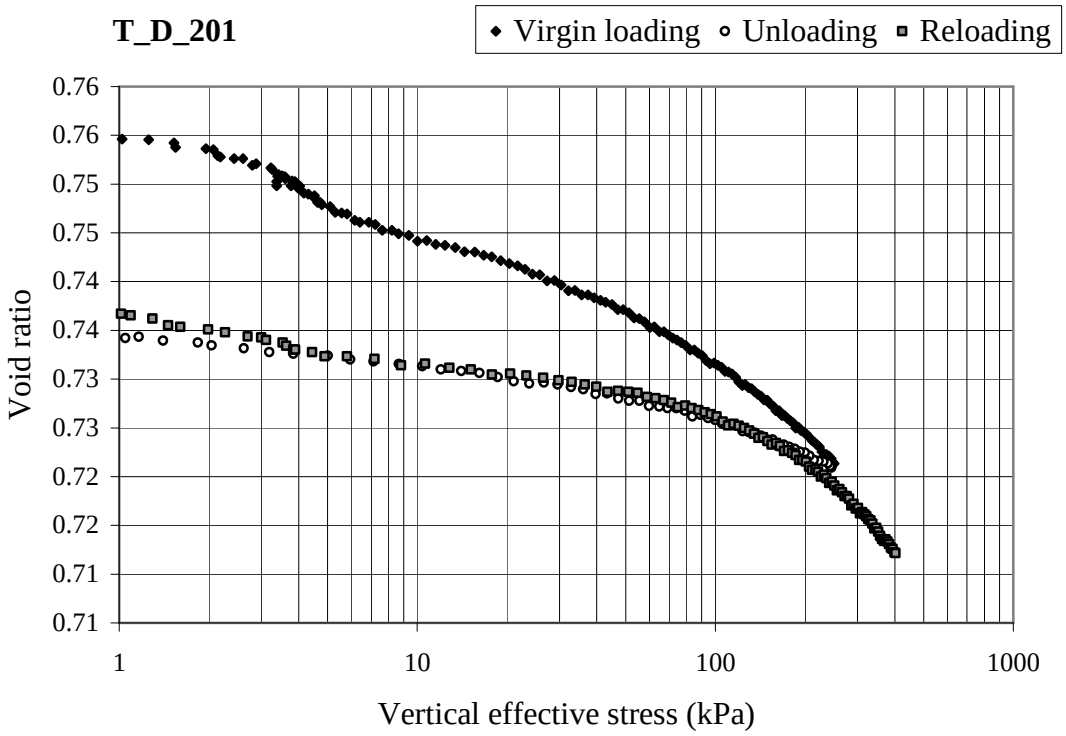

Figure 5.27. Void ratio vs. vertical effective stress for T_D_201

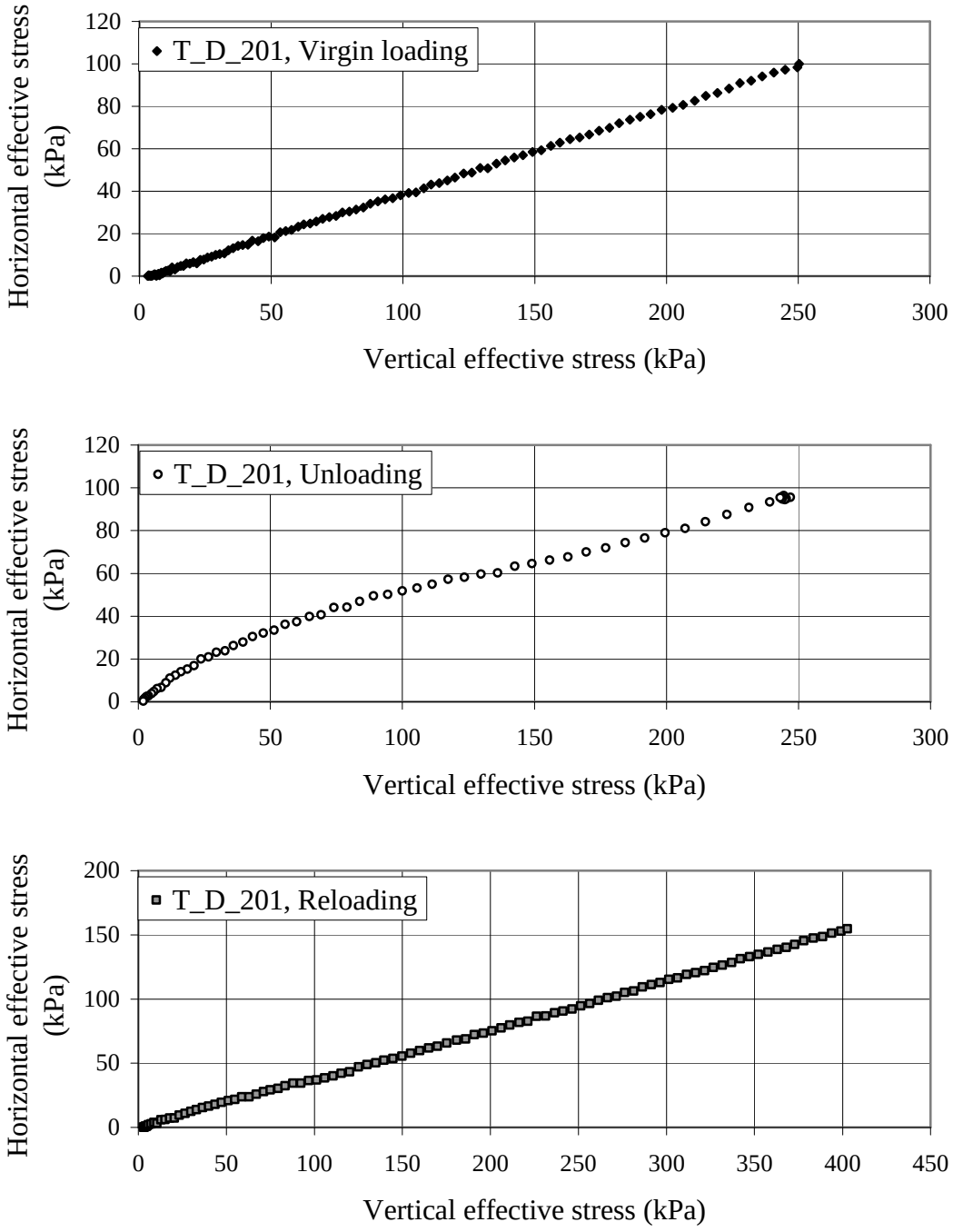

Figure 5.28. Horizontal vs. vertical effective stress for T_D_201

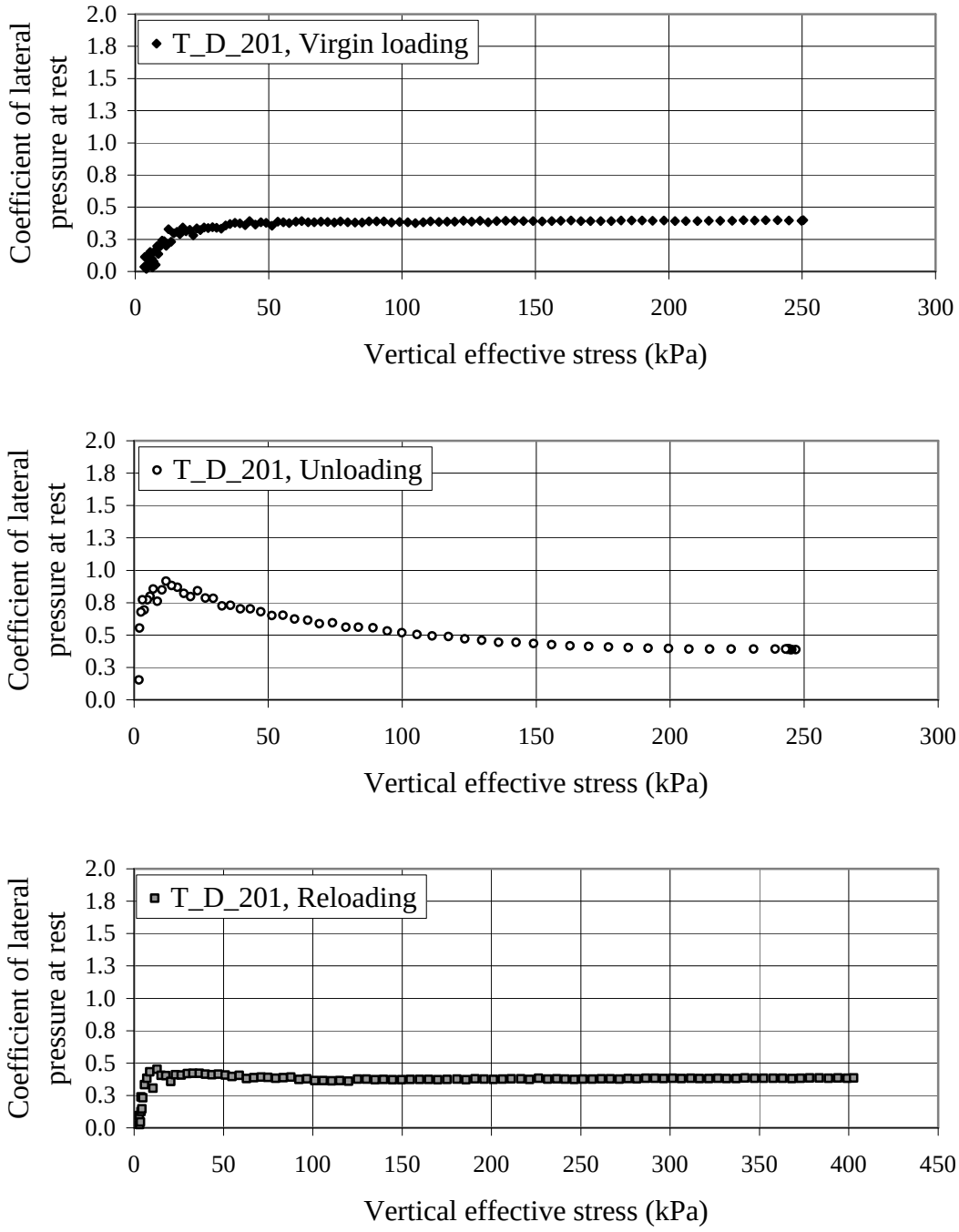

Figure 5.29. K_o vs. vertical effective stress for T_D_201

The coefficient of lateral pressure at rest for dense, tamped specimens was calculated for virgin loading, unloading and reloading phases (Table 5.17, Table 5.18 and Table 5.19).

Table 5.17. K_o values for T_D specimens subject to virgin loading

Test ID	**Reconstituted relative density (%)**	**K_o at end of virgin loading** (σ'_v = 250 kPa)
T_D_201	60	0.399
T_D_202	63	0.420
T_D_203	62	0.394
T_D_204	62	0.329
T_D_205	63	0.434
T_D_206	61	0.358

Table 5.18. K_o values for T_D specimens subject to unloading

Test ID	**Reconstituted relative density (%)**	**K_o for unloading**			
		OCR = 2	**OCR = 5**	**OCR = 10**	**OCR = 25**
T_D_201	60	0.471	0.650	0.842	0.849
T_D_202	63	0.522	0.762	0.957	1.14
T_D_203	62	0.485	0.689	0.774	0.750
T_D_204	62	0.443	0.651	0.789	0.929
T_D_205	63	0.535	0.750	0.895	0.966
T_D_206	61	0.456	0.637	0.782	0.917

Table 5.19. K_o values for T_D specimens subject to reloading

Test ID	**Reconstituted relative density (%)**	**K_o at end of reloading** $\left(\sigma'_v = 400 \text{ kPa}\right)$
T_D_201	60	0.383
T_D_202	63	0.404
T_D_203	62	0.375
T_D_204	62	0.317
T_D_205	63	0.412
T_D_206	61	0.342

5.3.3 Very dense specimens

Five (5) one-dimensional compression tests were performed on very dense, tamped (T_V) Fraser River sand specimens. The relative densities of the test specimens varied from 85 to 87%, with an average of 86%. Test data is presented herein to represent typical one-dimensional compression response of very dense, tamped sand specimens (Figure 5.30, Figure 5.31 and Figure 5.32). For very dense, tamped specimens, the complete set of testing data is available in Appendix B.3. Repeatability of the testing results was verified from comparisons of the compression responses plotted in Appendix B.3.

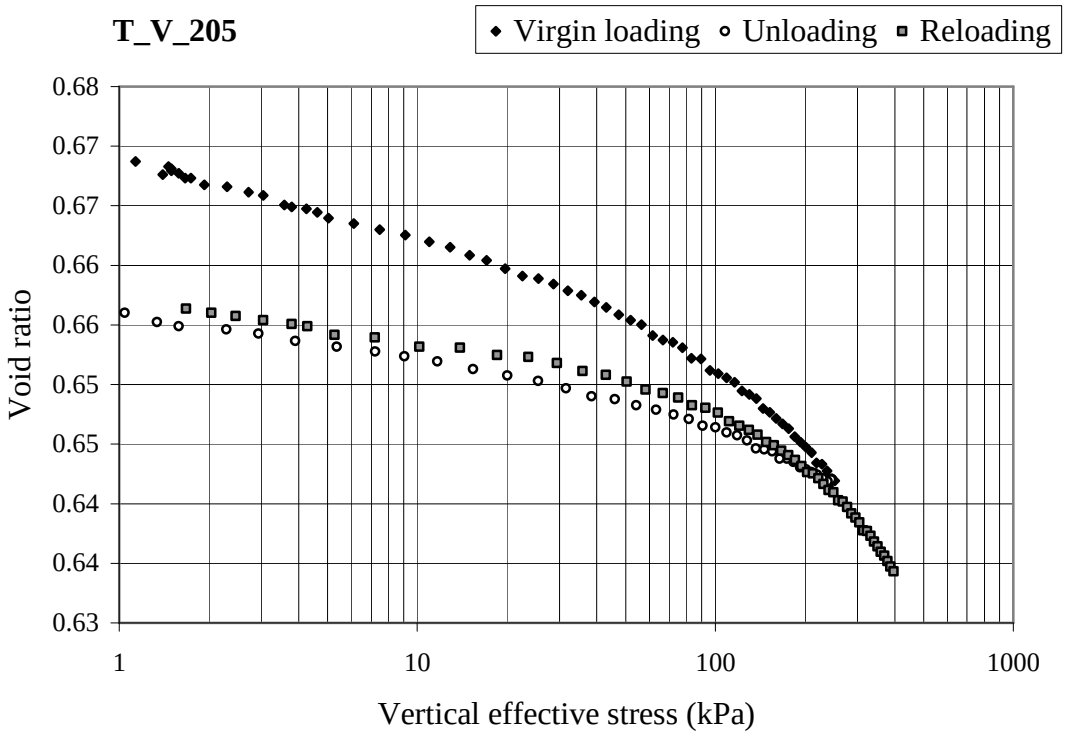

Figure 5.30. Void ratio vs. vertical effective stress for T_V_205

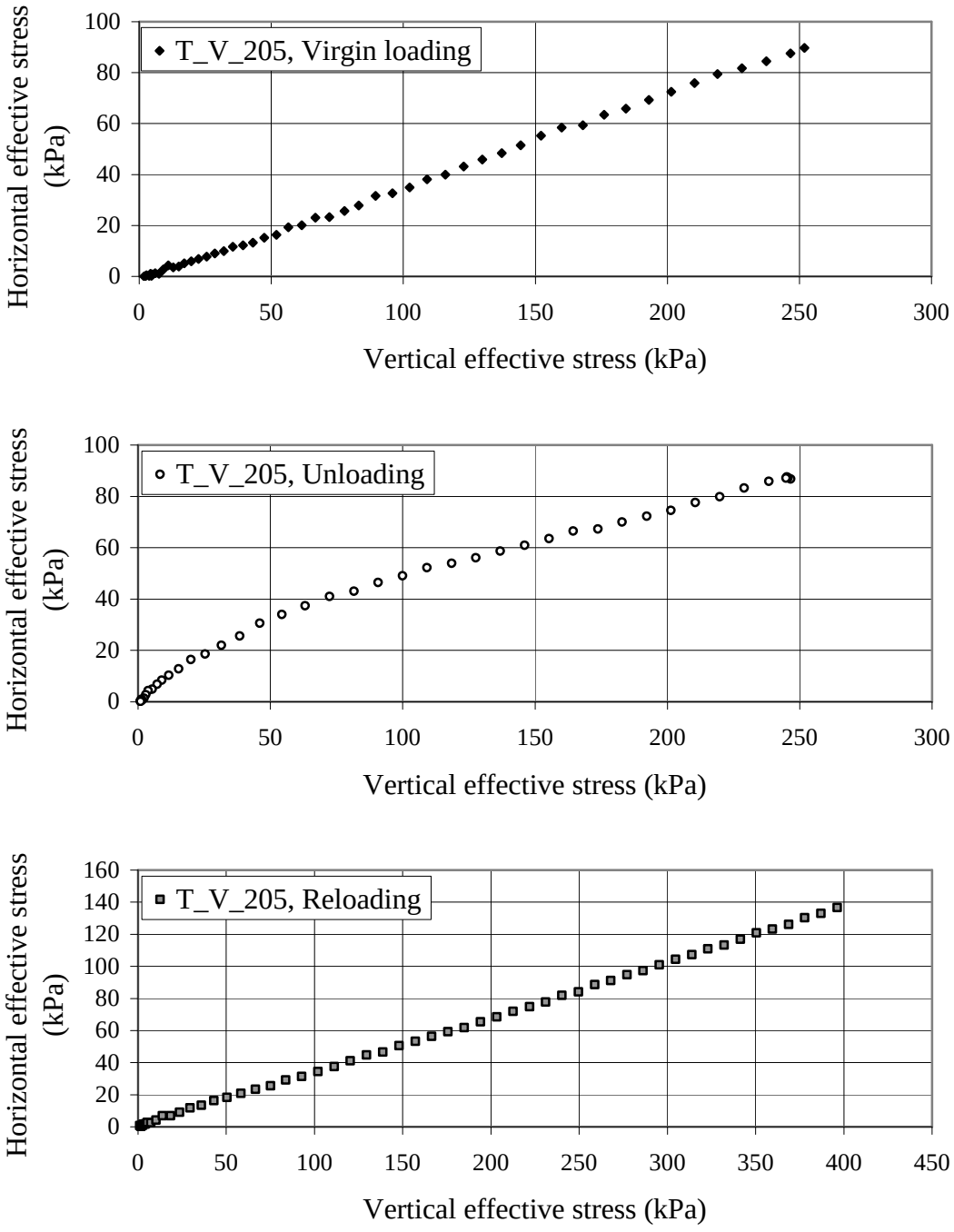

Figure 5.31. Horizontal vs. vertical effective stress for T_V_205

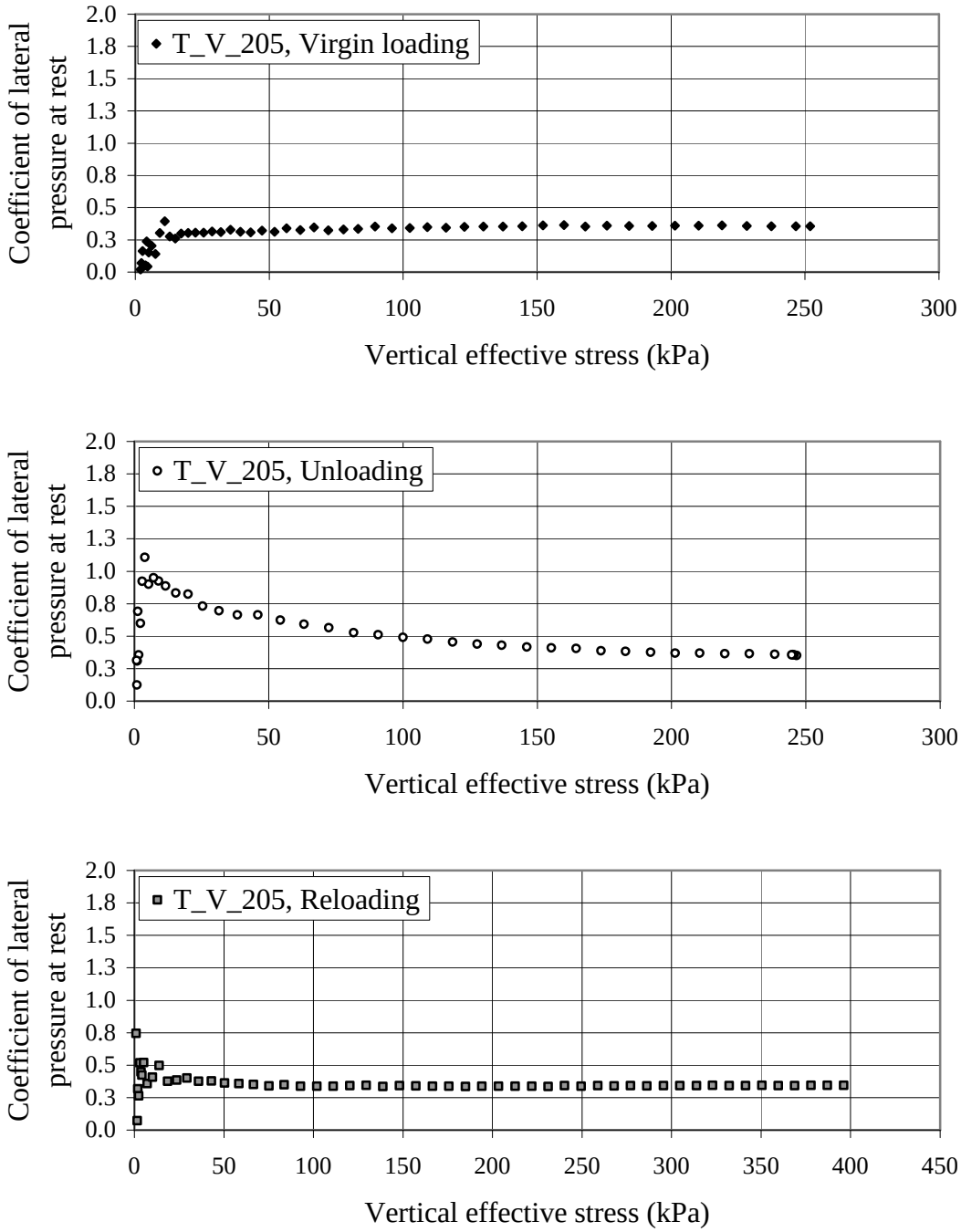

Figure 5.32. K_o vs. vertical effective stress for T_V_205

The coefficient of lateral pressure at rest for very dense, tamped specimens was computed for all loading phases (Table 5.20, Table 5.21 and Table 5.22).

Table 5.20. K_o values for T_V specimens subject to virgin loading

Test ID	**Reconstituted relative density (%)**	**K_o at end of virgin loading** ($\sigma_v^{'}$ = 250 kPa)
T_V_201	87	0.328
T_V_202	86	0.331
T_V_203	87	0.341
T_V_204	86	0.369
T_V_205	85	0.356

Table 5.21. K_o values for T_V specimens subject to unloading

Test ID	**Reconstituted relative density (%)**	**K_o for unloading**			
		OCR = 2	**OCR = 5**	**OCR = 10**	**OCR = 25**
T_V_201	87	0.403	0.606	0.763	0.799
T_V_202	86	0.434	0.677	0.829	0.868
T_V_203	87	0.461	0.661	0.785	0.822
T_V_204	86	0.491	0.680	0.845	0.868
T_V_205	85	0.439	0.624	0.732	0.926

Table 5.22. K_o values for T_V specimens subject to reloading

Test ID	**Reconstituted relative density (%)**	**K_o at end of reloading** $\left(\sigma_v^{'} = 400 \text{ kPa}\right)$
T_V_201	87	0.315
T_V_202	86	0.322
T_V_203	87	0.323
T_V_204	86	0.361
T_V_205	85	0.345

5.3.4 Effect of densification

For tamped specimens, the effect of densification during reconstitution may be observed by comparing the plotted compression test data. Figure 5.33 compares horizontal versus vertical effective stress during virgin loading, unloading and reloading for medium loose, dense and very dense tamped specimens.

From Figure 5.33, the slope of the stress plot, $\overset{o}{K}$, for virgin loading and reloading phases increases with decreasing reconstituted relative density. During unloading, similar curvature is observed for all reconstituted densities, with the curves gradually converging near zero vertical stress.

The coefficient of lateral pressure at rest as a function of the vertical effective stress is plotted in Figure 5.34 for medium loose, dense and very dense tamped specimens. In both virgin loading and reloading, the constant K_o value increases with decreasing relative density. During unloading, all reconstituted densities exhibit similar concave-up curvature.

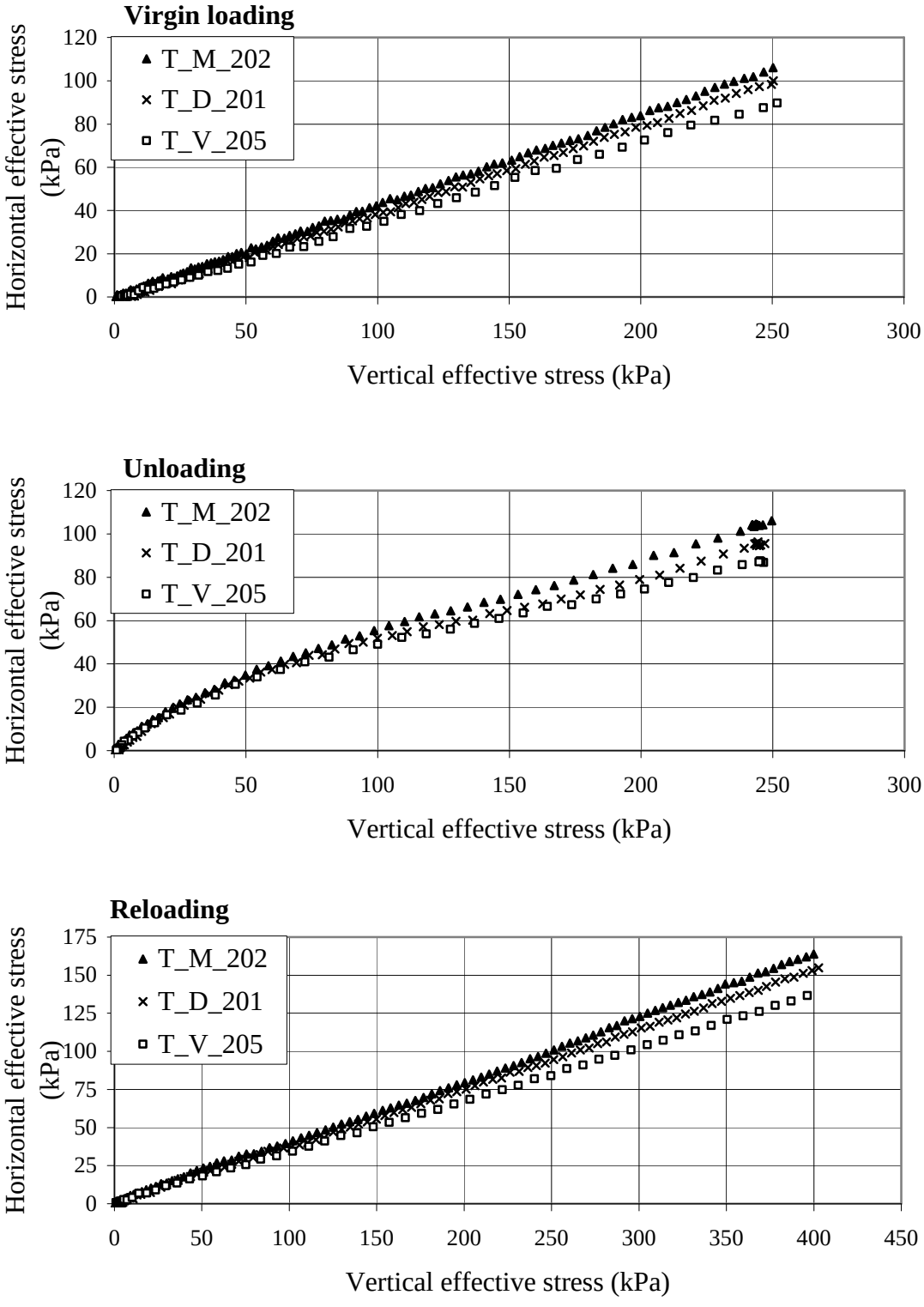

Figure 5.33. Comparison of horizontal vs. vertical effective stress for T specimens

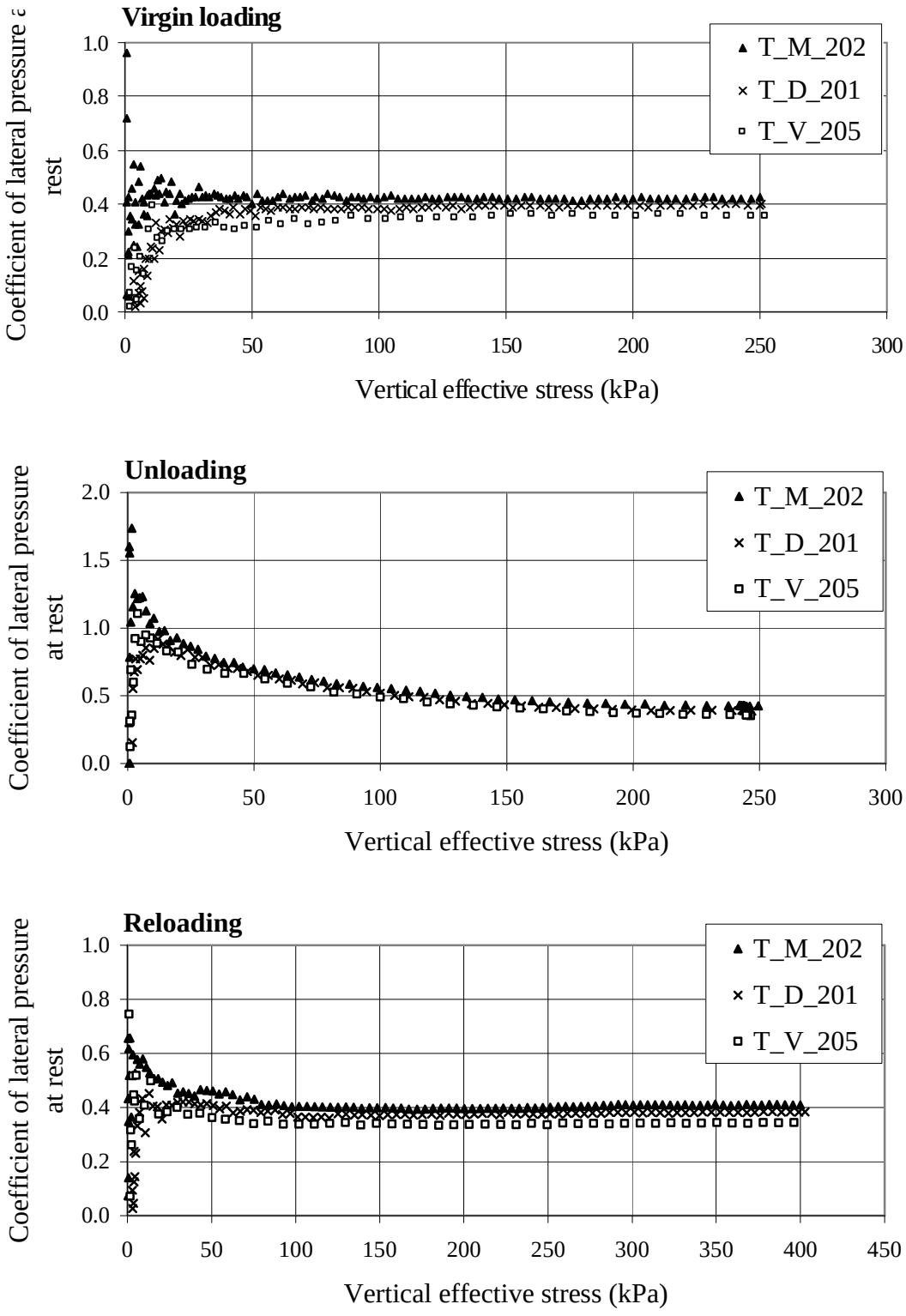

Figure 5.34. Comparison of K_o vs. vertical effective stress for T specimens

The coefficient of lateral pressure at rest, calculated at the end of virgin loading, was compared for all seventeen (17) one-dimensional compression tests performed on tamped specimens (see Figure 5.35). The shaded region in Figure 5.35 corresponds to a general envelope estimated from the compression test results.

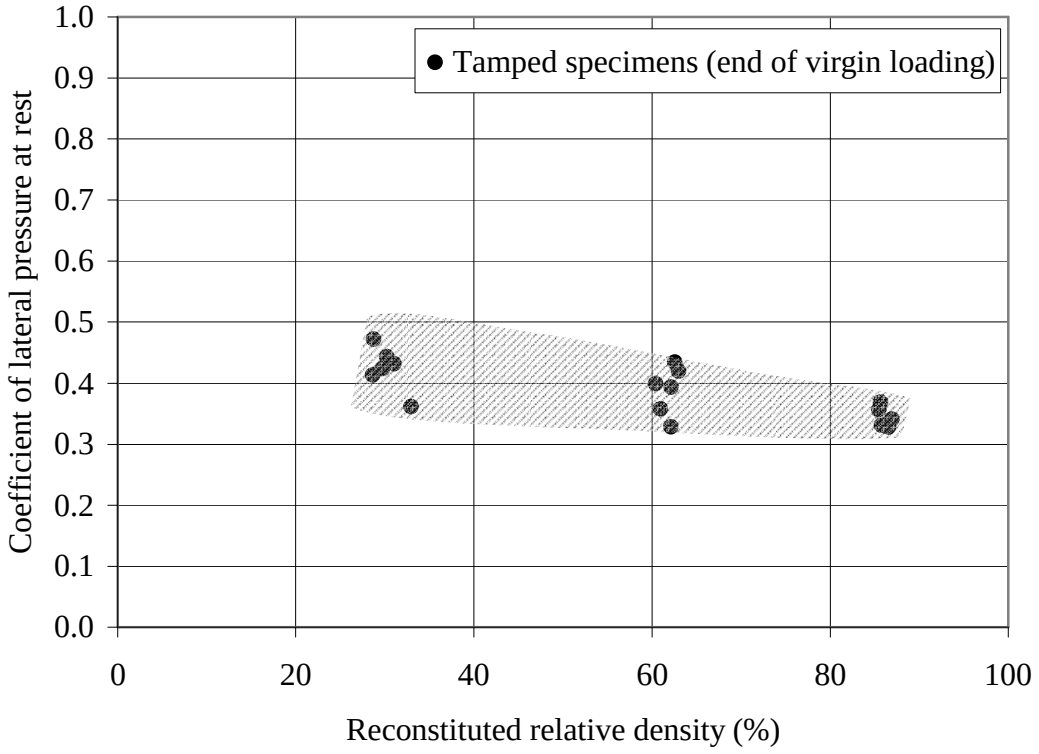

Figure 5.35. K_o at the end of virgin loading for T specimens

Figure 5.35 corroborates previous observations of a decrease in K_o with increasing relative density. Also, the plot suggests that with increasing reconstituted relative density, the scatter in measured K_o values is minimized.

5.3.5 Effect of loading history

The effect of specimen loading history may be observed for tamped specimens by comparing the plotted compression test data. Horizontal versus vertical effective stress is

shown in Figure 5.36 during virgin loading and reloading for a dense, tamped specimen. A marginal decrease in the slope is noted from virgin loading to reloading.

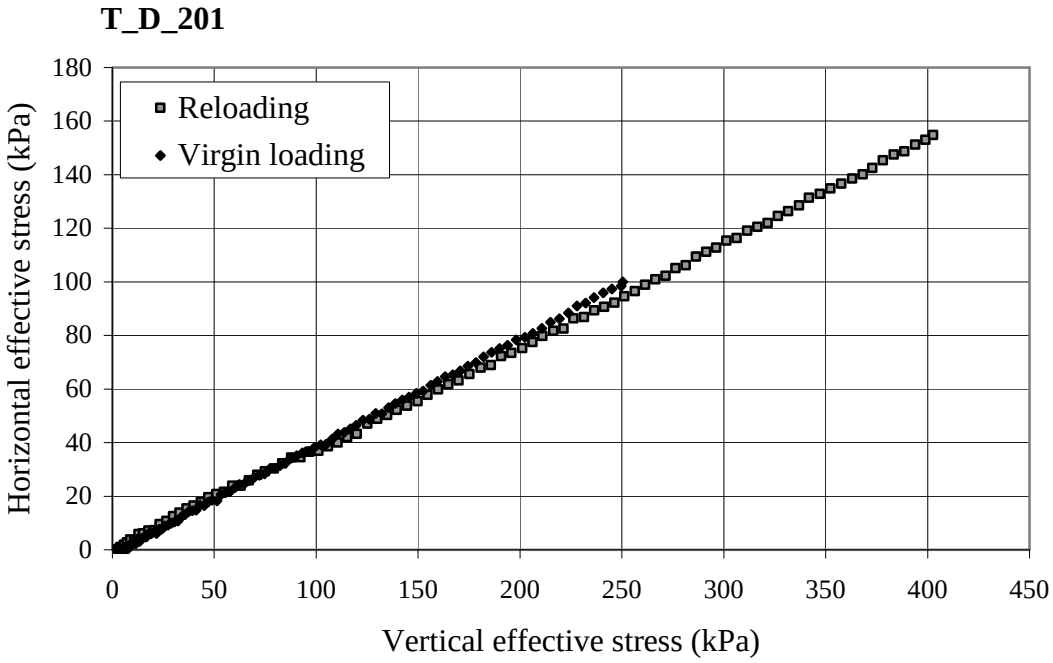

Figure 5.36. Comparison of horizontal vs. vertical effective stress during virgin loading and reloading for T_D_201

Figure 5.37 shows the coefficient of lateral pressure at rest during virgin loading and reloading for a dense, air-pluviated specimen. The plot also shows a slight decrease in the constant K_o value from virgin loading to reloading. As the specimen is reloaded past its preconsolidation pressure, no noticeable change in K_o is observed.

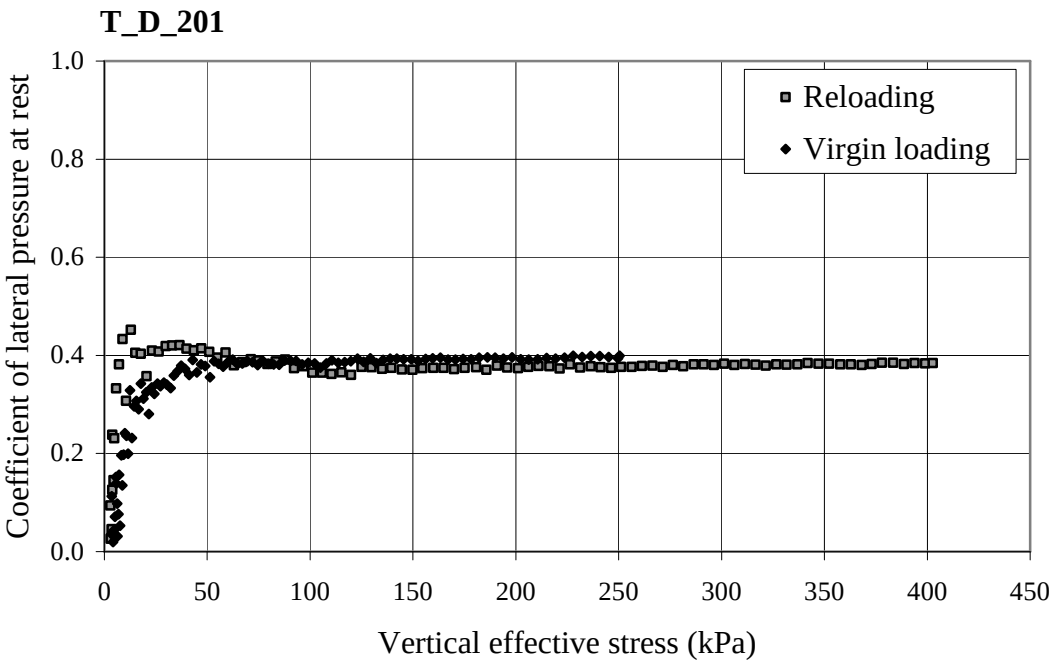

Figure 5.37. Comparison K_o vs. vertical effective stress during virgin loading and reloading for T_D_201

Although not shown here, the effect of loading history on very loose, medium loose and very dense tamped specimens was found to be comparable to that observed in dense, tamped specimens (see Figure 5.36, Figure 5.37).

To best observe the effect of loading history, the coefficient of lateral pressure at rest, at the end of both virgin loading and reloading was compared for all seventeen (17) one-dimensional compression tests performed on tamped specimens (see Figure 5.38). For all reconstituted densities, K_o values measured at the end of reloading are marginally lower than those at the end of virgin loading.

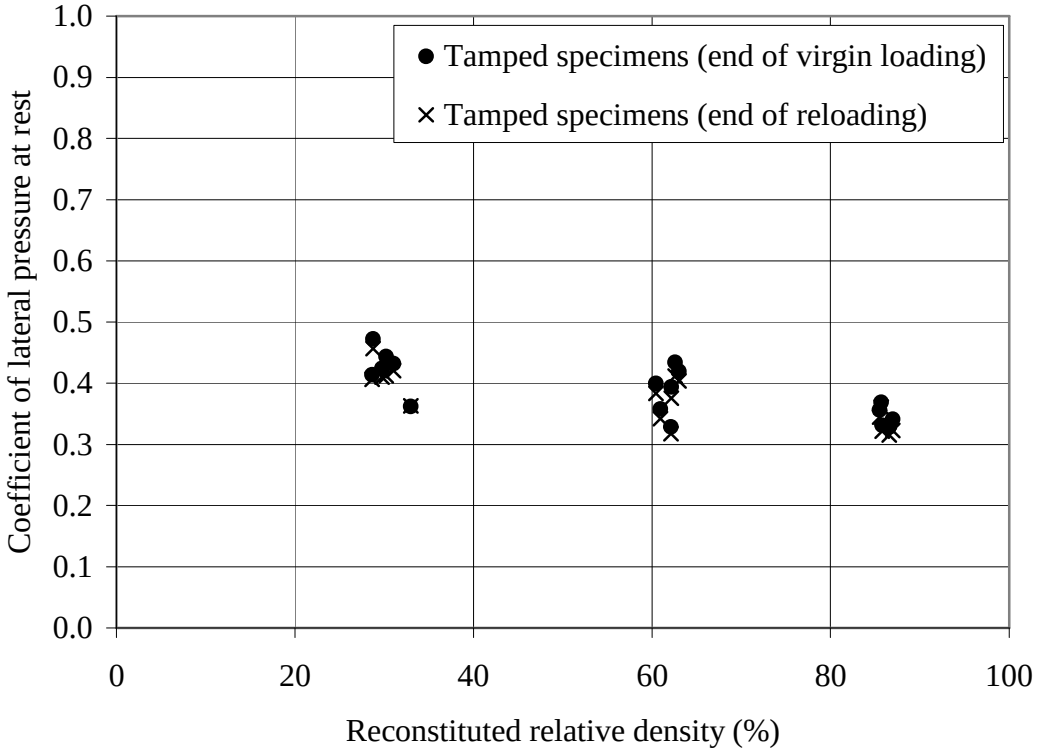

Figure 5.38. K_o at the end of virgin loading and reloading for T specimens

Additionally, the coefficient of lateral pressure at rest, determined for selected OCR values during unloading, was compared for all seventeen (17) one-dimensional compression tests on tamped specimens (see Figure 5.39). K_o values for all densities increase as OCR increases, although not as dramatically as observed for air-pluviated specimens. Again, the scatter in K_o values increases with increasing OCR, although not as greatly as for air-pluviated specimens.

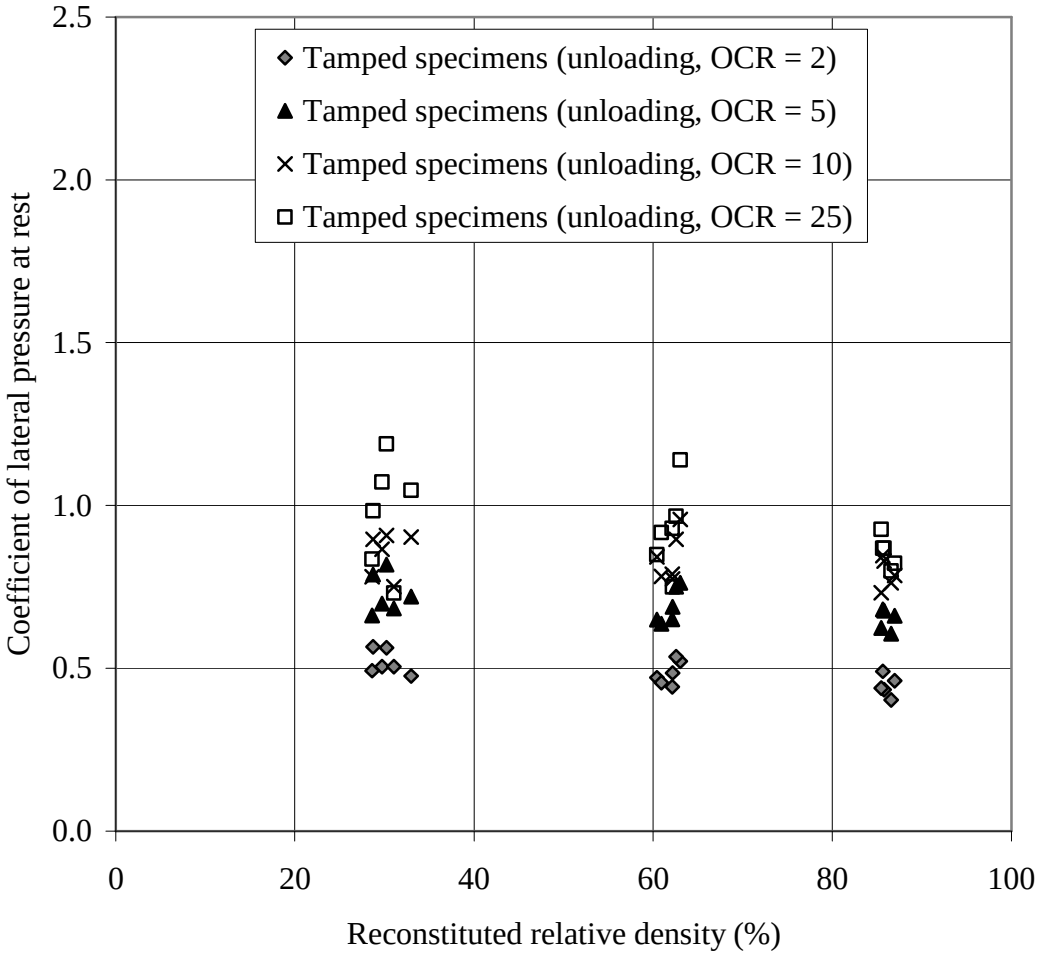

Figure 5.39. K_o at varied OCR values during unloading for T specimens

5.4 Vibrated Fraser River sand specimens

5.4.1 Medium loose specimens

Six (6) one-dimensional compression tests were performed on medium loose, vibrated (V_M) Fraser River sand specimens. The relative densities of the test specimens ranged from 24 to 34%, with an average value of 27%. The test data presented herein represents the typical one-dimensional compression response of medium loose, vibrated sand specimens (Figure 5.40, Figure 5.41 and Figure 5.42). For the complete set of medium loose, vibrated specimen testing data and verification of repeatability, refer to Appendix C.1.

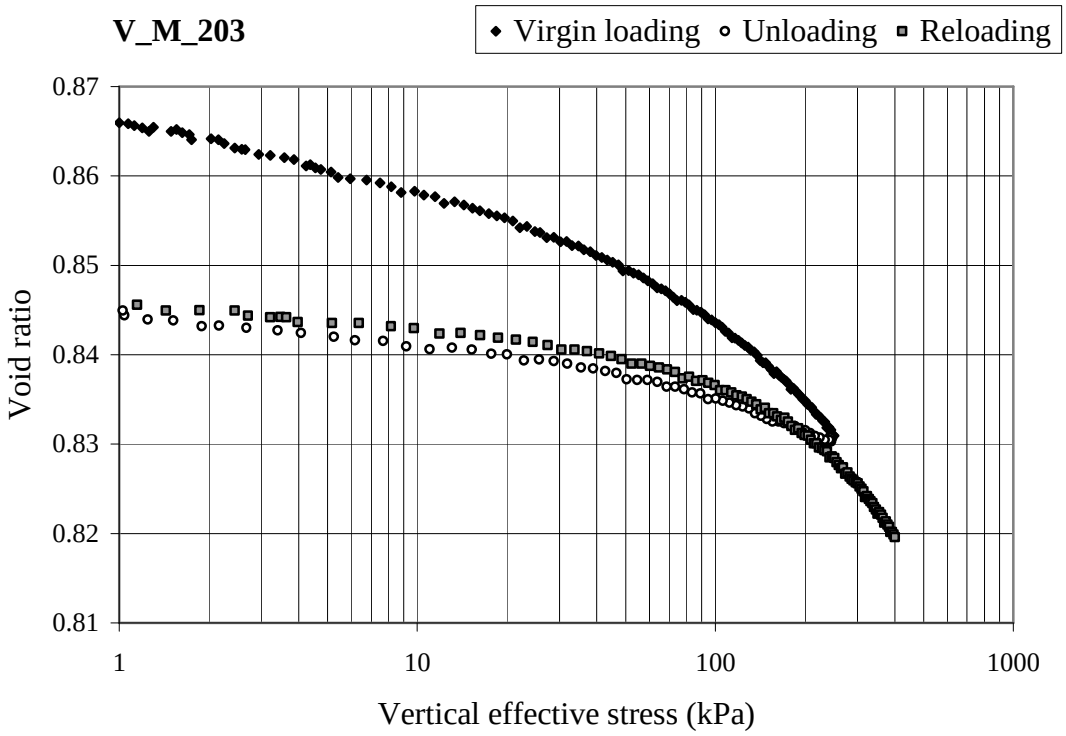

Figure 5.40. Void ratio vs. vertical effective stress for V_M_203

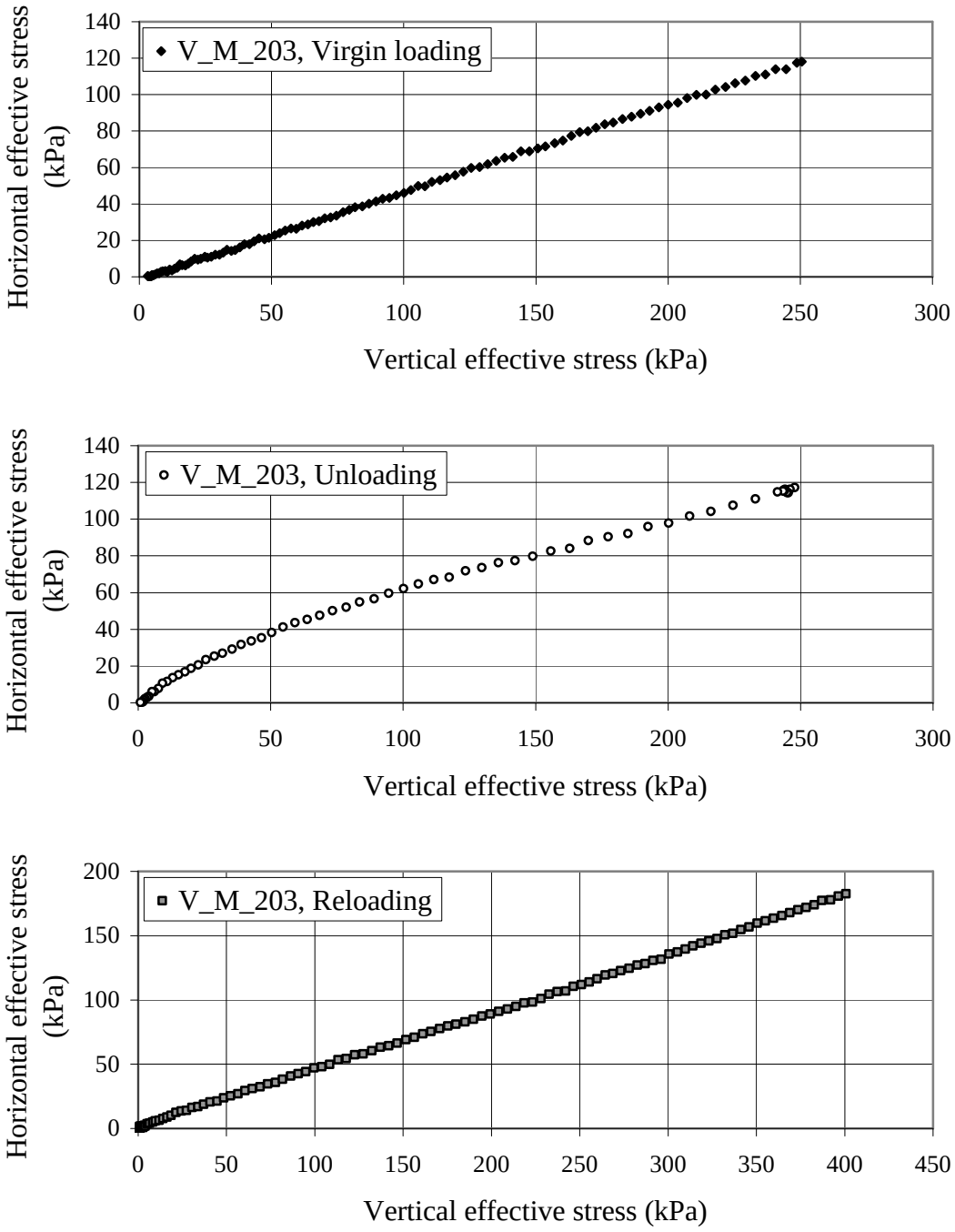

Figure 5.41. Horizontal vs. vertical effective stress for V_M_203

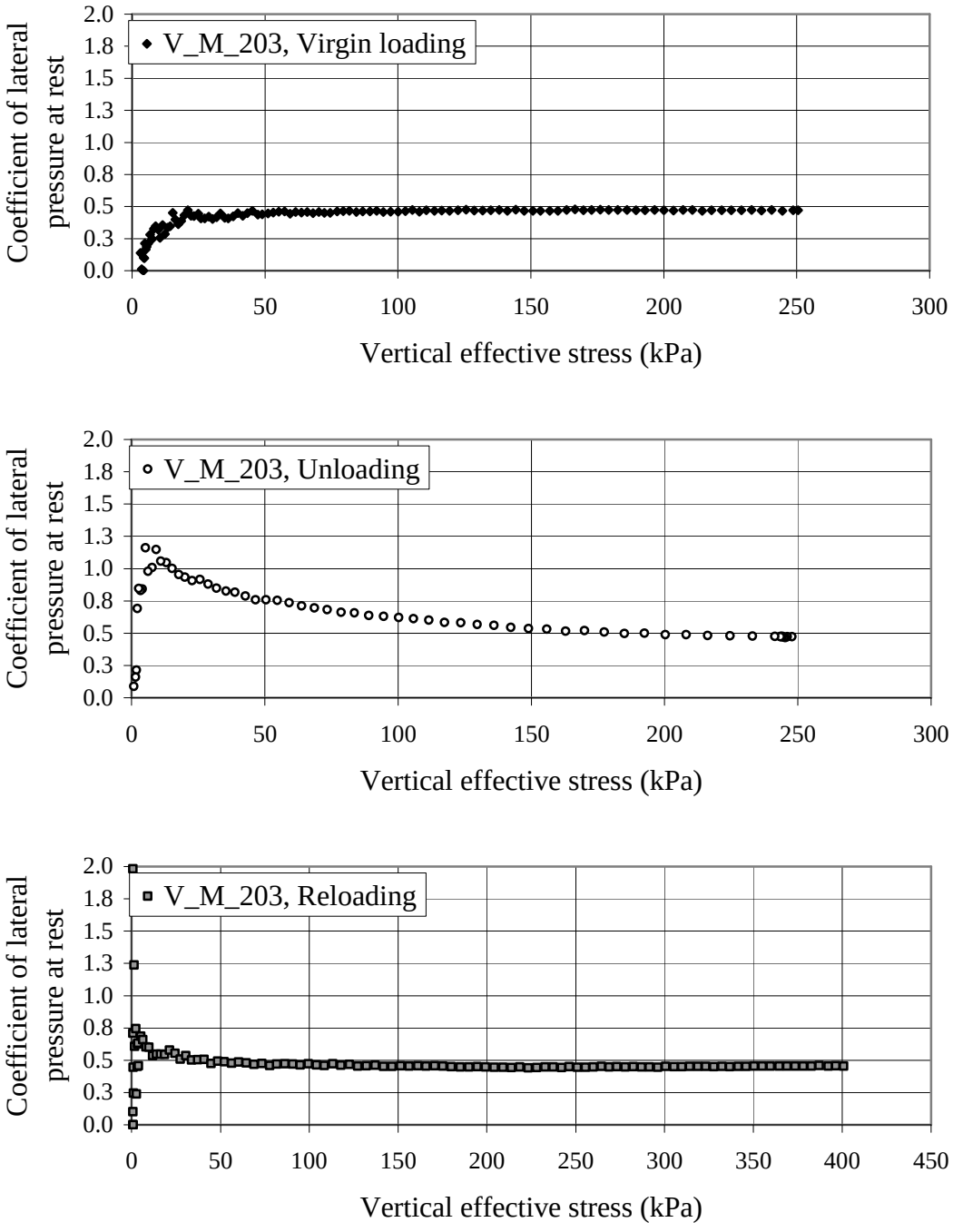

Figure 5.42. K_o vs. vertical effective stress for V_M_203

For all loading phases, the coefficient of lateral pressure at rest for medium loose, vibrated specimens was determined (Table 5.23, Table 5.24 and Table 5.25).

Table 5.23. K_o values for V_M specimens subject to virgin loading

Test ID	**Reconstituted relative density (%)**	**K_o at end of virgin loading** (σ'_v = 250 kPa)
V_M_201	26	0.485
V_M_202	24	0.463
V_M_203	28	0.471
V_M_204	34	0.455
V_M_205	26	0.448
V_M_206	26	0.461

Table 5.24. K_o values for V_M specimens subject to unloading

Test ID	**Reconstituted relative density (%)**	**K_o for unloading**			
		OCR = 2	**OCR = 5**	**OCR = 10**	**OCR = 25**
V_M_201	26	0.605	0.840	1.02	1.16
V_M_202	24	0.552	0.730	0.881	1.03
V_M_203	28	0.581	0.757	0.915	1.06
V_M_204	34	0.528	0.669	0.743	0.759
V_M_205	26	0.532	0.698	0.795	0.900
V_M_206	26	0.546	0.735	0.816	0.756

Table 5.25. K_o values for V_M specimens subject to reloading

Test ID	**Reconstituted relative density (%)**	**K_o at end of reloading** $\left(\sigma'_v = 400 \text{ kPa}\right)$
V_M_201	26	0.434
V_M_202	24	0.435
V_M_203	28	0.455
V_M_204	34	0.439
V_M_205	26	0.438
V_M_206	26	0.419

5.4.2 Dense specimens

Six (6) one-dimensional compression tests were performed on dense, vibrated (V_D) Fraser River sand specimens. Relative densities of the specimens ranged from 58 to 64% and had an average value of 62%. The test data, as presented herein, describes the representative one-dimensional compression response of dense, vibrated sand specimens (Figure 5.43, Figure 5.44 and Figure 5.45). The full set of testing data for dense, vibrated specimens is available in Appendix C.2. Repeatability of the results was verified from comparisons of the compression response plots in Appendix C.2.

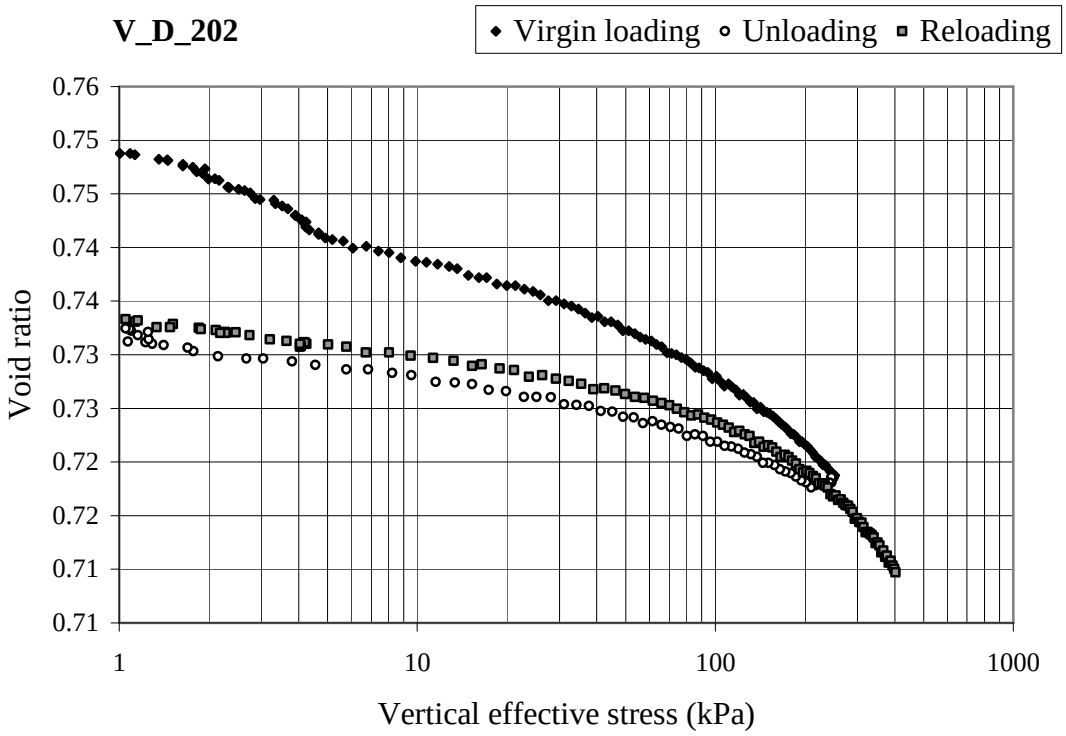

Figure 5.43. Void ratio vs. vertical effective stress for V_D_202

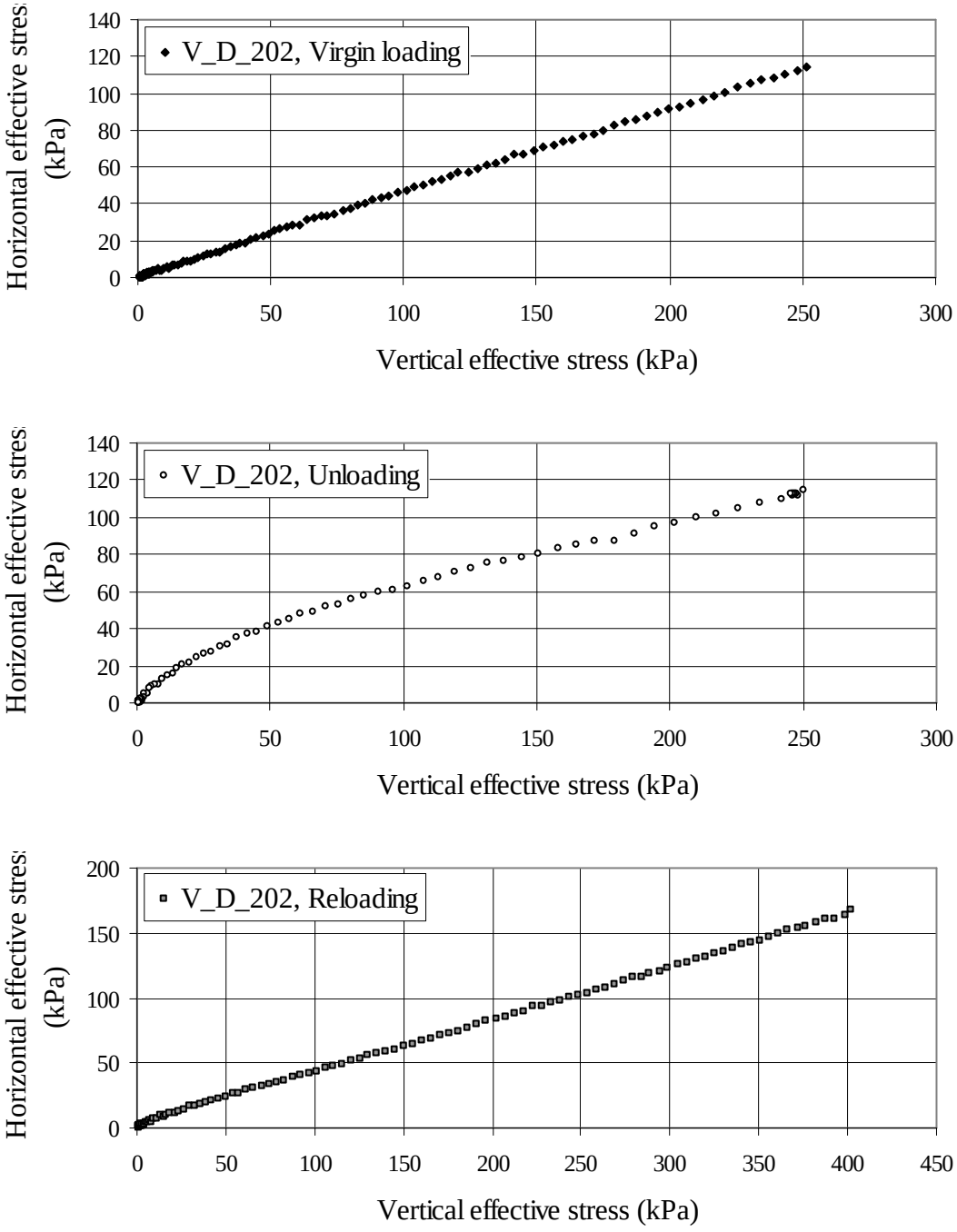

Figure 5.44. Horizontal vs. vertical effective stress for V_D_202

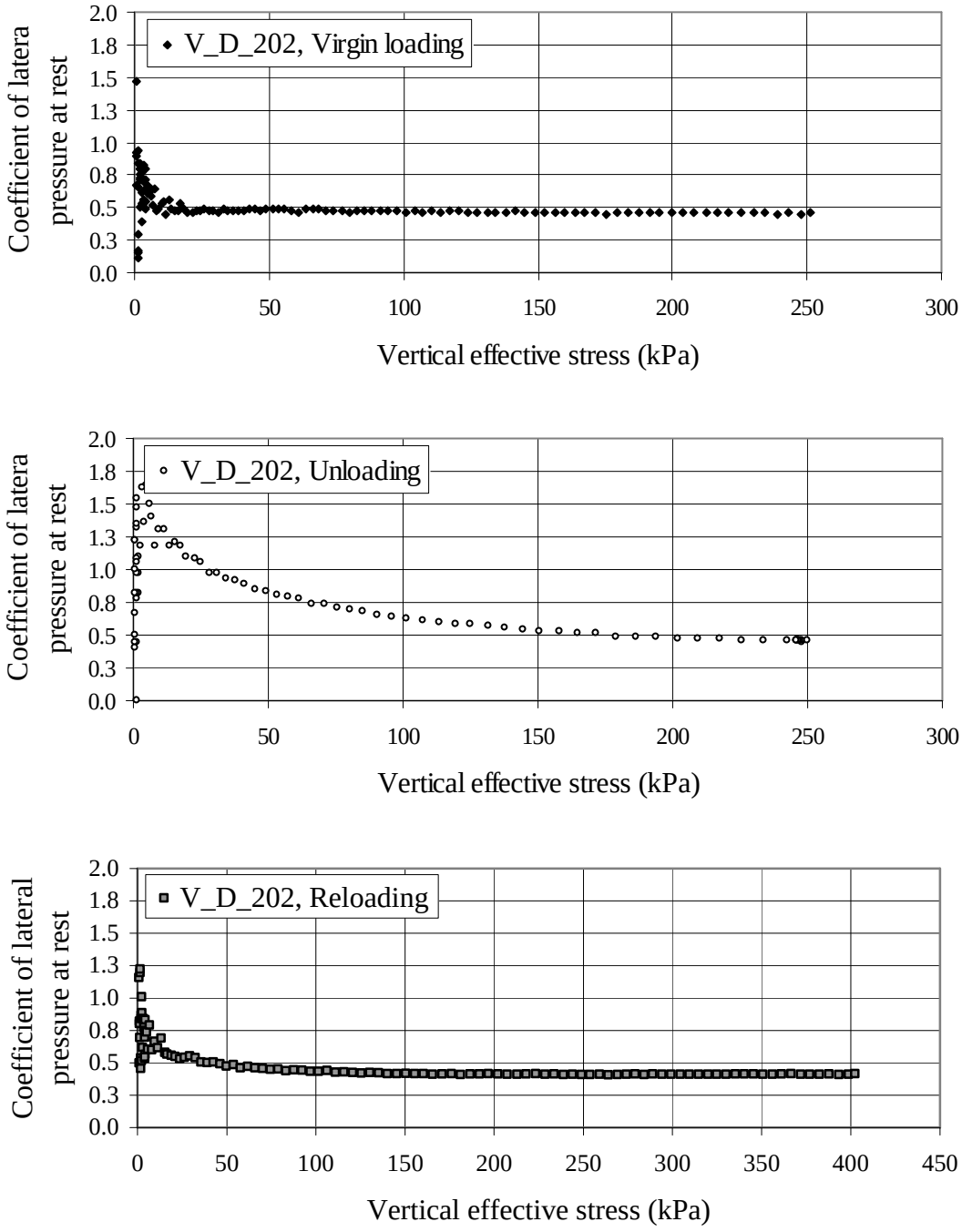

Figure 5.45. K_o vs. vertical effective stress for V_D_202

The coefficient of lateral pressure at rest for dense, vibrated specimens was computed for virgin loading, unloading and reloading phases, as detailed in Table 5.26, Table 5.27 and Table 5.28.

Table 5.26. K_o values for V_D specimens subject to virgin loading

Test ID	**Reconstituted relative density (%)**	**K_o at end of virgin loading** (σ'_v = 250 kPa)
V_D_201	62	0.508
V_D_202	62	0.456
V_D_203	64	0.493
V_D_204	63	0.391
V_D_205	64	0.511
V_D_206	58	0.454

Table 5.27. K_o values for V_D specimens subject to unloading

Test ID	**Reconstituted relative density (%)**	**K_o for unloading**			
		OCR = 2	**OCR = 5**	**OCR = 10**	**OCR = 25**
V_D_201	62	0.620	0.879	1.10	1.37
V_D_202	62	0.577	0.840	1.06	1.30
V_D_203	64	0.642	0.952	1.12	1.32
V_D_204	63	0.503	0.736	0.895	1.07
V_D_205	64	0.635	0.889	1.14	1.48
V_D_206	58	0.582	0.815	1.03	1.23

Table 5.28. K_o values for V_D specimens subject to reloading

Test ID	**Reconstituted relative density (%)**	**K_o at end of reloading** $\left(\sigma'_v = 400 \text{ kPa}\right)$
V_D_201	62	0.474
V_D_202	62	0.412
V_D_203	64	0.446
V_D_204	63	0.379
V_D_205	64	0.466
V_D_206	58	0.423

5.4.3 Very dense specimens

Five (5) one-dimensional compression tests were performed on very dense, vibrated (V_V) Fraser River sand specimens. The relative densities of the test specimens ranged from 84 to 86%, with an average of 85%. Test data presented herein represents the typical one-dimensional compression response for very dense, vibrated sand specimens (Figure 5.46, Figure 5.47, and Figure 5.48). Refer to Appendix C.3 for the full set of testing data for very dense, vibrated specimens. Comparisons of the plots in Appendix C.3 verifies repeatability of the testing results.

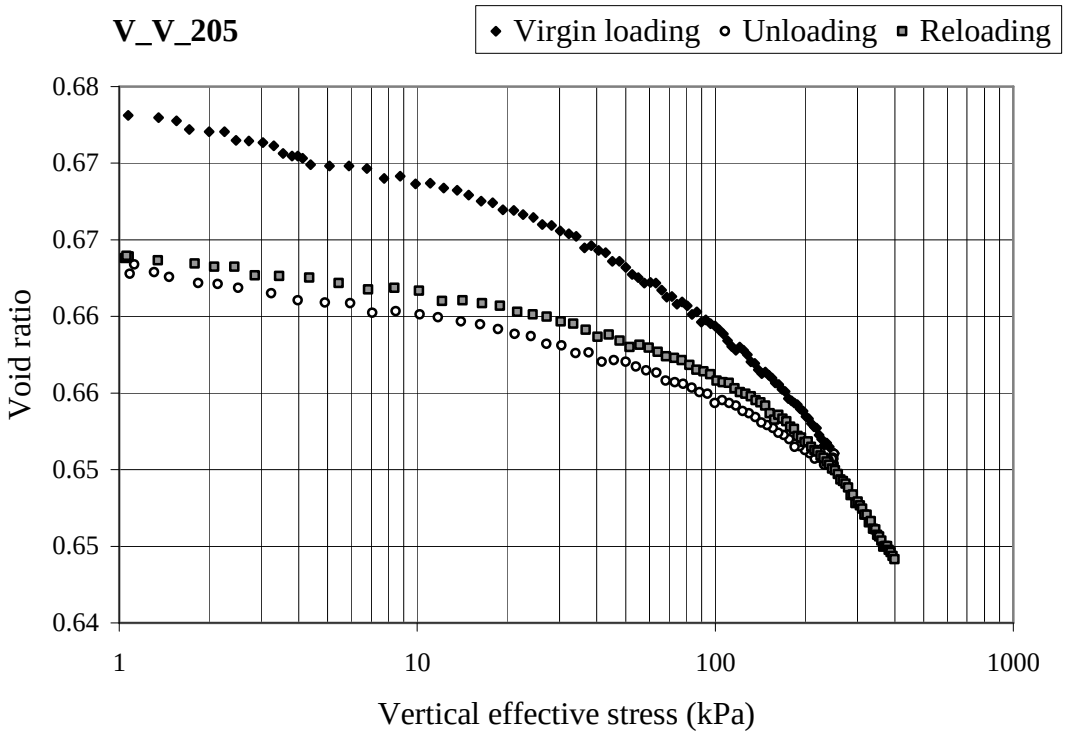

Figure 5.46. Void ratio vs. vertical effective stress for V_V_205

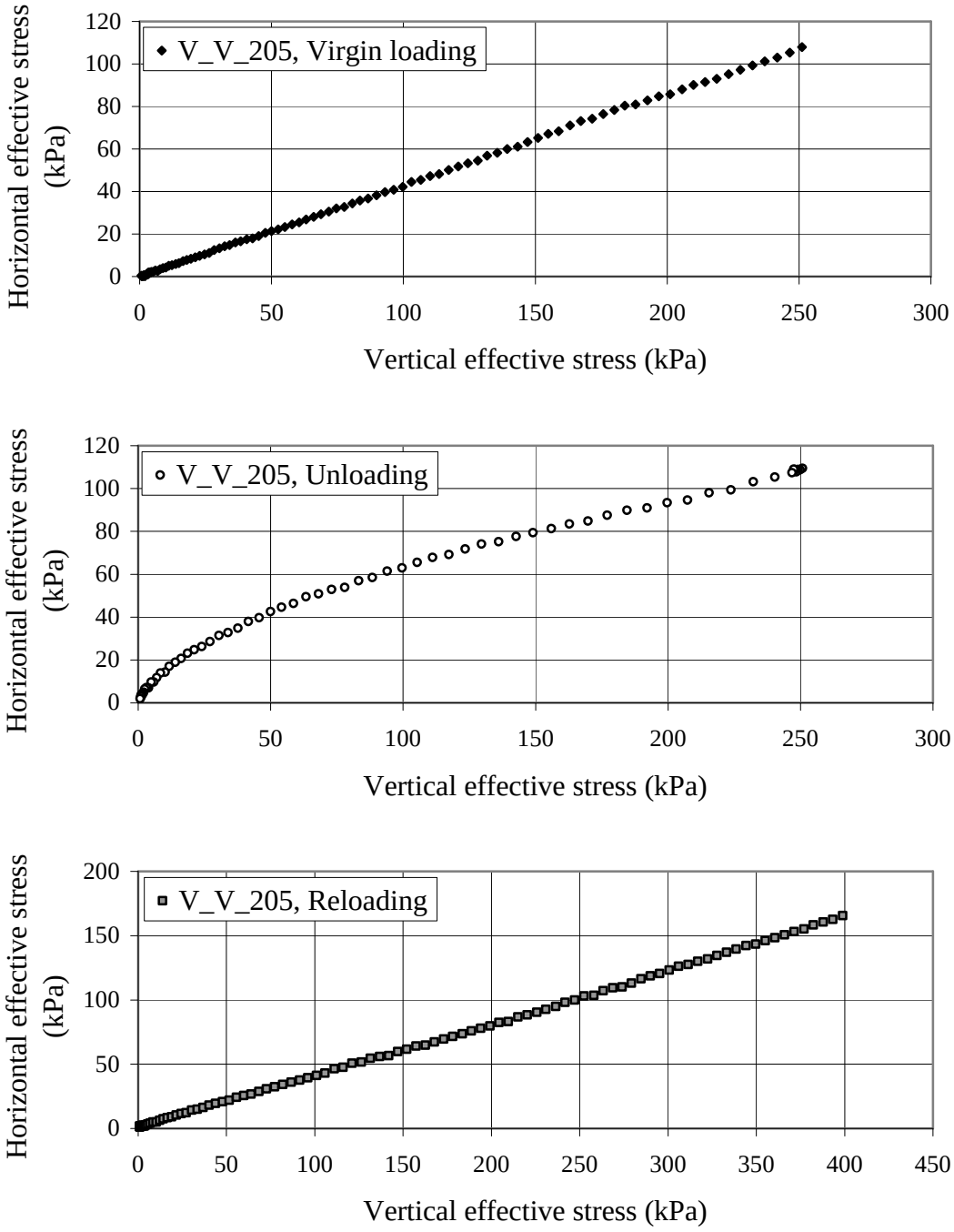

Figure 5.47. Horizontal vs. vertical effective stress for V_V_205

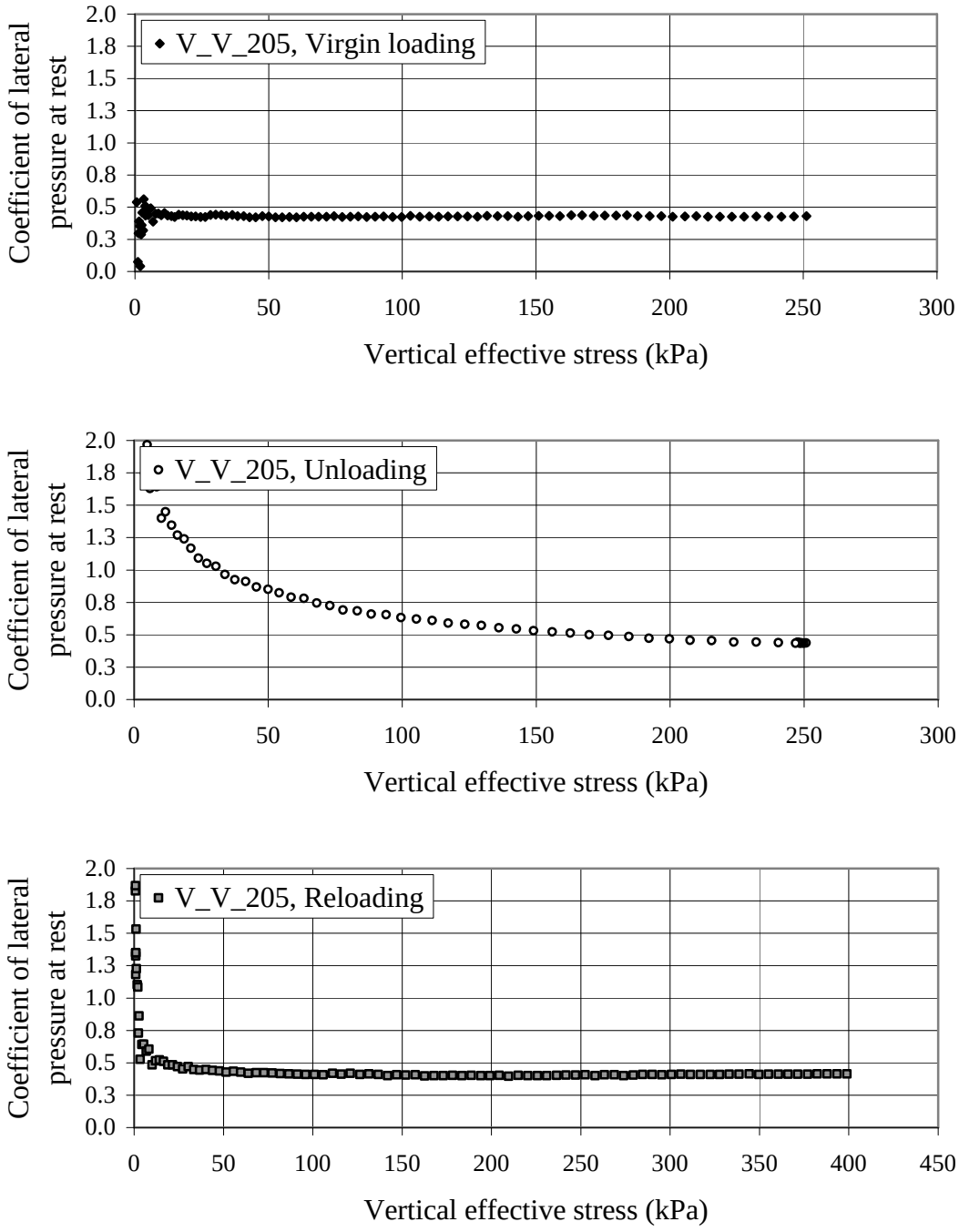

Figure 5.48. K_o vs. vertical effective stress for V_V_205

For very dense, vibrated specimens, the coefficient of lateral pressure at rest was calculated for all loading phases (Table 5.29, Table 5.30 and Table 5.31).

Table 5.29. K_o values for V_V specimens subject to virgin loading

Test ID	**Reconstituted relative density (%)**	**K_o at end of virgin loading** (σ'_v = 250 kPa)
V_V_201	86	0.466
V_V_202	84	0.398
V_V_203	86	0.432
V_V_204	85	0.415
V_V_205	84	0.430

Table 5.30. K_o values for V_V specimens subject to unloading

Test ID	**Reconstituted relative density (%)**	**K_o for unloading**			
		OCR = 2	**OCR = 5**	**OCR = 10**	**OCR = 25**
V_V_201	86	0.598	0.917	1.21	1.86
V_V_202	84	0.467	0.673	0.836	0.915
V_V_203	86	0.590	0.902	1.18	1.54
V_V_204	85	0.539	0.789	1.01	1.24
V_V_205	84	0.581	0.850	1.09	1.40

Table 5.31. K_o values for V_V specimens subject to reloading

Test ID	**Reconstituted relative density (%)**	**K_o at end of reloading** (σ'_v = 400 kPa)
V_V_201	86	0.434
V_V_202	84	0.383
V_V_203	86	0.395
V_V_204	85	0.377
V_V_205	84	0.415

5.4.4 Effect of densification

For vibrated specimens, the effect of specimen densification during reconstitution may be examined by comparing the plotted compression test results. In Figure 5.49, a plot of horizontal versus vertical effective stress during virgin loading, unloading and reloading is shown for medium loose, dense and very dense vibrated specimens.

From Figure 5.49, the slope of the linear stress plot, $\overset{o}{K}$, for virgin loading and reloading phases tends to increase slightly with decreasing reconstituted relative density. Still, the decrease in $\overset{o}{K}$ for vibrated specimens appears to be less prominent than that noted in both air-pluviated and tamped specimens. Similar curvature is observed for all reconstituted densities during unloading.

Figure 5.50 displays the coefficient of lateral pressure at rest versus the vertical effective stress for medium loose, dense and very dense vibrated specimens. The constant K_o values for both virgin loading and reloading tend to increase with decreasing relative density, if only slightly. During unloading, all reconstituted densities exhibit similar concave-up curvature. As unloading progresses to zero effective vertical stress, the curves slightly diverge.

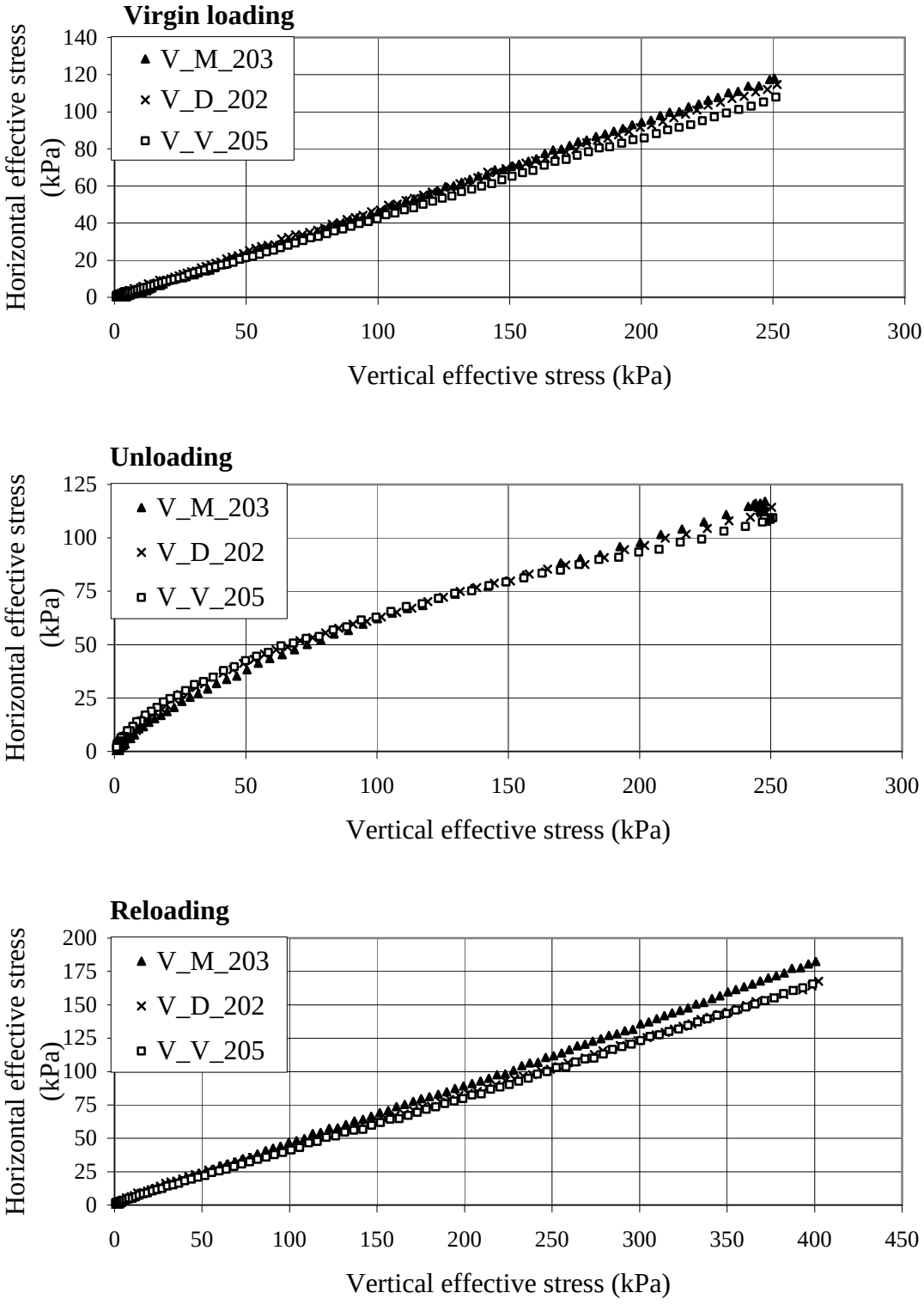

Figure 5.49. Comparison of horizontal vs. vertical effective stress for V specimens

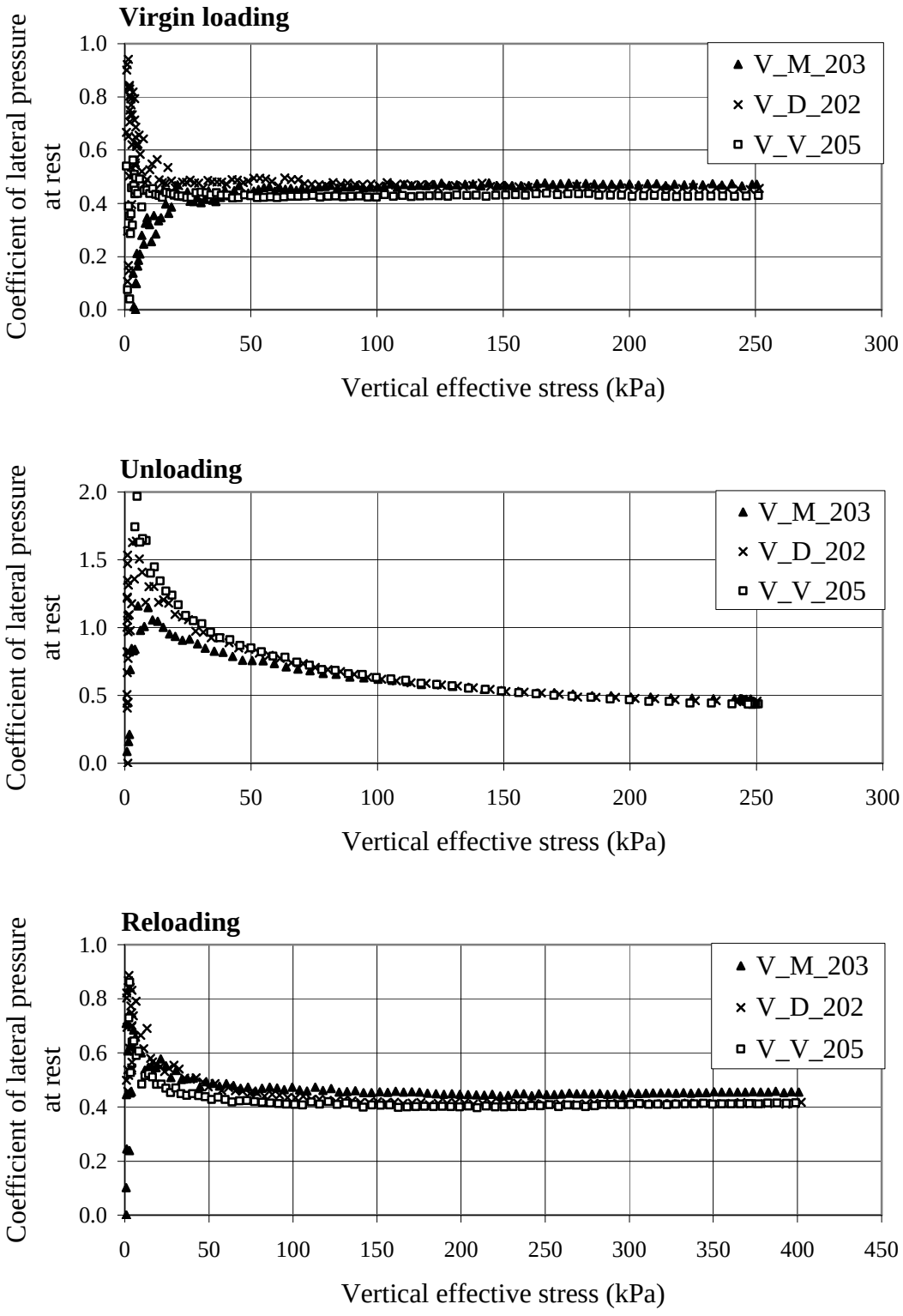

Figure 5.50. Comparison of K_o vs. vertical effective stress for V specimens

To examine the overall effect of densification, the coefficient of lateral pressure at rest at the end of virgin loading was compared for all seventeen (17) one-dimensional compression tests performed on vibrated specimens (see Figure 5.51). Note that the shaded area in Figure 5.51 corresponds to a general envelope derived from the testing results.

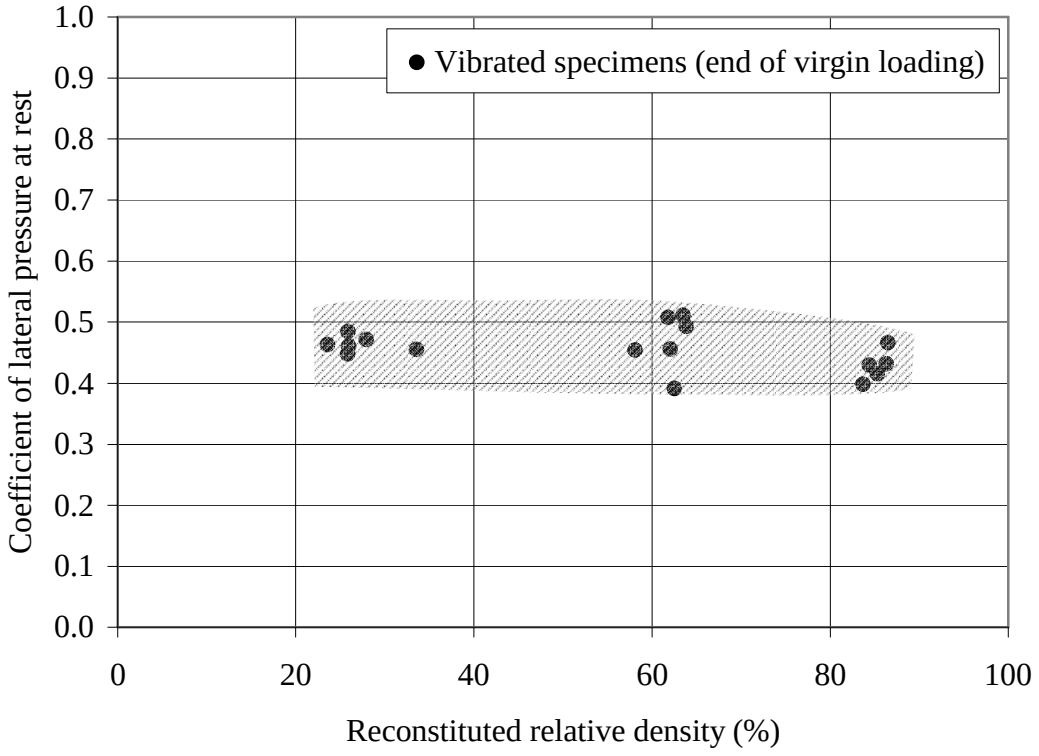

Figure 5.51. K_o at the end of virgin loading for V specimens

Figure 5.51 suggests K_o may decrease with increasing density for very dense vibrated specimens, however, the test data is less than convincing, especially when compared with the trends previously observed for air-pluviated and tamped specimens.

5.4.5 Effect of loading history

For vibrated specimens, the effect of specimen loading history may be observed by comparing the plotted compression test data. Figure 5.52 compares the horizontal versus

vertical effective stress during virgin loading and reloading for a dense, vibrated specimen. A decrease in slope is evident from virgin loading to reloading phases.

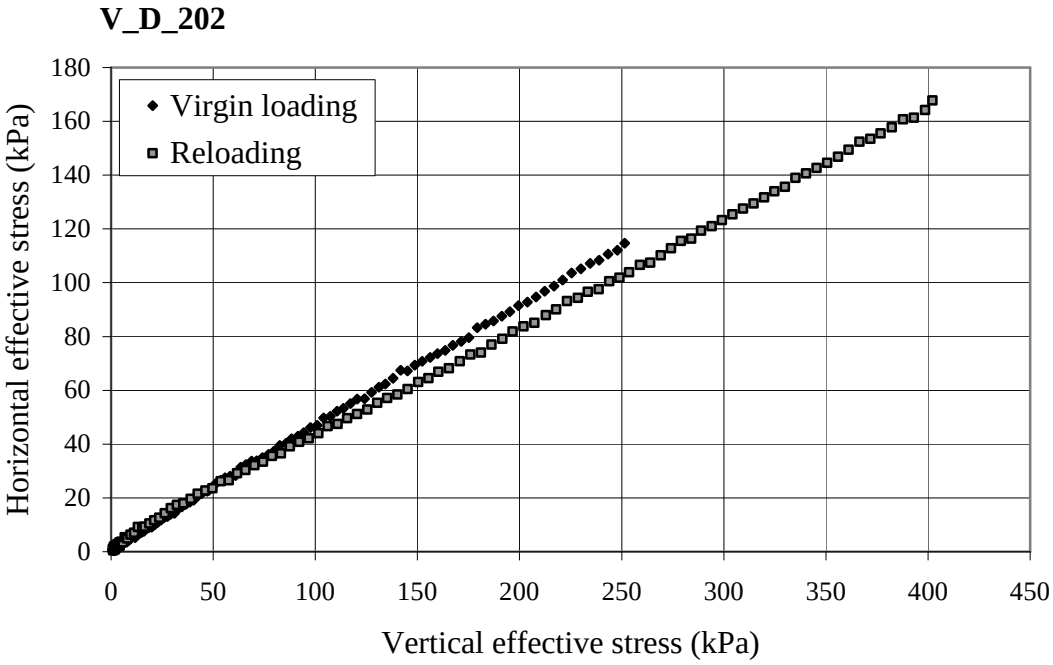

Figure 5.52. Comparison of horizontal vs. vertical effective stress during virgin loading and reloading for V_D_202

Figure 5.53 shows the coefficient of lateral pressure at rest versus vertical effective stress during virgin loading and reloading for a dense, air-pluviated specimen. The plot again indicates a decrease in the constant K_o value from virgin loading to reloading. No obvious variance in K_o is observed as the specimen is reloaded past its preconsolidation pressure.

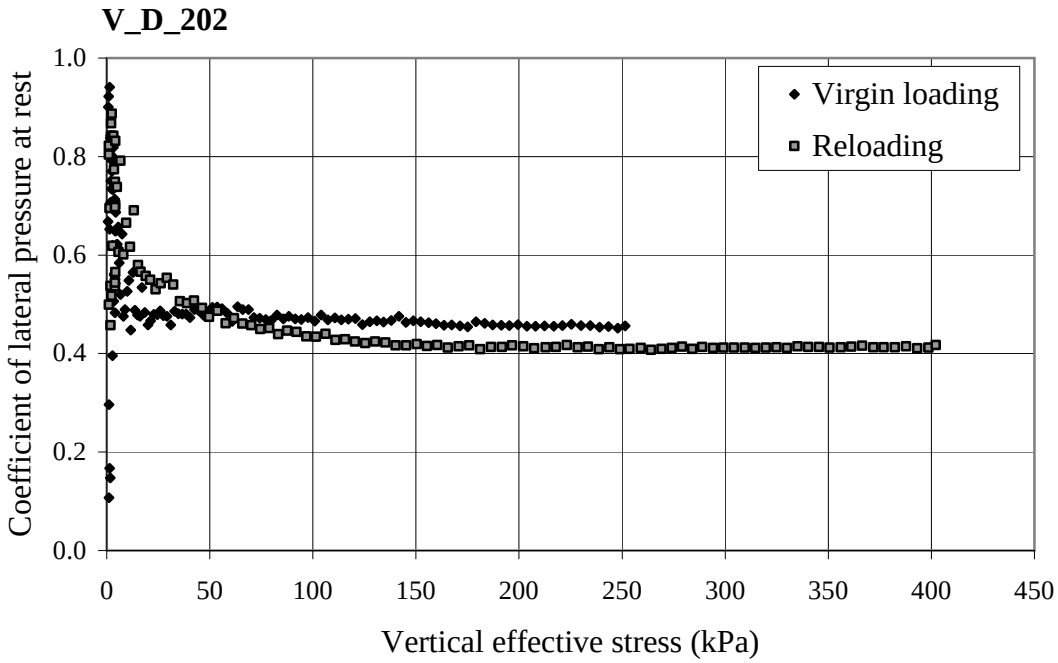

Figure 5.53. Comparison K_o vs. vertical effective stress during virgin loading and reloading for V_D_202

Although not shown here, the effect of loading history on very loose, medium loose and very dense vibrated specimens was found to be similar to that observed in dense, vibrated specimens (see Figure 5.52, Figure 5.53).

For all seventeen (17) one-dimensional compression tests performed on vibrated specimens, the coefficient of lateral pressure at rest, computed at the end of both virgin loading and reloading, was plotted to illustrate the overall effect of loading history (see Figure 5.54). For all densities, K_o values measured at the end of reloading are less than those at the end of virgin loading.

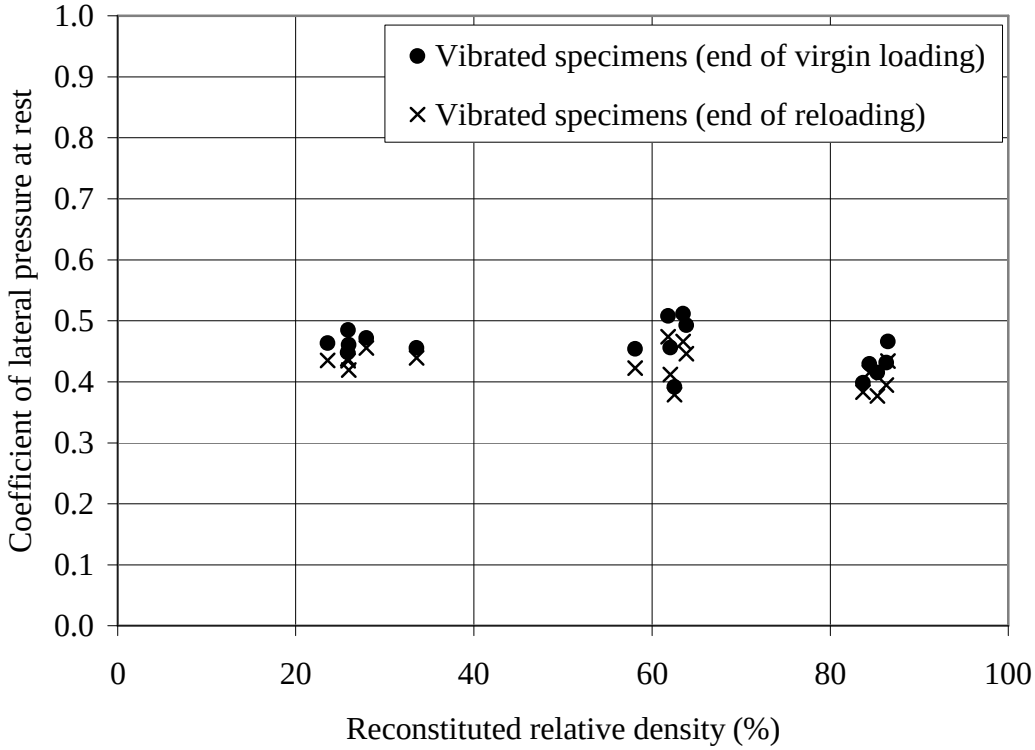

Figure 5.54. K_o at the end of virgin loading and reloading for V specimens

In addition, the coefficient of lateral pressure at rest, computed for selected OCR values over the unloading phase, was compared for all seventeen (17) one-dimensional compression tests performed on vibrated specimens (see Figure 5.55). K_o values increase as OCR increases for all reconstituted densities. This increase is noticeably greater at higher relative densities. As noted for other reconstitution methods, the scatter in K_o values increases markedly with increasing OCR. Again, this effect seems to present more prominently at higher densities.

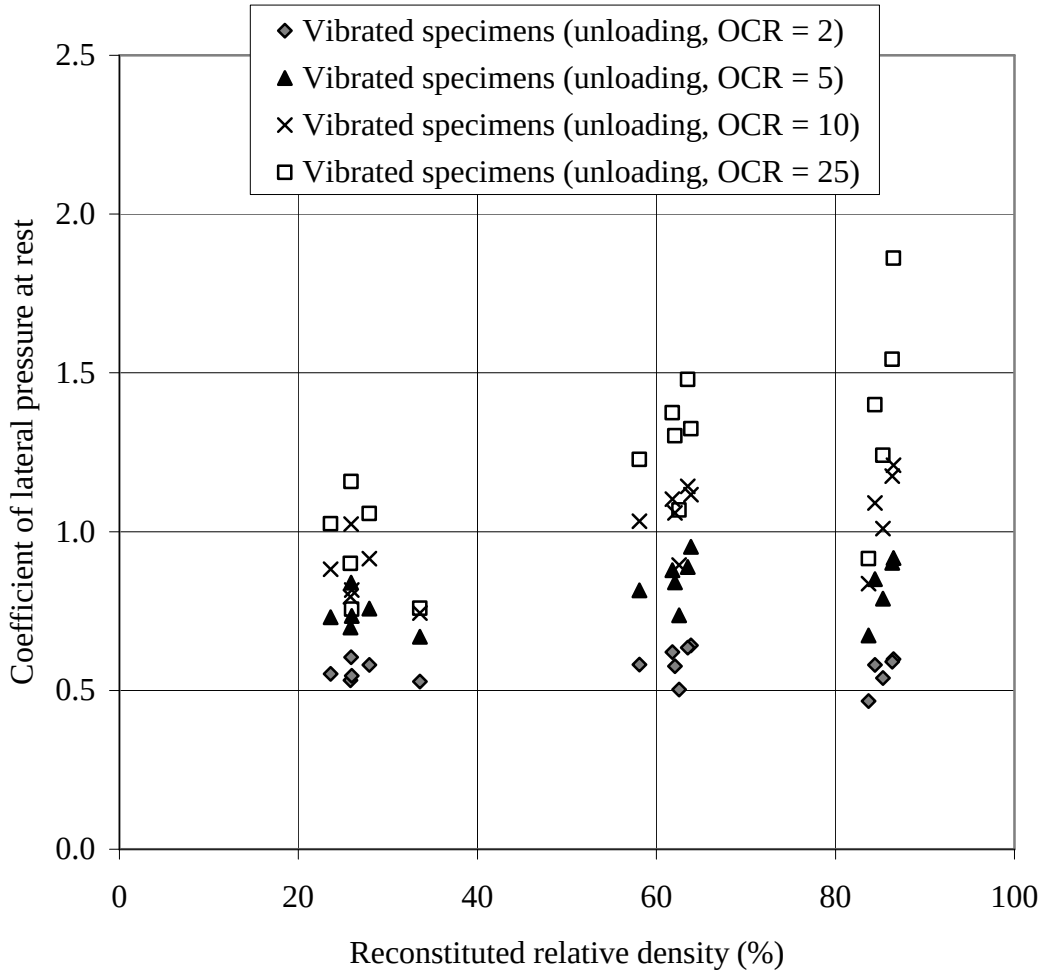

Figure 5.55. K_o at varied OCR values during unloading for V specimens

5.5 Fraser River sand specimens at varied strain rates

Six (6) one-dimensional compression tests were performed on dense Fraser River sand specimens at varied strain rates. The aim of this series of tests was to investigate whether the results of the core testing program, derived using one selected strain rate, would be significantly impacted if the tests were conducted at other rates of strain. Two strain rates were selected that differed by an approximate factor of ten from the 0.015 mm per minute standard rate used in the core testing program – i.e., a rate of 0.0018 mm per minute (about ten times slower than the standard rate) and a rate of 0.15 mm per minute (about ten times faster than the standard rate) were chosen herein.

At a given strain rate, one test was performed for each specimen reconstitution technique. All six tests were performed on dense specimens ranging from 60 to 65% relative density, with an average density of 62%.

The coefficient of lateral pressure at rest, calculated at the end of both virgin loading and reloading, was determined for all six (6) one-dimensional compression tests performed on dense specimens at varied strain rates. Figure 5.56 compares the K_o results for air-pluviated specimens at varied strain rates with the air-pluviated results from Chapter 5.2.3. These results suggest that the one-dimensional compression tests performed on dense, air-pluviated specimens are reasonably independent of the testing strain rate.

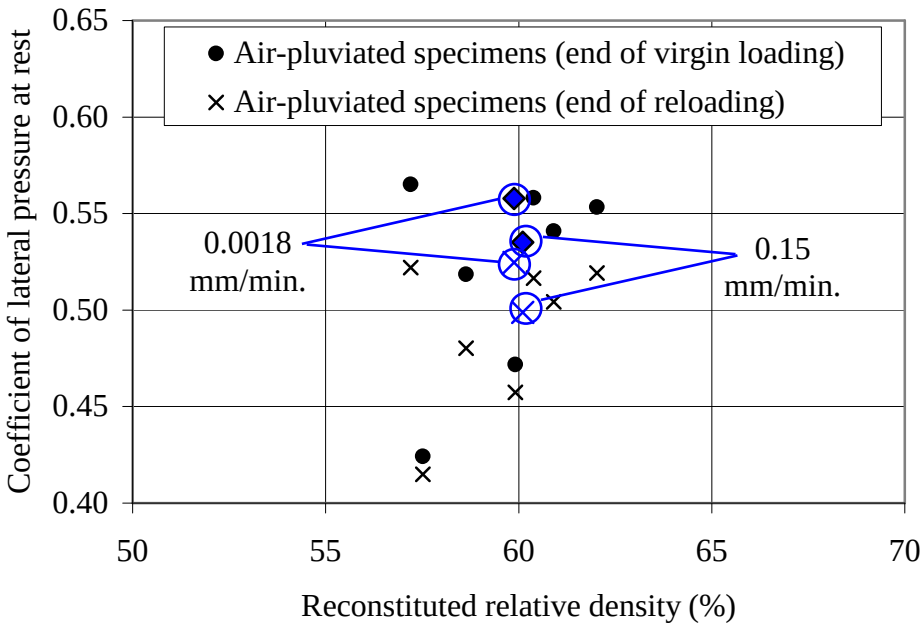

Figure 5.56. K_o for AP_D specimens at varied strain rates

In Figure 5.57, K_o results for tamped specimens at varied strain rates are compared with the tamped specimen results from Chapter 5.3.2. Again, the results indicate that the one-dimensional compression tests performed on dense, tamped specimens are practically independent of the testing strain rate.

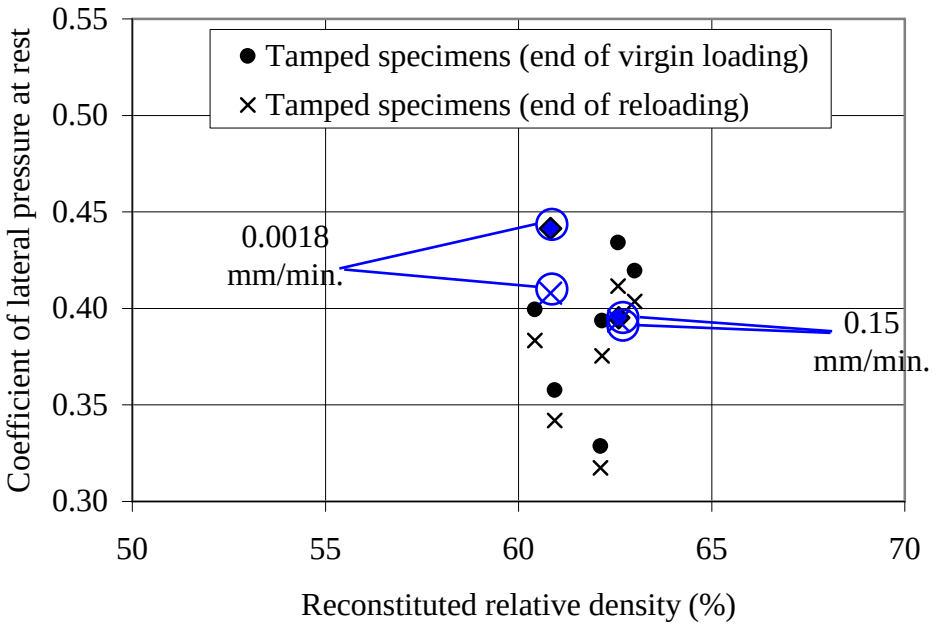

Figure 5.57. K_o for T_D specimens at varied strain rates

Figure 5.58 compares the K_o results for vibrated specimens at varied strain rates with the vibrated results from Chapter 5.4.2. These results likewise indicate that the one-dimensional compression tests performed on dense, vibrated specimens are practically independent of the rate of strain.

Although testing at varied strain rates was only performed on dense specimens, it may be reasonably inferred that very loose, medium loose and very dense specimen test results would also be independent of the rate of strain.

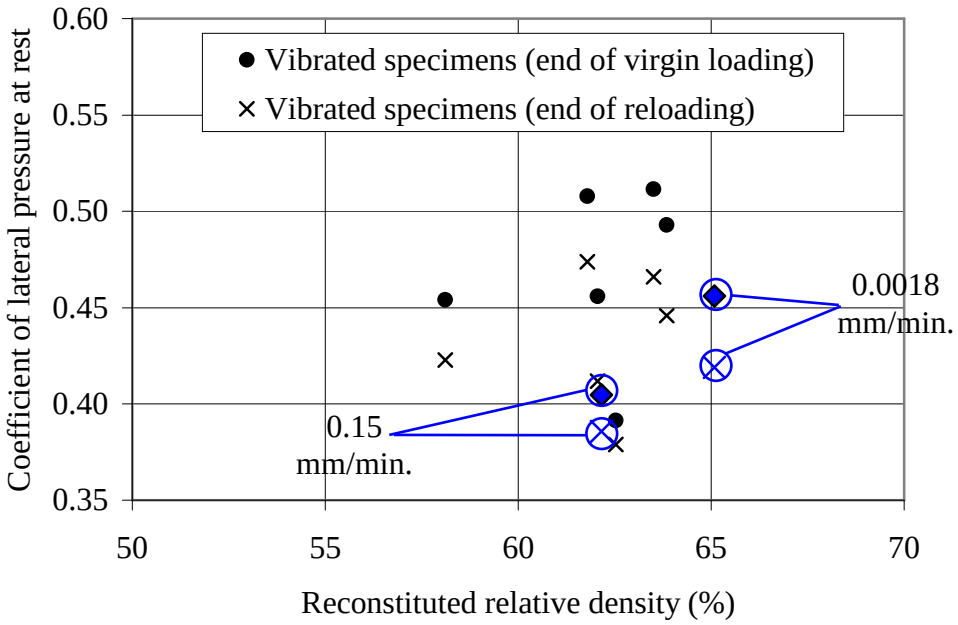

Figure 5.58. K_o for V_D specimens at varied strain rates

5.6 Saturated Fraser River sand specimens

Three (3) one-dimensional compression tests were performed on dense, saturated Fraser River sand specimens. The purpose of this sequence of tests was to investigate whether the results of the core testing program, derived using dry specimens, would be significantly impacted if the tests were conducted using saturated specimens instead. One saturated test was performed for each specimen reconstitution technique. Specimens ranged from 57 to 63% relative density, with an average of 61%. The procedure employed for specimen saturation is described in Chapter 4.5.

For the end of both virgin loading and reloading, the coefficient of lateral pressure at rest was determined for all three (3) one-dimensional compression tests performed on saturated specimens. Figure 5.59 compares the K_o result for the saturated, air-pluviated specimen with the air-pluviated results from Chapter 5.2.3. The results suggest that the one-dimensional compression tests performed on dense, air-pluviated specimens are reasonably independent of specimen saturation.

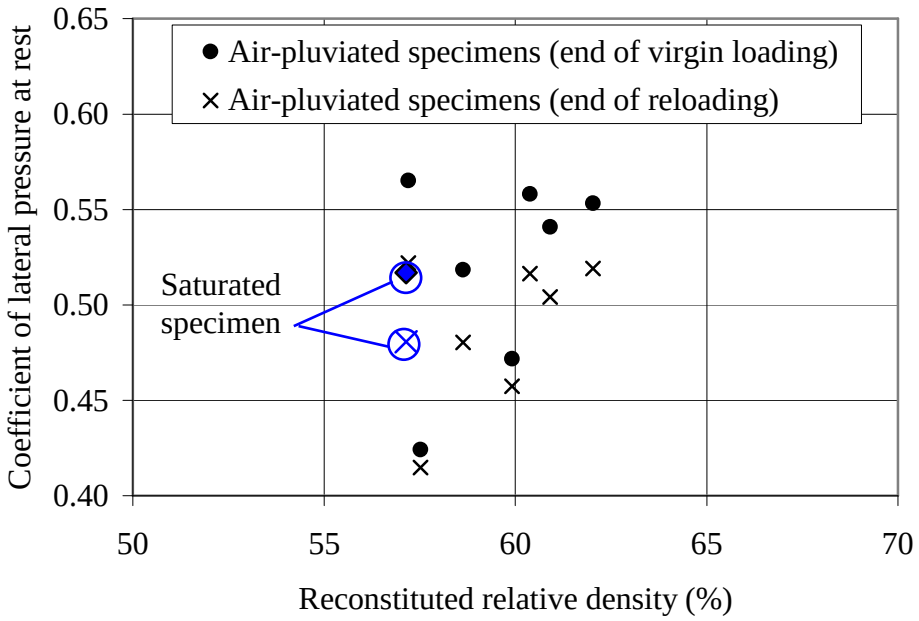

Figure 5.59. K_o for AP_D saturated specimen

Figure 5.60 compares the K_o result for the saturated, tamped specimen with the tamped results from Chapter 5.3.2. Again, the results indicate that the one-dimensional compression tests performed on dense, tamped specimens are practically independent of specimen saturation.

For saturated, vibrated specimens, Figure 5.58 compares the K_o results with the vibrated results from Chapter 5.4.2. Once more, the results show that the one-dimensional compression tests performed on dense, vibrated specimens are basically independent of specimen saturation.

Although saturated testing was only performed on dense specimens, it may be reasonably inferred that very loose, medium loose and very dense specimen test results would also be independent of specimen saturation.

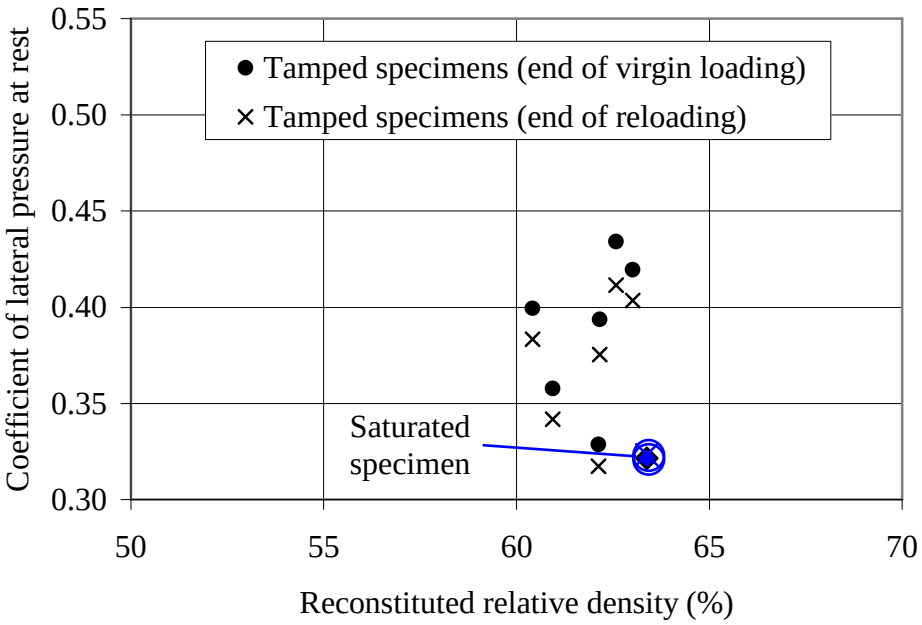

Figure 5.60. K_o for T_D saturated specimen

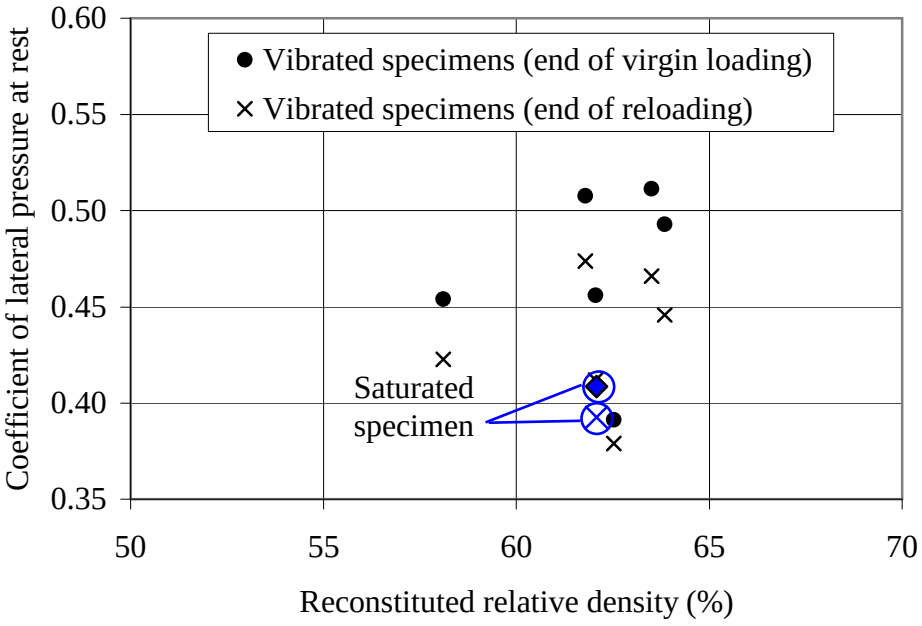

Figure 5.61. K_o for V_D saturated specimen

5.7 Post-test Fraser River sand gradations

A series of sieve analyses was performed on selected Fraser River sand specimens subsequent to one-dimensional compression testing. The goal of these analyses was to determine if any notable particle damage occurred during either specimen reconstitution or one-dimensional compression testing. Particle damage, easily identified by changes in the grain size distribution curve, has been shown to affect the one-dimensional compression response of sand (Nakata, Hyodo, Hyde, Kato, & Murata, 2001).

Figure 5.62 compares representative post-test gradations for very dense specimens reconstituted by air pluviation, tamping and vibration with the material gradation determined prior to specimen reconstitution and compression testing. No major changes are visible in the particle size distributions of the tested specimens.

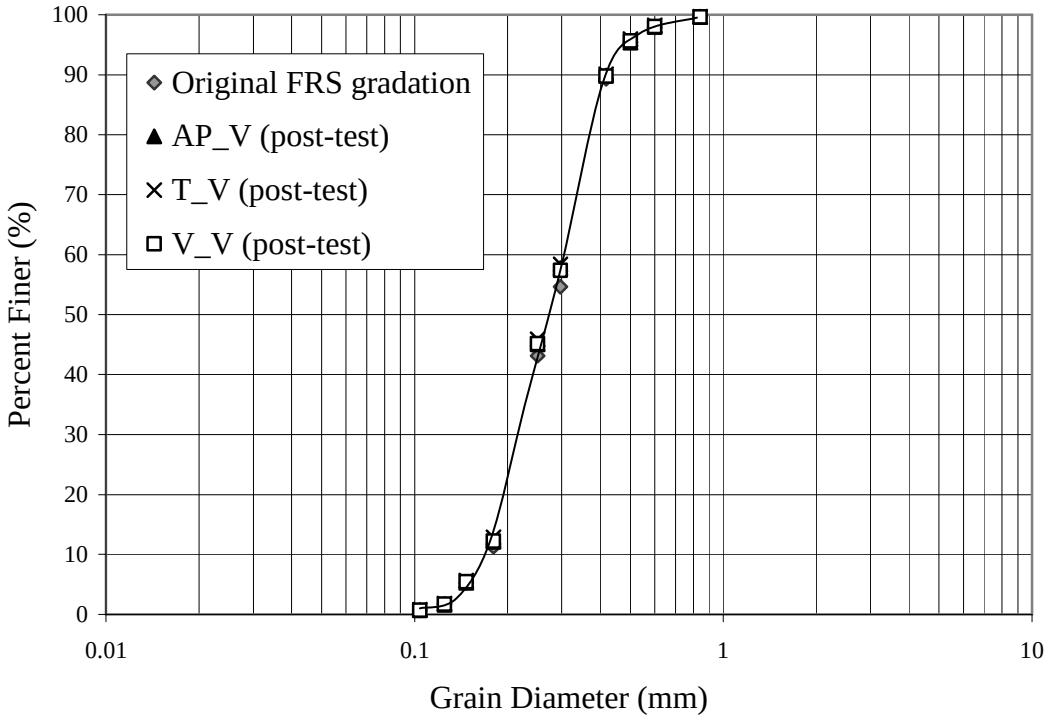

Figure 5.62. Post-test particle size distributions of Fraser River sand

6 ANALYSIS AND DISCUSSION

6.1 Role of particle fabric in one-dimensional compression of sand

As noted earlier, when studying the mechanical behaviour of soil, it is important to account for the effect of particle fabric. Granular soil fabric in both reconstituted laboratory specimens and in-situ soil deposits should be carefully considered. Often, methods utilized in engineering practice for determination of soil behavioural properties do not acknowledge the possible influence of fabric. Neglecting to address fabric effects may result in inaccurate estimation, jeopardizing design safety, cost or both. As discussed herein, results from the present study demonstrate that the coefficient of lateral pressure at rest can indeed be affected by granular particle fabric.

The effect of initial particle fabric may be observed by comparing individual compression test results and by evaluating representative K_o values over the entire core testing program. For brevity, only compression response plots for dense specimens will be presented herein. Regardless, the effect of initial particle fabric on medium loose and very dense specimens was found to be analogous to that observed in dense specimens. Data sets of K_o values for all specimens tested will be offered subsequently.

Figure 6.1 compares the horizontal versus vertical effective stress response during virgin loading and reloading for dense specimens prepared by air pluviation, tamping and vibration. For both virgin loading and reloading, the slope of the linear stress plot, $\overset{o}{K}$, is greatest for the dense, air-pluviated specimen and least for the dense, tamped specimen. The $\overset{o}{K}$ value for the dense, vibrated specimen falls in between these two extremes.

Figure 6.2 displays K_o as a function of the vertical effective stress during virgin loading and reloading for dense specimens prepared by air pluviation, tamping and vibration. The stabilized K_o value is greatest for dense, air-pluviated specimens and least for dense, tamped specimens. K_o for dense, vibrated specimens lies in between these two extremes. This is observed for both virgin loading and reloading phases.

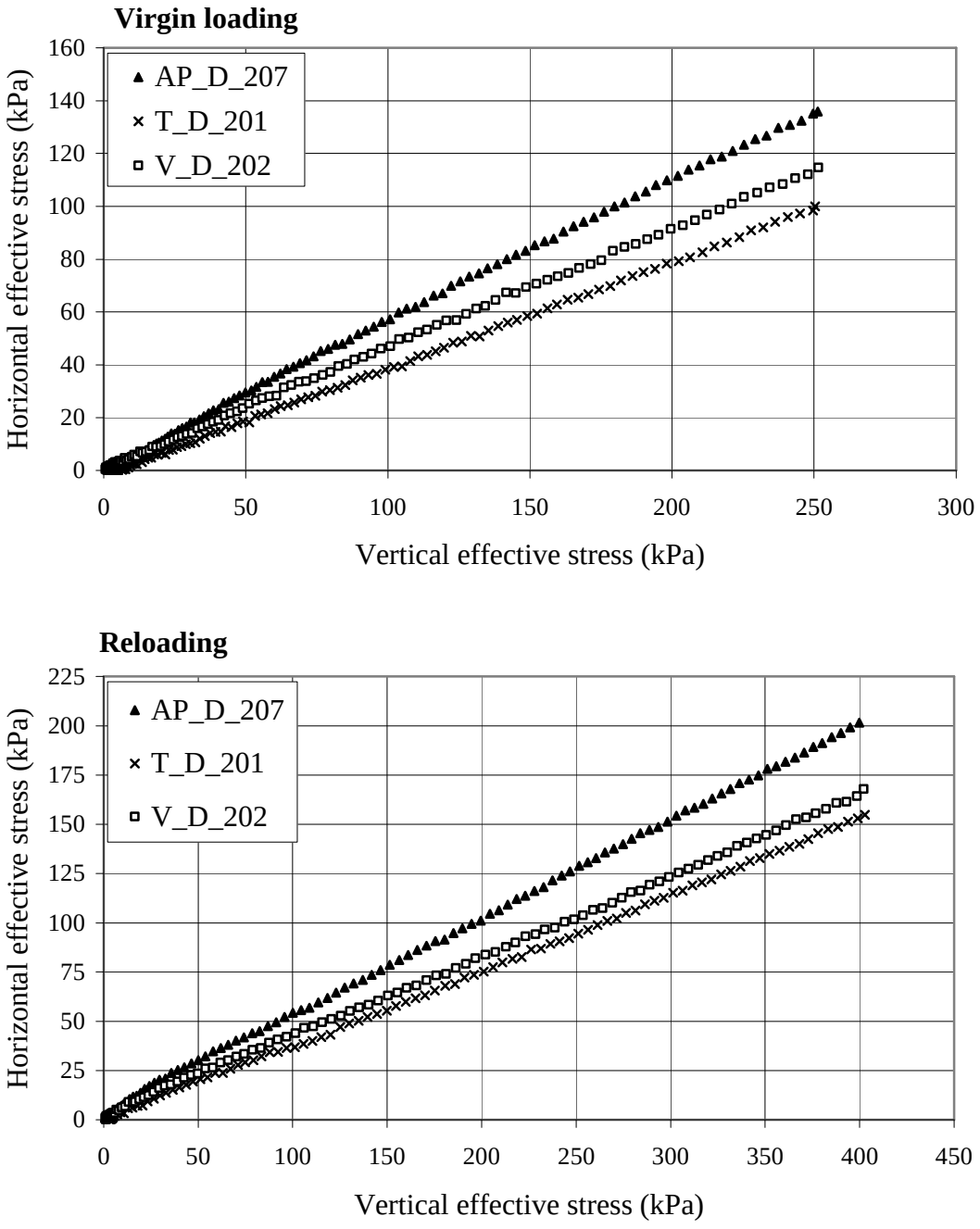

Figure 6.1. Comparison of horizontal vs. vertical effective stress for dense specimens of different initial fabrics

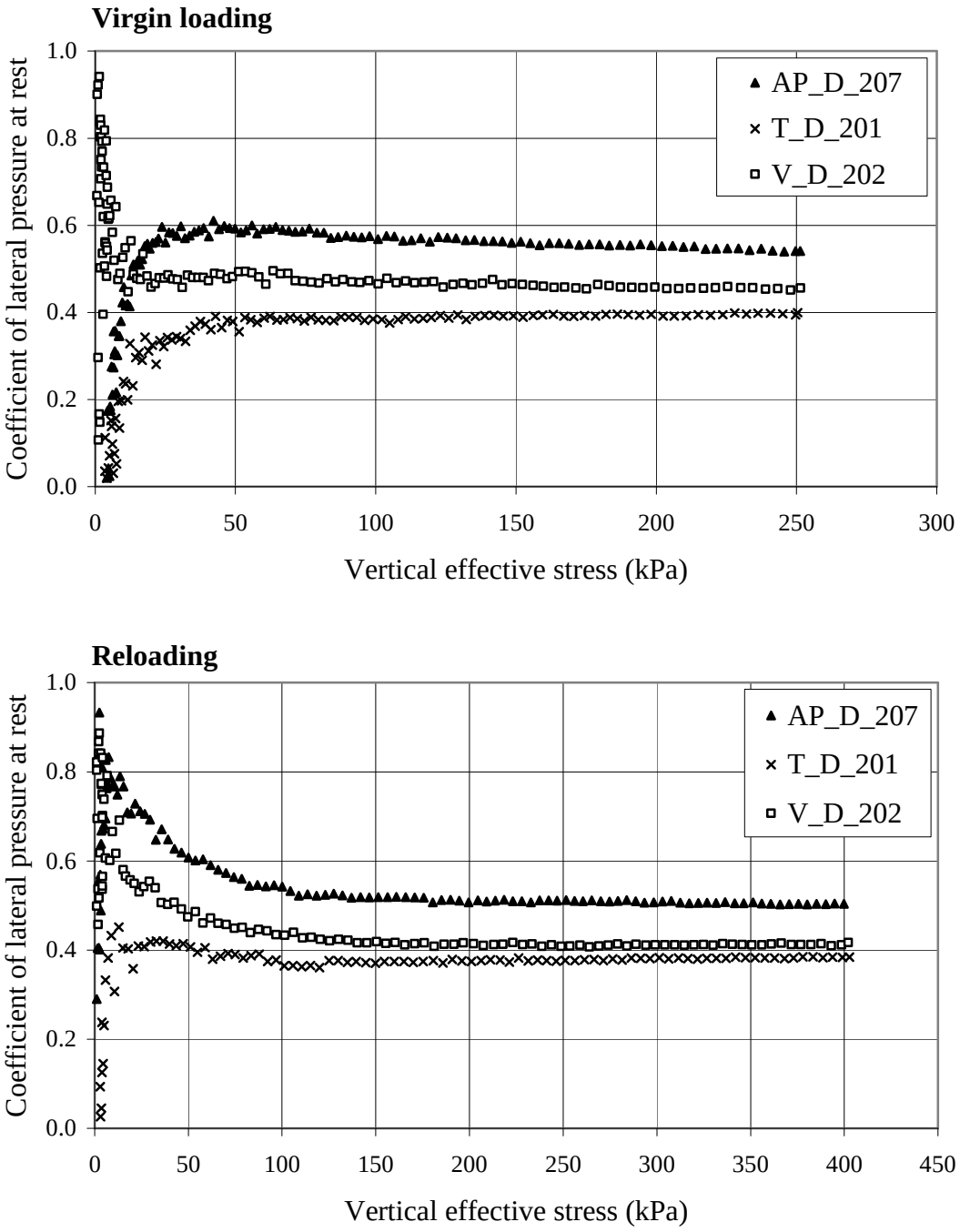

Figure 6.2. Comparison of K_o vs. vertical effective stress for dense specimens of different fabrics

6.1.1 Medium loose specimens

To provide a comprehensive overview of the effect of initial particle fabric, K_o at the end of virgin loading and reloading was calculated and compared for all nineteen (19) one-dimensional compression tests on medium loose specimens (see Figure 6.3). Air-pluviated specimens produced the highest K_o values, tamped specimens ranked the lowest and vibrated specimens produced intermediate values. Scatter was slightly more prominent for air-pluviated specimens.

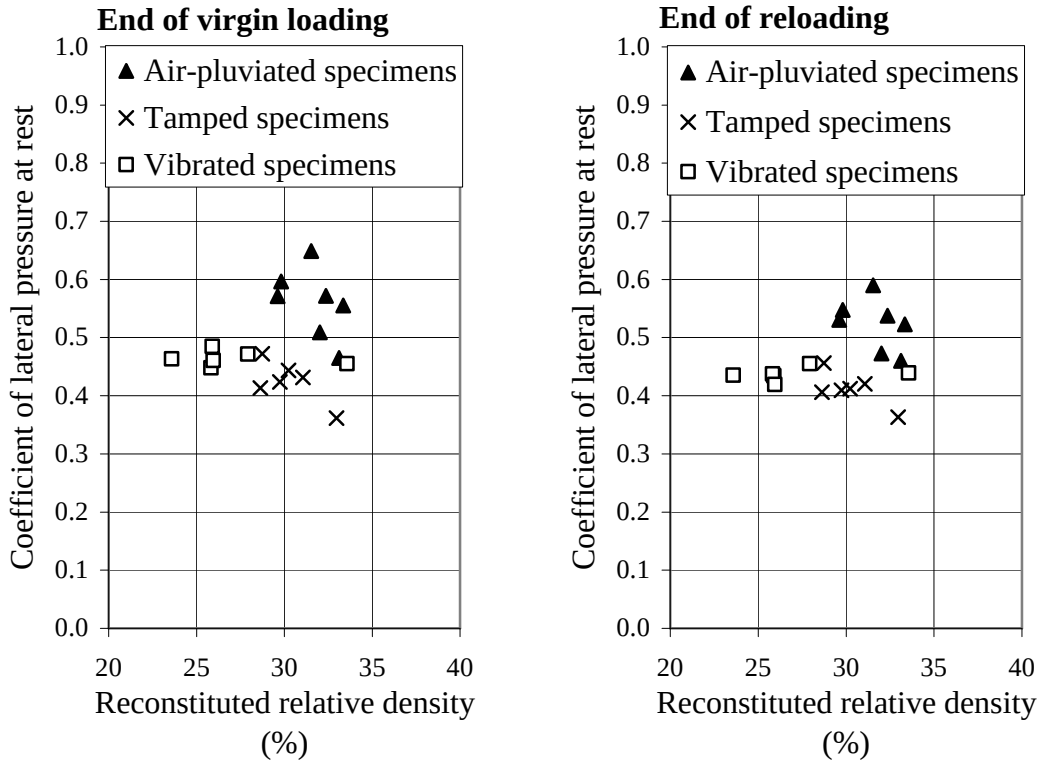

Figure 6.3. K_o during loading for medium loose specimens of different initial fabrics

Additionally, K_o for four approximate OCR values during unloading was compared for tests performed on medium loose specimens (see Figure 6.4). Again, air-pluviated K_o values ranked the highest while tamped specimens were generally the lowest. Vibrated K_o values were similar to those from tamping, except marginally greater overall. K_o increased with increasing OCR, most notably for air-pluviated specimens. Scatter also increased with increasing OCR and was greater for air-pluviated specimens.

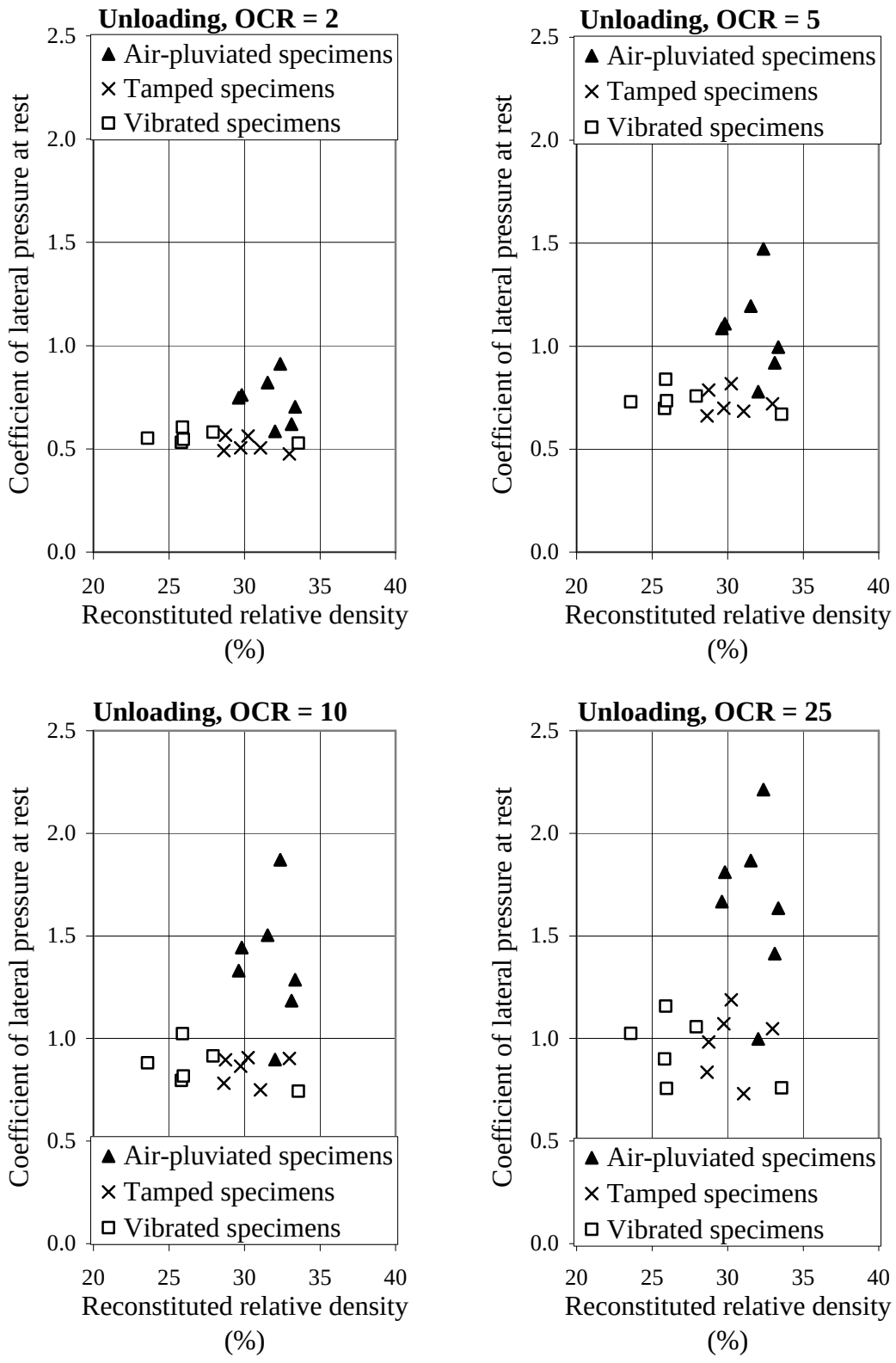

Figure 6.4. K_o during unloading for medium loose specimens of different initial fabrics

6.1.2 Dense specimens

Similarly, K_o at the end of virgin loading and reloading was compared for all nineteen (19) one-dimensional compression tests performed on dense specimens (see Figure 6.5). Air-pluviated specimens produced the highest K_o values, tamped specimens ranked the lowest and vibrated specimens gave intermediary values.

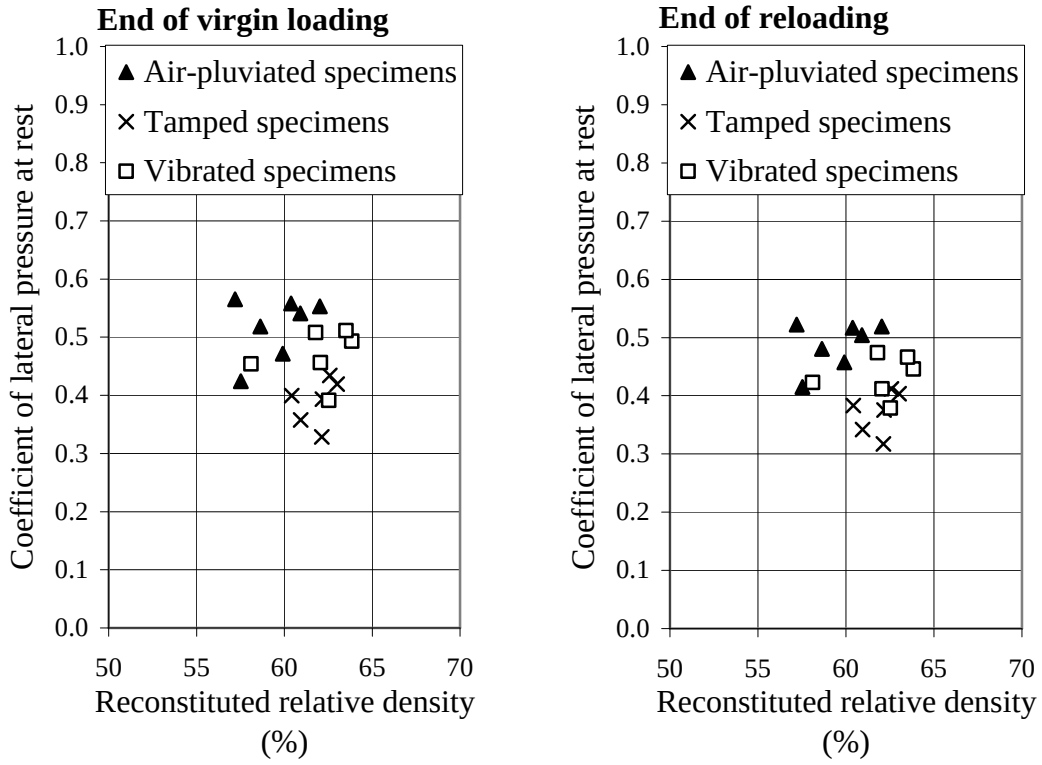

Figure 6.5. K_o during loading for dense specimens of different initial fabrics

As well, K_o calculated during the unloading phase was compared for tests performed on dense specimens (see Figure 6.6). As observed previously, dense air-pluviated K_o values ranked the highest while tamped specimens were the lowest. Vibrated K_o values ranked in the middle. K_o increased with increasing OCR, most notably for the air-pluviated specimens. Scatter also increased with increasing OCR and was only slightly more prominent for air-pluviated specimens.

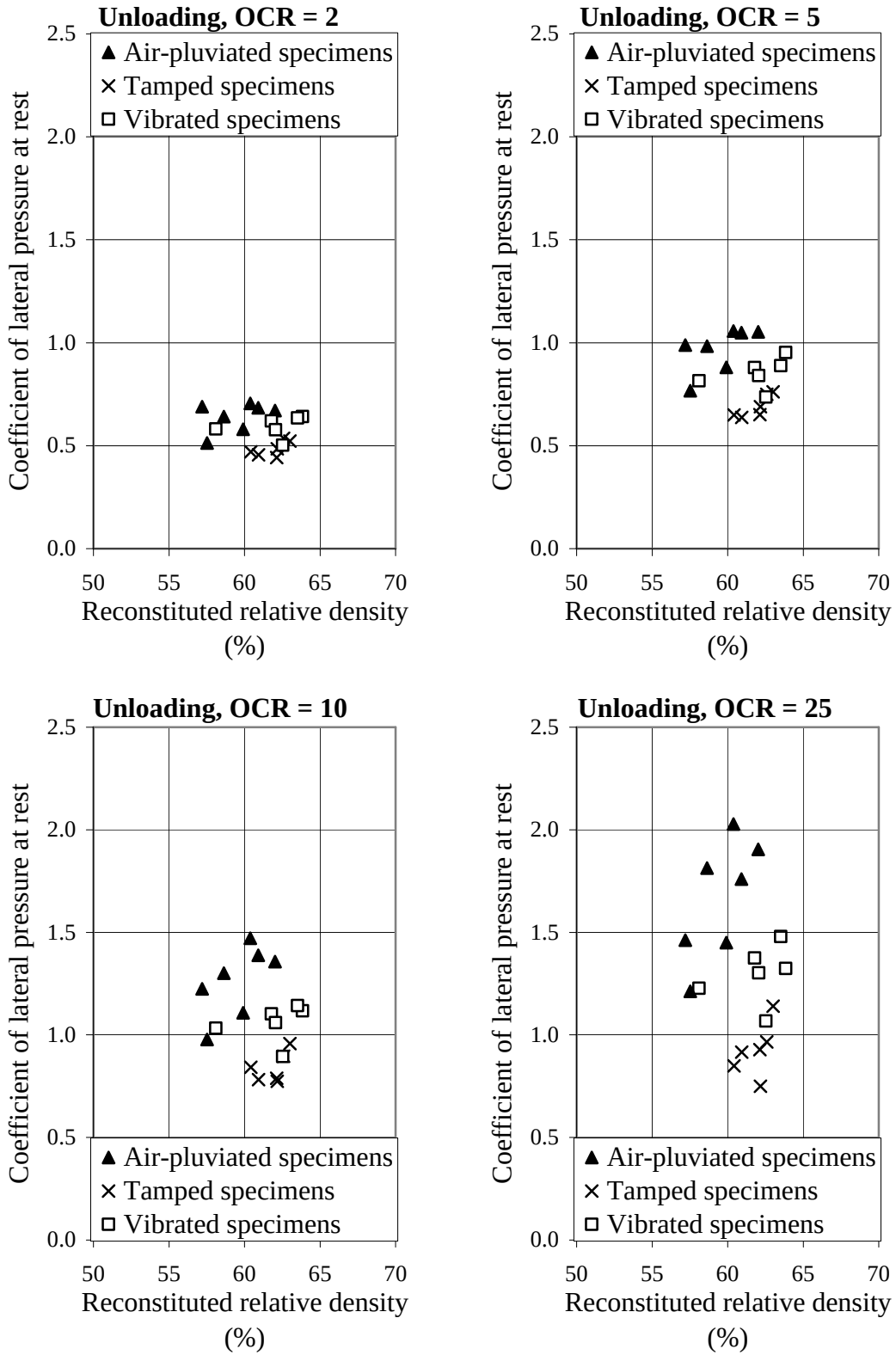

Figure 6.6. K_o during unloading for dense specimens of different initial fabrics

6.1.3 Very dense specimens

Lastly, K_o at the end of virgin loading and reloading was compared for all sixteen (16) one-dimensional compression tests performed on very dense specimens (see Figure 6.7). Air-pluviated specimens produced the highest K_o values, tamped specimens ranked the lowest and vibrated specimens gave intermediate values.

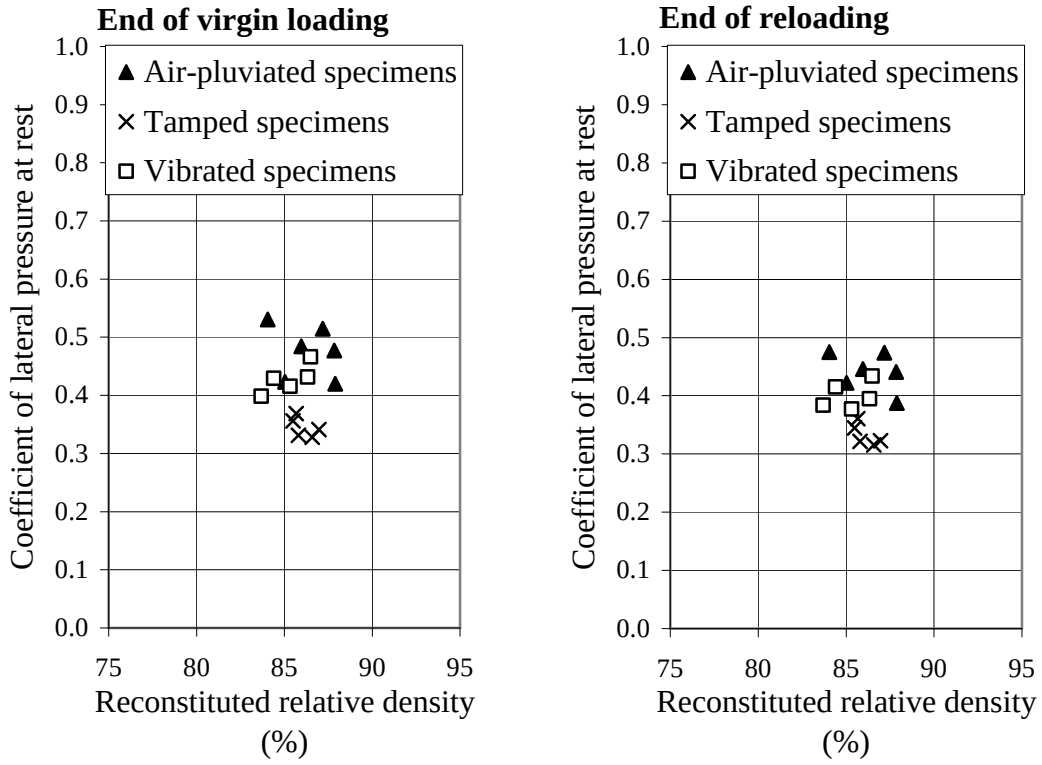

Figure 6.7. K_o during loading for very dense specimens of different initial fabrics

Also, K_o was compared for tests performed on very dense specimens (see Figure 6.8). Although not significantly different at low OCR values, air-pluviated K_o values ranked the highest while tamped specimens were the lowest. Vibrated K_o values ranked in the middle. K_o increased with increasing OCR, primarily for vibrated and air-pluviated specimens. Scatter also increased with increasing OCR for air-pluviated and vibrated specimens only.

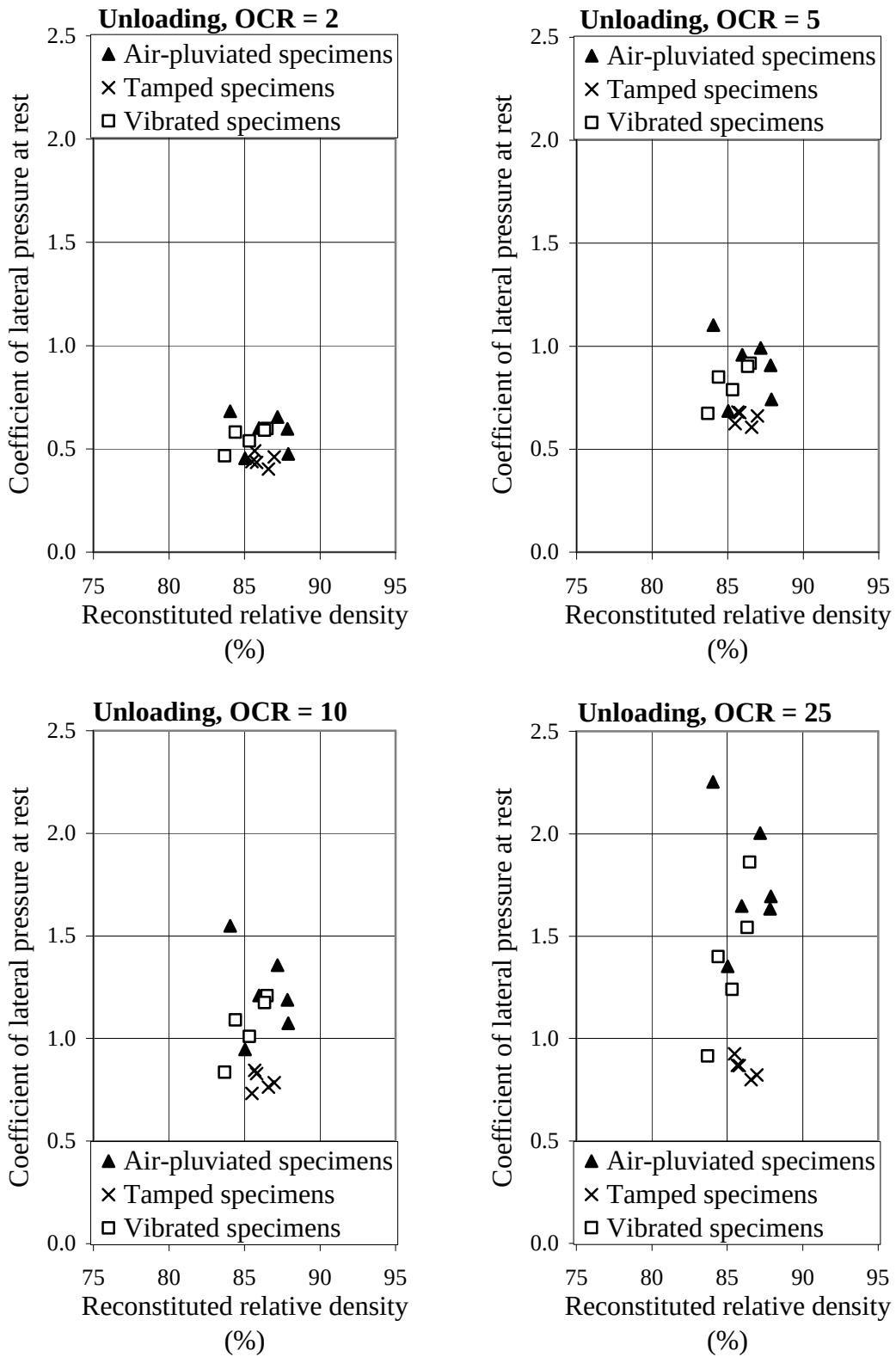

Figure 6.8. K_o during unloading for very dense specimens of different initial fabrics

6.1.4 General remarks

An interesting observation can be made about the behaviour of the tested specimens with respect to their reconstituted fabrics. As described in Chapter 2.2, different specimen reconstitution techniques have been shown to produce variable particle fabrics. To obtain a precise description of the initial specimen fabrics prepared in the present study, further research is required. Reliable assessment and comparison of fabric would involve microscopic examination of preserved and dissected specimen sections and is outside the scope of the present study.

Still, there is opportunity to offer some general remarks about the probable initial particle fabric arising from the different reconstitution techniques. From Chapter 2.2.1, pluviated granular specimens, once preserved and sectioned, have been shown to exhibit a strongly preferred grain orientation in vertical sections, with the long particle axes normal to the vertical plane (Mahmood & Mitchell, 1974). Tamped granular specimens in Chapter 2.2.2 have been shown to exhibit a weakly bimodal preferential grain orientation in vertical sections, with the long particle axes aligned at about 45° from the horizontal (Mahmood & Mitchell, 1974). Finally, from Chapter 2.2.3, vibrated granular specimens have been shown to exhibit practically random grain orientation (Mahmood & Mitchell, 1974).

Considering that the stress-strain response of granular specimens has been linked to the particle fabric, it is not unreasonable to expect that the grain orientation would have some correlation with the measured coefficient of lateral present at rest. Air-pluviated specimens consistently showed the greatest K_o values, and as presented above, this would correspond to the case where the long particle axes are primarily oriented normal to the vertical plane. Vibrated specimens consistently showed intermediate K_o values, with presumably random grain orientation. Tamped specimens consistently yielded the smallest K_o values, with the long particle axes presumably tending to be oriented at 45° from the horizontal. It is possible that as grain orientations shift from normal positioning, with respect to the vertical plane, to more parallel orientation along the vertical plane, the coefficient of lateral pressure at rest decreases.

While further research is obviously needed, the idea that a mechanical behaviour property, in this case K_o, could be linked to the general characteristics of initial particle fabric is intriguing. From the results of the present study, a reasonable approach may be to empirically correlate K_o to the method of specimen reconstitution, in addition to accounting for the effects arising due to density and overconsolidation.

6.2 Determination of the coefficient of lateral pressure at rest

In this section, the methods described in Chapter 2.1 for determination of the coefficient of lateral pressure at rest will be evaluated with respect to the test results from the present study.

6.2.1 Determination of K_o during virgin loading

The first method for the coefficient of lateral pressure at rest to be examined is the Jaky (1948) simplified formula (Eq. 2.2). Recall that Jaky's formula is intended for the virgin loading phase only and is designed to be used with the effective friction angle (ϕ') of the soil (Mayne & Kulhawy, 1982). Estimating the effective friction angle of soil for use in this equation can be a complex task. Not only is the effective friction angle a function of initial relative density, but also, it is a function of confining pressure. Moreover, the value of friction angle measured in the laboratory can be affected by the loading modes (i.e., specific testing apparatus utilized) and also likely, by the particle fabric (Bolton, 1986; Lee & Seed, 1967).

In line with previous researchers, it may be prudent to examine the applicability of the effective friction angle in determination of $K_{o,}$ with respect to observations from the present study. Chapters 5.2.5, 5.3.4 and 5.4.4 detailed the observed effects of initial relative density on the measured coefficient of lateral pressure at rest. Overall, K_o had a tendency to decrease with increasing initial relative density. If K_o can indeed be represented as Jaky's function of the effective friction angle, then $(1-\sin\phi')$ must also decrease with increasing relative density. Because ϕ' has been shown to be greater at higher degrees of relative density, this implies that $(1-\sin\phi')$ would be expected to

decrease with increasing relative density, thus supporting Jaky's supposition (Cornforth, 1973).

In contrast, the plots of K_o versus vertical effective stress, presented in Chapter 5 for each reconstituted fabric and initial density, yield a different observation with respect to the dependence on ϕ'. Compression tests in the present study, executed up to 400 kPa vertical effective stress, indicate that after a limited period of initial loading, K_o is reasonably independent of the vertical effective stress. If K_o is truly a singular function of ϕ', this observation would be inconsistent with the accepted fact that ϕ' is dependent on confining stress (Lee & Seed, 1967).

Furthermore, Chapter 6.1 clearly demonstrates that K_o is a function of the reconstituted particle fabric. If K_o can be reasonably represented as a function of the effective friction angle, among other parameters, then the effect of particle fabric on ϕ' must be quantified. While the influence of fabric on the drained strength of Fraser River sand specimens has not yet been experimentally assessed, it may be noted that the undrained strength of Fraser River sand has been shown to be a function of the particle fabric (Vaid, Sivathayalan, & Stedman, 1999).

Collectively, these observations suggest that the determination of K_o using ϕ' alone may be inherently flawed. Based on results from the present study, it seems that there is opportunity to examine and propose an approach to define K_o in a more appropriate manner, while accounting for the effects of relative density, confining stress and particle fabric.

As an initial step in this effort, it was decided to build upon the well-established assertion that K_o is related to the drained strength (Jaky, 1944; Mayne & Kulhawy, 1982). Knowing the uncertainties associated with ϕ', it was considered prudent to instead use the constant-volume friction angle, ϕ'_{cv}, as the parameter representing drained strength. The constant-volume friction angle represents the lower bound of shearing resistance (Negussey, Wijewickreme, & Vaid, 1988). For sands in a loose state, the effective friction angle is considered to be equivalent to the constant-volume friction angle.

Importantly, the constant-friction angle is generally accepted to be a unique function of mineral composition alone and independent of initial relative density and confining stress (Negussey et al., 1988). Additionally, experimental studies on Fraser River sand confirm that ϕ'_{cv} is also independent of the specimen reconstitution technique and hence, is independent of particle fabric (Vaid et al., 1999). Constant-volume friction angles reported for Fraser River sand range from 32 to 34° (Sivathayalan, 2000; Uthayakumar, 1996).

Based exclusively on results from the present study, the following relationship was constructed to describe the coefficient of lateral pressure at rest during virgin loading as a function of ϕ'_{cv}, the reconstituted particle fabric and the initial relative density:

$$K_{onc} = (F - m)(1 - \sin \phi'_{cv}); \text{ where } K_{onc} = K_o \text{ during virgin loading}$$

F = fabric factor

m = density parameter

Eq. 6.1

To account for the effect of initial particle fabric, a "fabric factor" is introduced. The fabric factor, *F*, attempts to express the effect of a given initial particle fabric with respect to the initial fabric conditions prevalent in a very loose specimen. As such, the value of the fabric factor would be a constant for a given specimen reconstitution method, determined by calibration with respect to laboratory K_o measurements. Based on examination of the present study's data using this approach, the following fabric factors are proposed for use with Fraser River sand:

Table 6.1. Fabric factors for different specimen reconstitution methods in present study

Specimen reconstitution method	**Fabric factor, *F***
Air pluviation	F_{AP} = 1.20
Tamping	F_T = 0.95
Vibration	F_V = 1.05
No densification	F_N = 1.00

The density parameter, *m*, dictates the slope of the K_{onc} curve and is designed to be a function of the initial relative density. Working backwards from the results of the present study, *m* may be estimated by the following equation:

$$m = \frac{D_r^2}{4}; \qquad \text{where } D_r = \text{initial relative density}$$

Eq. 6.2

Therefore, the equation for K_{onc} becomes:

$$K_{onc} = \left(F - \frac{D_r^2}{4} \right)\left(1 - \sin \phi'_{cv}\right)$$

Eq. 6.3

In accordance with ϕ'_{cv} values reported in literature for Fraser River sand, ϕ'_{cv} was assumed to be equal to 32° for the present study.

For the case of non-densified specimens, $F_N = 1.00$ and $D_R \approx 0$. Therefore, the equation for K_{onc} for non-densified specimens simplifies to the following:

$$K_{onc} = \left(1 - \frac{(0)^2}{4} \right)\left(1 - \sin \phi'_{cv}\right) = 1 - \sin \phi'_{cv}$$

Eq. 6.4

Note that this equation (Eq. 6.4) is equivalent to Jaky's relation for very loose specimens during virgin loading, and it also coincides with that suggested by Mesri and Hayat (1993) for granular soils not subject to densification. The test results at the end of virgin loading and the K_{onc} approximation for non-densified specimens using the proposed K_{onc} formula (Eq. 6.3) are presented in Figure 6.9. The new equation provides a reasonable fit for the very loose (D_r = 0%), non-densified sand specimens from the present study.

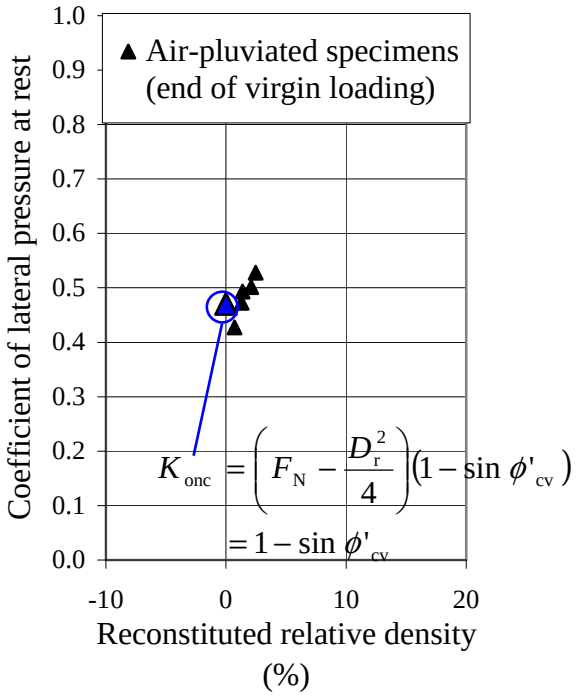

Figure 6.9. K_{onc} at the end of virgin loading for non-densified specimens compared with the proposed K_{onc} relation (Eq. 6.3)

Figure 6.10 plots the test results at the end of virgin loading and the K_{onc} approximations for densified specimens using the proposed K_{onc} formula (Eq. 6.3). The new equation provides a reasonable fit for the densified specimens from the present study.

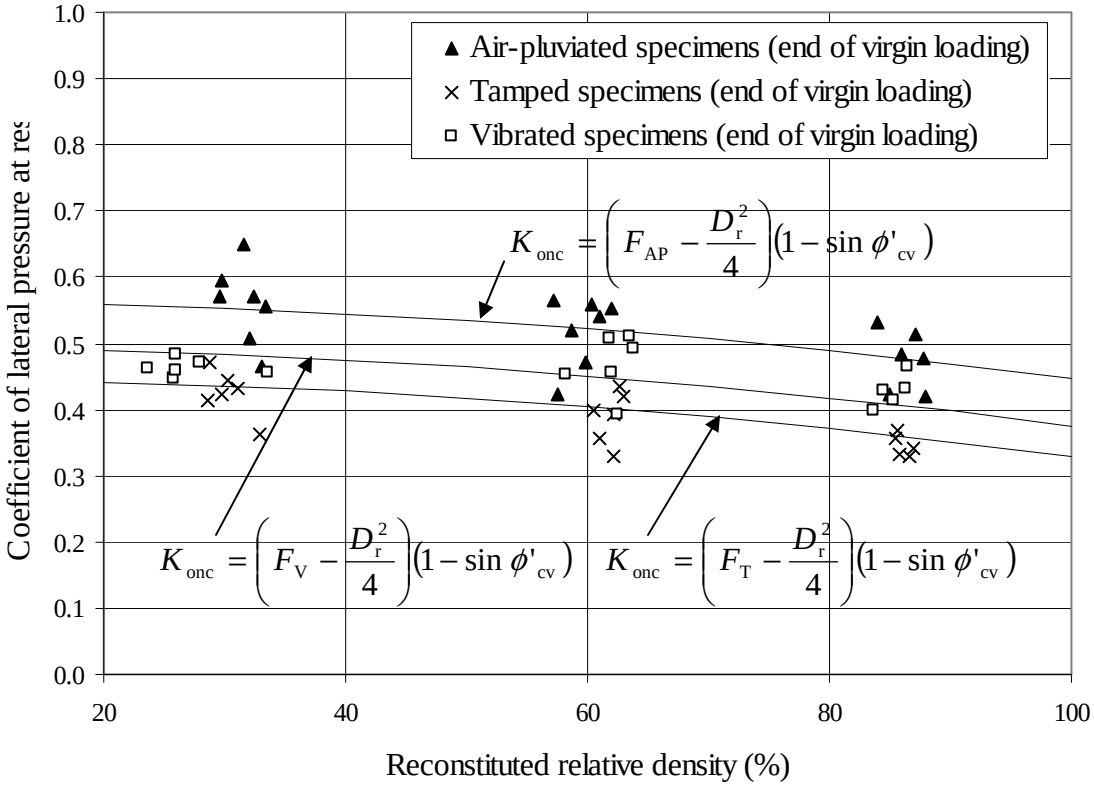

Figure 6.10. K_{onc} at the end of virgin loading for densified specimens compared with the proposed K_{onc} relation (Eq. 6.3)

6.2.2 Determination of K_o during unloading

The next method for the coefficient of lateral pressure at rest to be evaluated is the Schmidt (1976) equation for specimen unloading (Eq. 2.3). Recall that the formula for K_{ou} requires the coefficient of lateral pressure during virgin loading, the overconsolidation ratio (OCR) and the at-rest rebound parameter (α). As OCR is continually increasing during the unloading phase of tests conducted in this program, four different values of OCR were selected for assessment of K_{ou}. Approximate values of 2, 5, 10 and 25 were chosen to represent the range of OCR during unloading.

The appropriate estimation for α has been defined differently by Schmidt (1976), Mayne and Kulhawy (1982) and Mesri and Hayat (1993). Schmidt proposed a constant value

between 0.3 and 0.5 for sands. Mayne and Kulhawy contended that $\alpha = \sin\phi'$. Mesri and Hayat recommended $\alpha = \sin\phi'_{cv}$. For the present study, a constant value of 0.35 was selected for α, in accordance with Schmidt's original suggestion. Therefore, the equation proposed for determination of the coefficient of lateral pressure at rest during unloading is as follows:

$$K_{ou} = \left[\left(F - \frac{D_r^2}{4}\right)\left(1 - \sin\phi'_{cv}\right)\right]\mathrm{OCR}^{0.35}$$

Eq. 6.5

For the case of non-densified specimens, the equation for K_{ou} simplifies to the following:

$$K_{ou} = \left(1 - \sin\phi'_{cv}\right)\mathrm{OCR}^{0.35}$$

Eq. 6.6

Figure 6.11 plots the test results at selected OCR values during unloading and the K_{ou} approximation for non-densified specimens using the proposed formula for the coefficient of lateral pressure at rest during unloading (Eq. 6.5). For OCR = 2, 5 and 10, the proposed equation fits the test data quite well. At OCR = 25, the equation slightly overestimates K_{ou}. Overall, the new equation provides a reasonable fit for the non-densified specimens from the present study.

Figure 6.12 and Figure 6.13 compare K_{ou} for densified specimens at selected OCR values during unloading with the proposed K_{ou} equation (Eq. 6.5). At OCR = 2 and OCR = 5, the proposed equation matches the test data reasonably well for all reconstituted densities and particle fabrics. As unloading progresses, scatter observed in the data increases appreciably. At OCR = 10 and OCR = 25, the proposed equation tends to slightly overestimate K_{ou} at lower relative densities. Still, the new equation seems to provide a reasonable fit for the densified specimens from the present study.

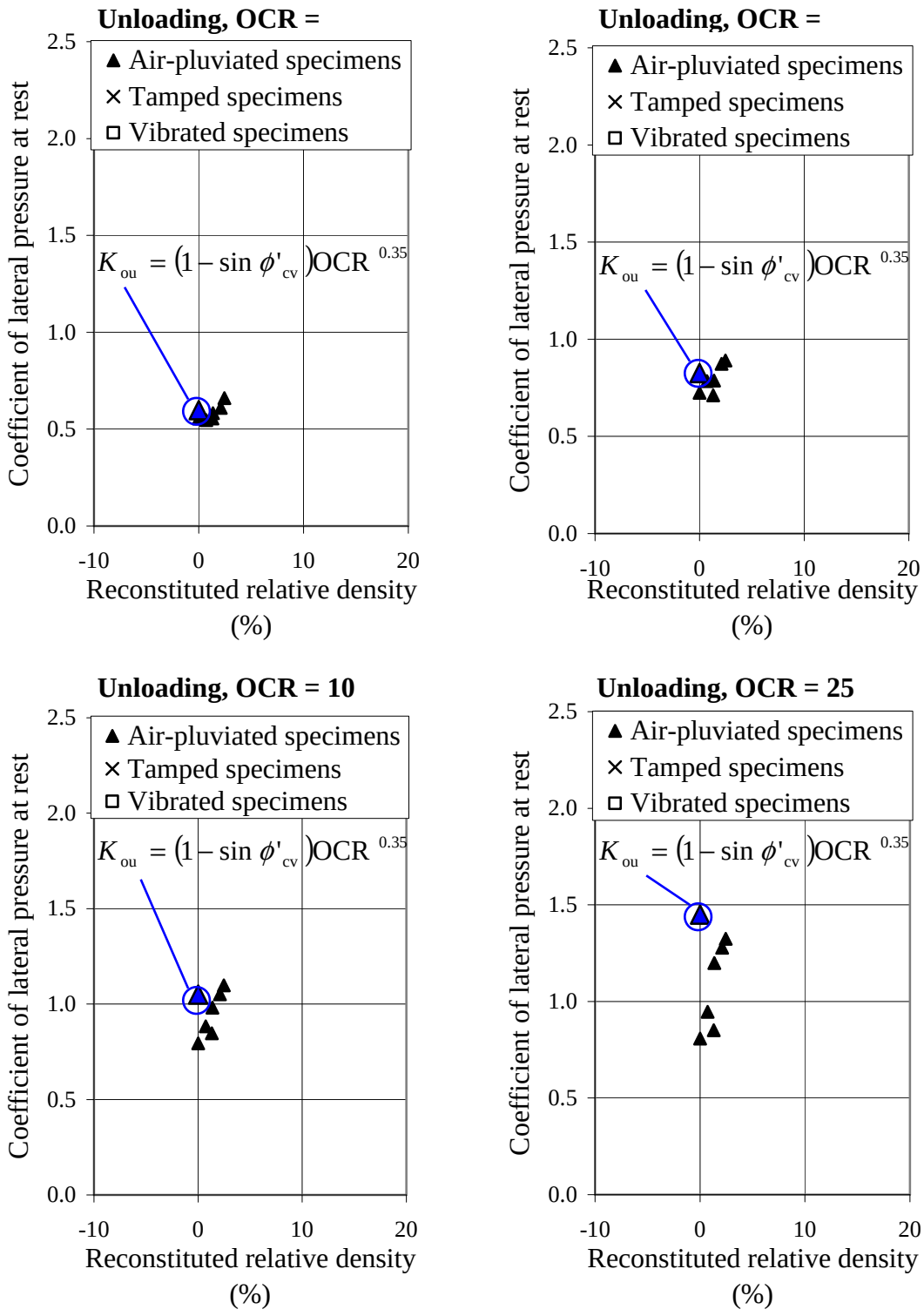

Figure 6.11. K_{ou} at OCR = 2, 5, 10 and 25 during unloading for non-densified specimens compared with the proposed K_{ou} relation (Eq. 6.5)

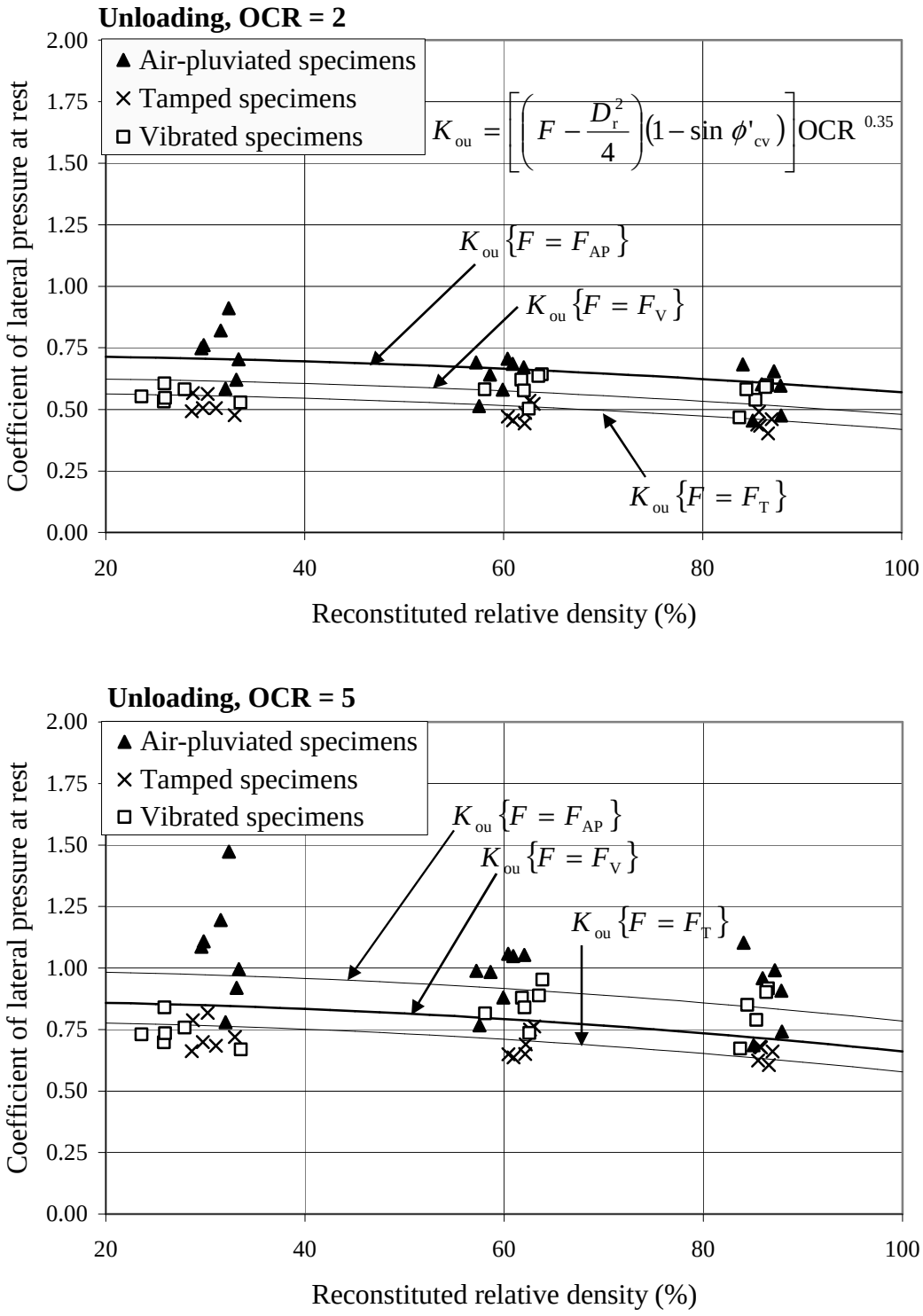

Figure 6.12. K_{ou} at OCR = 2 and OCR = 5 during unloading for densified specimens compared with the proposed K_{ou} relation (Eq. 6.5)

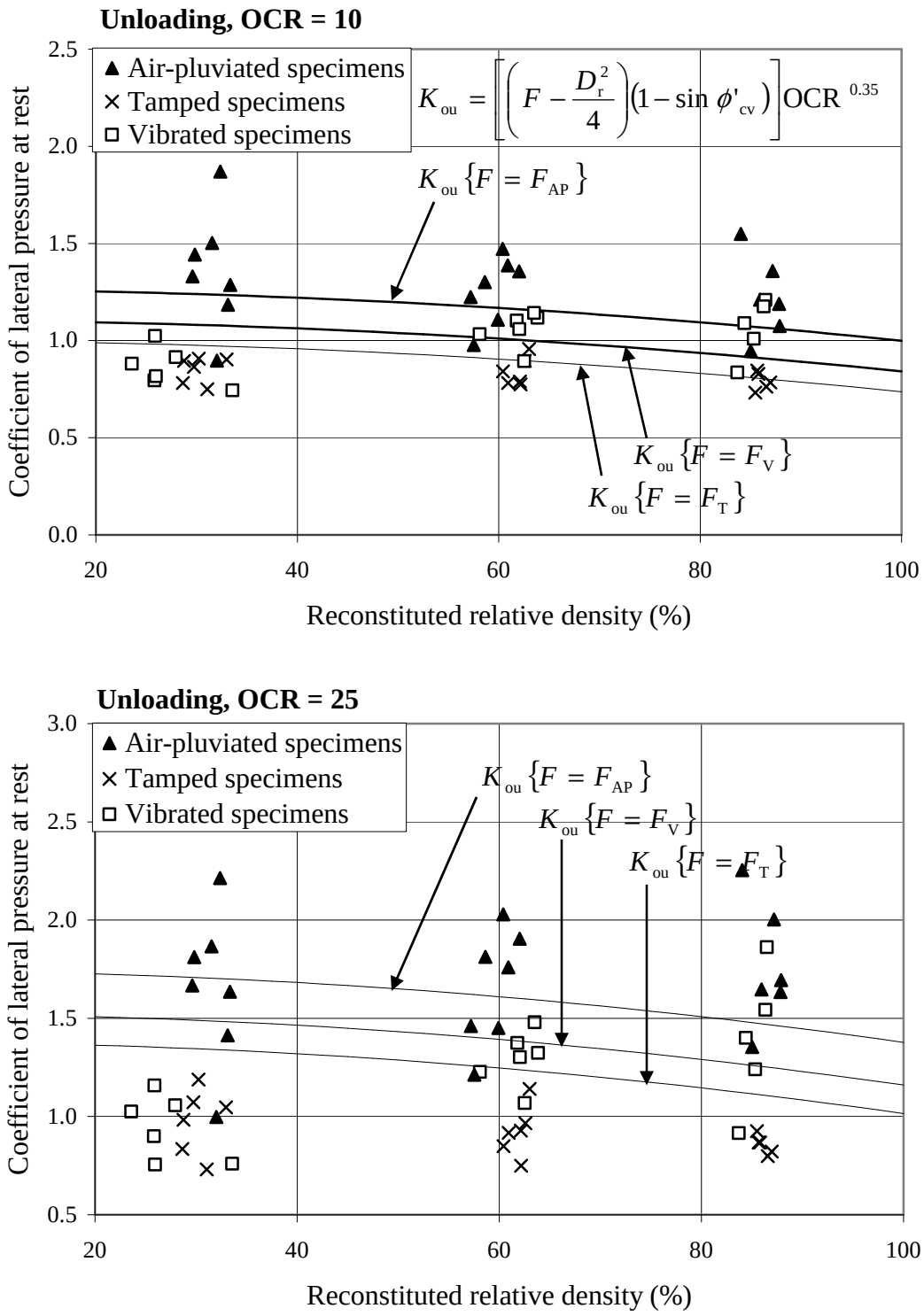

Figure 6.13. K_{ou} at OCR = 10 and OCR = 25 during unloading for densified specimens compared with the proposed K_{ou} relation (Eq. 6.5)

6.2.3 Determination of K_o during reloading

Two primary approaches exist for determination of the coefficient of lateral pressure at rest during reloading: the Mayne and Kulhawy (1982) equation (Eq. 2.6) and the Mesri and Hayat (1993) formula (Eq. 2.12). The equation proposed by Mesri and Hayat (1993) incorporates $\overset{o}{K}_r$, the slope of the horizontal versus vertical effective stress plot in recompression. While the introduction of the $\overset{o}{K}$ parameter is an interesting concept, its relevancy to the present study is questionable. Ideally, an equation for the coefficient of lateral pressure at rest would not only provide reasonable estimations, but moreover, would be computed without requiring specific K_o-laboratory testing data. The $\overset{o}{K}$ parameter itself is a product of one-dimensional compression testing data of the material of interest. To be of practical significance, any parameters introduced to determine K_o should preferably serve to absolve the need for advance laboratory testing. Therefore, only the Mayne and Kulhawy (1982) approach will be evaluated with respect to the present study.

Recall that the Mayne and Kulhawy (1982) formula for K_{or} requires the effective friction angle of the soil, the overconsolidation ratio, the maximum overconsolidation ratio (OCR_{max}), the at-rest rebound parameter and the empirical reload coefficient (m_r). In the present study, specimens are unloaded to near zero effective vertical effective stress before reloading. The stress history parameter, OCR_{max}, is therefore approaching infinity for the reloading phase, and the equation for K_{or} becomes:

$$K_{or} = K_{onc}\left(\frac{OCR}{OCR_{max}^{(1-\alpha)}}\right) + m_r\left(1 - \frac{OCR}{OCR_{max}}\right) = K_{onc}\left(\frac{OCR}{(\to\infty)^{(1-\alpha)}}\right) + m_r\left(1 - \frac{OCR}{(\to\infty)}\right)$$

$$= K_{onc}(\to 0) + m_r(1 - (\to 0)) = m_r$$

Eq. 6.7

Estimated empirically, based on data from the present study, $m_r = 0.9K_{onc}$. Combining the simplified equation for K_{or} (Eq. 6.7) and the proposed formula for K_{onc} during virgin loading (Eq. 6.3), the following results:

$$K_{or} = m_r = 0.9K_{onc} = (0.9)\left[\left(F - \frac{D_r^2}{4}\right)(1 - \sin\phi'_{cv})\right]$$

Eq. 6.8

For the case of non-densified specimens, the equation for K_{or} simplifies to the following:

$$K_{or} = m_r = 0.9K_{onc} = (0.9)(1 - \sin\phi'_{cv})$$

Eq. 6.9

Figure 6.14 plots the test results at the end of virgin loading and the K_{or} approximation for non-densified specimens using the proposed K_{or} formula (Eq. 6.8). The new equation provides a reasonable fit for the non-densified specimens from the present study.

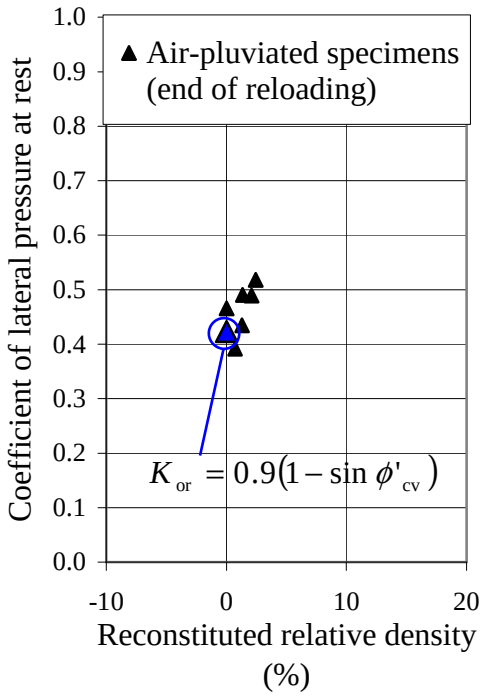

Figure 6.14. K_{or} at the end of reloading for non-densified specimens compared with the proposed K_{or} relation (Eq. 6.8)

Figure 6.15 plots the test results at the end of reloading and the K_{or} approximations for densified specimens using the proposed K_{or} formula (Eq. 6.8). The new equation provides a reasonable fit for the densified specimens from the present study.

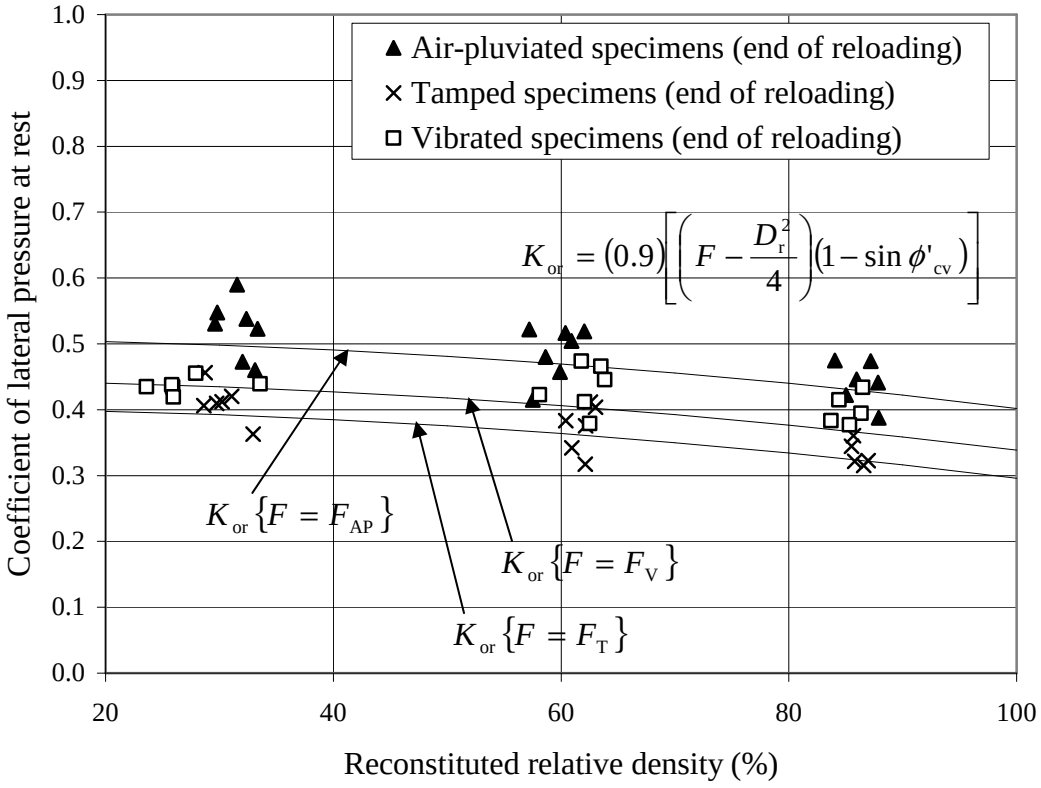

Figure 6.15. K_{or} at the end of reloading for densified specimens compared with the proposed K_{or} relation (Eq. 6.8)

7 CONCLUSIONS AND RECOMMENDATIONS

In conclusion, the primary objective of the present study is to examine the effect of initial particle fabric on the one-dimensional compression response of reconstituted sand specimens. One-dimensional compression tests with lateral stress measurement were carried out on reconstituted Fraser River sand specimens. Laboratory specimen reconstitution methods were developed in order to construct different initial particle fabrics. Three different techniques were utilized: air pluviation, tamping and vibration. In addition, the effects of initial relative density and loading history on the compression response were evaluated. The principal observations from the present study are summarized herein.

General compression response observed in the present study was parallel to that reported by other researchers. During both virgin loading and reloading, K_o achieves a near constant value early in loading and continues at this constant value for the remainder of the loading phase. Measured K_o values during unloading increase markedly, in excess of unity. In reloading, measured K_o values are slightly reduced from those observed in virgin loading. Furthermore, observations regarding the effects of initial relative density showed that measured K_o values generally decrease with increasing reconstituted relative density.

More importantly, the characteristic response observed in one-dimensional compression was found to be significantly affected by the laboratory reconstitution method (i.e., initial particle fabric). Air-pluviated specimens yield the highest K_o values, tamped specimens produce the lowest K_o values and vibrated specimens ranked intermediate. Given that the current methods utilized in practice for determination of K_o do not account for particle fabric, it is deemed appropriate to propose a new relation to describe the one-dimensional compression response of Fraser River sand based on the results of the present study.

A “fabric factor” is introduced to account for the effect of the initial particle fabric on the measured coefficient of lateral pressure at rest. Using the fabric factor, F, the constant-volume friction angle and the initial relative density, a new equation defining the

coefficient of lateral pressure at rest during virgin loading is proposed. The equation is shown to fit well with the results from the present study.

Further research should be pursued to more thoroughly investigate the behaviour of sand in one-dimensional compression. Specific attention should be paid to specimen densification and the effect of both inherent and evolving particle fabric on the coefficient of lateral pressure at rest. Also, the response behaviour of K_o for different loading phases should be carefully examined. Moreover, further research may help to define the most appropriate methods for determination of K_o in practice. The applicability of a more general "fabric factor" for other sands and granular materials should be considered.

In a more universal sense, the present study should serve as a reminder that the particle fabric in laboratory specimens and in-situ deposits must be duly acknowledged. Diverse particle fabric can have a distinct effect on a soil's mechanical behaviour, as demonstrated herein, and must not be ignored in practice or in the laboratory. Further in-depth research and laboratory testing is required to assist in clarifying the link between particle fabric and response behaviour.

REFERENCES

Alpan, I. (1967). "The empirical evaluation of the coefficient K_o and K_{or}." *Soils and Foundations*, 7(1), 31-40.

Bishop, A. W. (1958). "Test requirements for measuring the coefficient of earth pressure at rest." *Proc., Brussels Conference on Earth Pressure Problems*, 1, 2-14.

Bolton, M. D. (1986). "The strength and dilatancy of sands." *Géotechnique*, 36(1), 65-78.

Brand, E. W. (1973). "Some observations on the control of density by vibration." *Evaluation of Relative Density and its Role in Geotechnical Projects Involving Cohesionless Soils*, ASTM STP 523, 121-132.

Cornforth, D. H. (1973). "Prediction of drained strength of sand from relative density measurements." *Evaluation of Relative Density and its Role in Geotechnical Projects Involving Cohesionless Soils*, ASTM STP 523, 281-303.

Cresswell, A., Barton, M. E., & Brown, R. (1999). "Determining the maximum density of sands by pluviation." *ASTM Geotechnical Testing Journal*, 22(4), 324-328.

Dobry, R., & Whitman, R. V. (1973). "Compaction of sand on a vertically vibrating table." *Evaluation of Relative Density and its Role in Geotechnical Projects Involving Cohesionless Soils*, ASTM STP 523, 156-170.

Frost, J. D., & Park, J. (2003). "A critical assessment of the moist tamping technique." *Geotechnical Testing Journal*, 26(1), 57-70.

Garrison, R. E., Luternauer, J. L., Grill, E. V., Macdonald, R. D., & Murray, J. W. (1969). "Early diagenetic cementation of recent sands, Fraser River delta, British Columbia." *Sedimentology*, 12(1-2), 27-46.

Guo, P. J., & Stolle, D. F. E. (2006). "Fabric and particle shape influence on K_o of granular materials." *Soils and Foundations*, 46(5), 639-652.

Harr, M. E. (1977). *Mechanics of particulate media: a probabilistic approach.* New York: McGraw-Hill Companies.

Hendron, A. J., Jr. (1963). *The Behavior of Sand in One-Dimensional Compression*. Ph.D. thesis, Department of Civil and Environmental Engineering, University of Illinois, Urbana-Champaign, 300 pp.

Jaky, J. (1944). "The coefficient of earth pressure at rest (in Hungarian)." *Journal of the Society of Hungarian Architects and Engineers*, 355-358.

Jaky, J. (1948). "Pressure in silos." *Proc., 2nd International Conference on Soil Mechanics and Foundation Engineering*, Rotterdam, 1, 103–107.

Kolbuszewski, J. (1948). "General investigation of the fundamental factors controlling loose packing of sands." *Proc., 2nd International Conference on Soil Mechanics and Foundation Engineering*, Rotterdam, 7, 47-49.

Ladd, R. S. (1974). "Specimen preparation and liquefaction of sands." *Journal of the Geotechnical Engineering Division*, 100(10), 1180-1184.

Ladd, R. S. (1978). "Preparing test specimens using undercompaction." *Geotechnical Testing Journal*, 1(1), 16-23.

Lee, K. L., & Seed, H. B. (1967). "Drained strength characteristics of sands." *Proc., ASCE Journal of the Soil Mechanics and Foundations Division*, 93, 117-141.

Lo Presti, D. C. F., Pedroni, S., & Crippa, V. (1992). "Maximum dry density of cohesionless soils by pluviation and by ASTM D 4253-83: a comparative study." *Geotechnical Testing Journal*, 15(2), 180-189.

Mahmood, A., & Mitchell, J. K. (1974). "Fabric-property relationships in fine granular materials." *Clays and Clay Minerals*, 22, 396-408.

Mahmood, A., Mitchell, J. K., & Lindblom, U. (1976). “Effect of specimen preparation method on grain arrangement and compressibility in sand.” *Soil Specimen in Preparation for Laboratory Testing*, ASTM STP 599, 169-192.

Mayne, P. W., & Kulhawy, F. H. (1982). “K_o-OCR relationships in soil.” *Proc., ASCE Journal of the Geotechnical Engineering Division*, 108, 851-872.

Mesri, G., & Hayat, T. M. (1993). “Coefficient of earth pressure at rest.” *Canadian Geotechnical Journal*, 30(4), 647-666.

Michalowski, R. L. (2005). “Coefficient of Earth pressure at rest.” *Journal of Geotechnical and Geoenvironmental Engineering*, ASCE, 131(11), 1429-1433.

Mitchell, J. K., & Soga, K. (2005). *Fundamentals of Soil Behavior* (3rd ed.). New Jersey: John Wiley & Sons, Inc.

Mulilis, J. P., Seed, H. B., Chan, C. K., Mitchell, J. K., & Arulanandan, K. (1977). “Effects of sample preparation on sand liquefaction.” *Proc., ASCE Journal of the Geotechnical Engineering Division*, 103(2), 91-108.

Nakata, Y., Hyodo, M., Hyde, A. F. L., Kato, Y., & Murata, H. (2001). “Microscopic particle crushing of sand subjected to high pressure one-dimensional compression.” *Soils and Foundations*, 41(1), 69-82.

Negussey, D., Wijewickreme, W. K. D., & Vaid, Y. P. (1988). “Constant-volume friction angle of granular materials.” *Canadian Geotechnical Journal*, 25(1), 50-55.

Oda, M. (1972a). “Initial fabrics and their relations to mechanical properties of granular material.” *Soils and Foundations*, 12(1), 17-36.

Oda, M. (1972b). “The mechanism of fabric changes during compressional deformation of sand.” *Soils and Foundations*, 12(2), 1-18.

Okochi, Y., & Tatsuoka, F. (1984). “Some factors affecting K_o-values of sand measured in triaxial cell.” *Soils and Foundations*, 24(3), 52-68.

Papadimitriou, A. G., Dafalias, Y. F., & Yoshimine, M. (2005). “Plasticity modeling of the effect of sample preparation method on sand response.” *Soils and Foundations*, 45(2), 109-123.

Pettibone, H. C., & Hardin, J. (1965). “Research on vibratory maximum density test for cohesionless soils.” *Compaction of Soils*, ASTM STP 377, 3-19.

Rad, N. S., & Tumay, M. T. (1987). “Factors affecting sand specimen preparation by raining.” *Geotechnical Testing Journal*, 10(1), 31-37.

Schmidt, B. (1967). “Lateral stresses in uniaxial strain.” *Danish Geotechnical Institute, Bulletin No. 23*, 5-12.

Selig, E. T. (1963). “Effect of vibration on density of sand.” *Proc., 2nd Pan-American Conference on Soil Mechanics and Foundation Engineering*, 129-144.

Sivathayalan, S., & Vaid, Y. P. (2002). “Influence of generalized initial state and principal stress rotation on the undrained response of sands.” *Canadian Geotechnical Journal*, 39(1), 63-76.

Sivathayalan, S. (2000). *Fabric, Initial State and Stress path Effects on Liquefaction Susceptibility of Sands*. Ph.D. thesis, Department of Civil Engineering, University of British Columbia, Vancouver, 307 pp.

Soiltest. (1990). *Materials Testing Catalog*. England: ELE International.

Sriskandakumar, S. (2004). *Cyclic Loading Response of Fraser River Sand for Validation of Numerical Models Simulating Centrifuge Tests*. M.A.Sc. thesis, University of British Columbia, Vancouver, 159 pp.

Terzaghi, K., Peck, R. B., & Mesri, G. (1996). *Soil Mechanics in Engineering Practice* (3rd ed.). New York: John Wiley & Sons, Inc.

Uthayakumar, M. (1996). *Liquefaction of Sands under Multi-Axial Loading*. Ph.D. thesis, University of British Columbia, Vancouver, 223 pp.

Vaid, Y. P., & Negussey, D. (1988). “Preparation of reconstituted sand specimens.” *Advanced Triaxial Testing of Soil and Rock*, ASTM STP 977, 405-417.

Vaid, Y. P., & Negussey, D. (1984). “Relative density of pluviated sand samples.” *Soils and Foundations*, 24(2), 101-105.

Vaid, Y. P., & Sivathayalan, S. (2000). “Fundamental factors affecting liquefaction susceptibility of sands.” *Canadian Geotechnical Journal*, 37(3), 592-606.

Vaid, Y. P., Sivathayalan, S., & Stedman, D. (1999). “Influence of specimen-reconstituting method on the undrained response of sand.” *Geotechnical Testing Journal*, 22(3), 187-195.

Wanatowski, D., & Chu, J. (2008). “Effect of specimen preparation method on the stress-strain behavior of sand in plane-strain compression tests.” *Geotechnical Testing Journal*, 31(4), 308-320.

Wijewickreme, D., Sriskandakumar, S., & Byrne, P. (2005). “Cyclic loading response of loose air-pluviated Fraser River sand for validation of numerical models simulating centrifuge tests.” *Canadian Geotechnical Journal*, 42(2), 550-561.

APPENDIX A. TEST DATA FOR AIR PLUVIATION

Appendix A.1. Very loose specimens

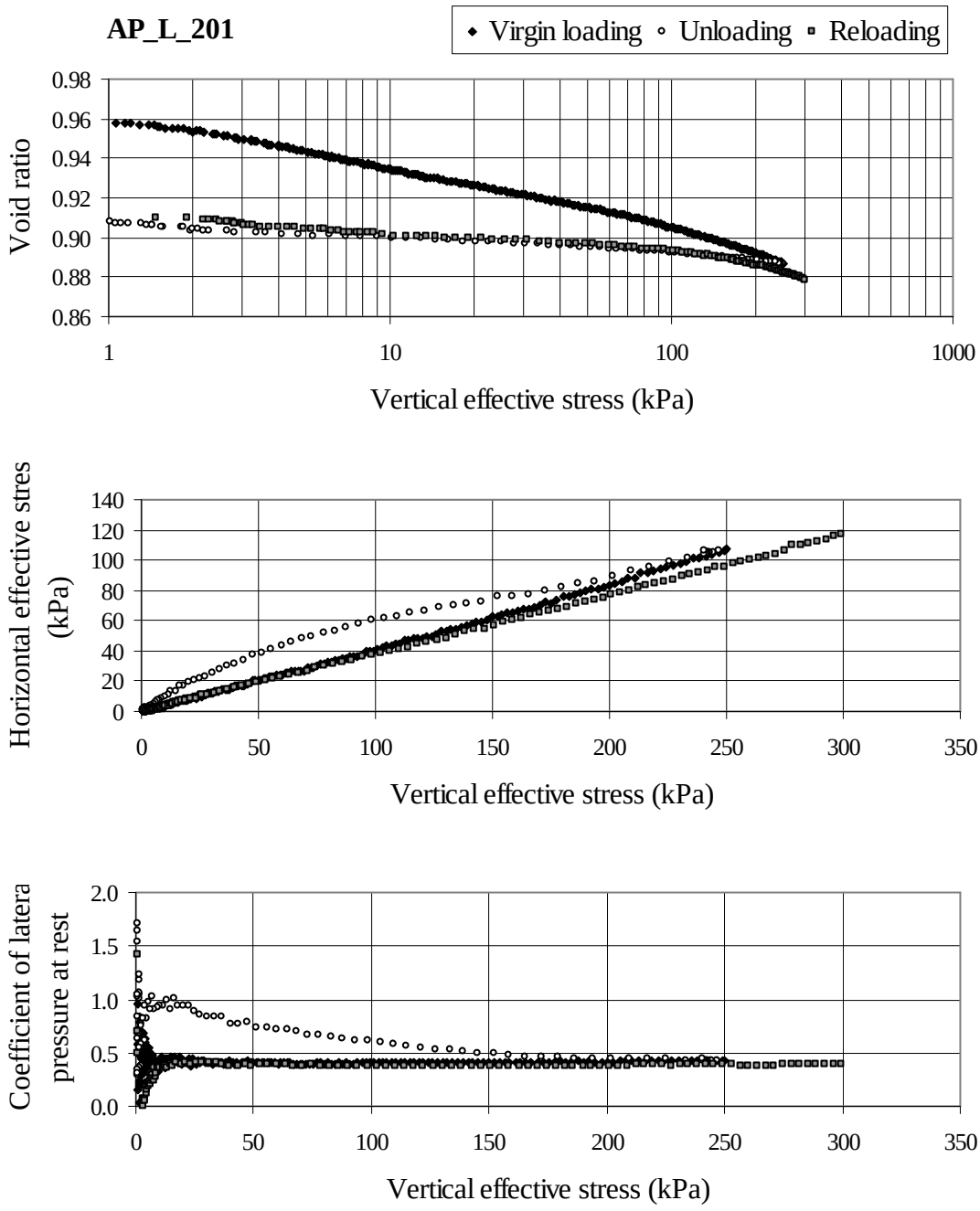

Figure A.1.1. Test data for AP_L_201

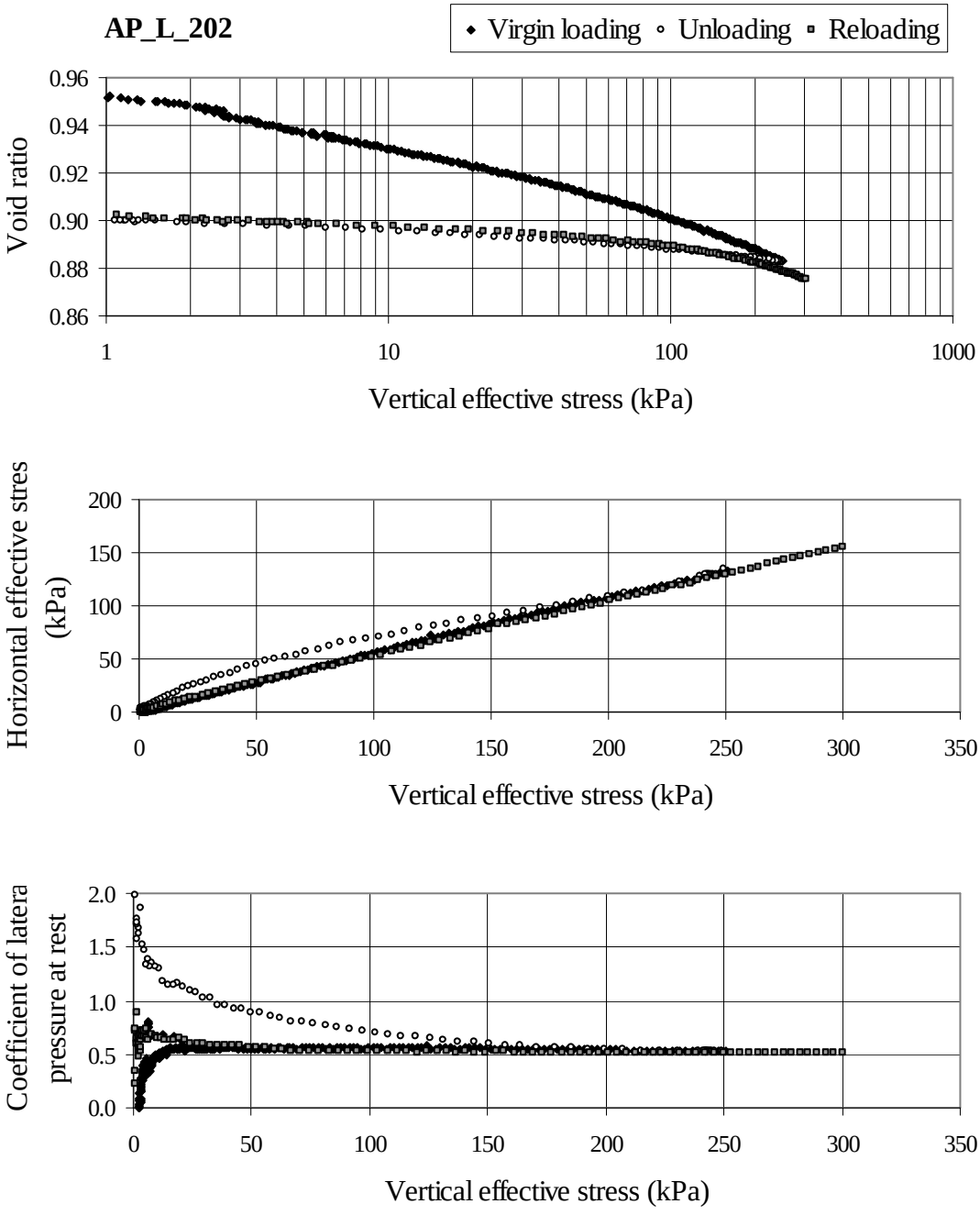

Figure A.1.2. Test data for AP_L_202

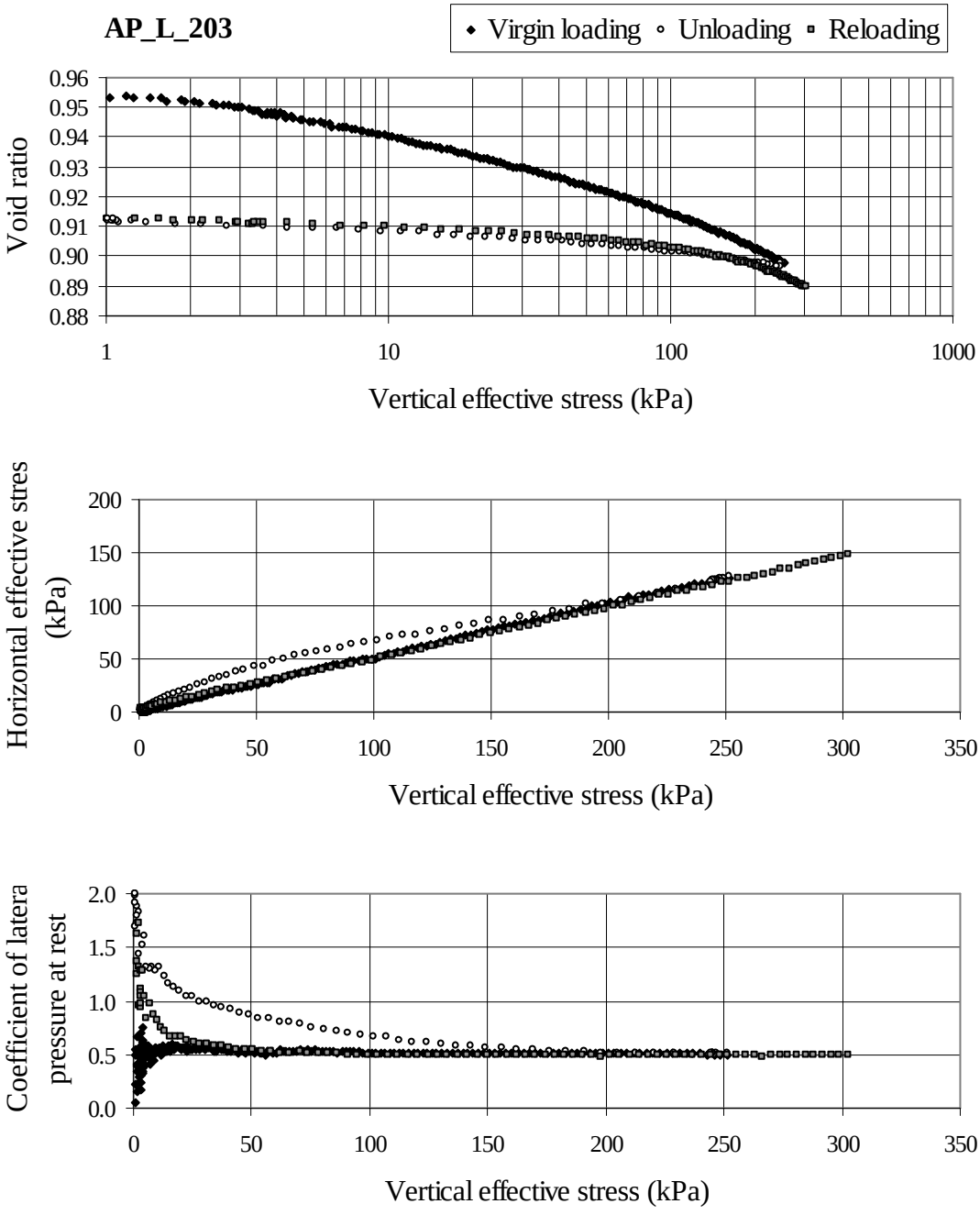

Figure A.1.3. Test data for AP_L_203

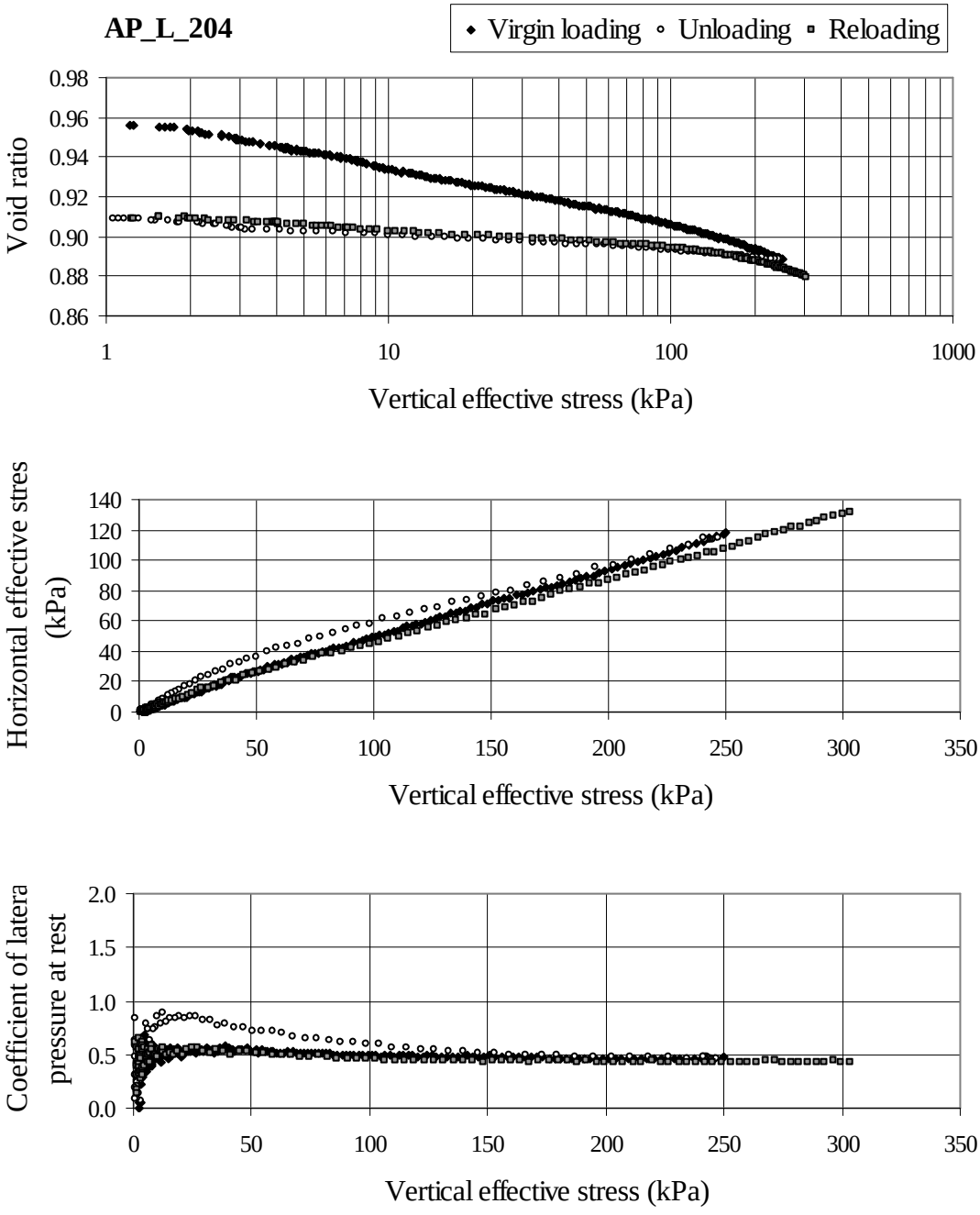

Figure A.1.4. Test data for AP_L_204

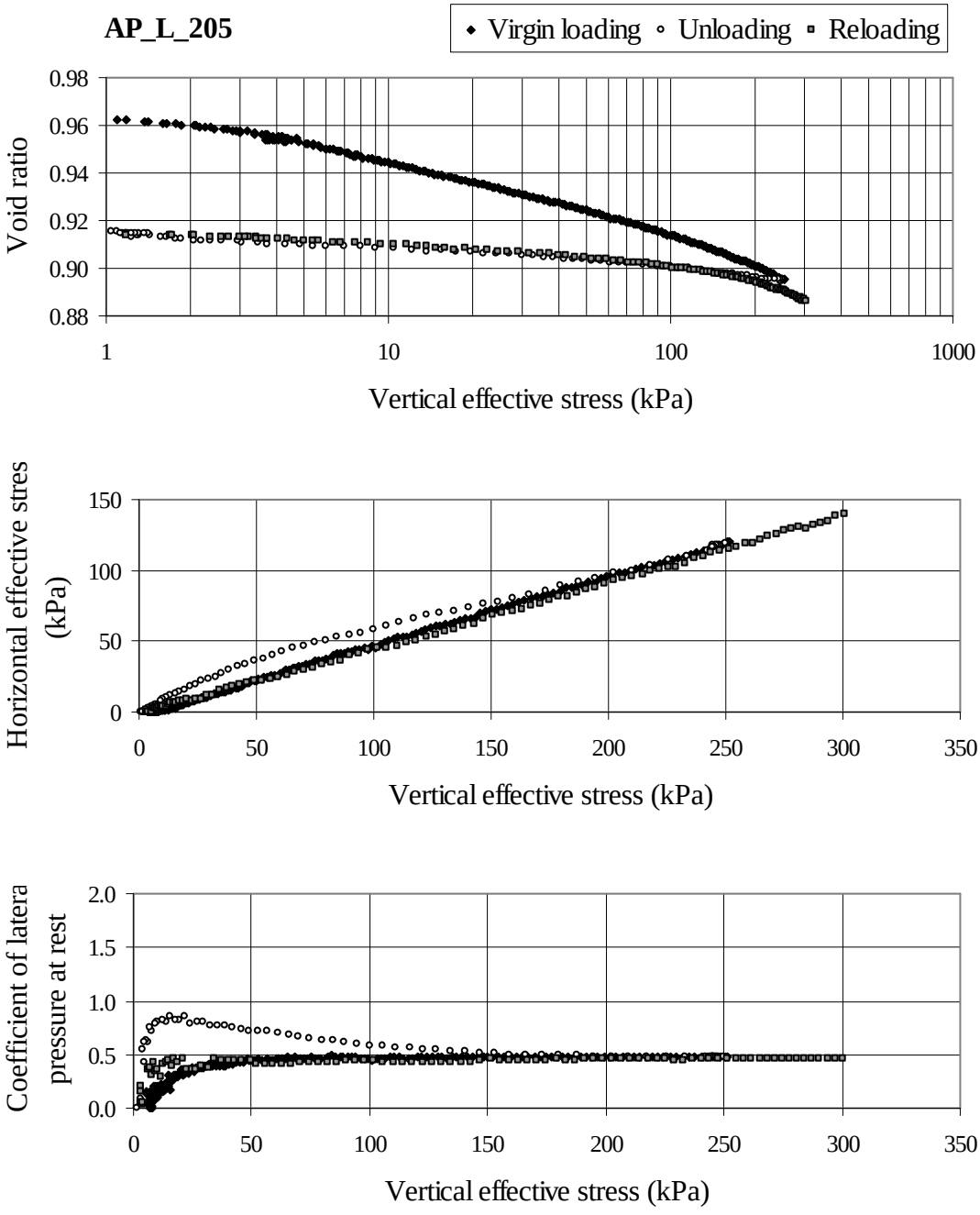

Figure A.1.5. Test data for AP_L_205

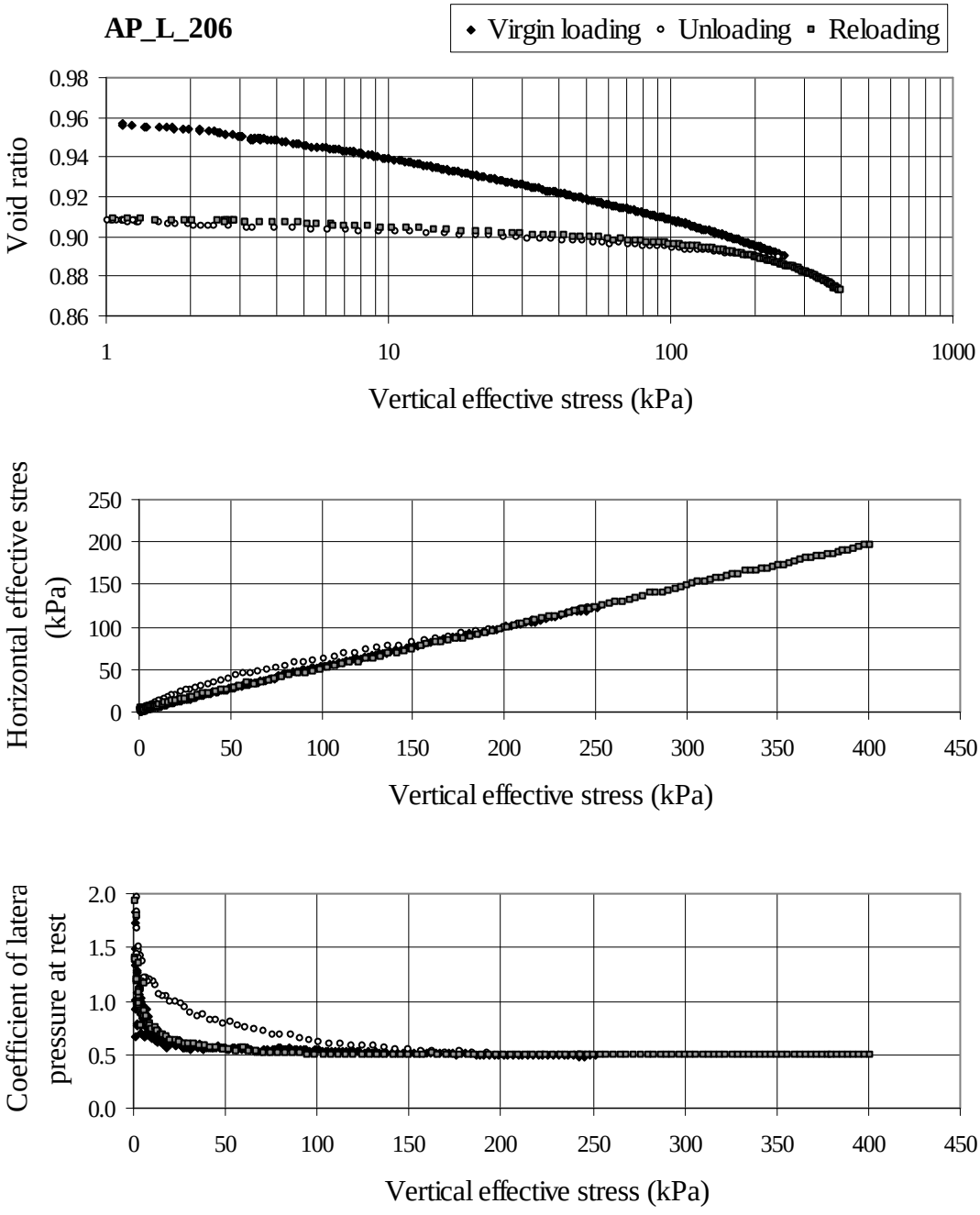

Figure A.1.6. Test data for AP_L_206

Appendix A.2. Medium loose specimens

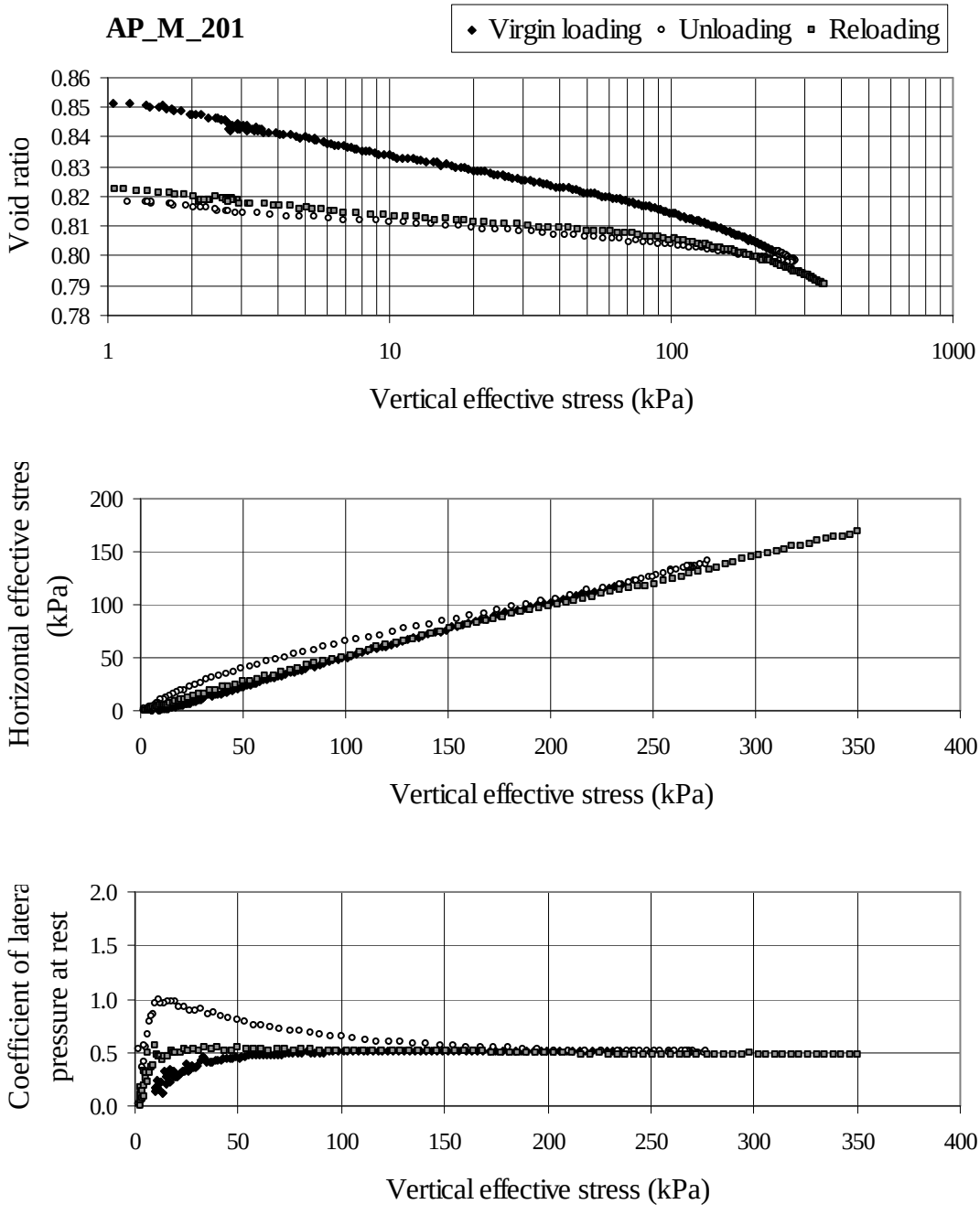

Figure A.2.1. Test data for AP_M_201

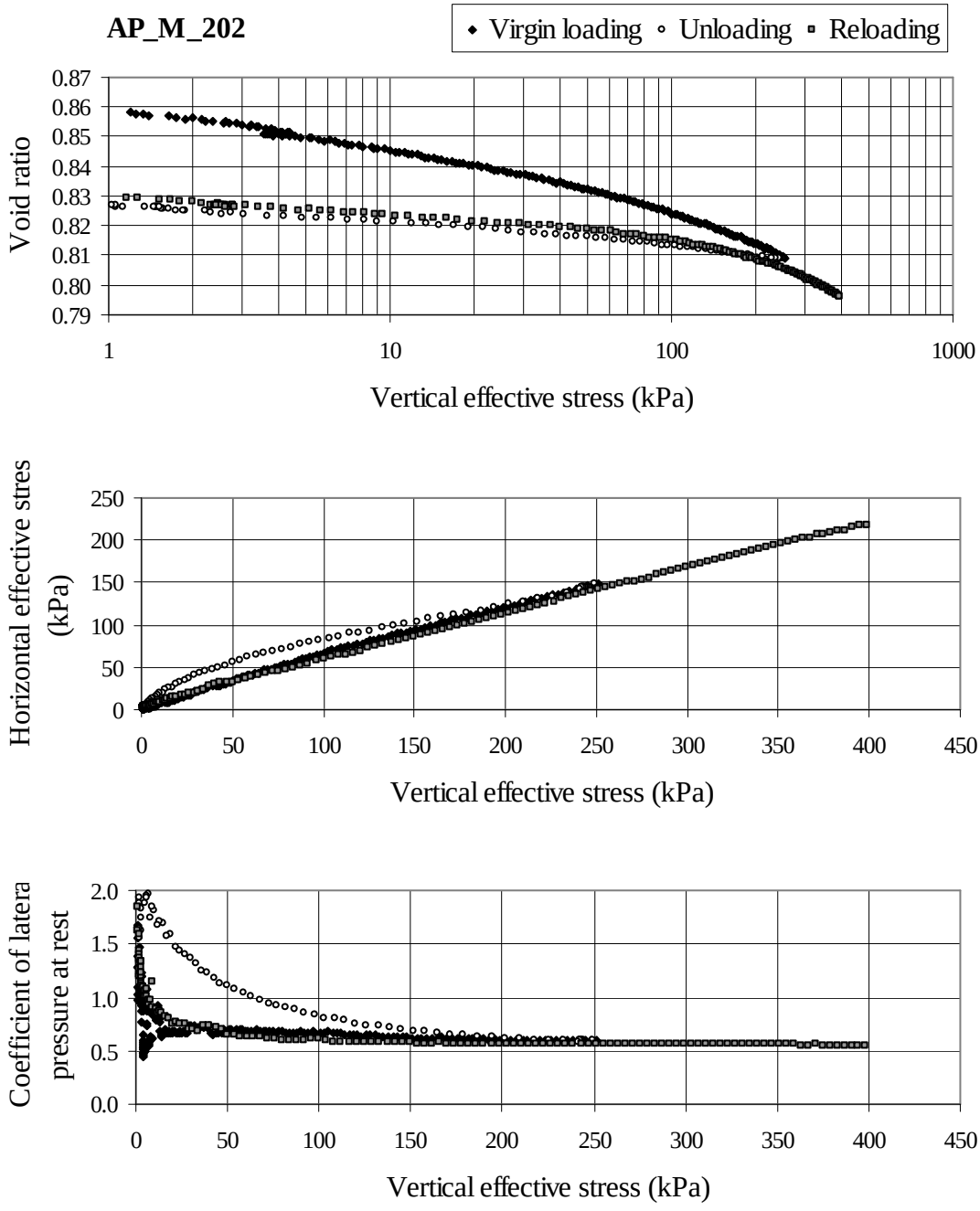

Figure A.2.2. Test data for AP_M_202

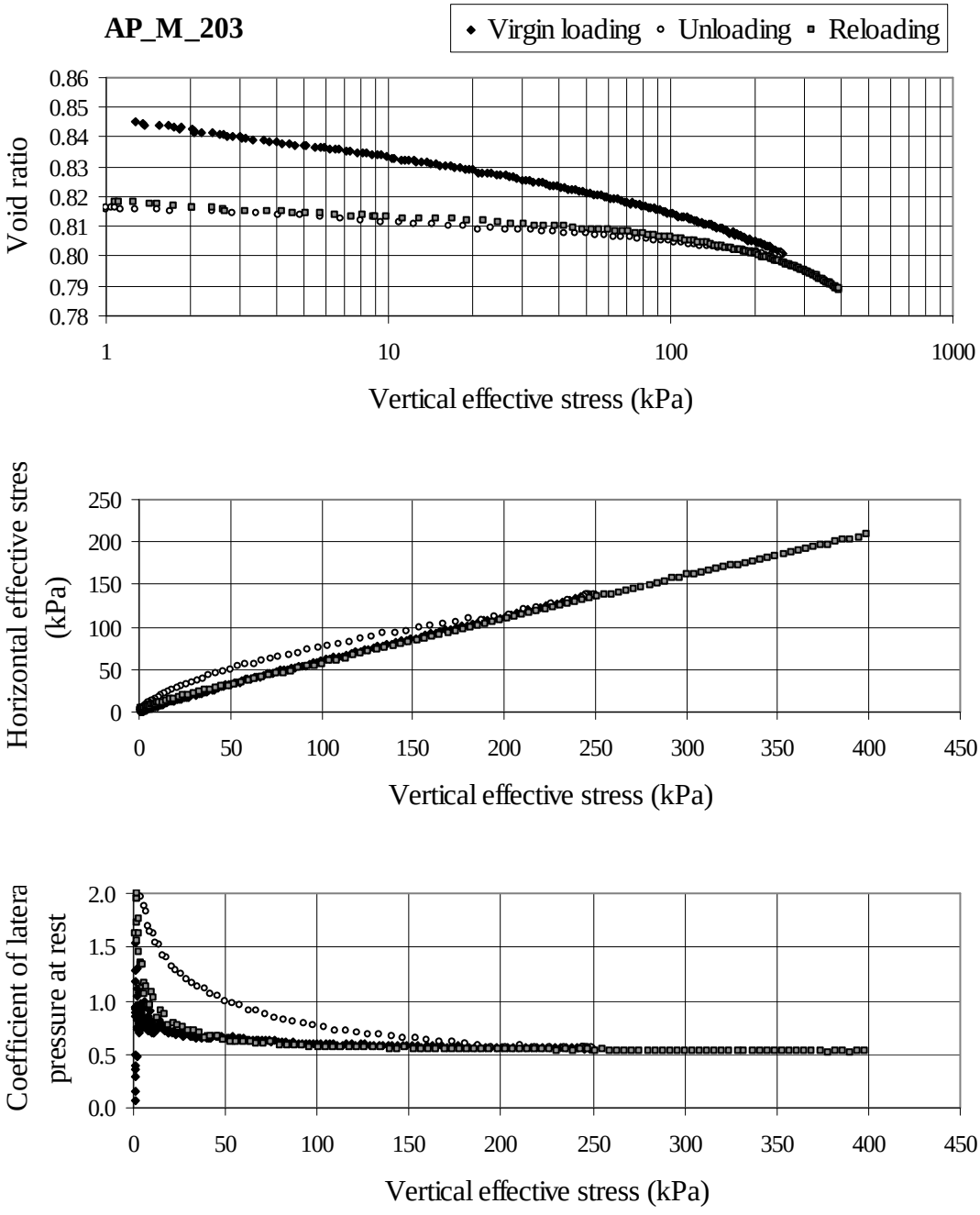

Figure A.2.3. Test data for AP_M_203

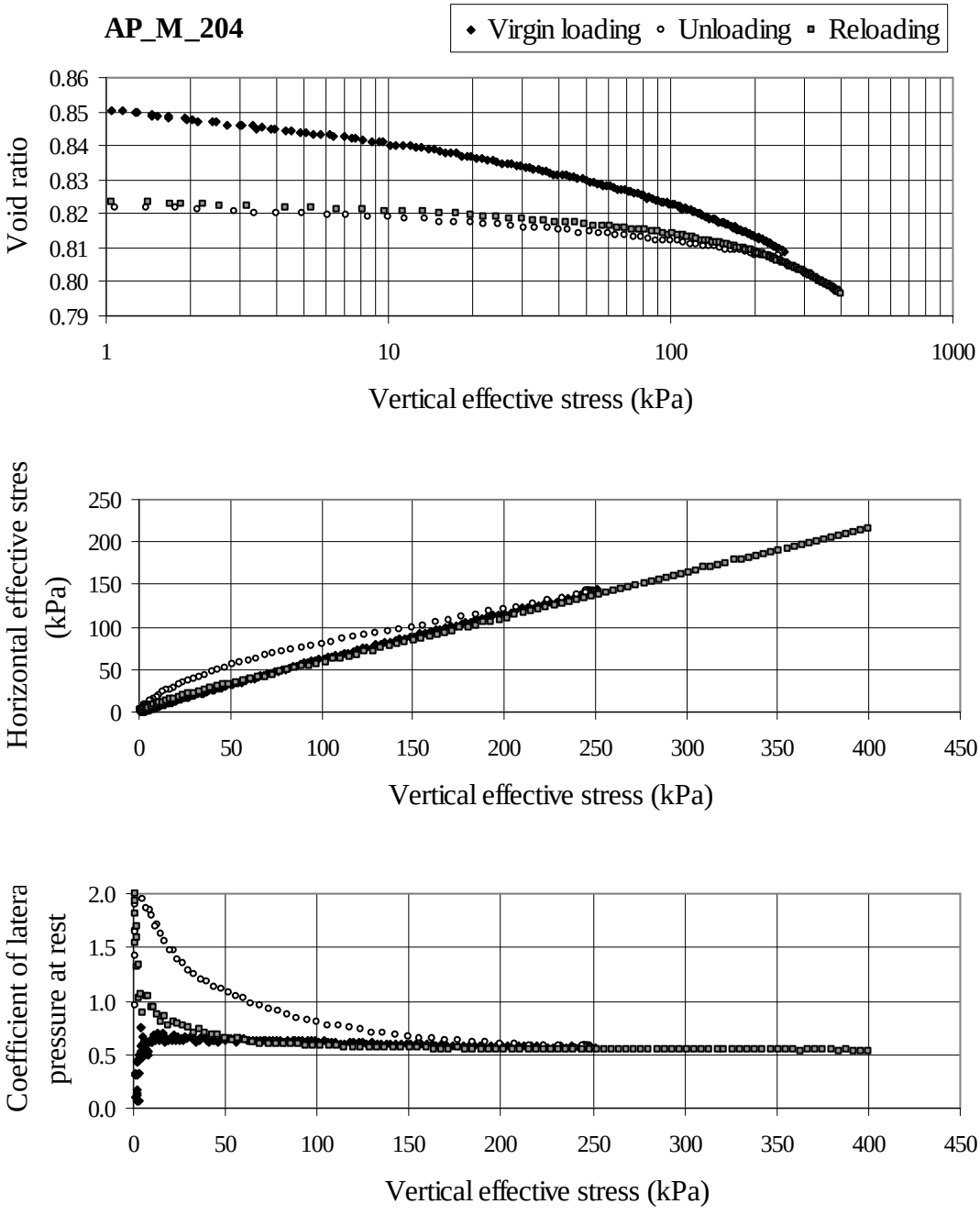

Figure A.2.4. Test data for AP_M_204

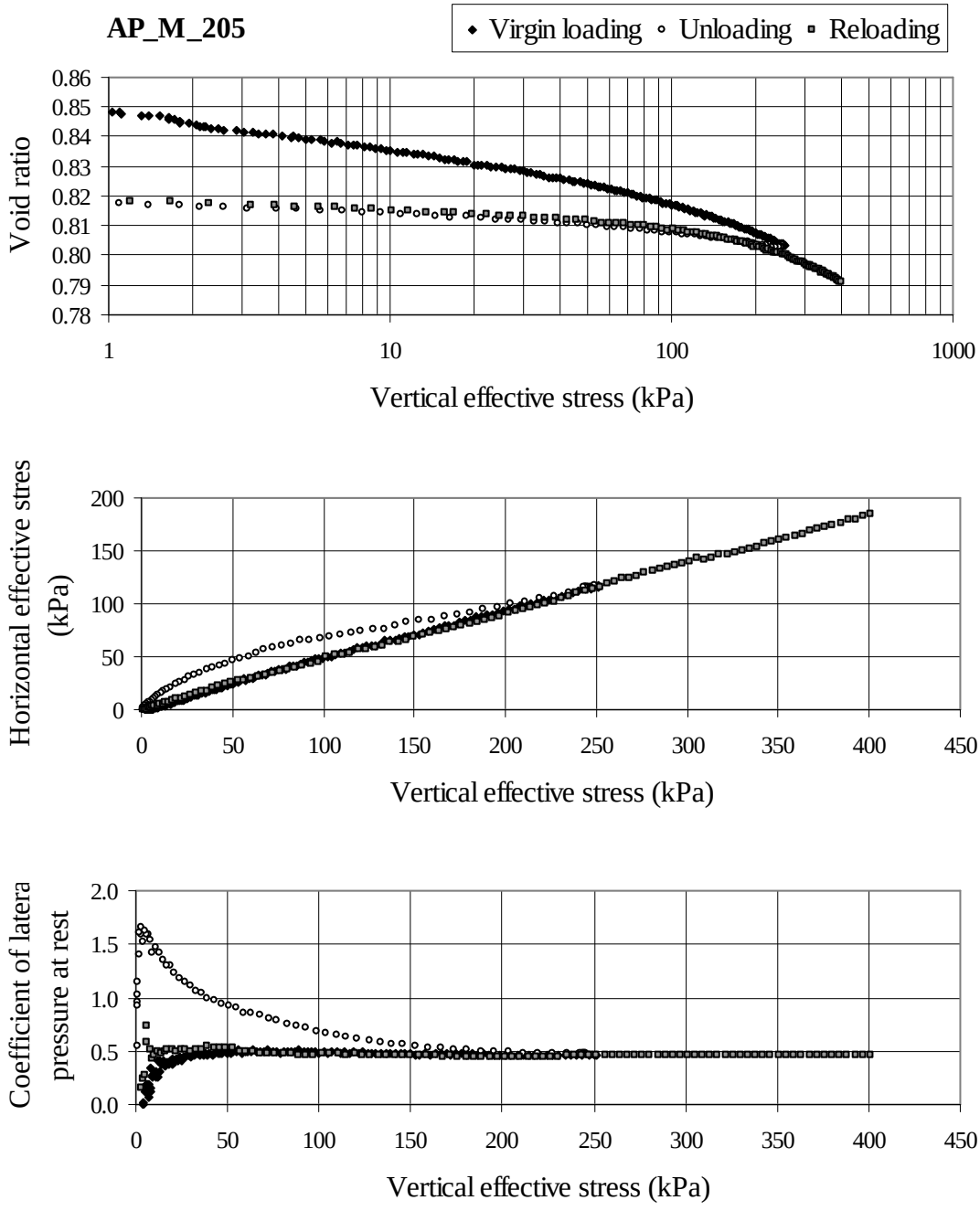

Figure A.2.5. Test data for AP_M_205

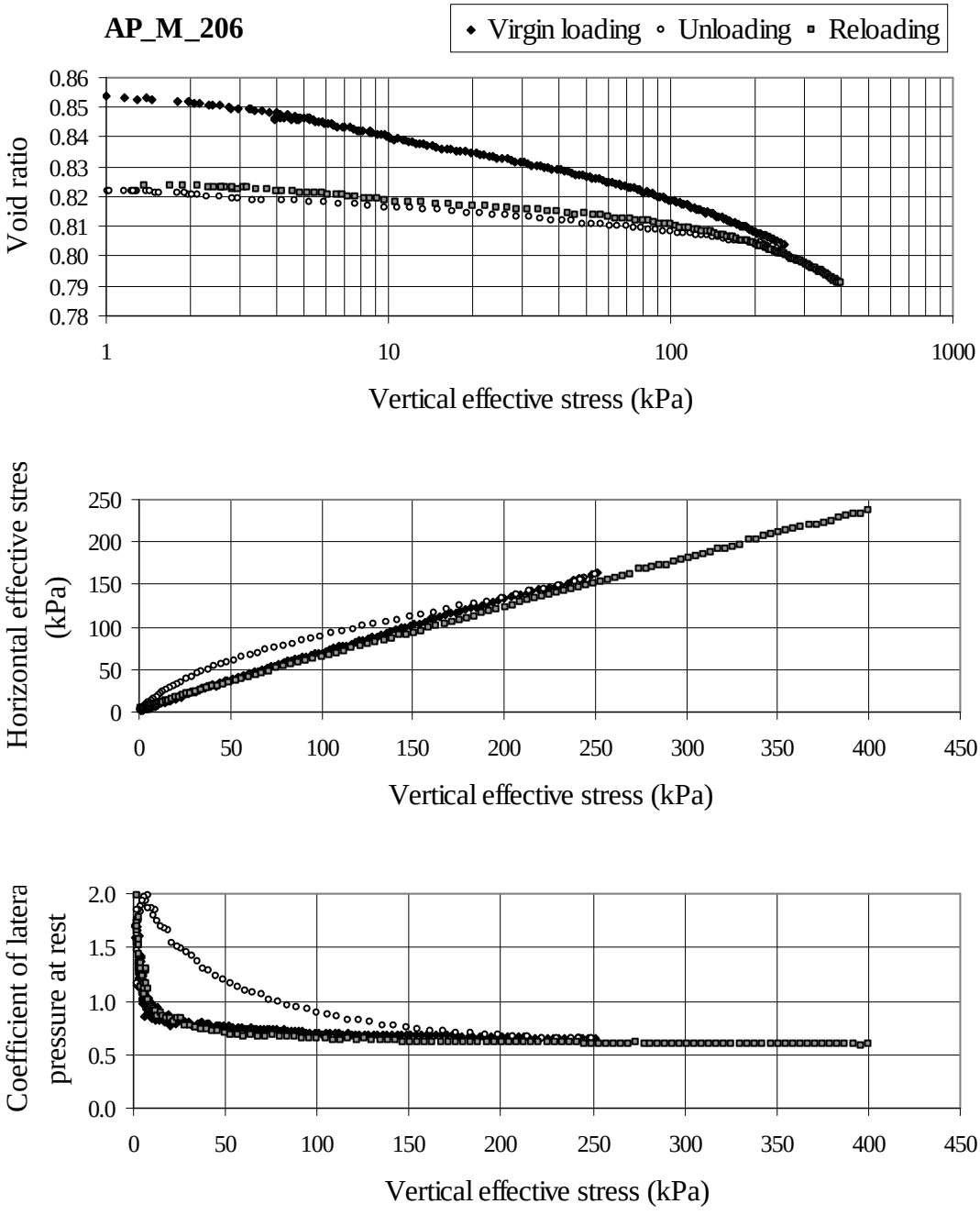

Figure A.2.6. Test data for AP_M_206

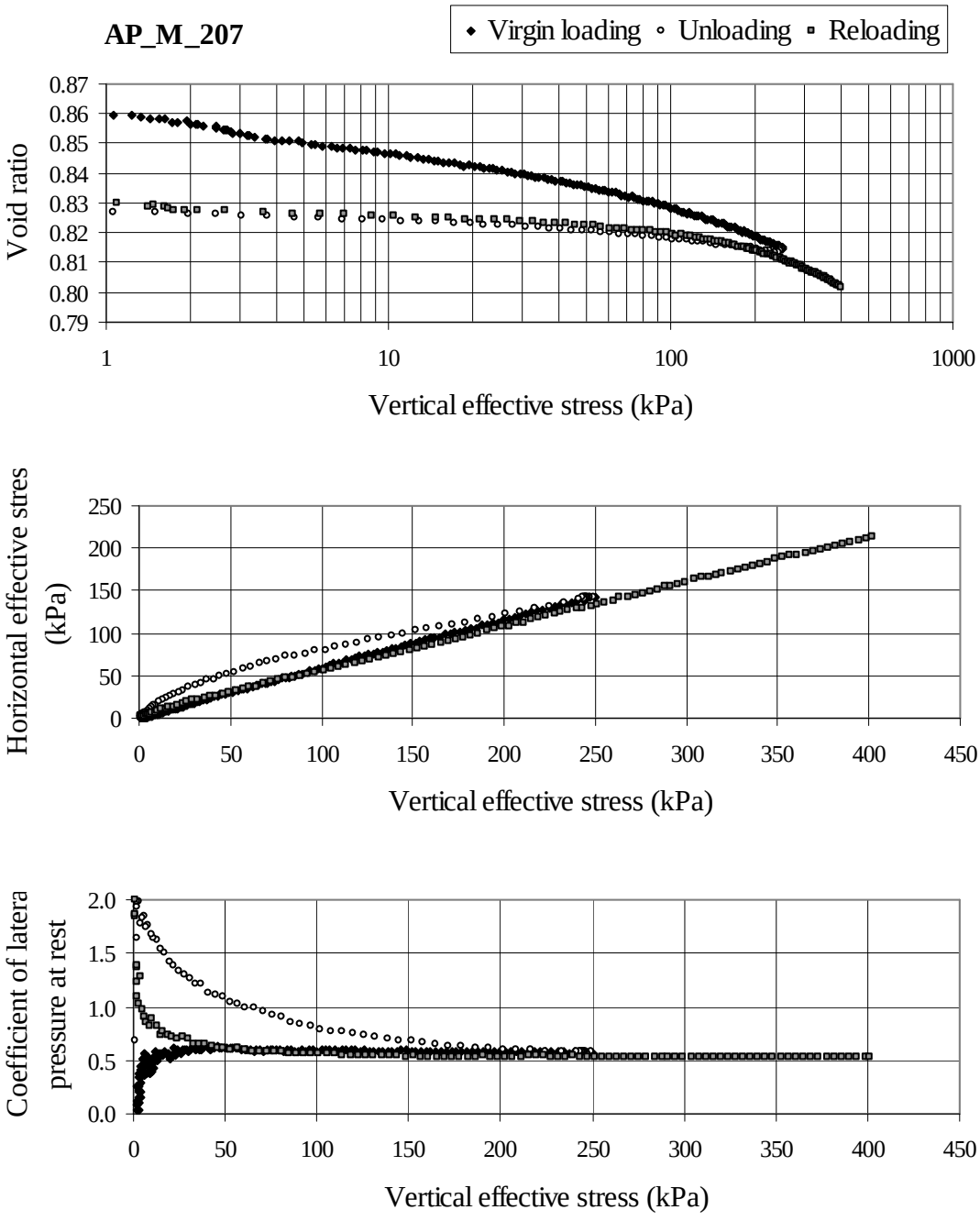

Figure A.2.7. Test data for AP_M_207

Appendix A.3. Dense specimens

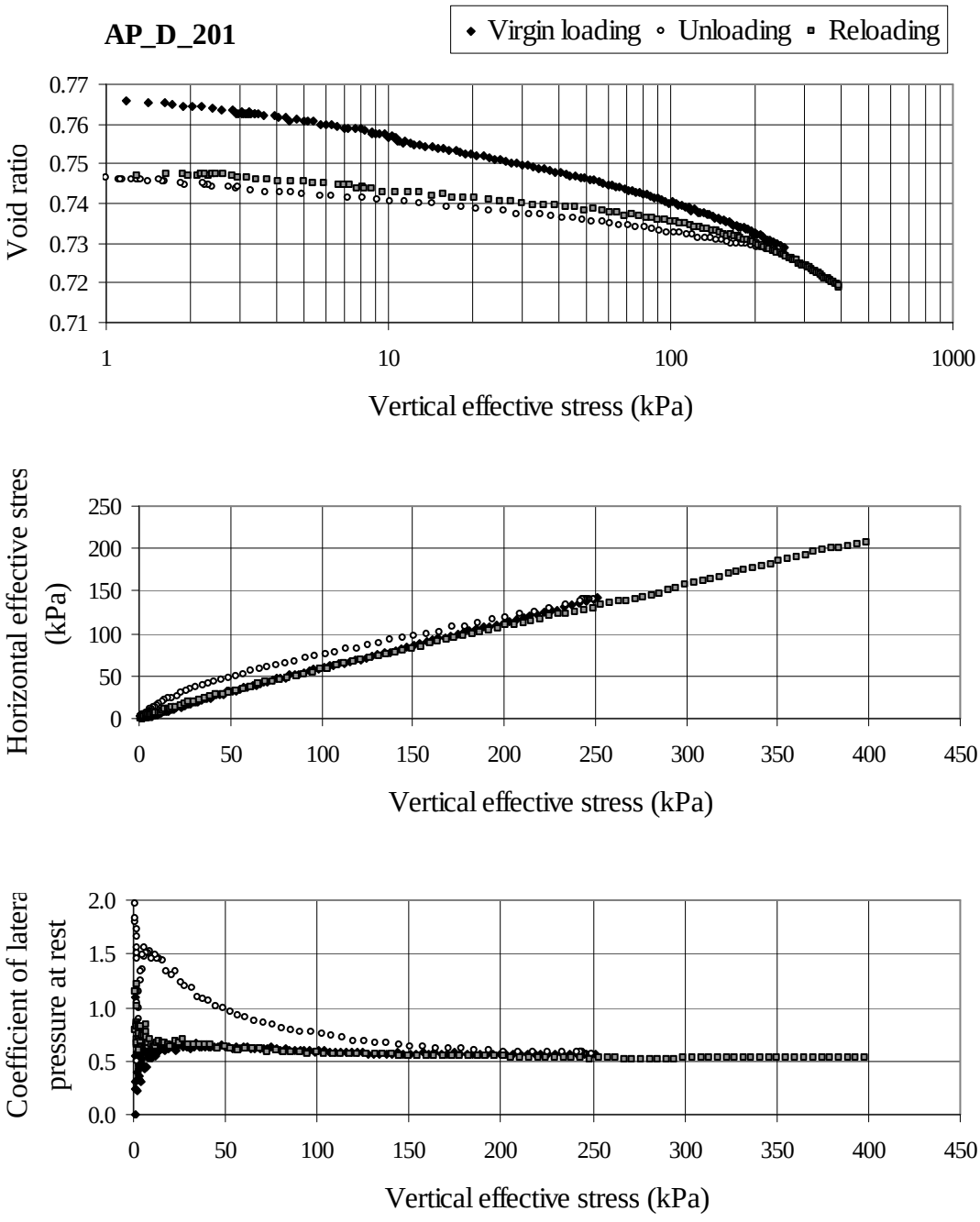

Figure A.3.1. Test data for AP_D_201

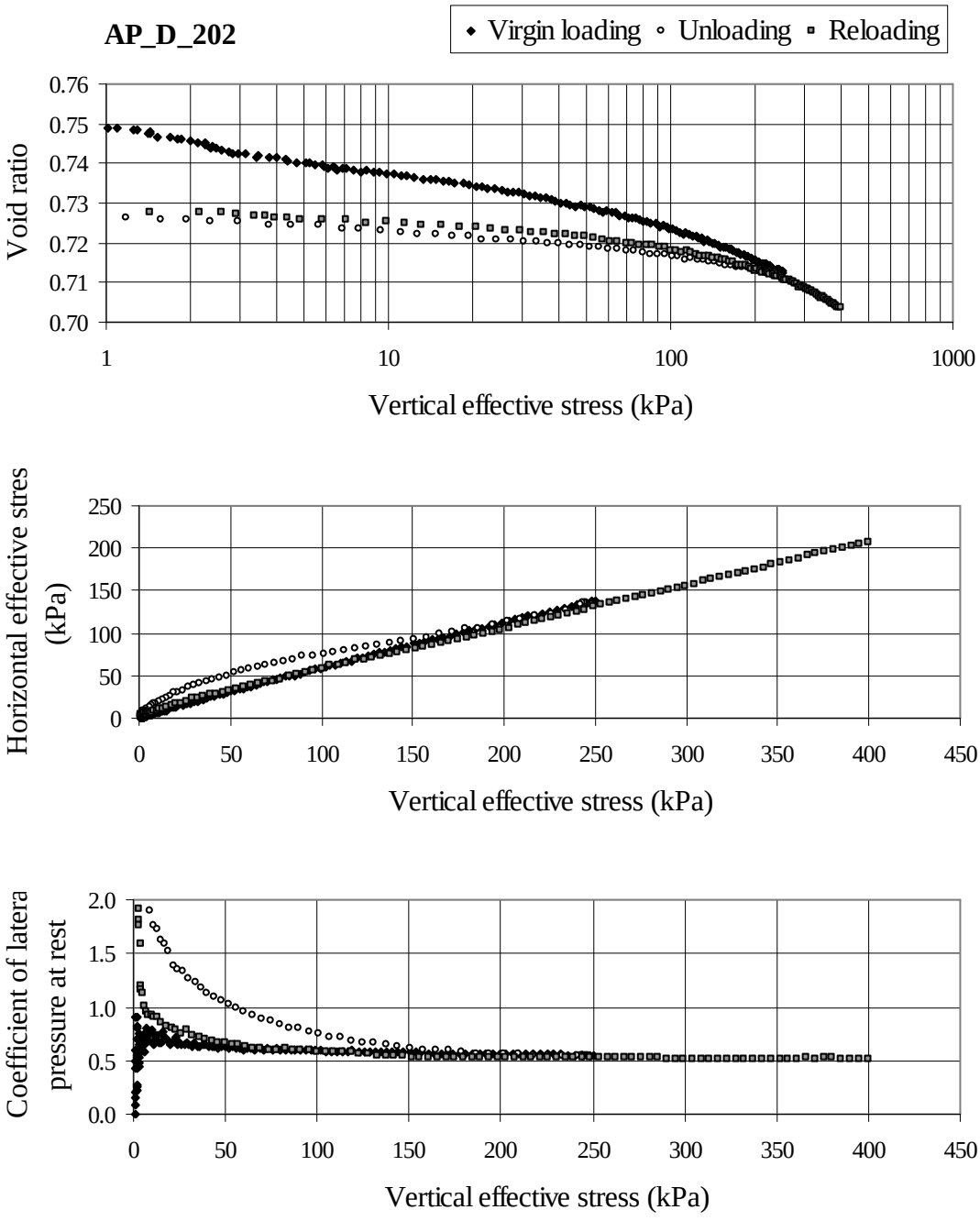

Figure A.3.2. Test data for AP_D_202

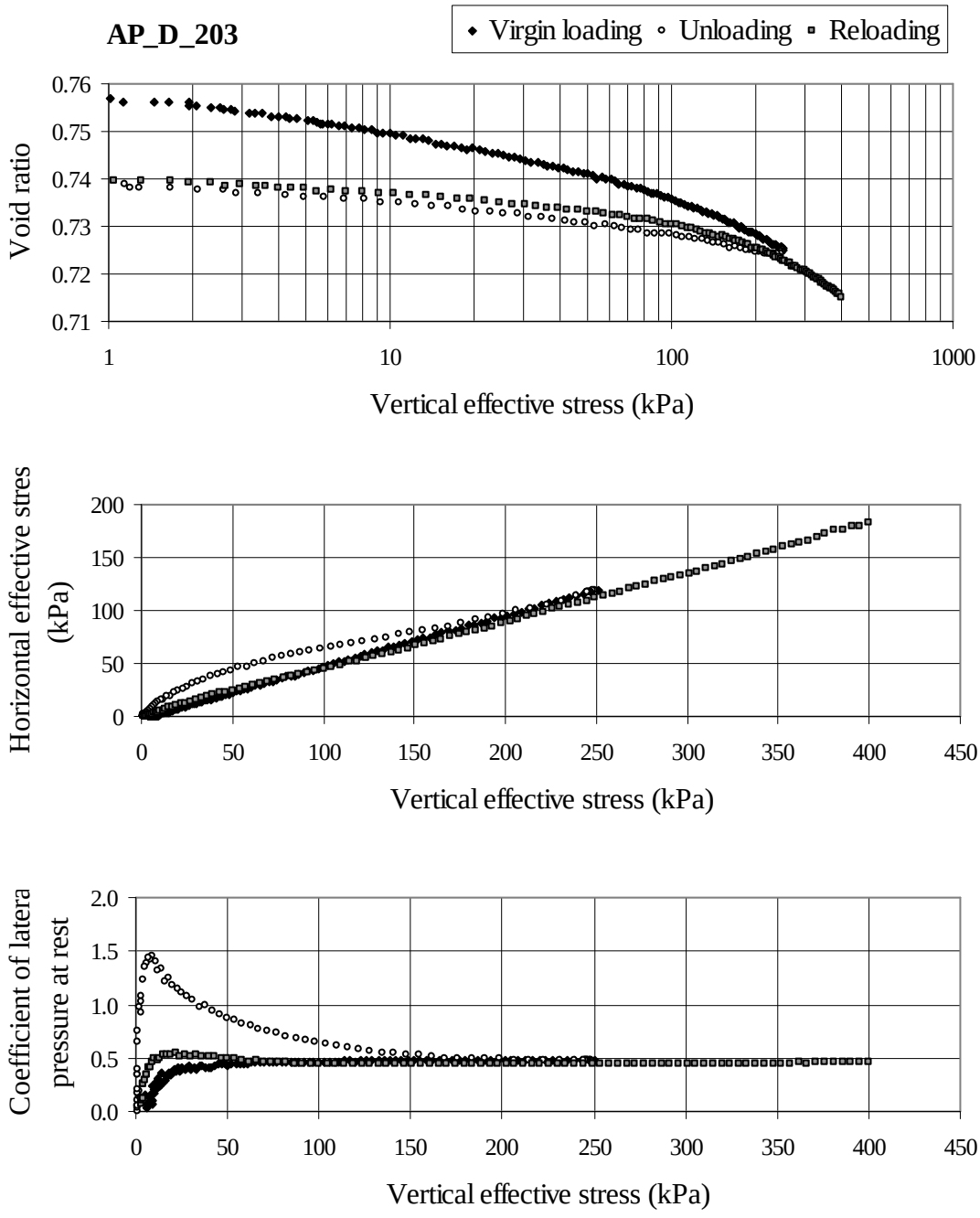

Figure A.3.3. Test data for AP_D_203

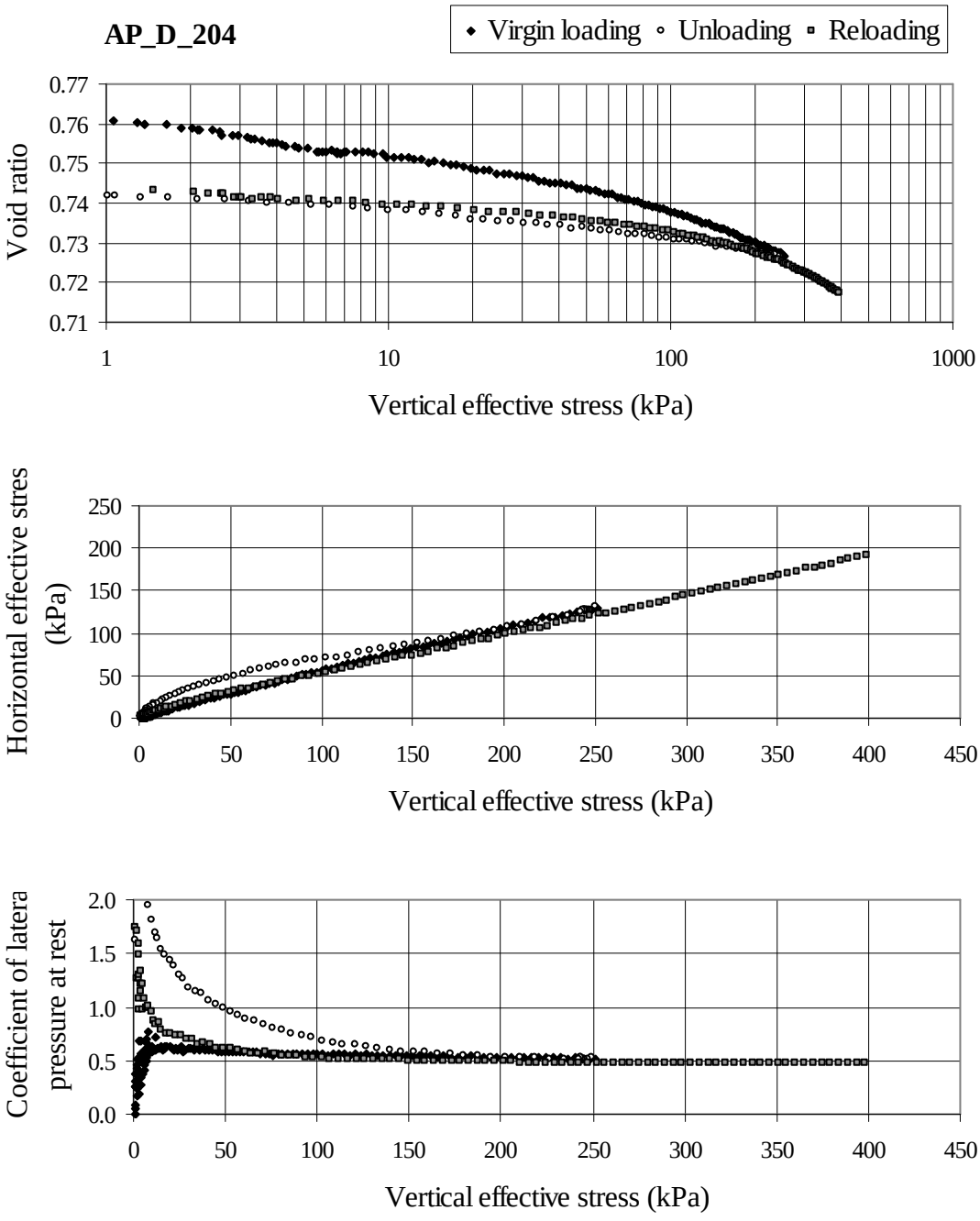

Figure A.3.4. Test data for AP_D_204

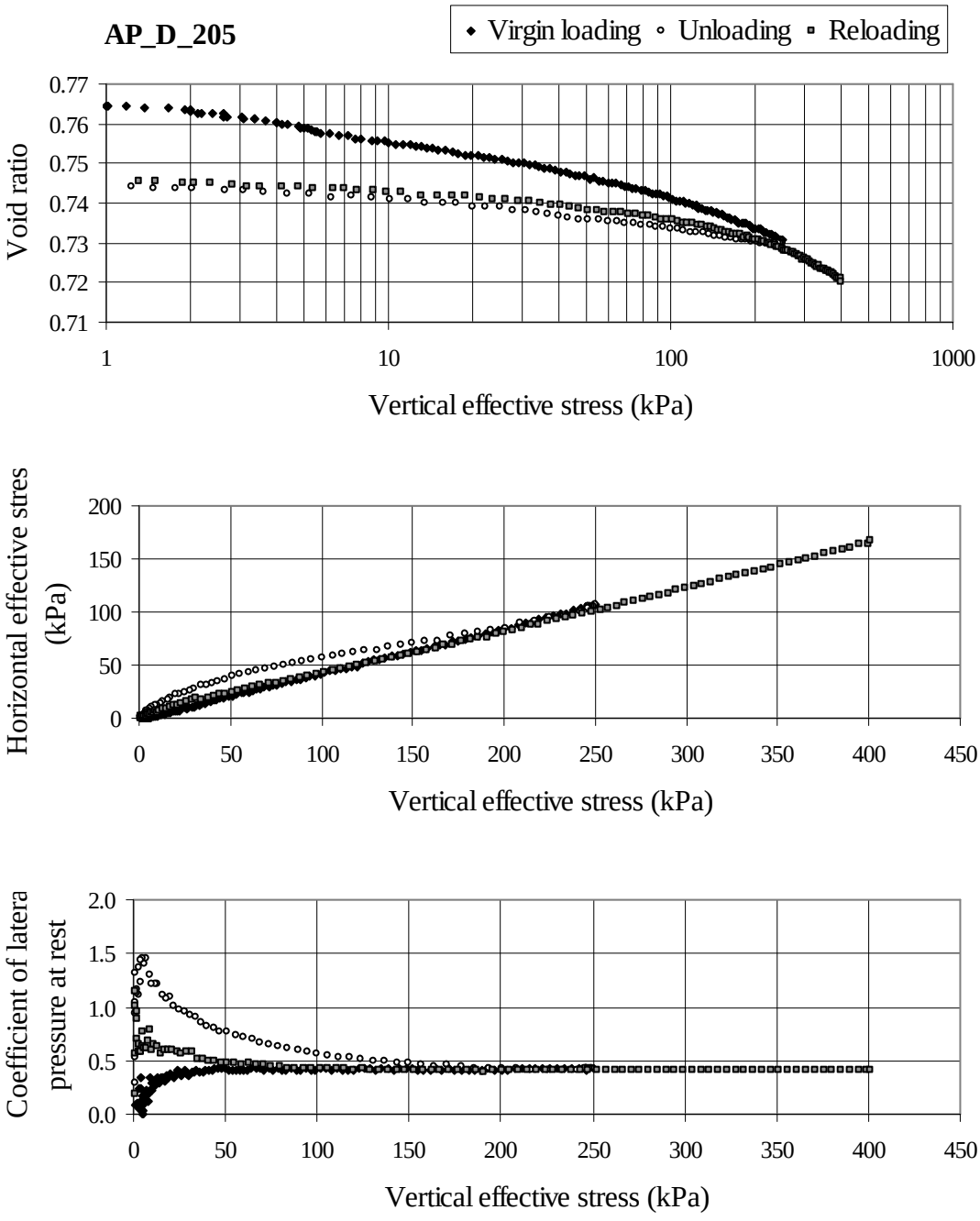

Figure A.3.5. Test data for AP_D_205

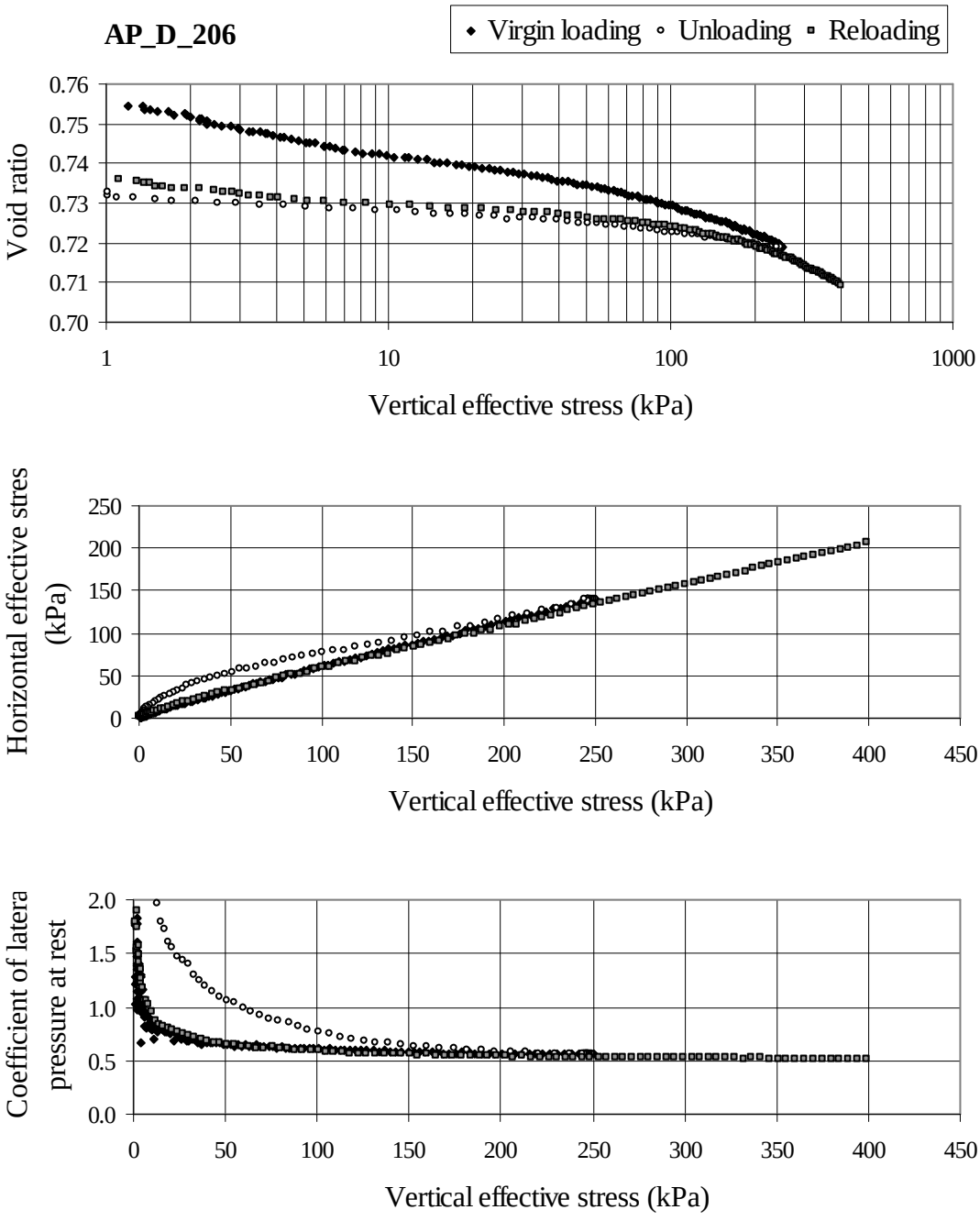

Figure A.3.6. Test data for AP_D_206

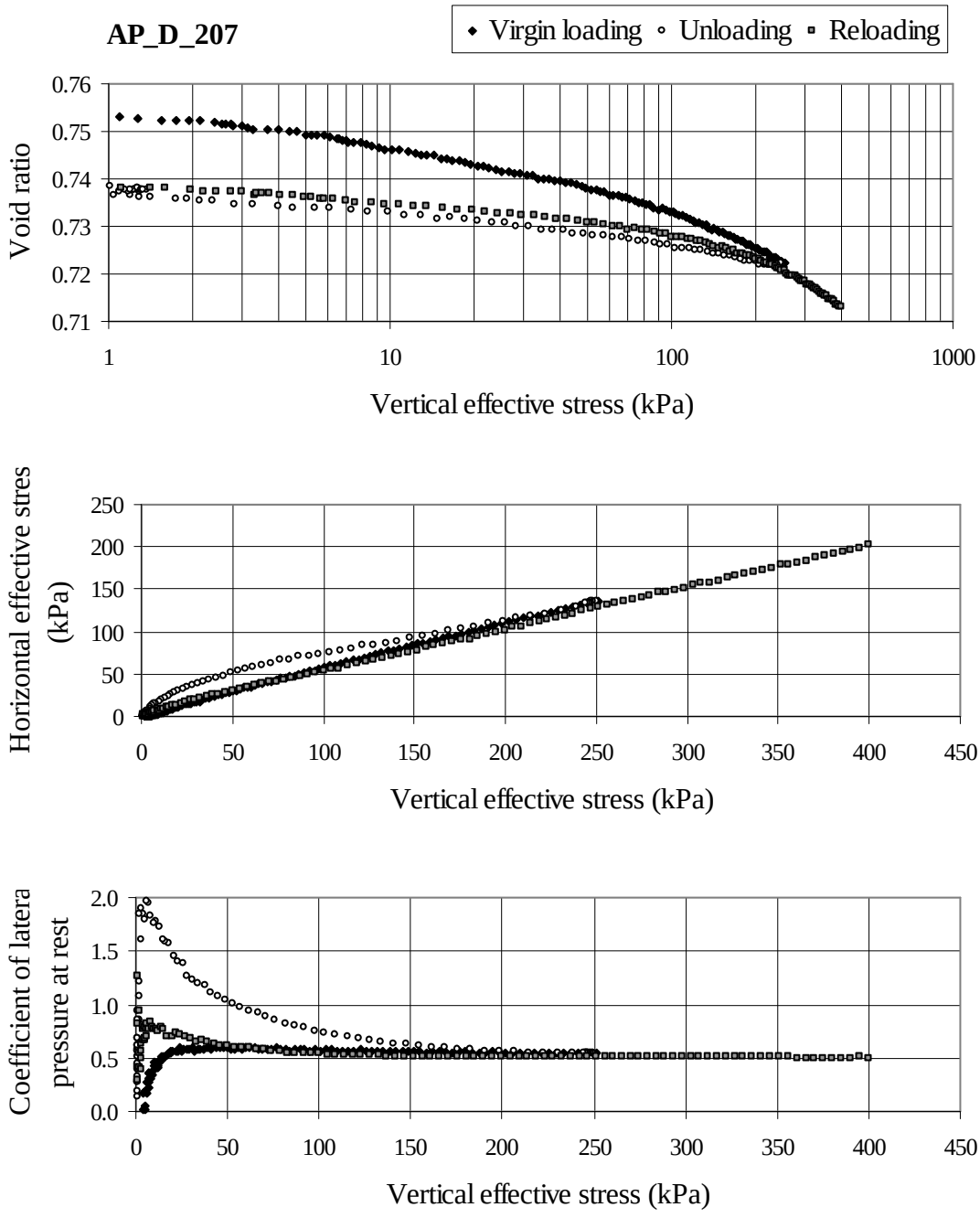

Figure A.3.7. Test data for AP_D_207

Appendix A.4. Very dense specimens

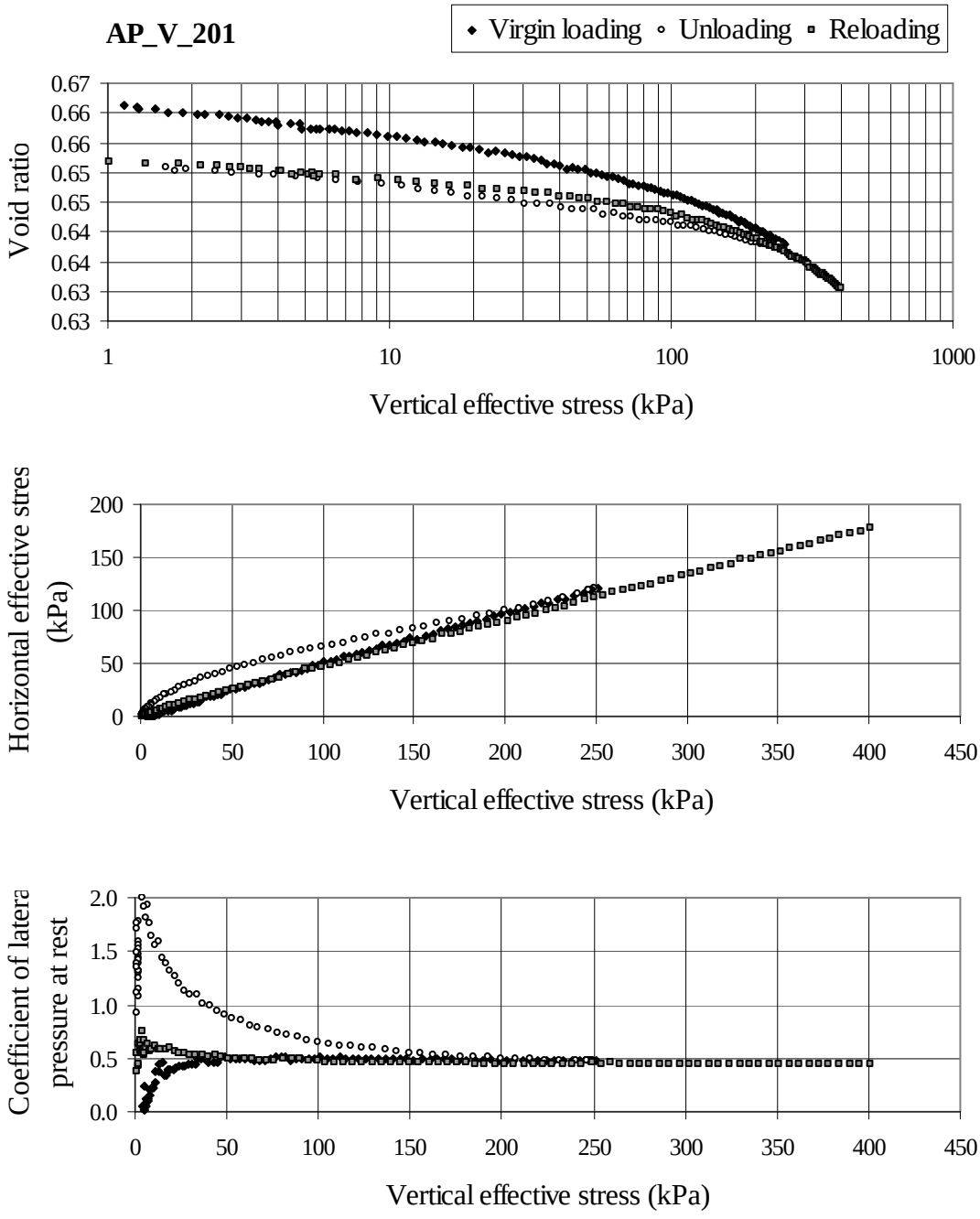

Figure A.4.1. Test data for AP_V_201

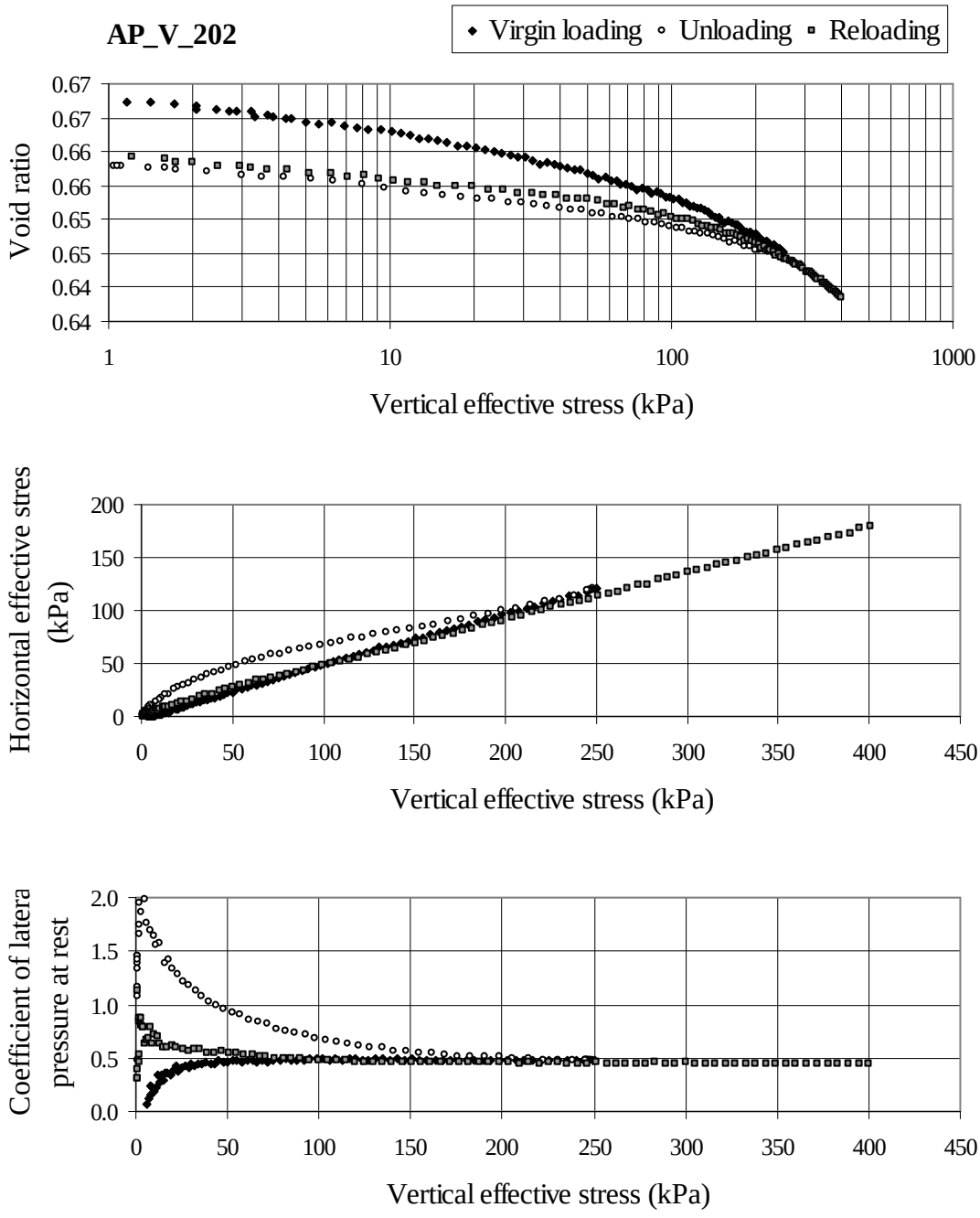

Figure A.4.2. Test data for AP_V_202

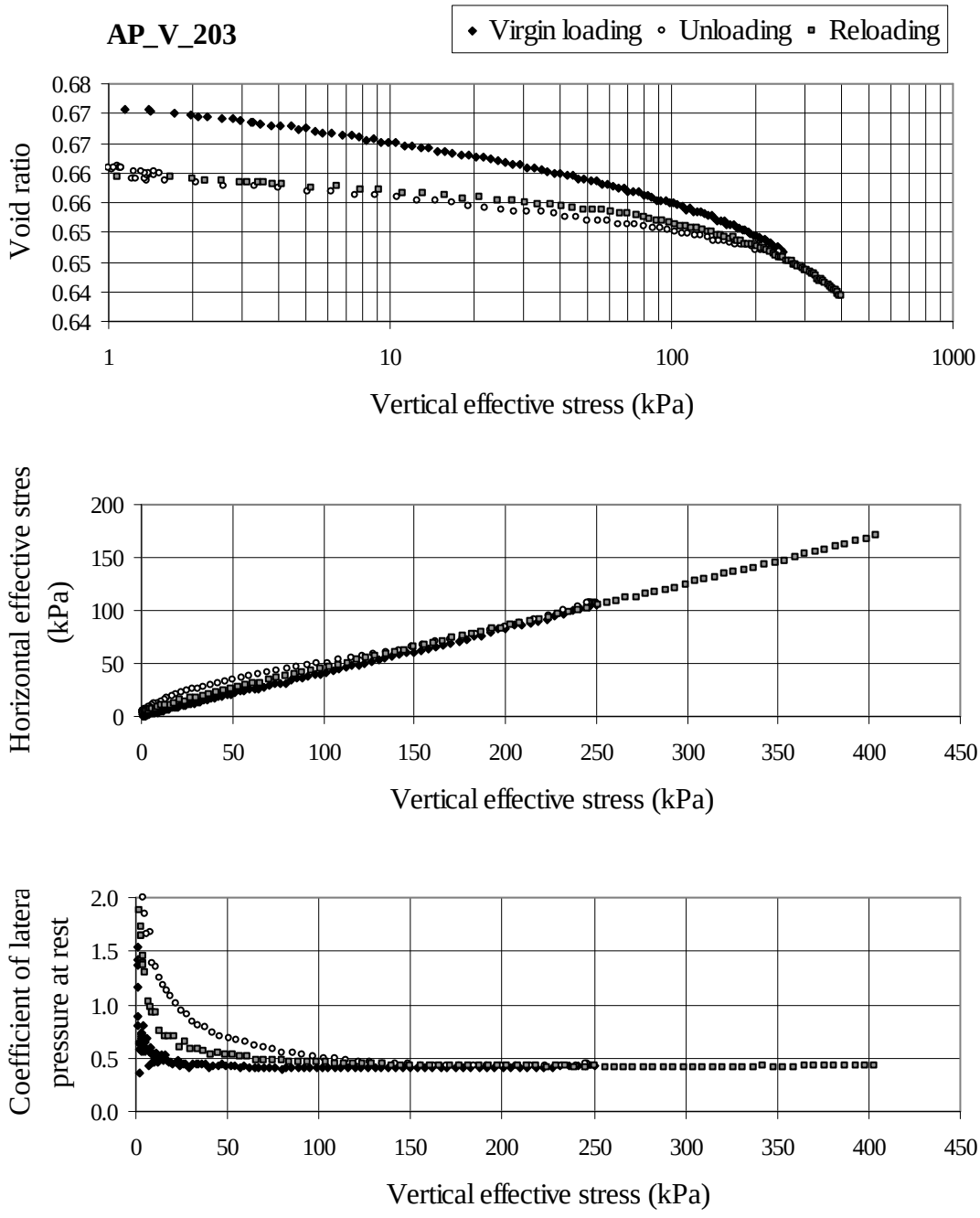

Figure A.4.3. Test data for AP_V_203

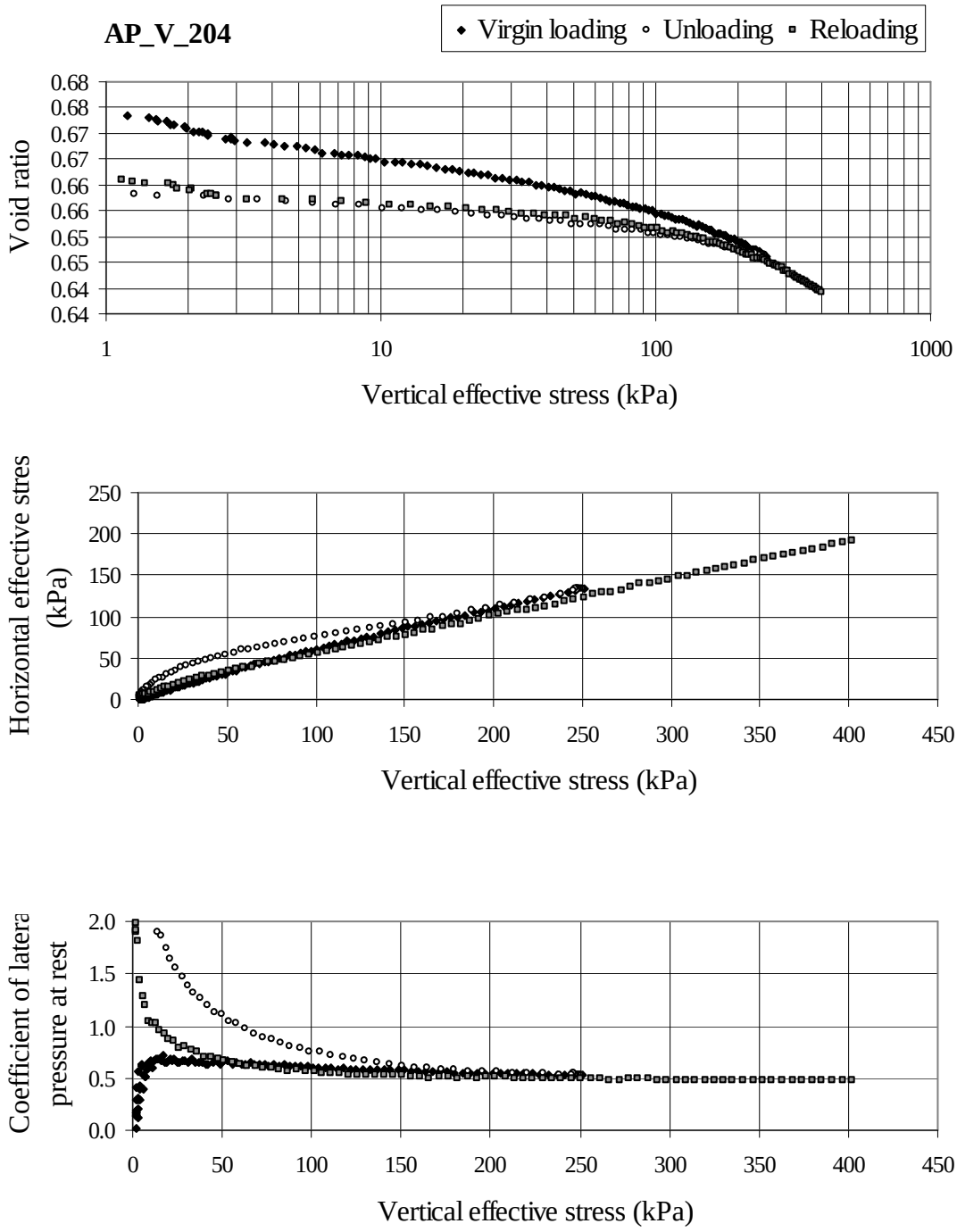

Figure A.4.4. Test data for AP_V_204

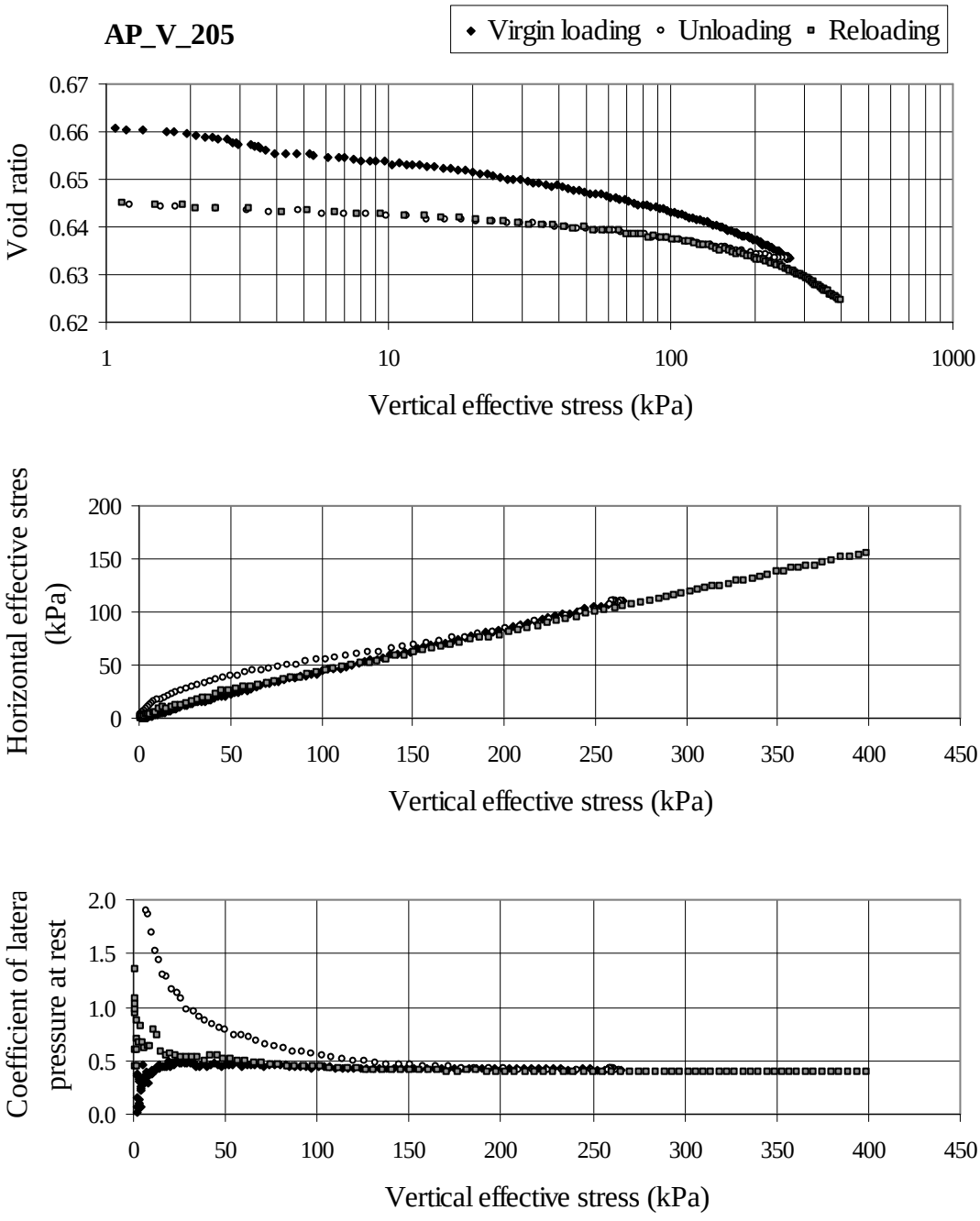

Figure A.4.5. Test data for AP_V_205

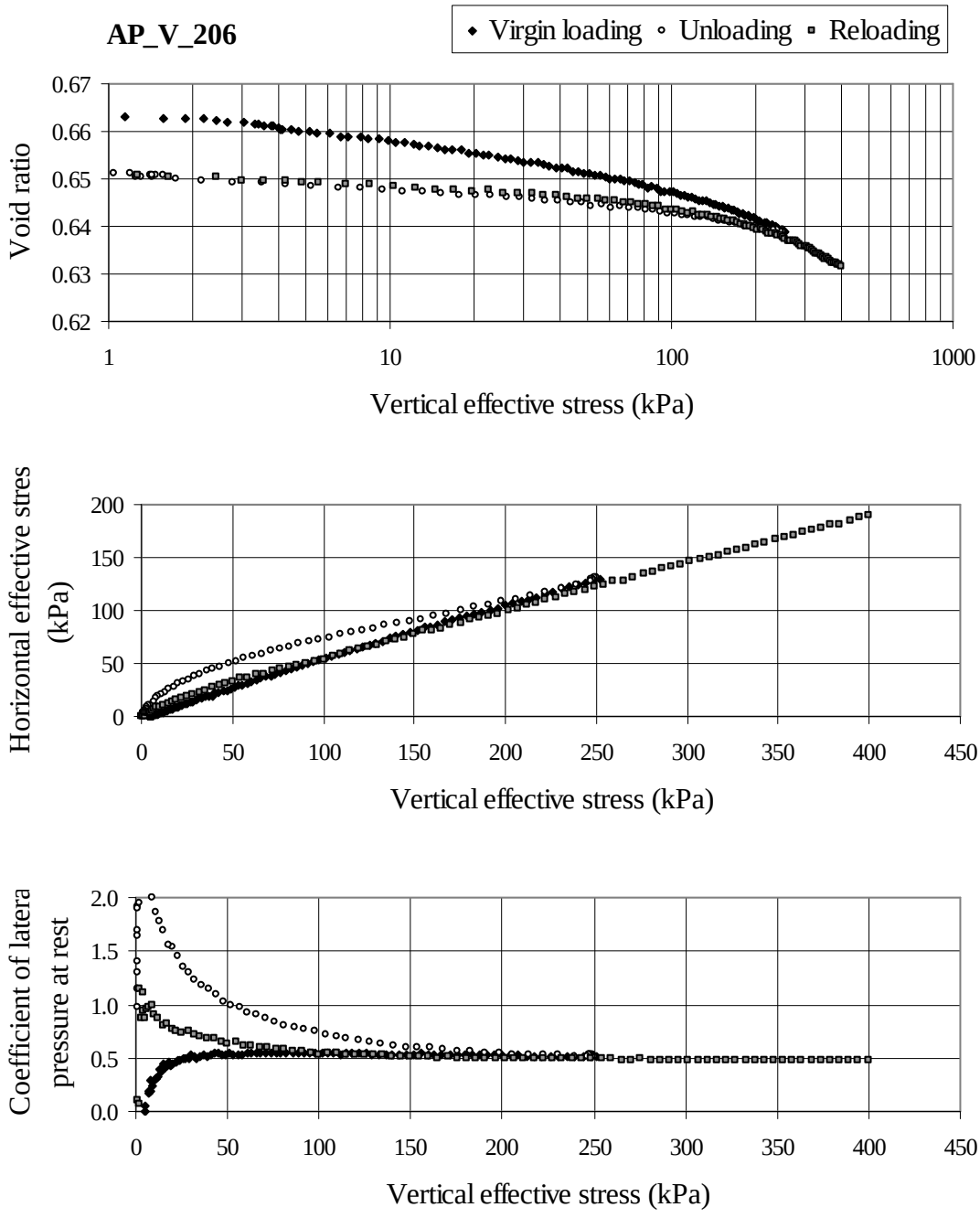

Figure A.4.6. Test data for AP_V_206

APPENDIX B: TEST DATA FOR TAMPING

Appendix B.1. Medium loose specimens

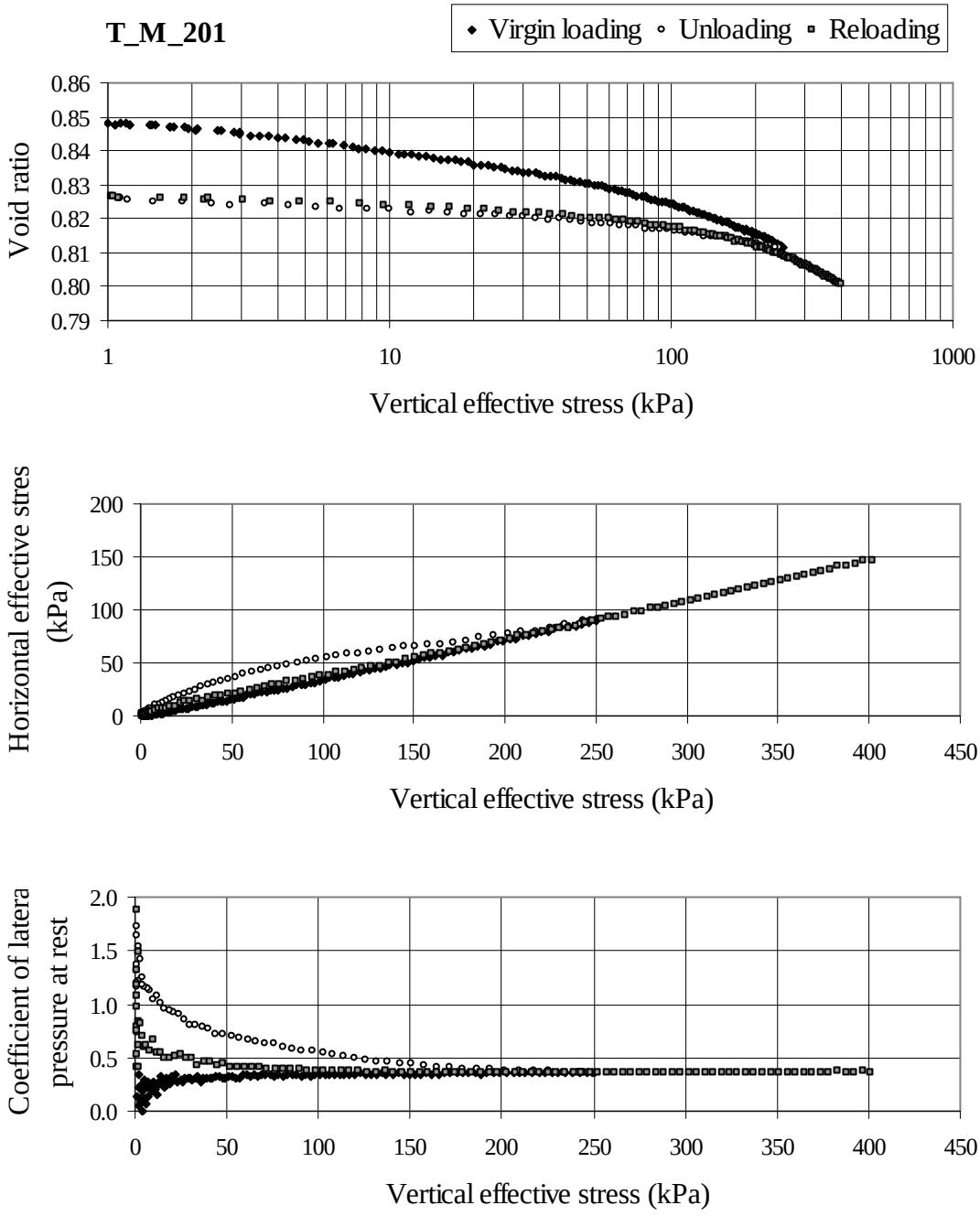

Figure B.1.1. Test data for T_M_201

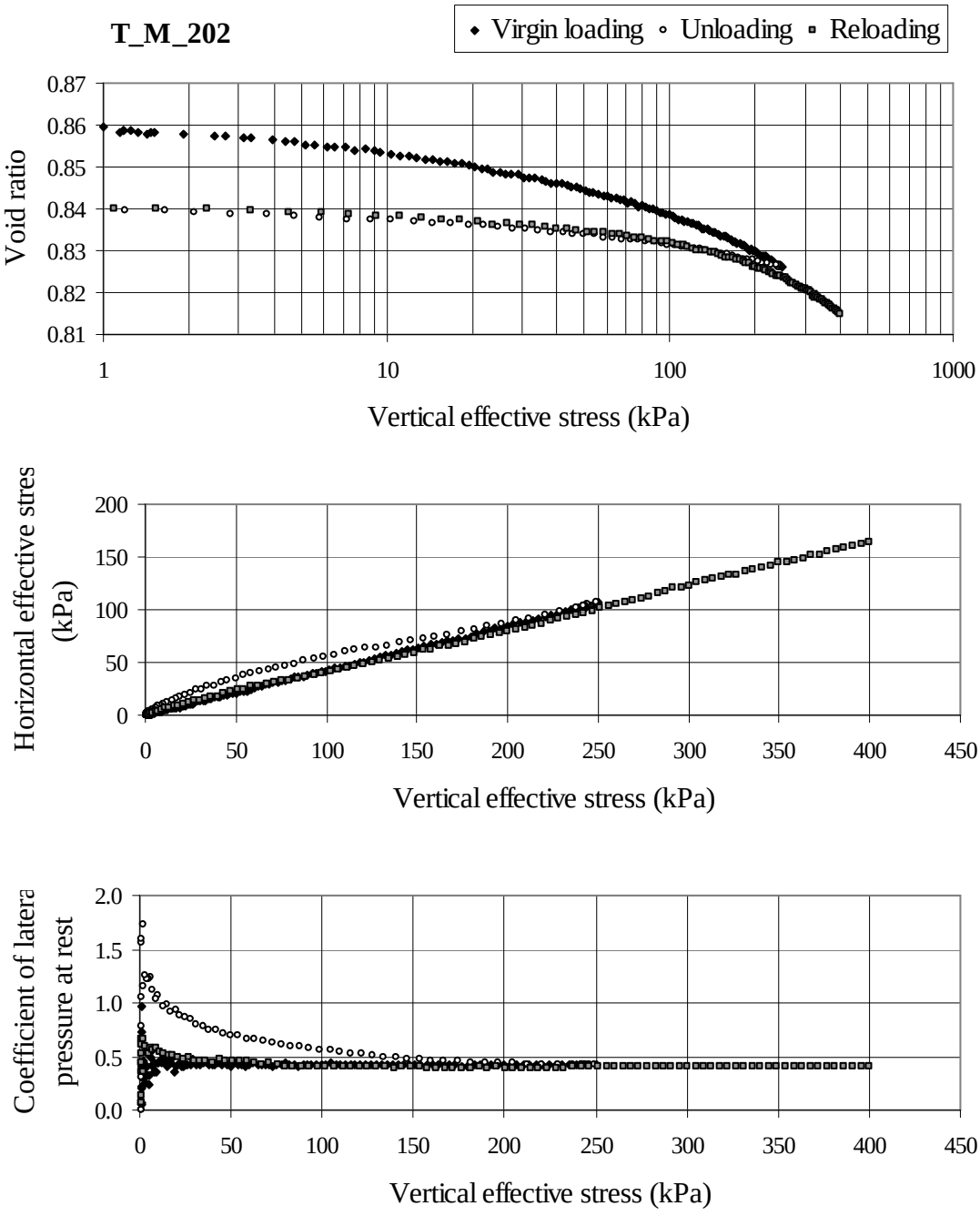

Figure B.1.2. Test data for T_M_202

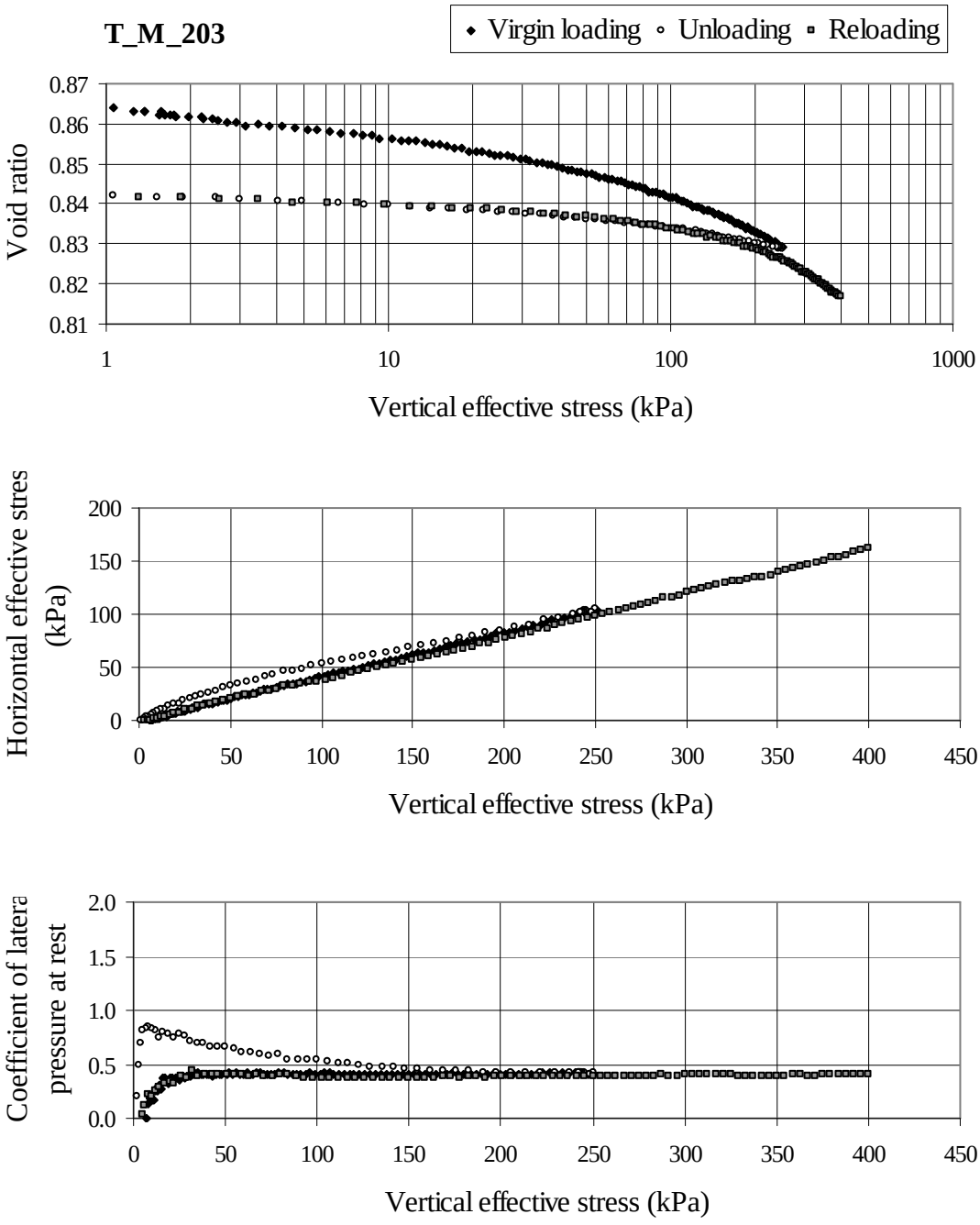

Figure B.1.3. Test data for T_M_203

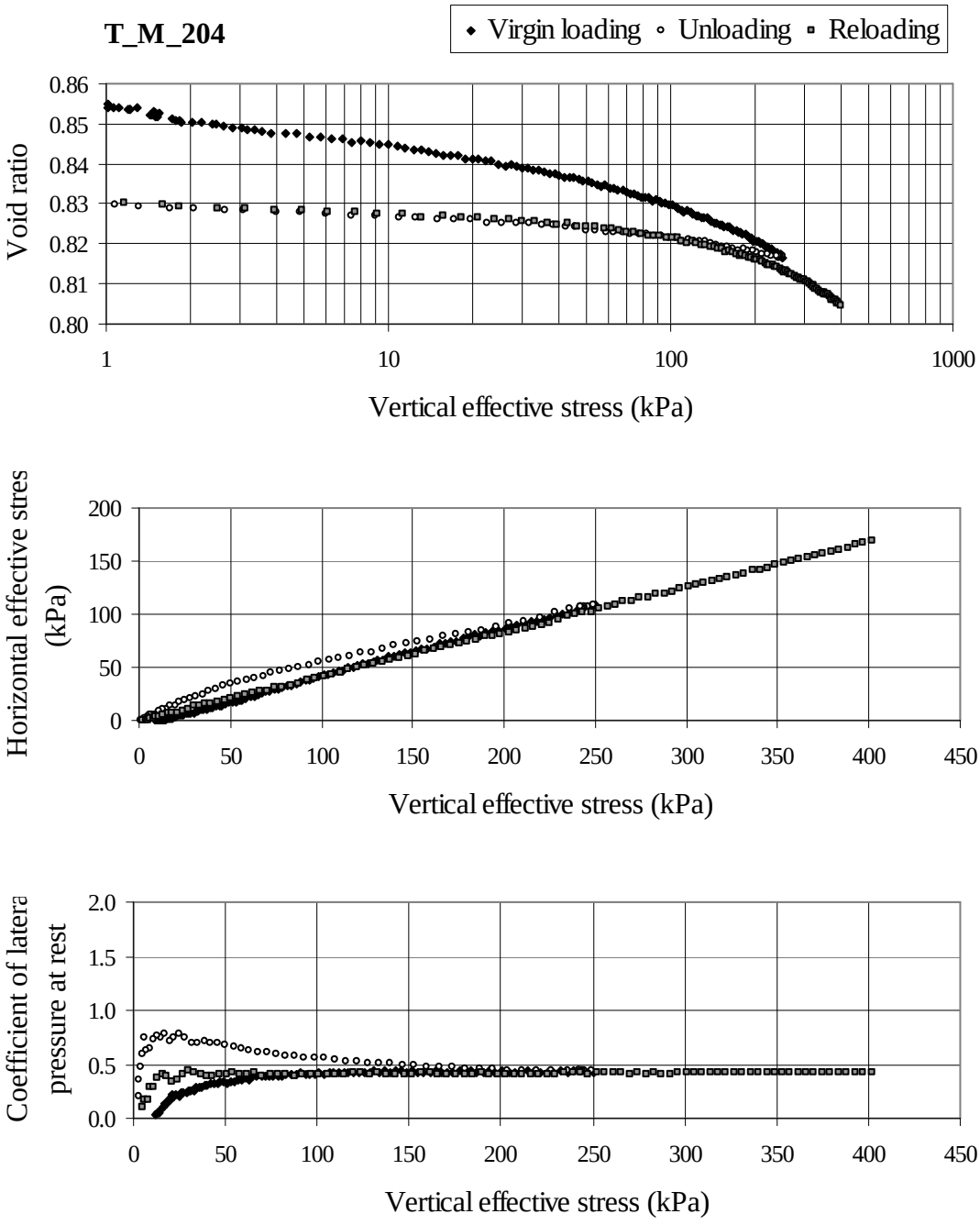

Figure B.1.4. Test data for T_M_204

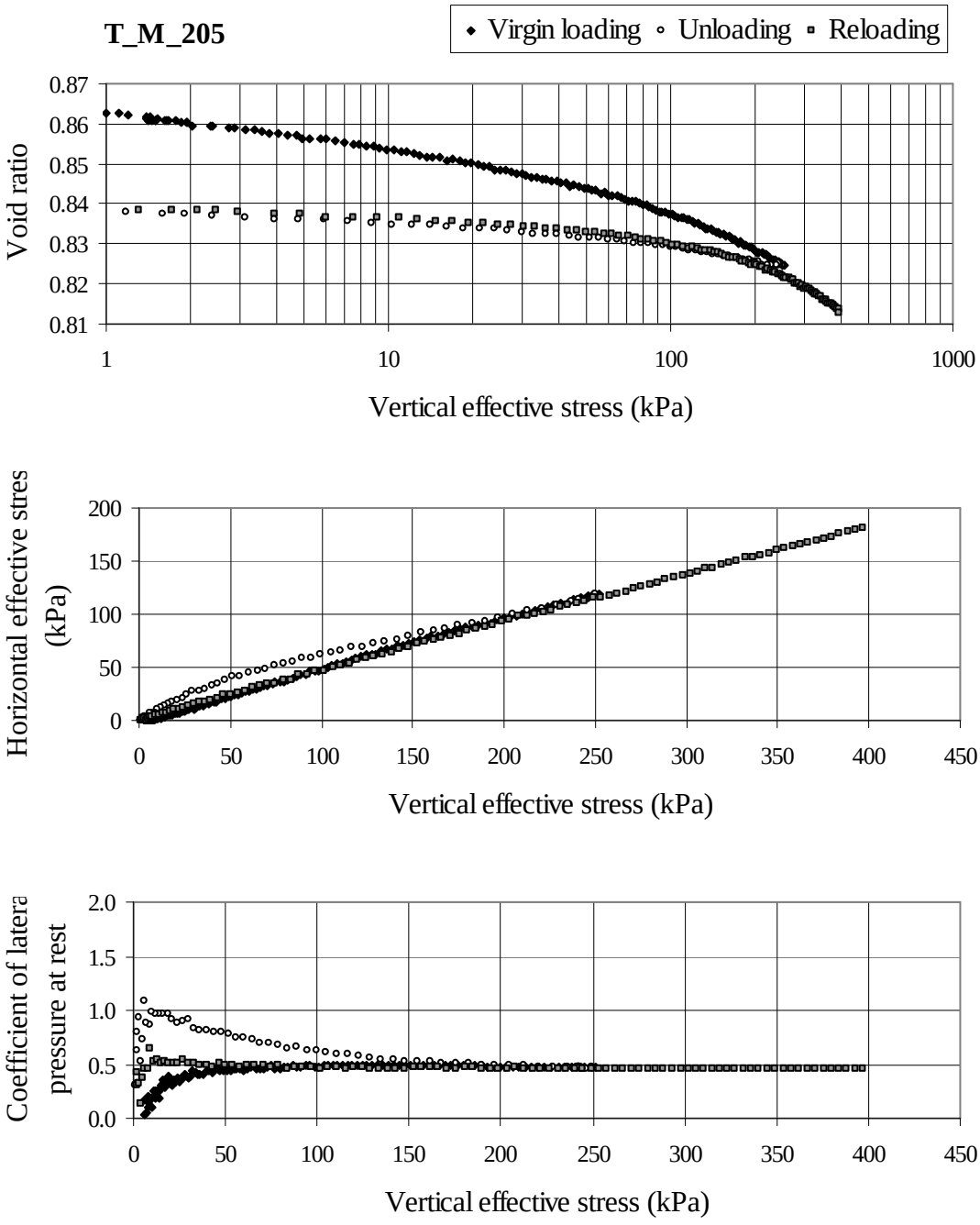

Figure B.1.5. Test data for T_M_205

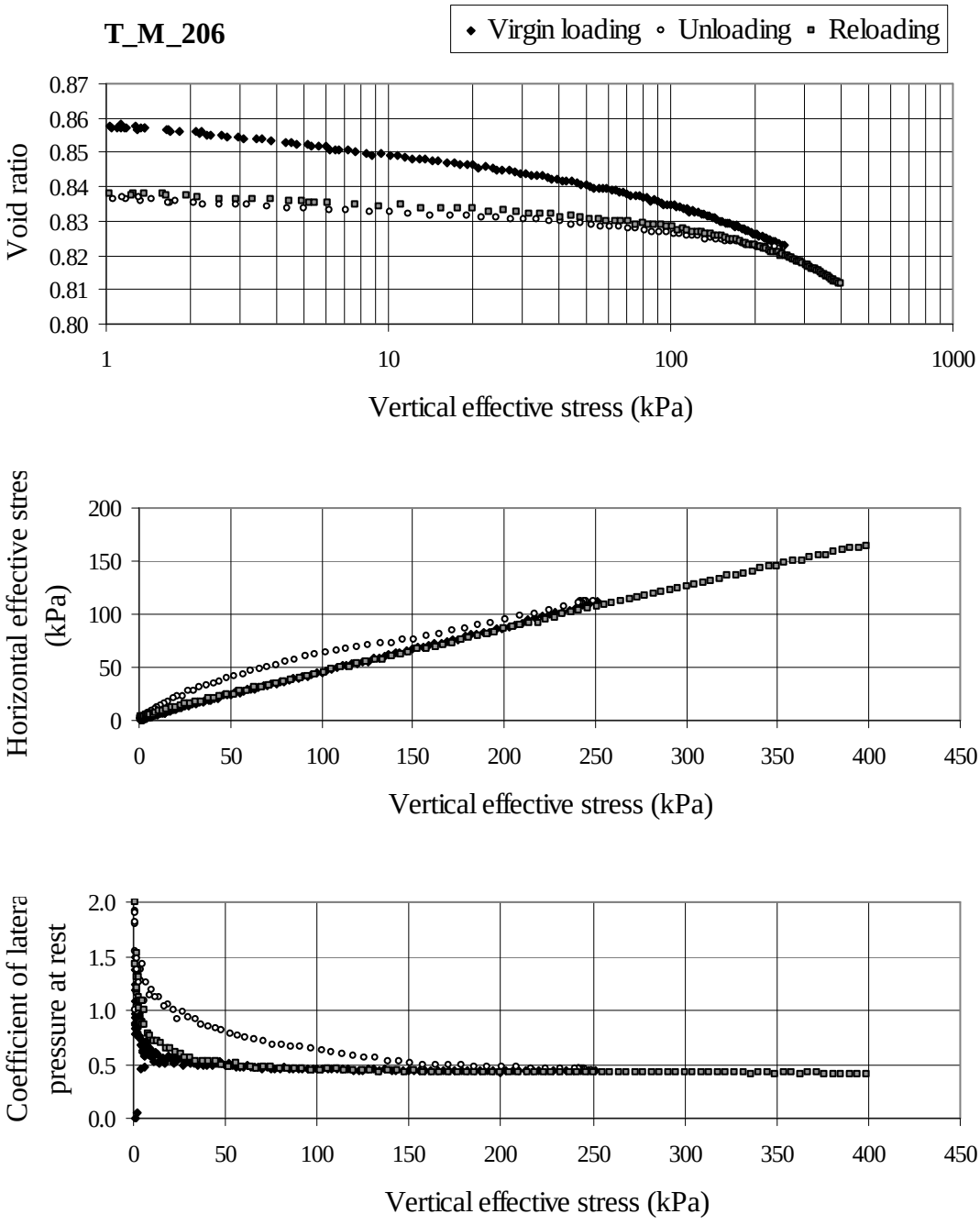

Figure B.1.6. Test data for T_M_206

Appendix B.2. Dense specimens

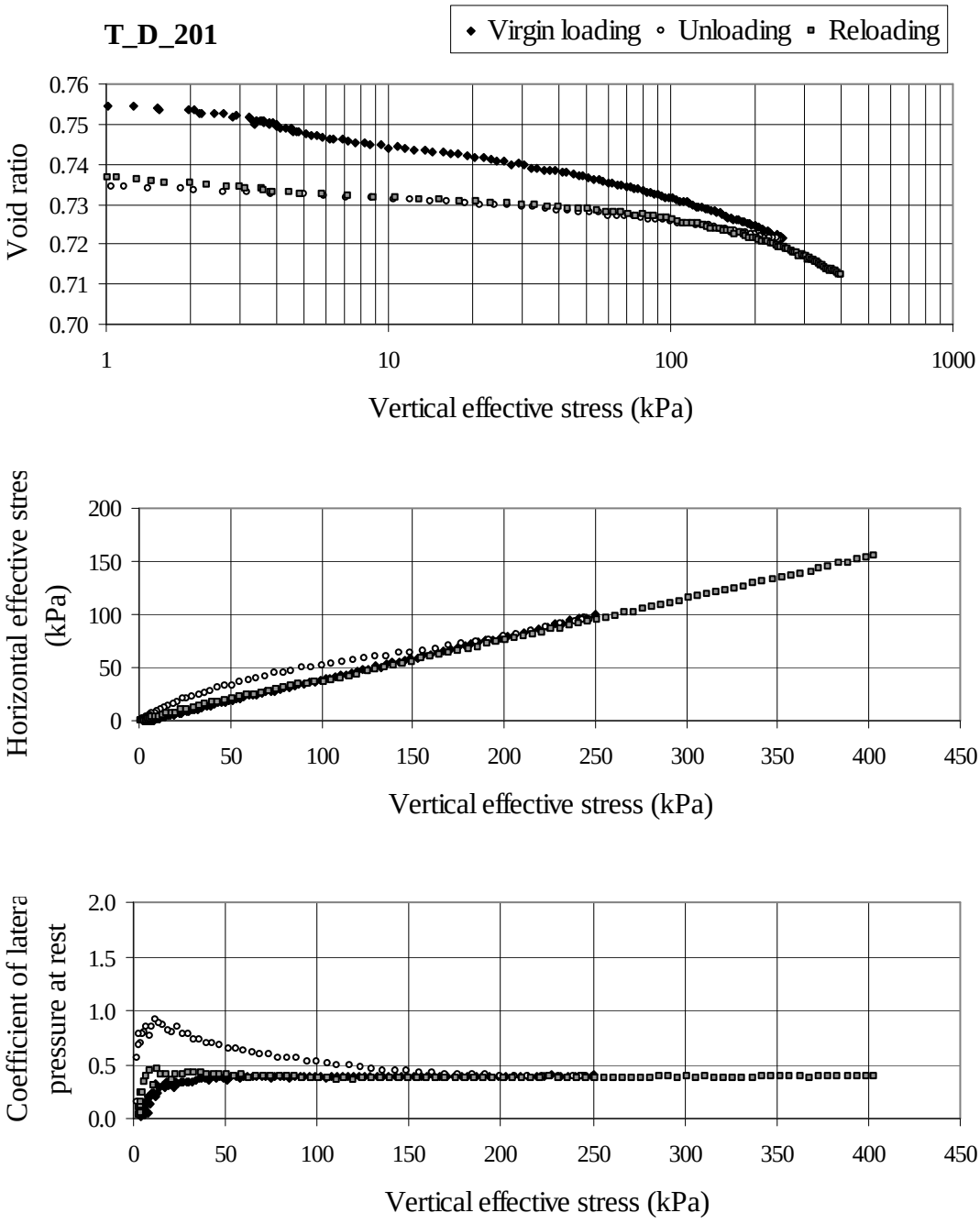

Figure B.2.1. Test data for T_D_201

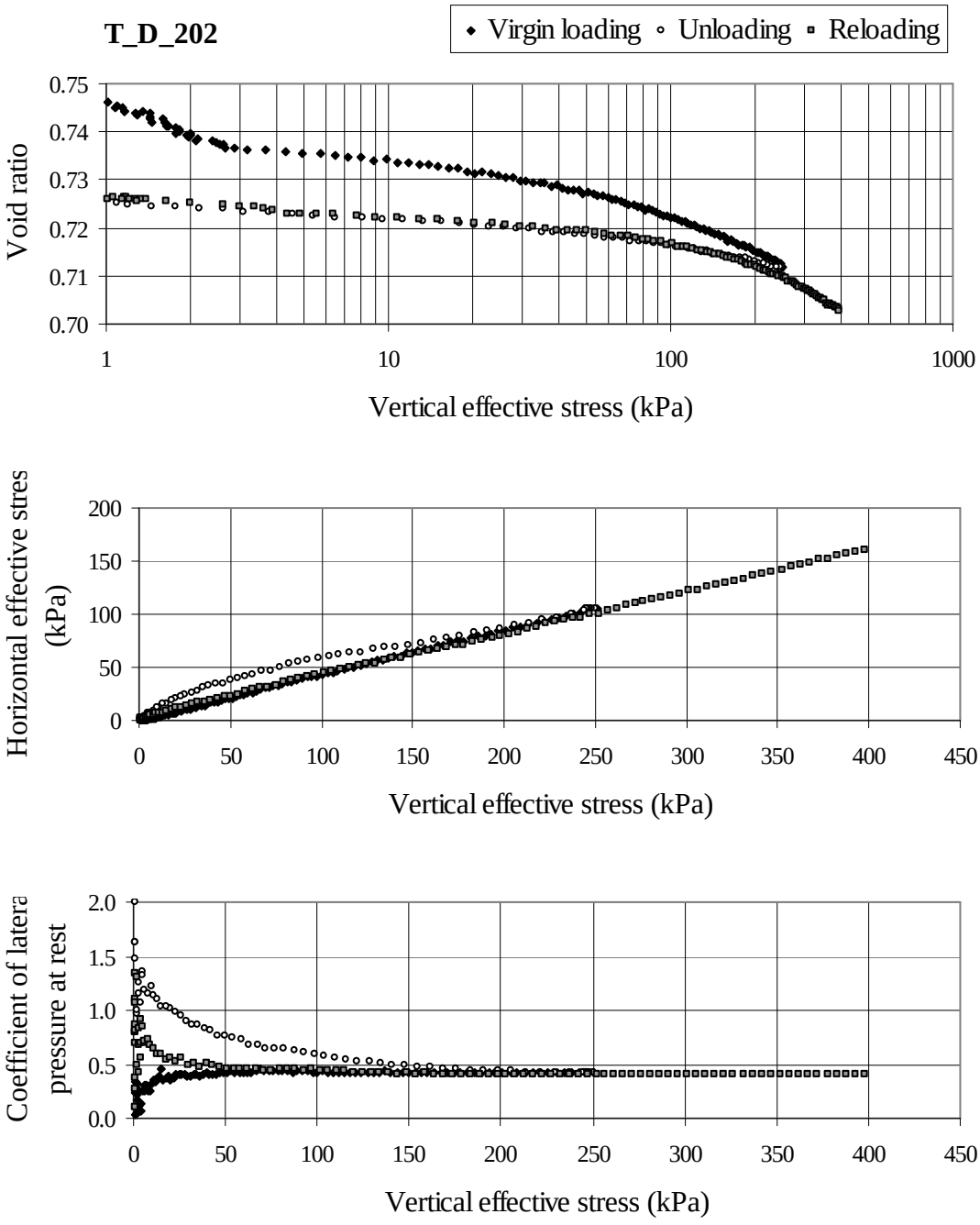

Figure B.2.2. Test data for T_D_202

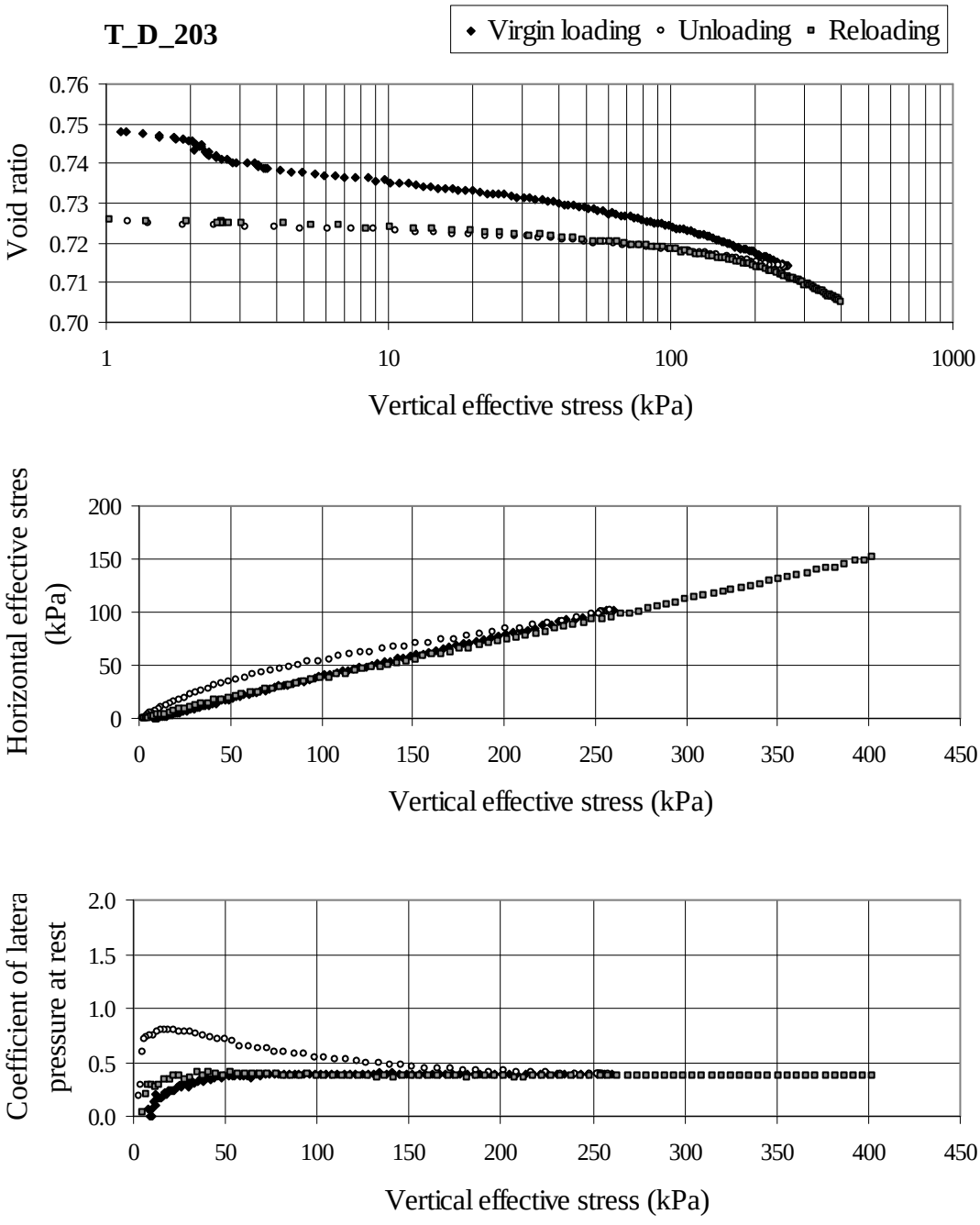

Figure B.2.3. Test data for T_D_203

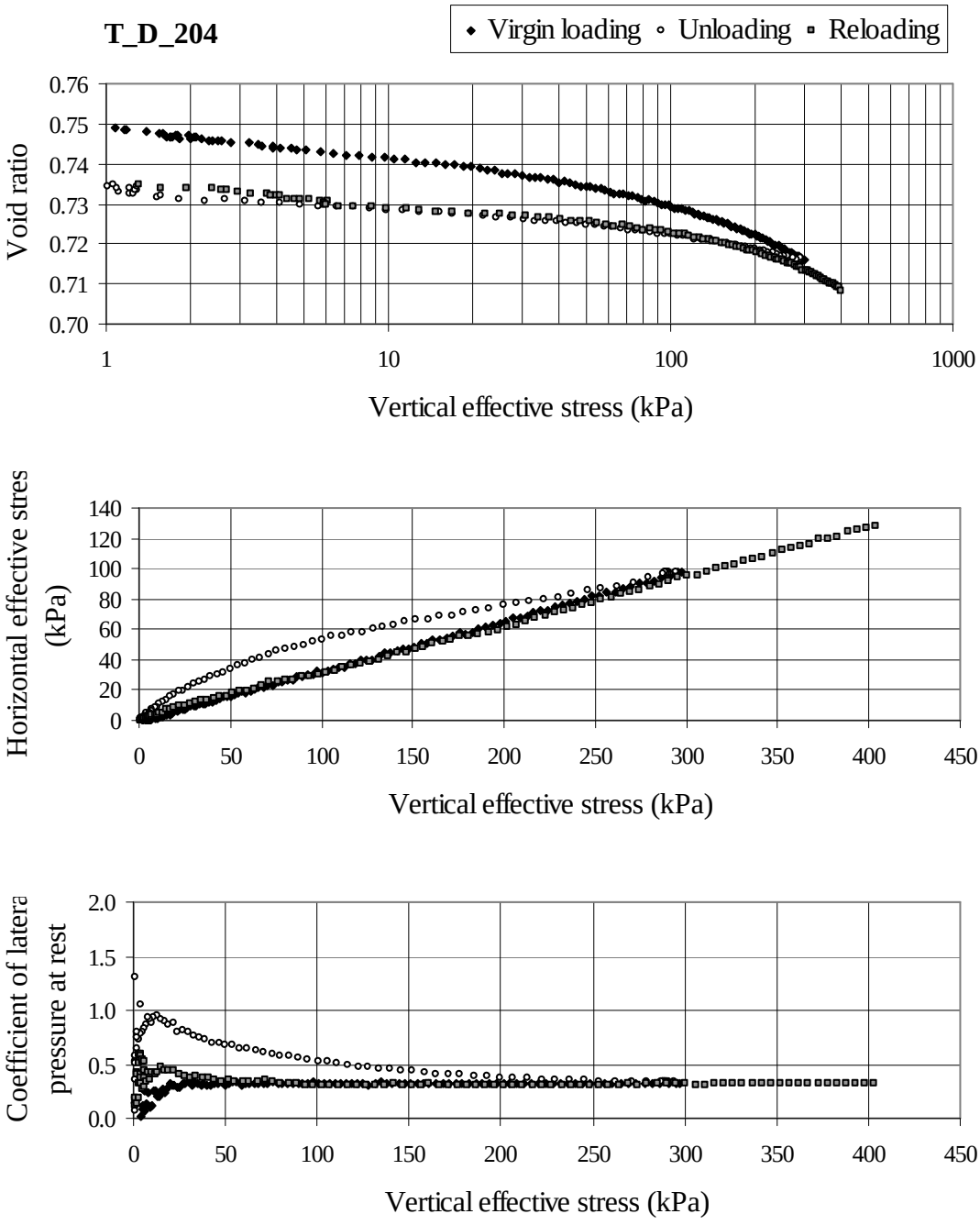

Figure B.2.4. Test data for T_D_204

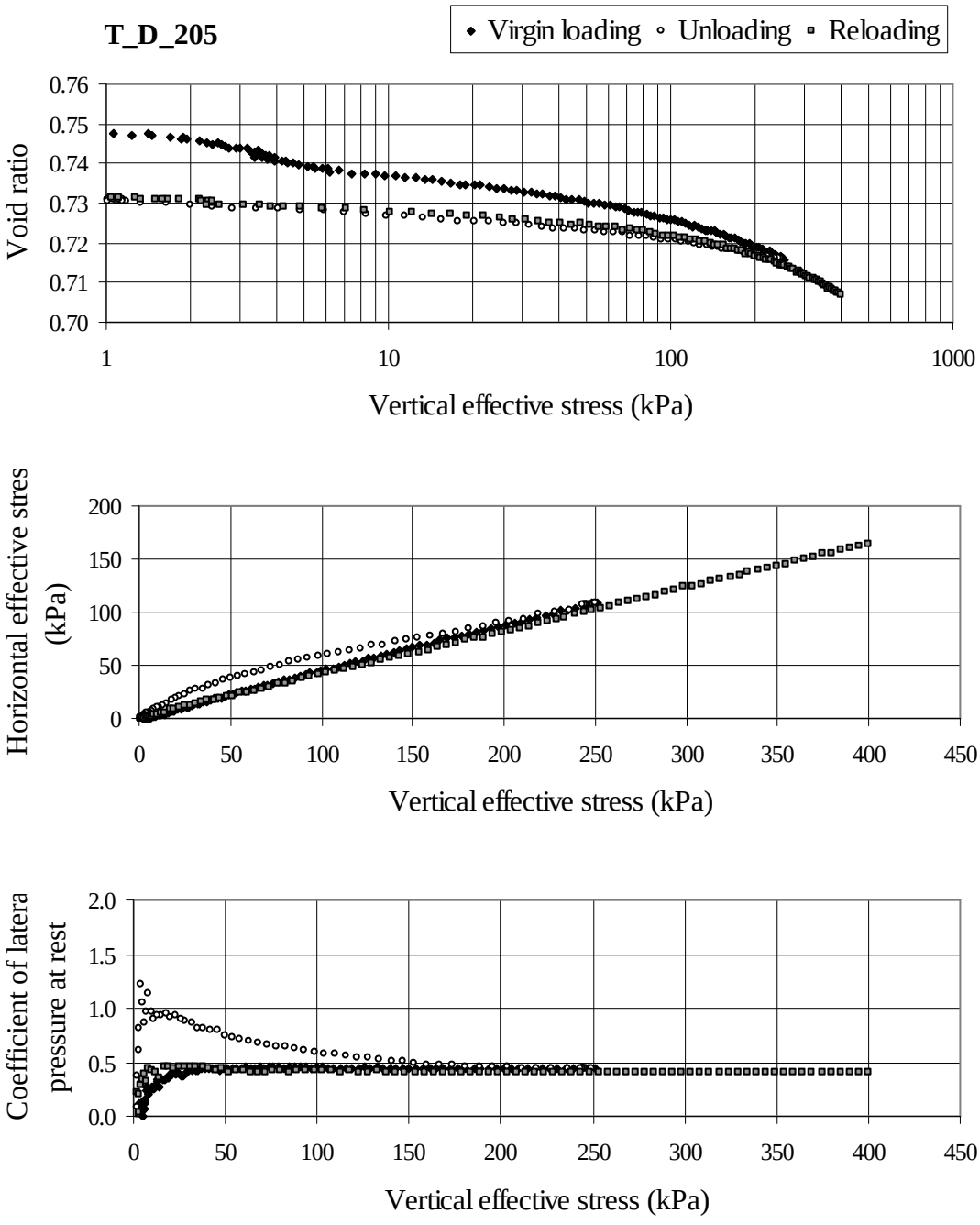

Figure B.2.5. Test data for T_D_205

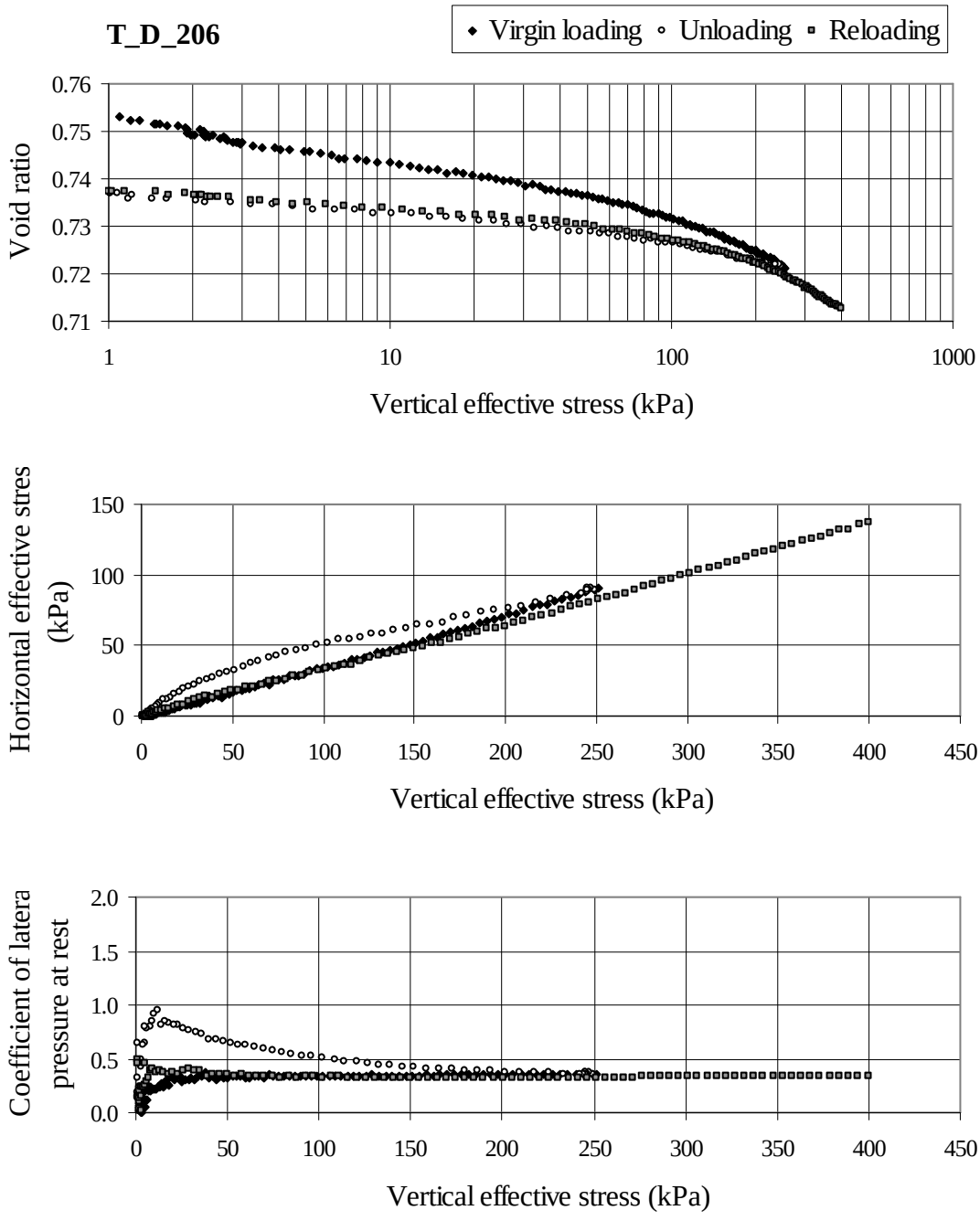

Figure B.2.6. Test data for T_D_206

Appendix B.3. Very dense specimens

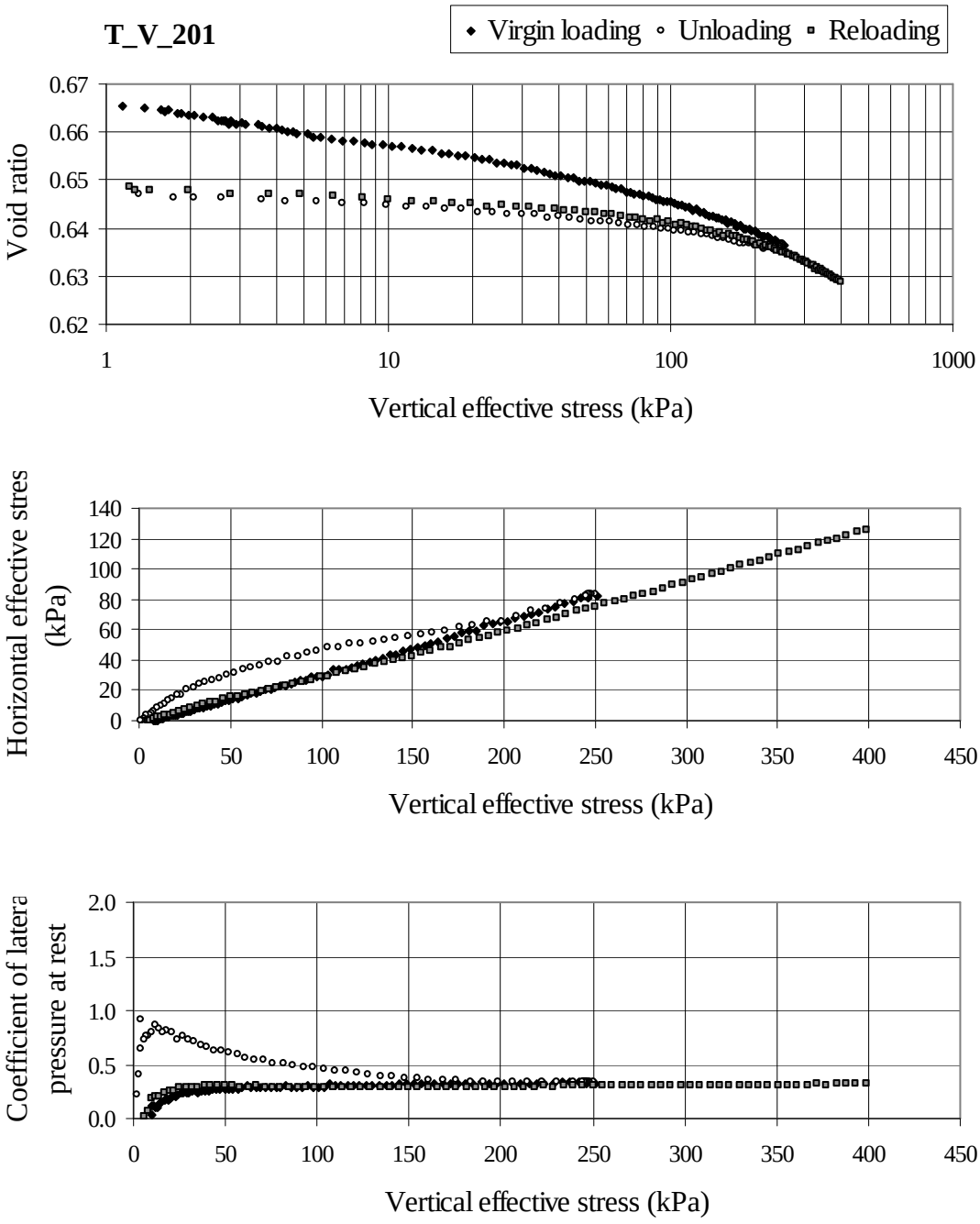

Figure B.3.1. Test data for T_V_201

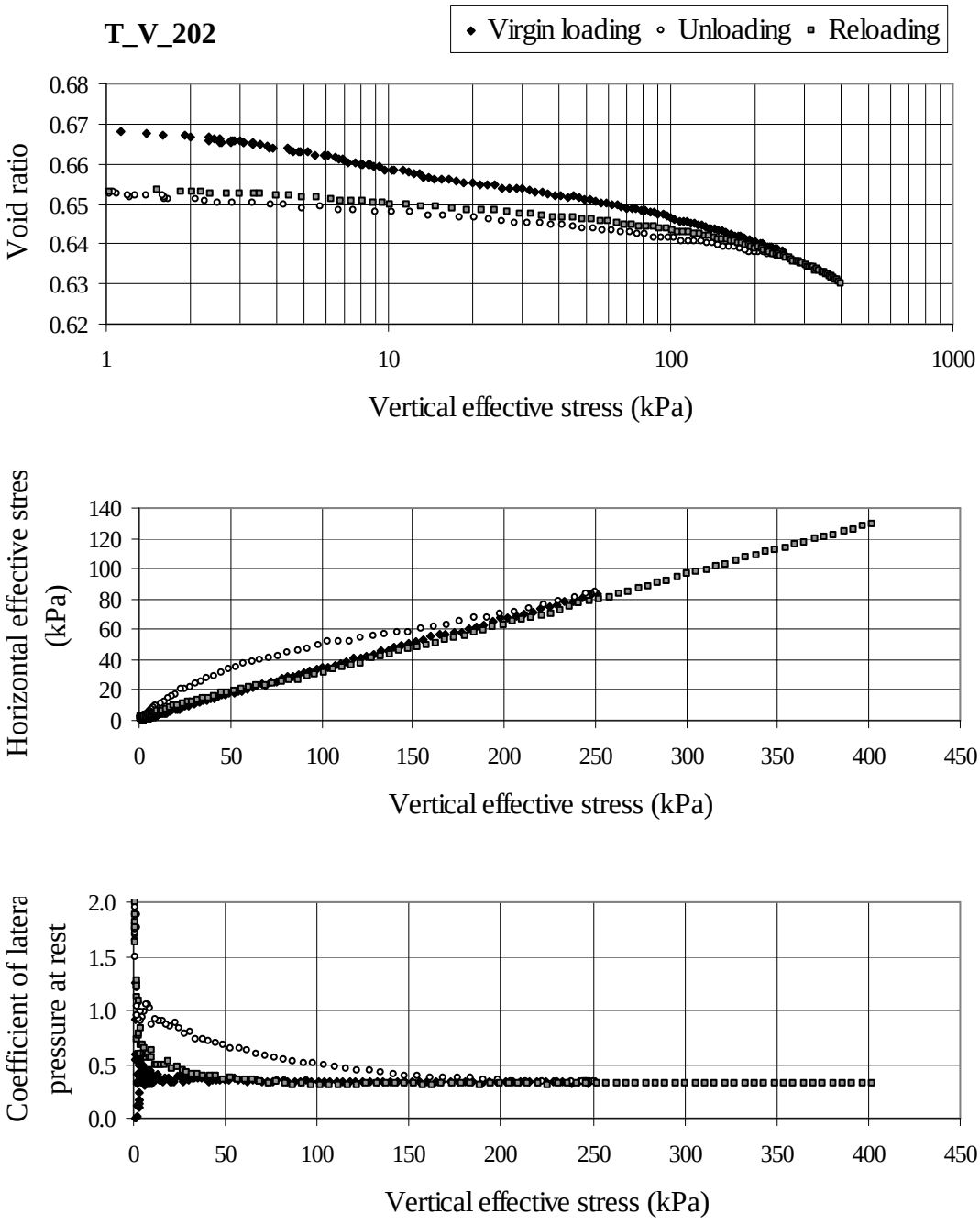

Figure B.3.2. Test data for T_V_202

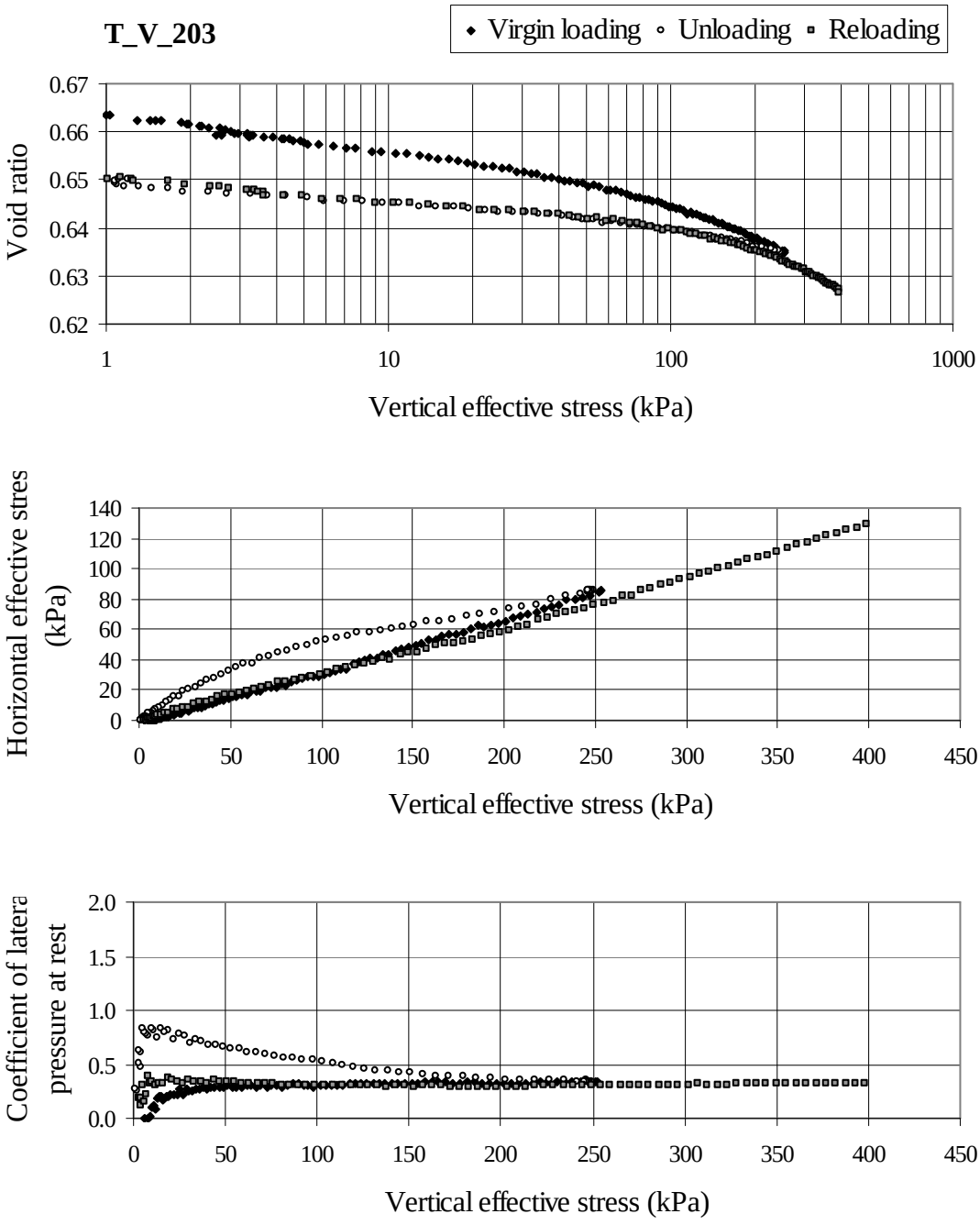

Figure B.3.3. Test data for T_V_203

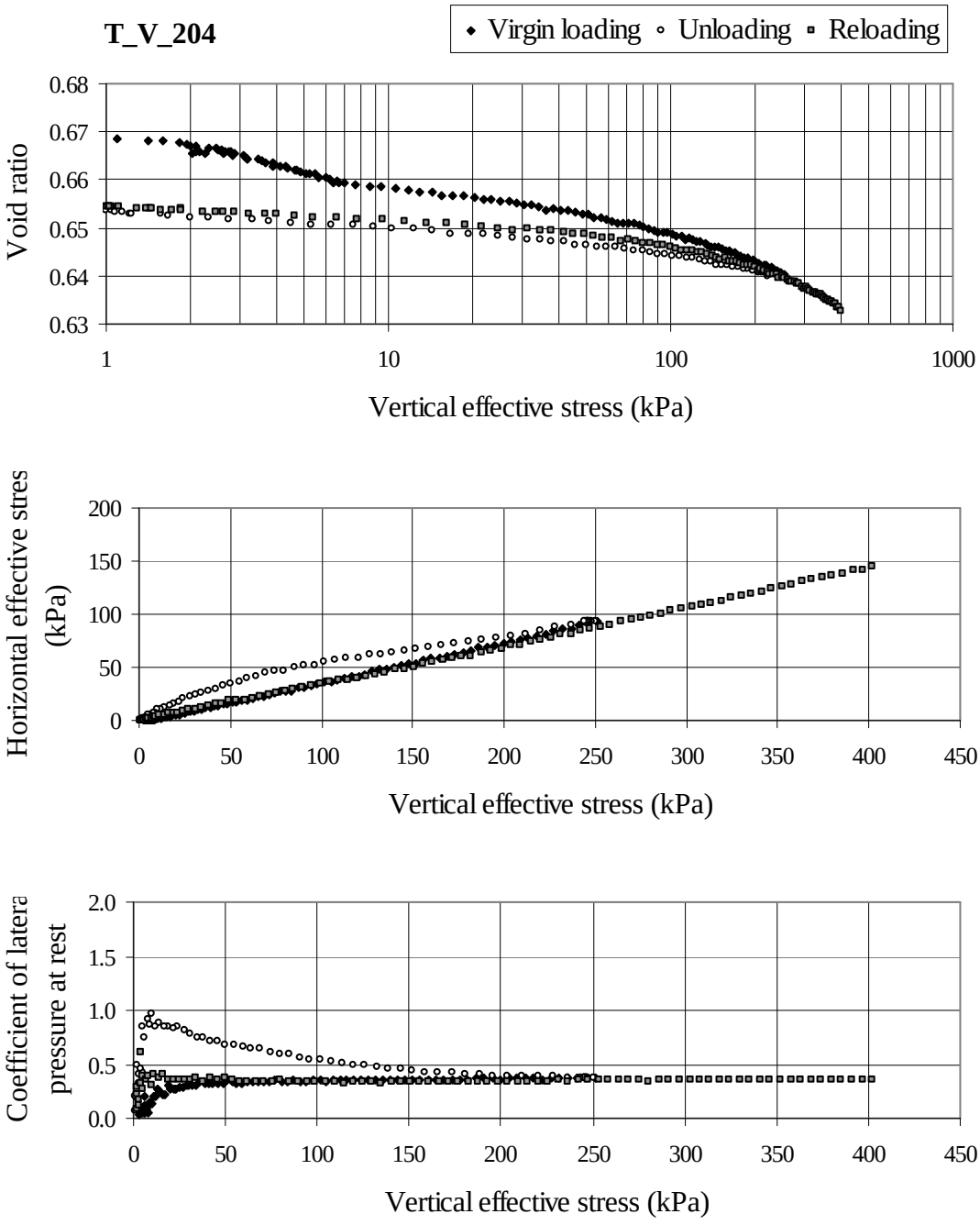

Figure B.3.4. Test data for T_V_204

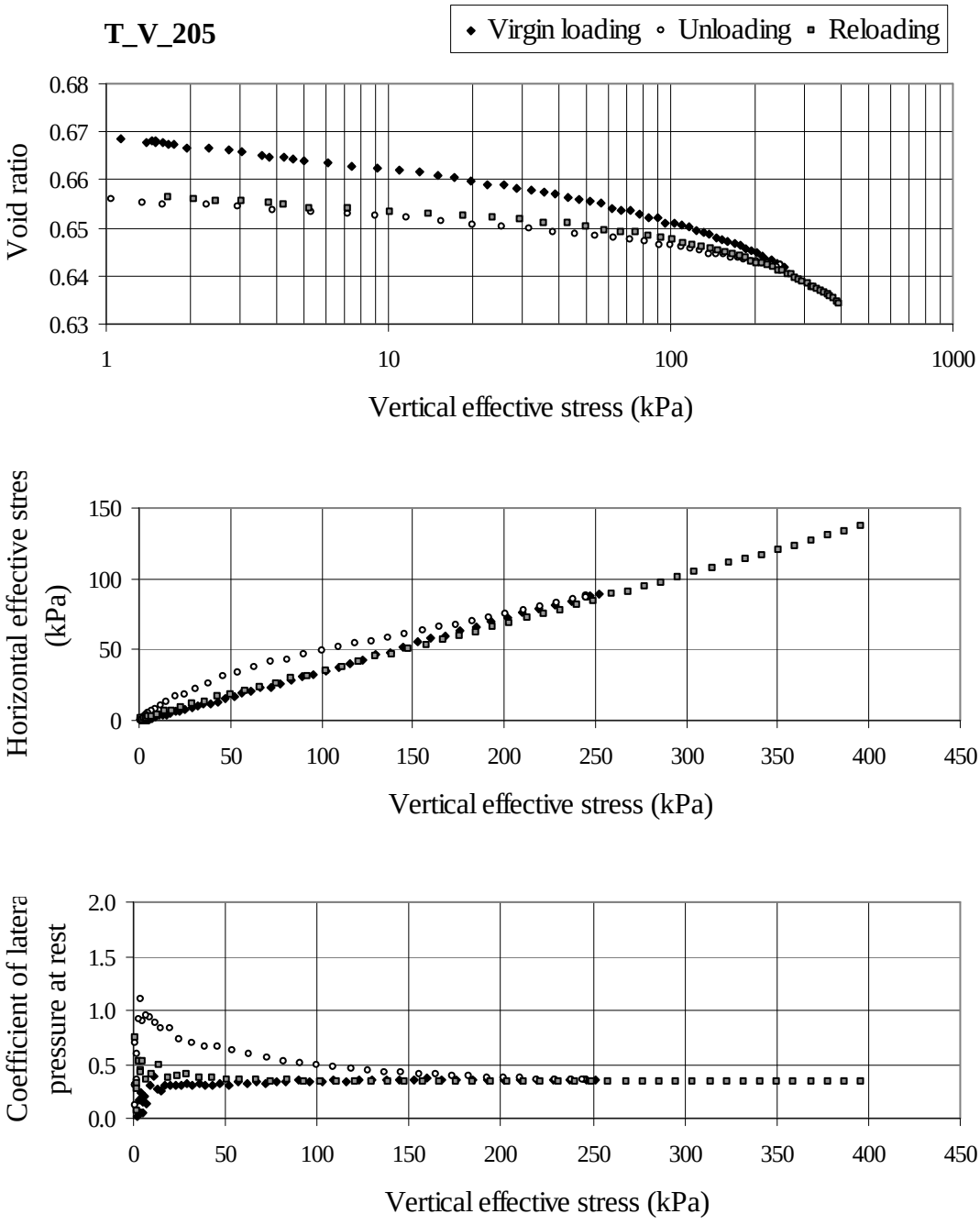

Figure B.3.5. Test data for T_V_205

APPENDIX C: TEST DATA FOR VIBRATION

Appendix C.1. Medium loose specimens

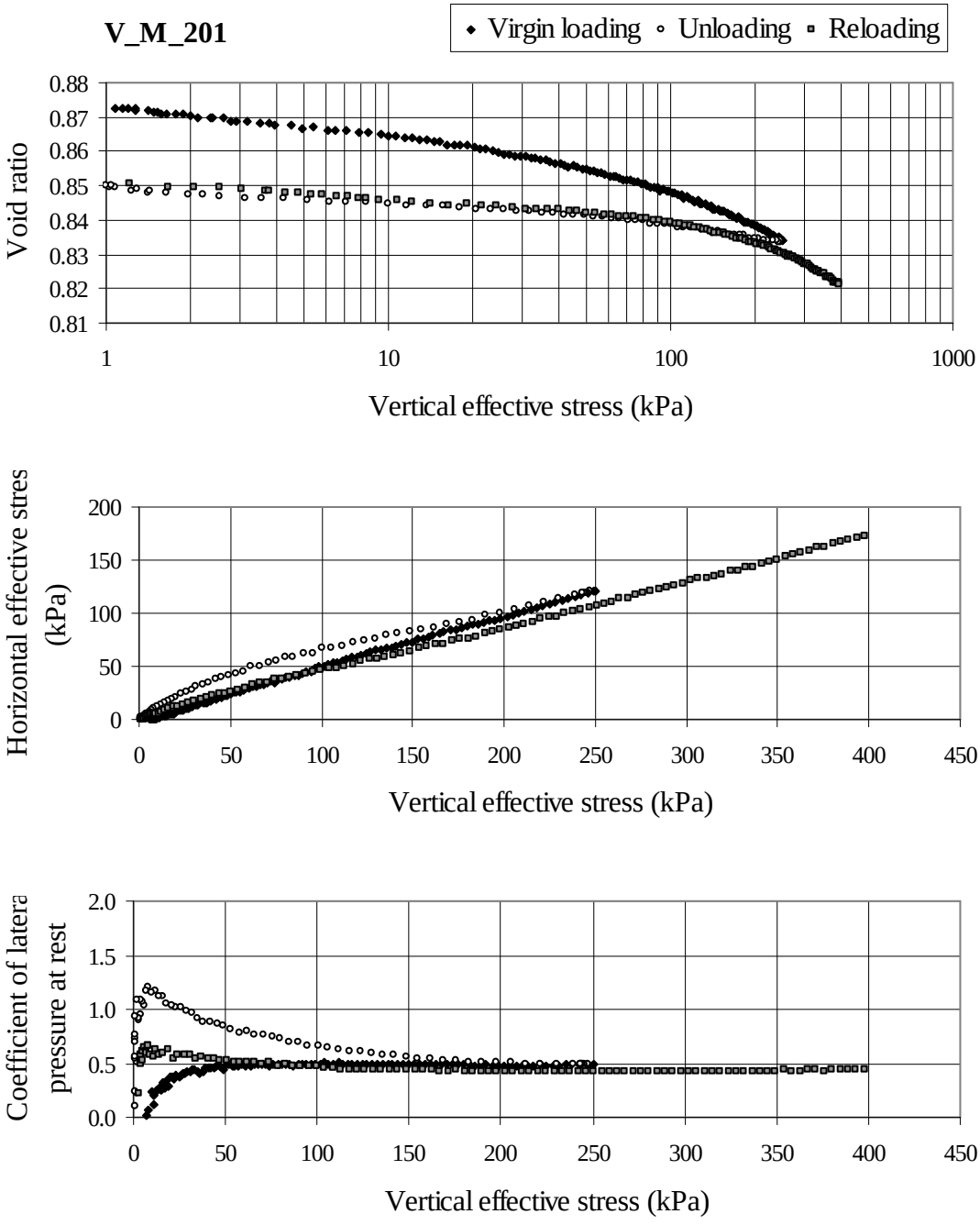

Figure C.1.1. Test data for V_M_201

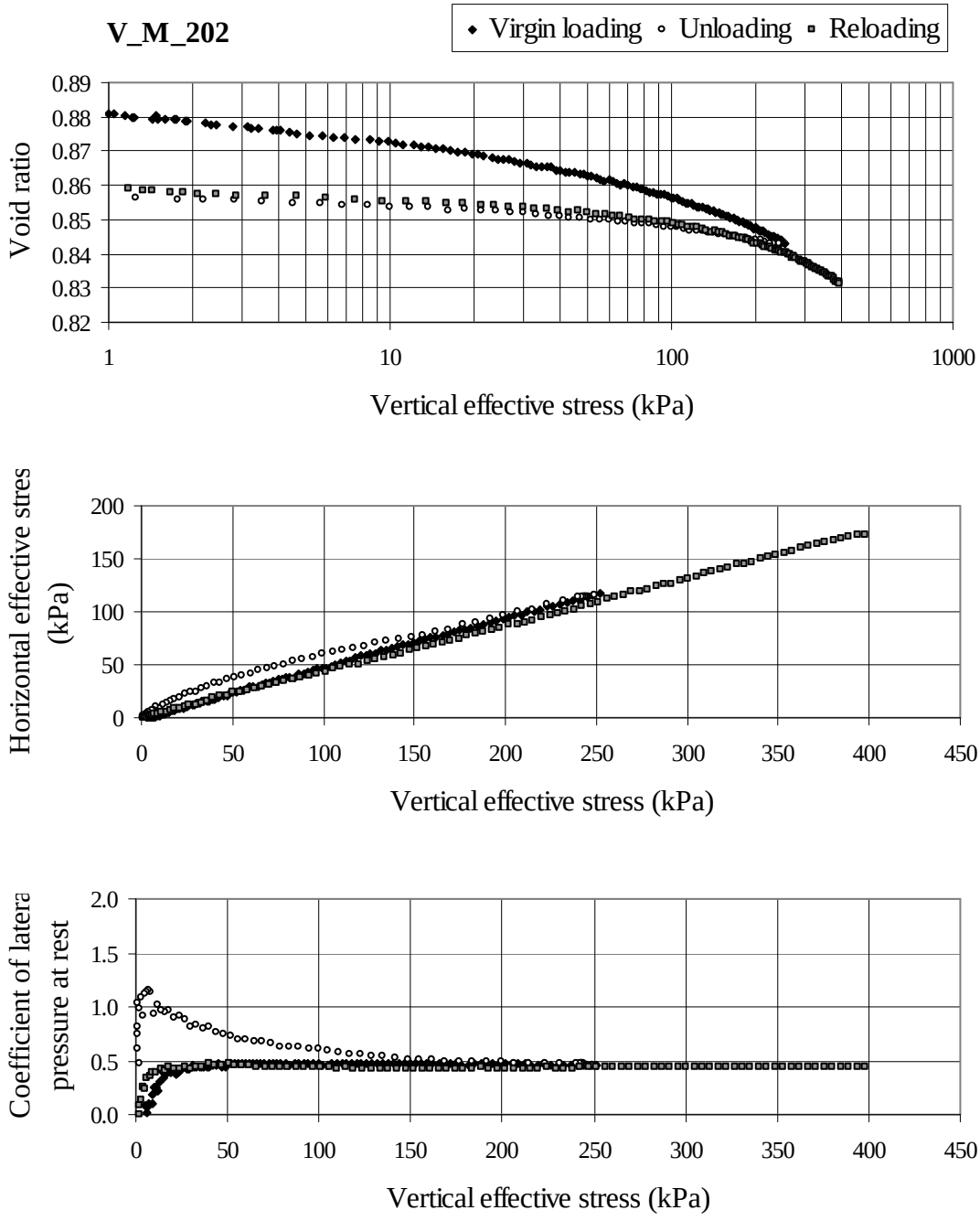

Figure C.1.2. Test data for V_M_202

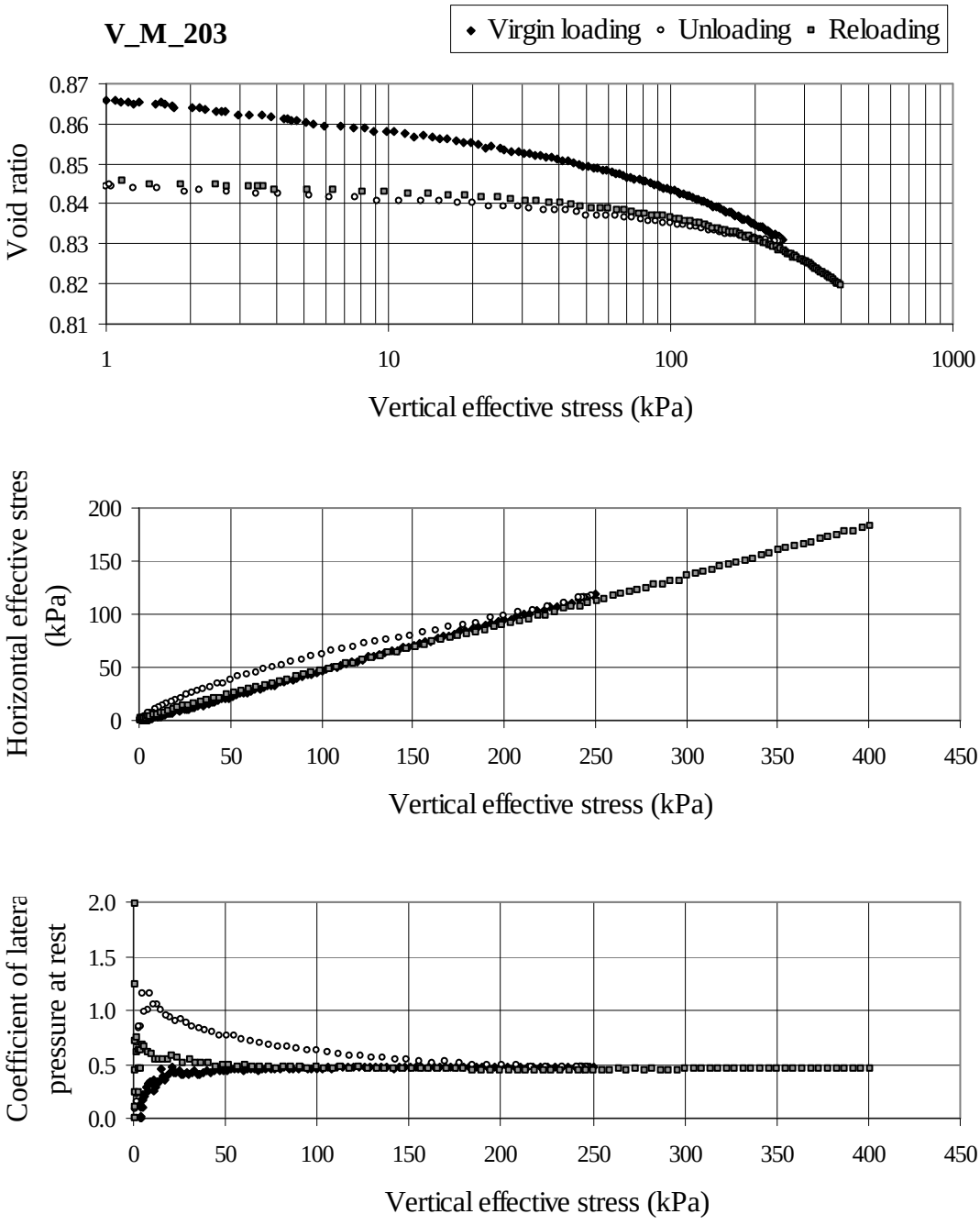

Figure C.1.3. Test data for V_M_203

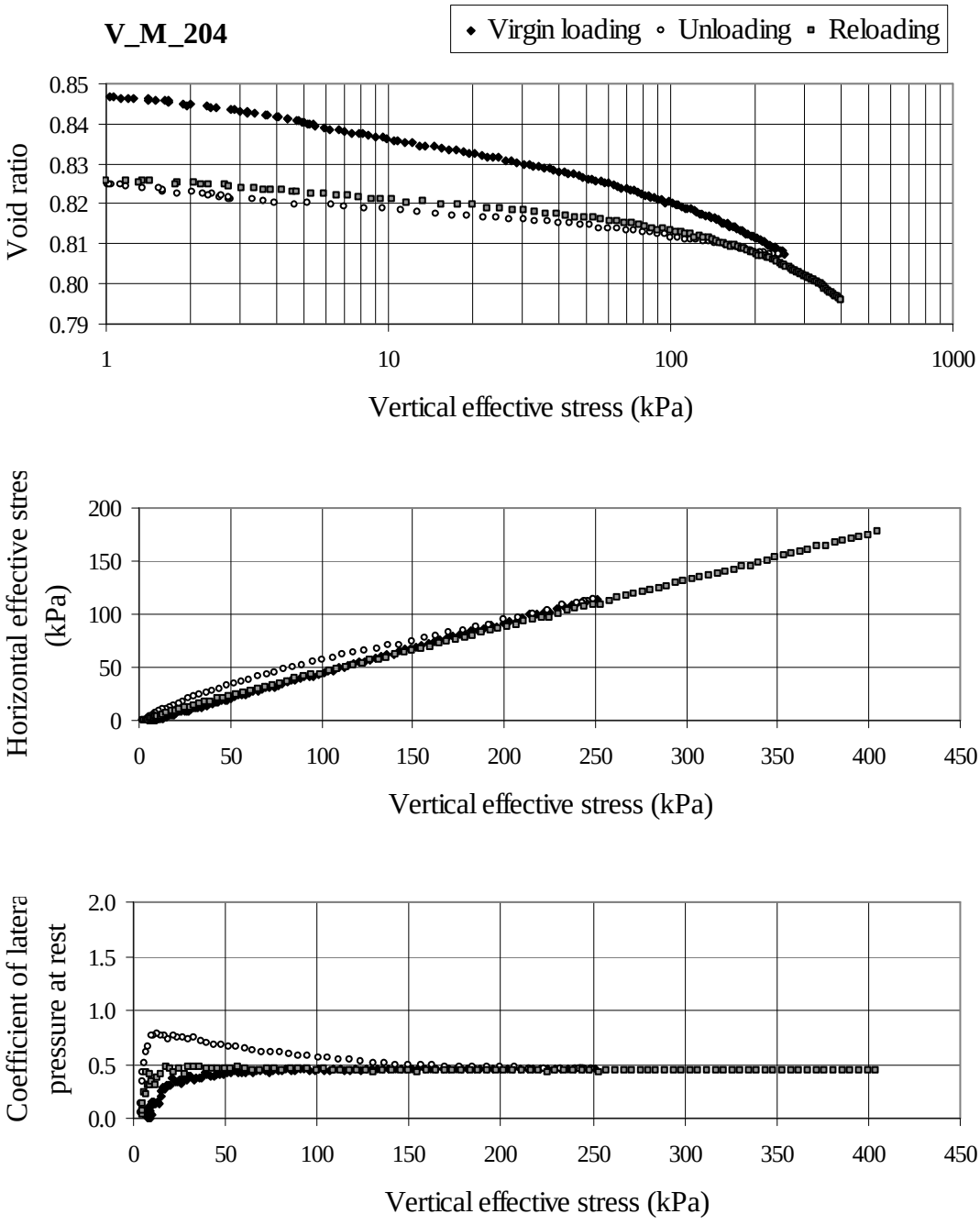

Figure C.1.4. Test data for V_M_204

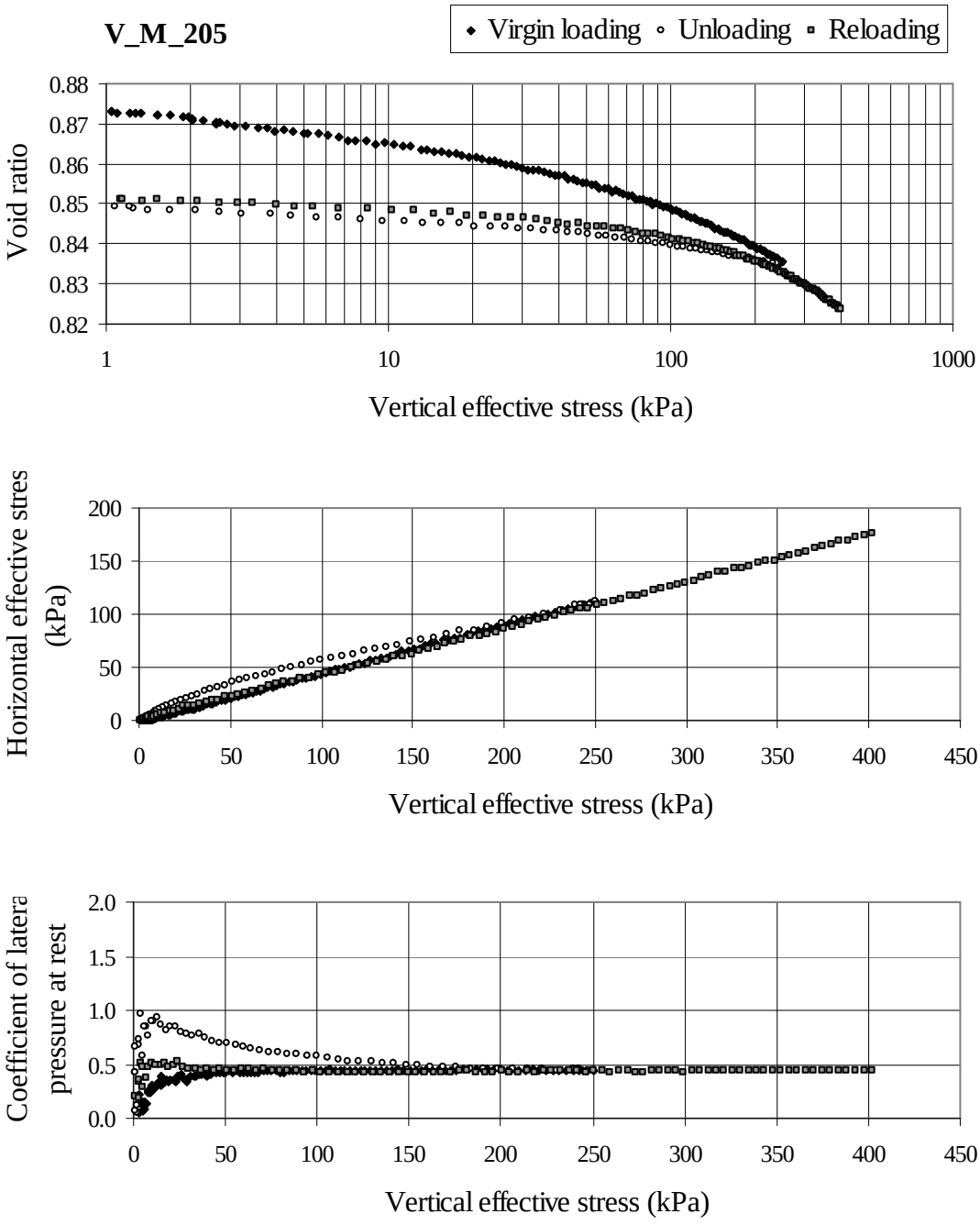

Figure C.1.5. Test data for V_M_205

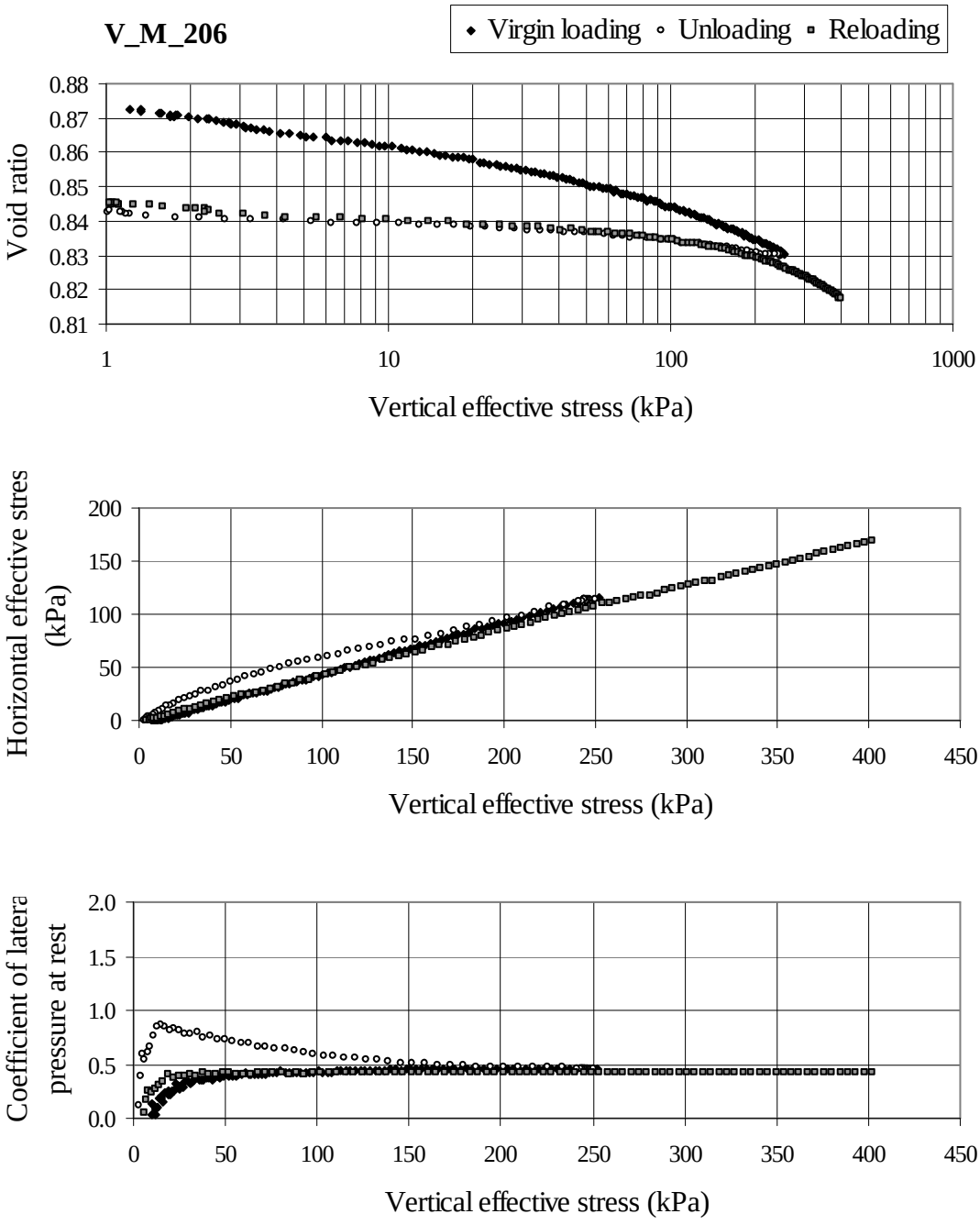

Figure C.1.6. Test data for V_M_206

Appendix C.2. Dense specimens

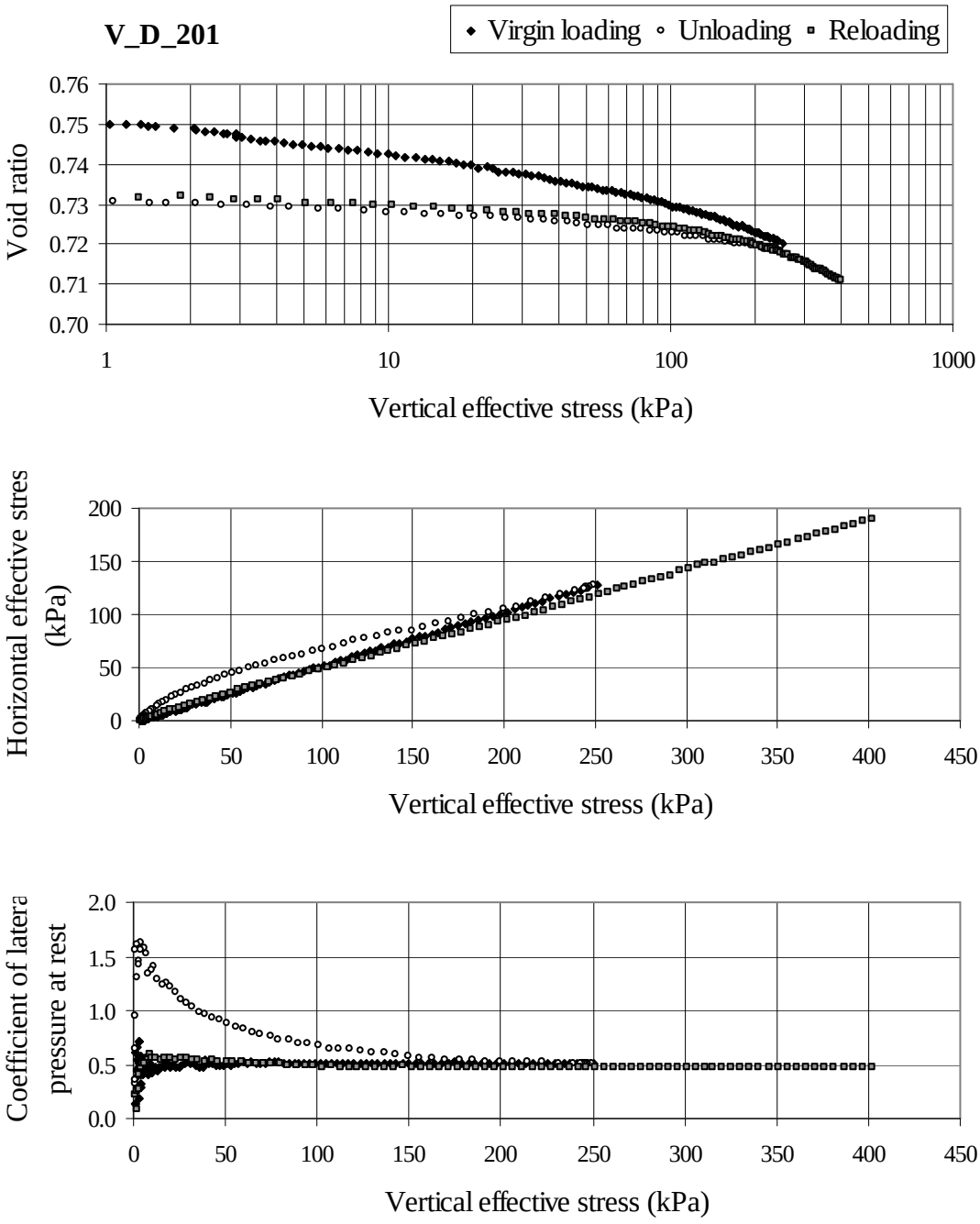

Figure C.2.1. Test data for V_D_201

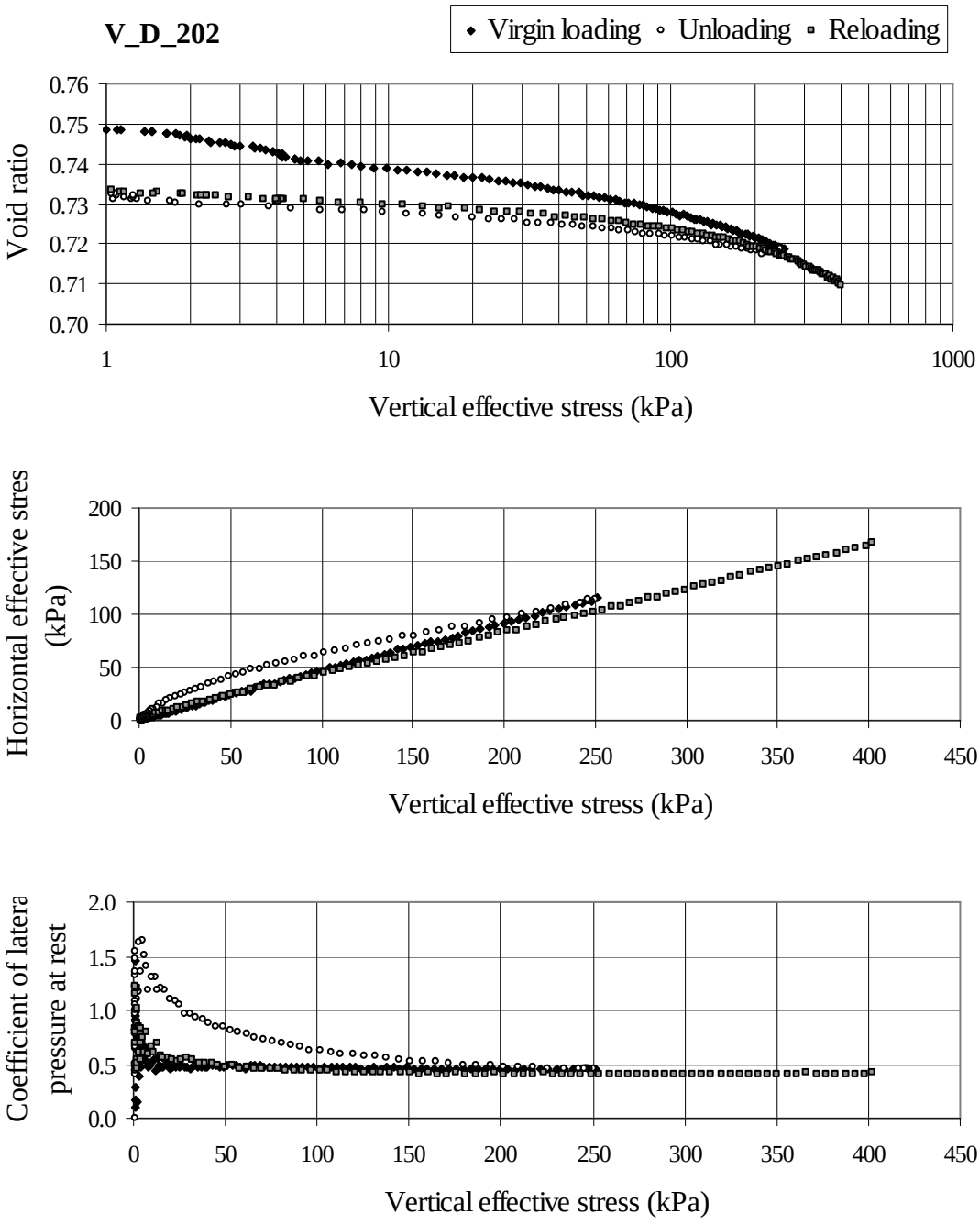

Figure C.2.2. Test data for V_D_202

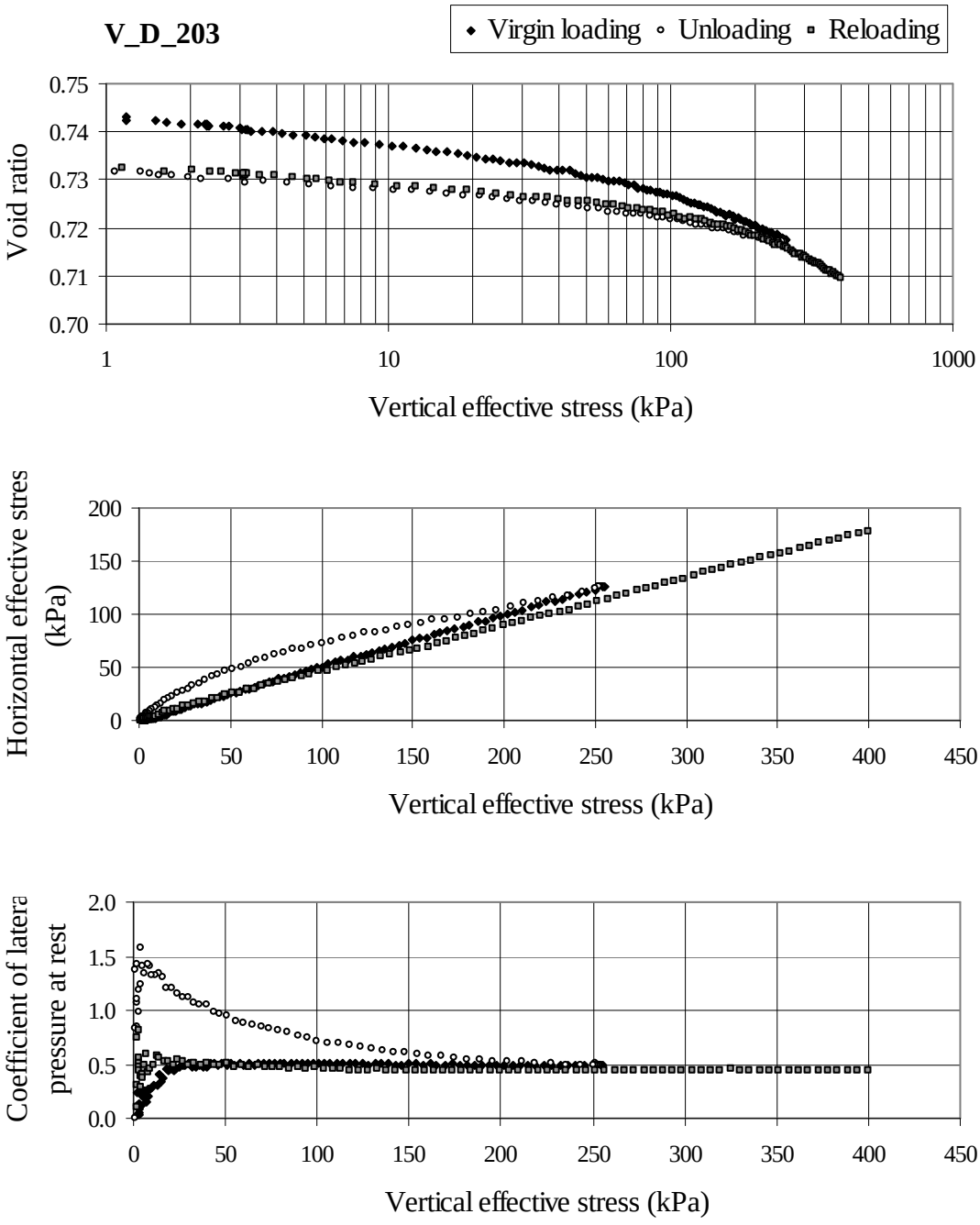

Figure C.2.3. Test data for V_D_203

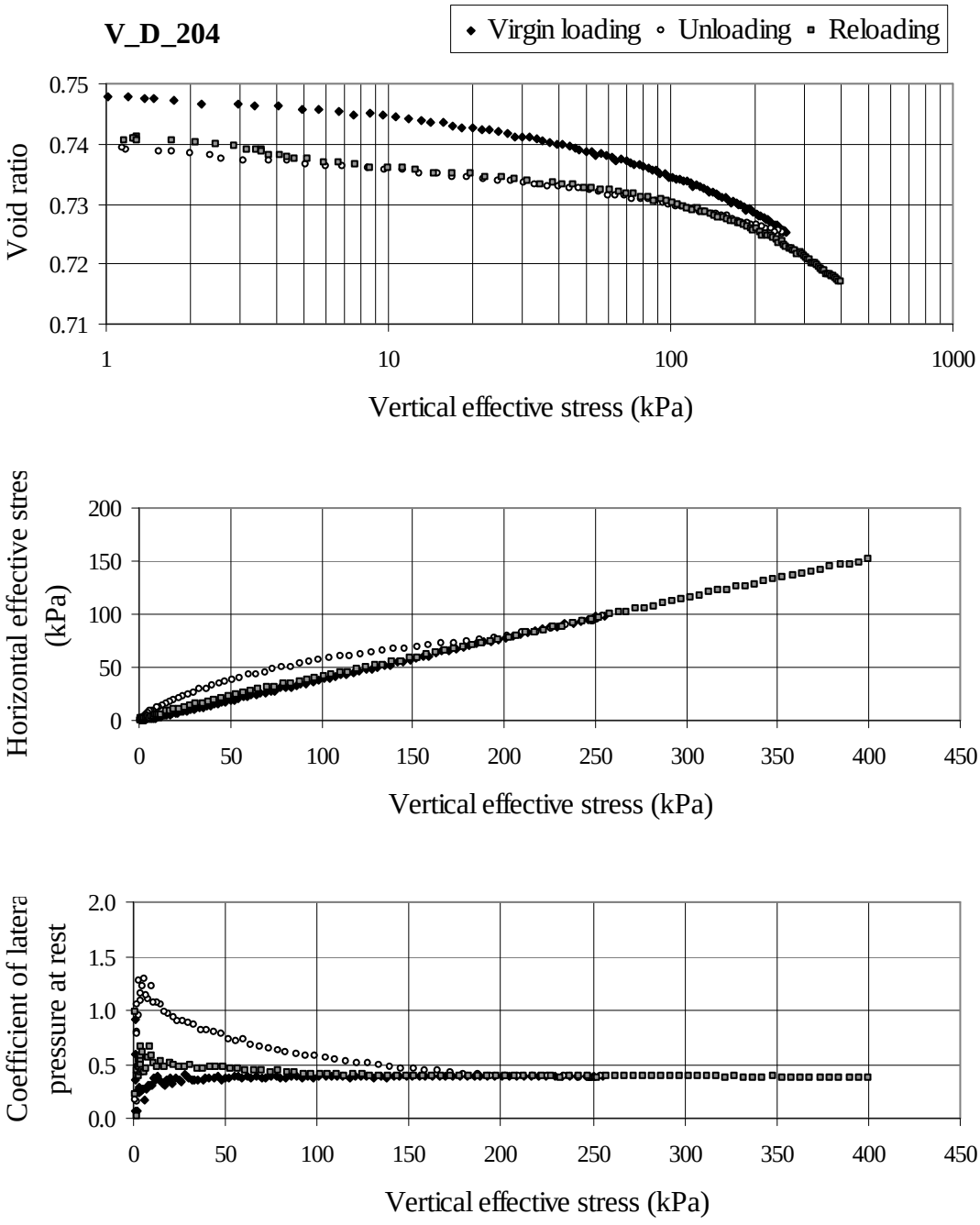

Figure C.2.4. Test data for V_D_204

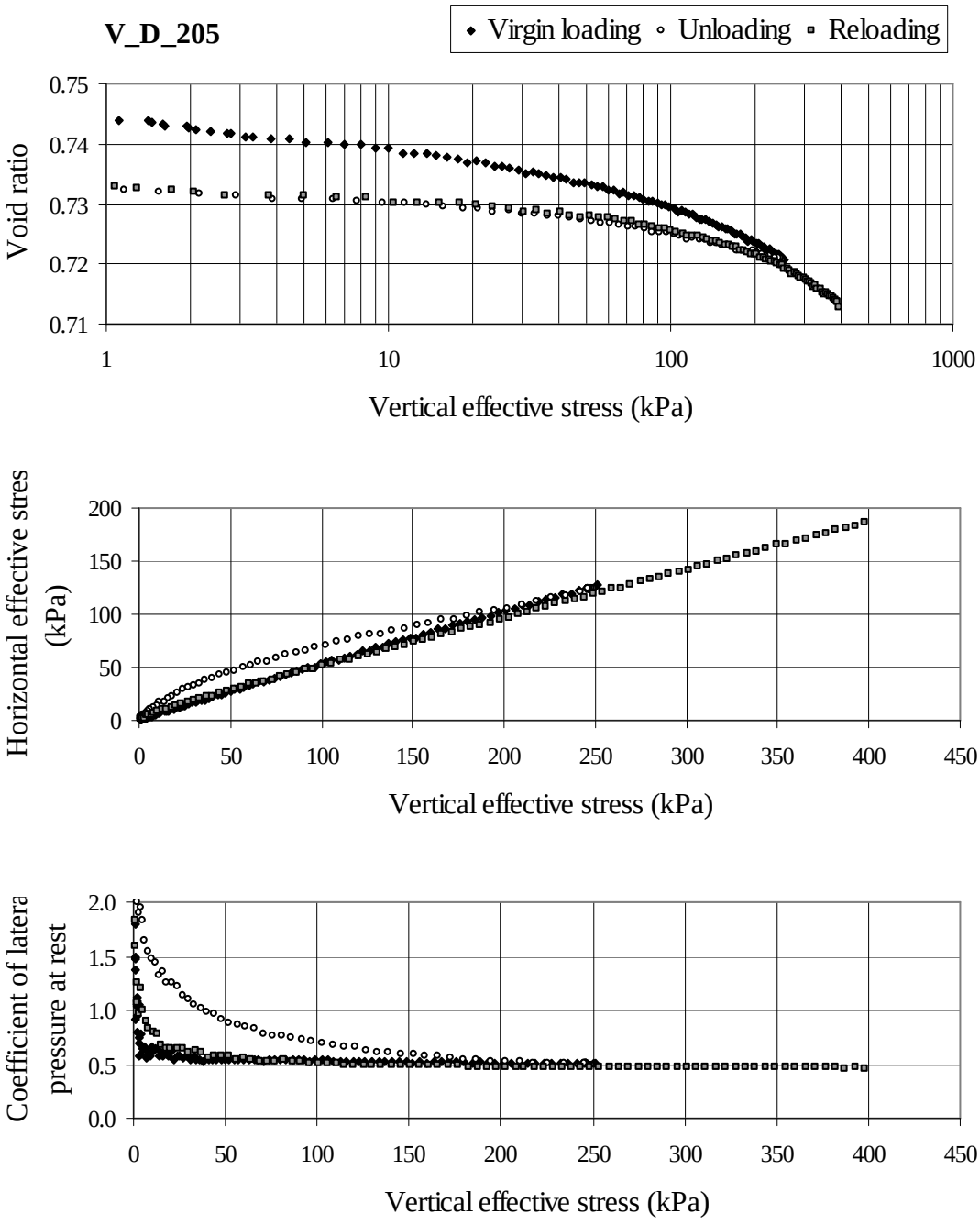

Figure C.2.5. Test data for V_D_205

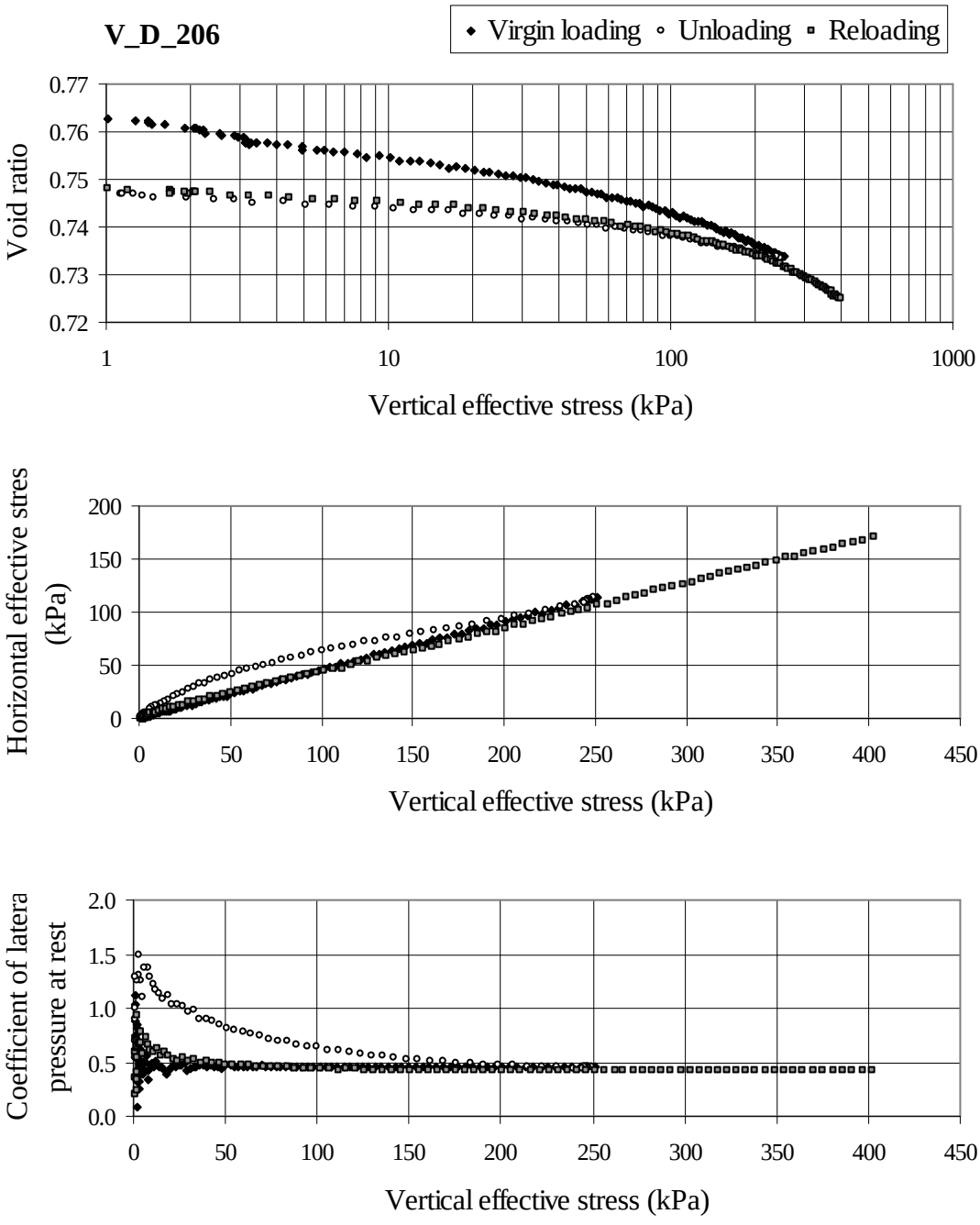

Figure C.2.6. Test data for V_D_206

Appendix C.3. Very dense specimens

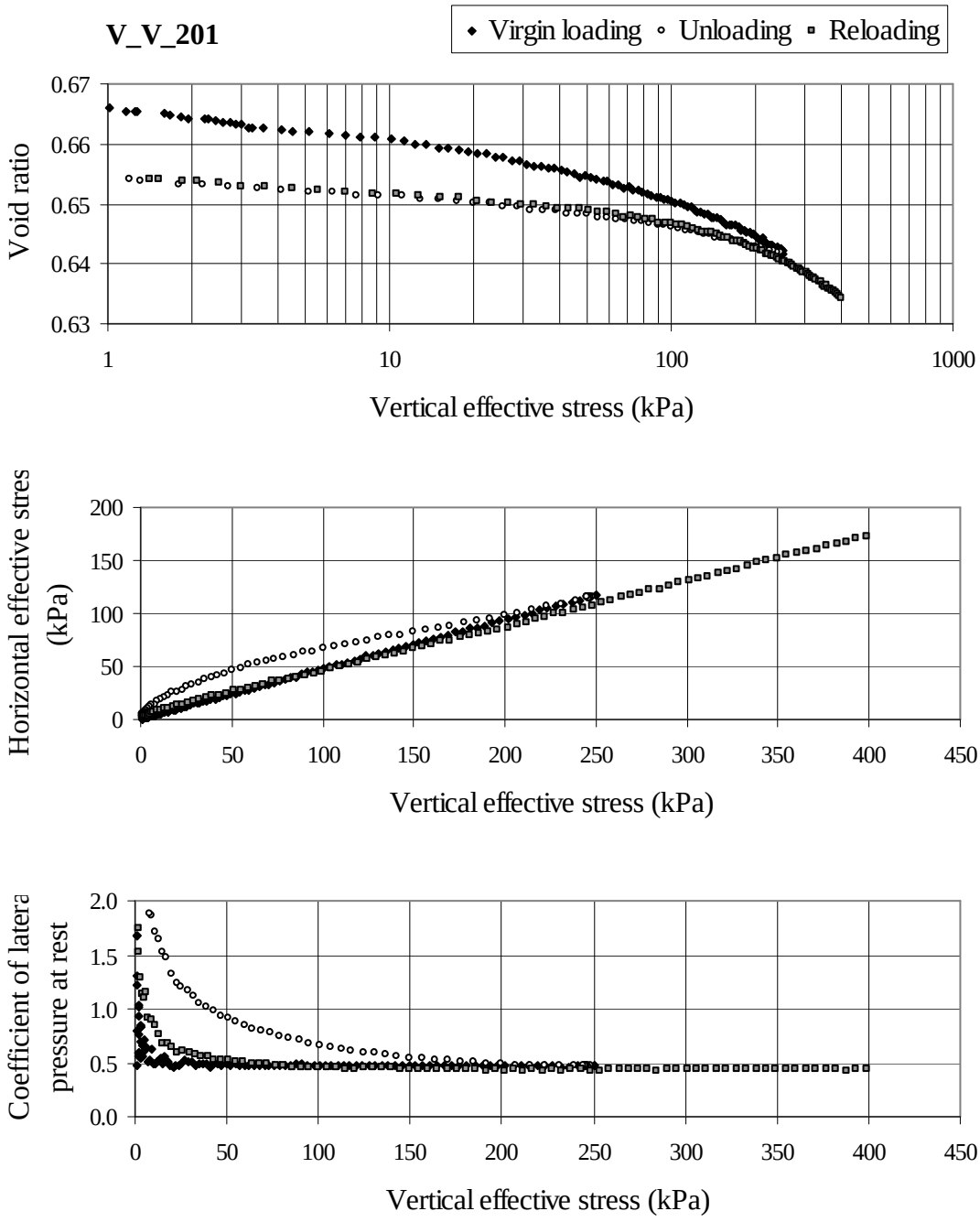

Figure C.3.1. Test data for V_V_201

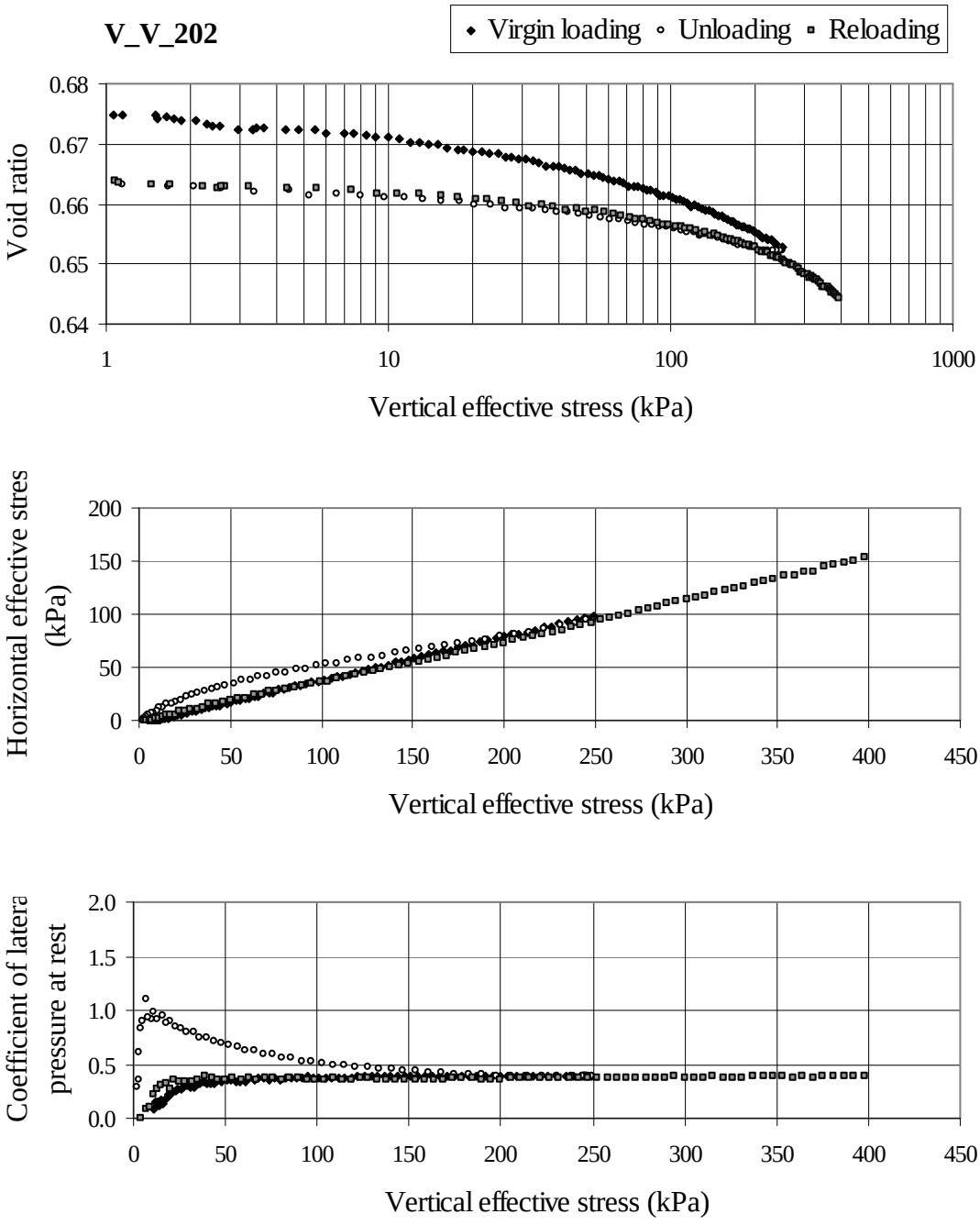

Figure C.3.2. Test data for V_V_202

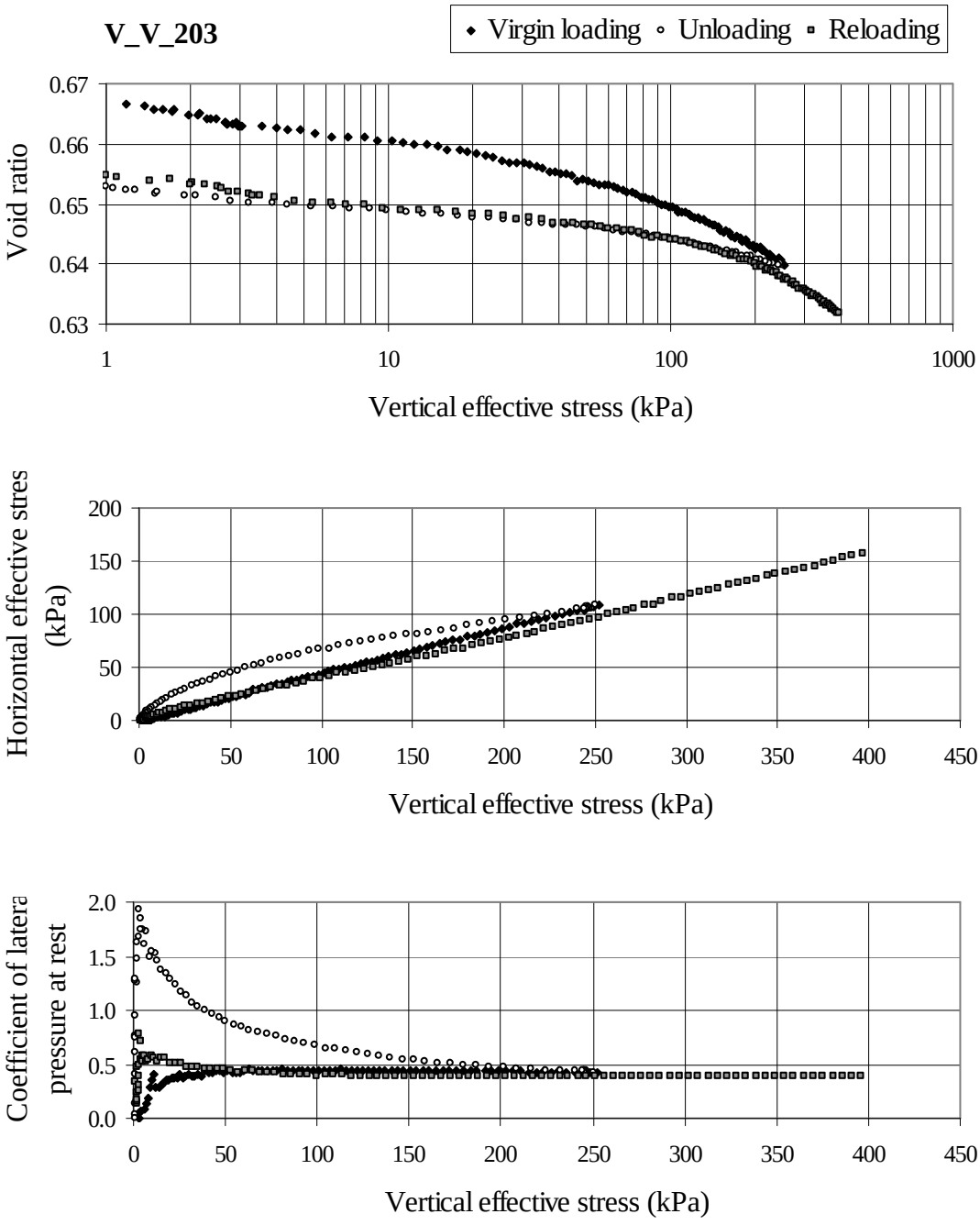

Figure C.3.3. Test data for V_V_203

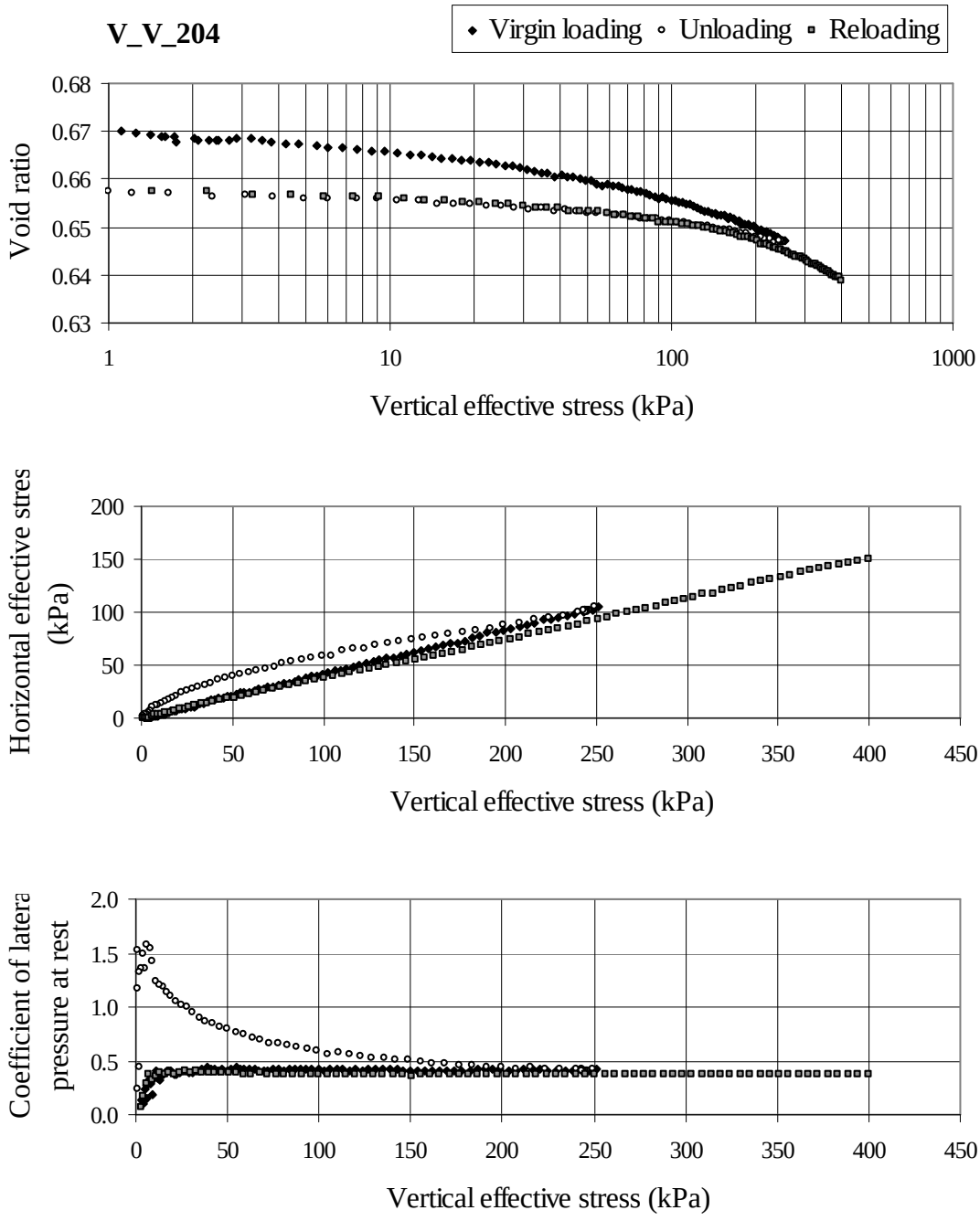

Figure C.3.4. Test data for V_V_204

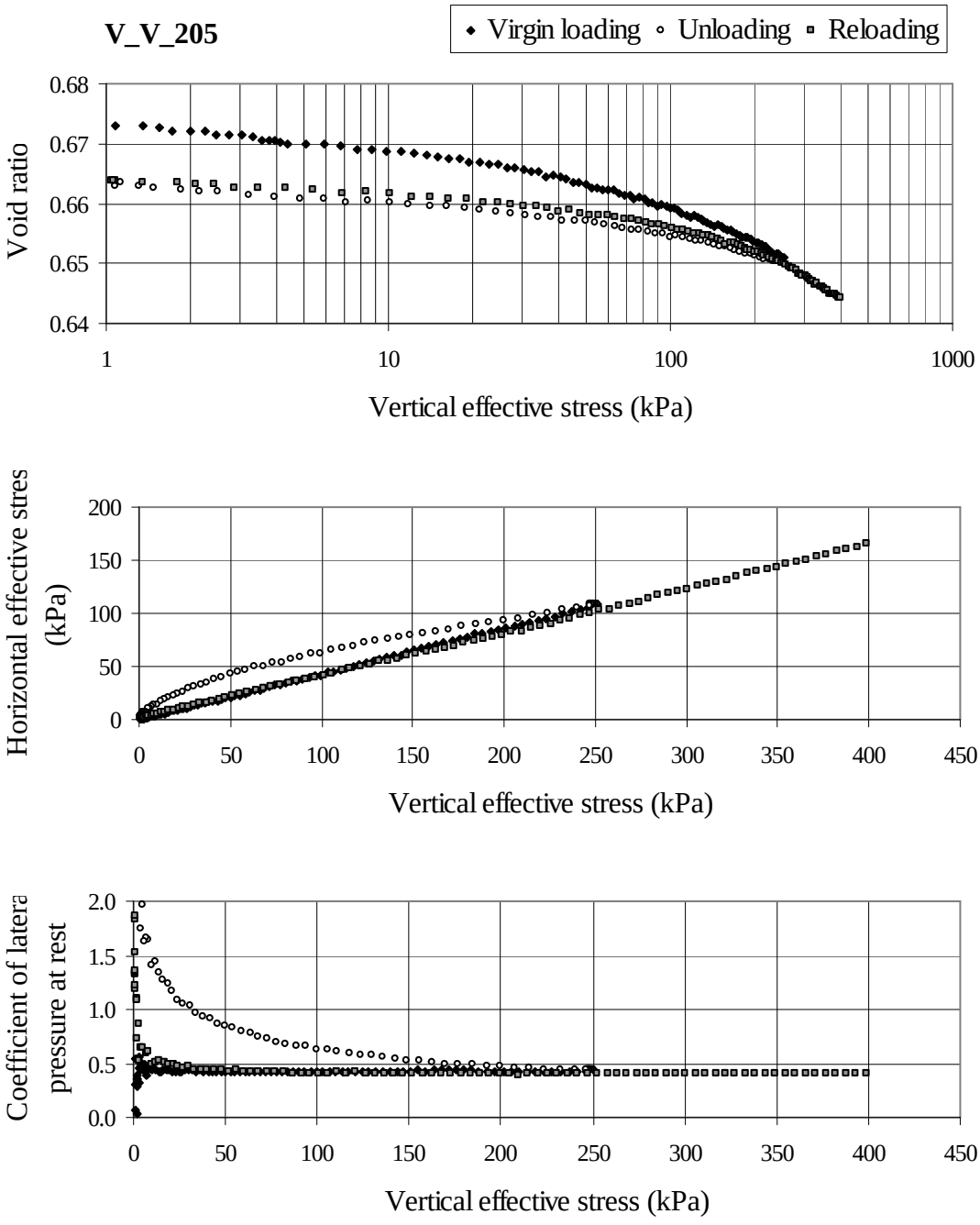

Figure C.3.5. Test data for V_V_205